New Approaches to the Labelling of Biological Targeting Vectors with ^{18}F

by

James Andrew Howard Inkster

M.Sc. (Chemistry), Simon Fraser University, 2003
B.Sc. (Hons., Chemistry), University of Saskatchewan, 1998

Thesis Submitted in Partial Fulfillment
of the Requirements for the Degree of
Doctor of Philosophy

in the
Department of Chemistry
Faculty of Science

SIMON FRASER UNIVERSITY

Fall 2012

Approval

Name: **James Andrew Howard Inkster**

Degree: **Doctor of Philosophy (Chemistry)**

Title of Thesis: ***New Approaches to the Labelling of Biological Targeting Vectors with ^{18}F***

Examining Committee: **Michael Eikerling,** Chair
Professor

Dr. Timothy Storr
Senior Supervisor
Assistant Professor

Dr. Thomas J. Ruth
Supervisor
Adjunct Professor

Dr. Paul Schaffer
Supervisor
Adjunct Professor

Dr. Dipankar Sen
Committee Member
Professor

Dr. Robert A. Britton
Committee Member
Associate Professor

Dr. Robert N. Young
Internal Examiner
Professor

Dr. Leonard I. Wiebe
External Examiner
Professor Emeritus
Faculty of Pharmacy and Pharmaceutical Sciences
University of Alberta

Date Defended/Approved: December 13, 2012

Partial Copyright Licence

Abstract

Positron emission tomography (PET) is currently the premiere molecular imaging technique for the detection and staging of cancer *in vivo*. Owing to the desirable nuclear properties of the short- lived positron emitter ^{18}F, and the remarkable targeting potential of many peptides, proteins and nucleic acid- based compounds, the efficient radiolabelling of these sensitive biomolecules with ^{18}F remains a fundamental objective in nuclear diagnostic medicine. Antisense imaging remains a promising tool for the identification and treatment of genetic diseases, particularly cancer. Herein, we expand the utility of the 2-[^{18}F]fluoropyridine- bearing labelling agent [^{18}F]FPy5yne to include nucleic acid- based probes for PET imaging. We describe the conjugation of [^{18}F]FPy5yne by way of a copper-catalyzed azide-alkyne cycloaddition (CuAAC) reaction to a 5'-azide-modified antisense oligodeoxyribonucleotide, which was first prepared from a 5'-aminohexyl-modified DNA 20mer. This work also describes protocols suitable for the coupling of [^{18}F]FPy5yne and mini-PEGylated analog PEG-[^{18}F]FPyKYNE to azide-modified peptide receptor ligands derived from bombesin and neuropeptide Y. These ^{18}F- labelled targeting vectors were assayed by collaborators for the detection of prostate, breast and brain cancer in mouse models by way of PET imaging and *ex vivo* autoradiography. Finally, a new approach for the ^{18}F- labelling of biological molecules is introduced and investigated. Sulfonyl [^{18}F]fluorides can be prepared under aqueous conditions and at room temperature, yet they have not yet been assayed as a potential means to ^{18}F- label biomarkers. A general route was developed for the synthesis of bifunctional arylsulfonyl [^{18}F]fluorides from their sulfonyl chloride precursors in 1:1 mixtures of MeCN, THF, or *t*-BuOH and Cs[^{18}F]F/Cs_2CO_3 over 15 minutes at room temperature. In most cases, pyridine could be used to selectively degrade the precursor without significantly affecting observed yields. As proof-of-principle, 3-formylmesitylenesulfonyl [^{18}F]fluoride was synthesized in excellent preparative yields and used to radiolabel an oxyamino-modified bombesin(6-14) analog. The ^{18}F bioconjugate showed signs of both defluorination and modification in mouse serum.

Keywords: positron emission tomography; ^{18}F; antisense; peptide receptors; sulfonyl fluorides

This work is dedicated to my daughters,
Frances (2009-) and Aoife (2012-),
who arrived late to the party.
And to my father George (1940-2011),
who left too soon.

Acknowledgements

I'd like to first thank my supervisory committee for their guidance and support. Most research efforts in radiochemistry today would be well served by more consistently seeking advice from those in the general field. In this regard, I am very lucky to have Profs. Britton and Sen review this document.

I would like to thank the TR13 cyclotron operators at TRIUMF- Cornelia Höehr, Wade English, and Linda Graham- for regularly providing me with [^{18}F]F^{-} despite a beam schedule packed with other projects. At the BC Cancer Radiopharmaceutical Facility, I'm indebted to radiochemists Dr. Kuo-Shyan Lin and Jennifer Greene for orientating me about the new facility, as well as cyclotron operators J.P. Appiah and Milan Vuckovic. I'd also like to acknowledge the assistance of the Michael Smith Proteomics Unit, the UBC Mass Spec lab and UBC NMR lab for their analytical contributions.

In my time at TRIUMF, both as a research assistant and a student, I've had the privilege of supervising a number of undergraduate co-op students. They were often a great help to me during radiosyntheses. In particular I am grateful for the efforts of Simon Gosslein and Kate Liu, who, ancillary to their own research goals, made direct contributions to this work. (More specific acknowledgements can be found in the preface to each chapter.)

The genuine advancement of PET imaging as field of science and medicine depends on strong collaborations between physicists, chemists, biological scientists and clinicians. In this regard, I am very grateful to have had the opportunity to work with Dr. François Bénard and his student Maral Pourghiasian. To have Maral's PhD. dependent on my radiochemistry was a statement of trust which I will not soon forget.

The peptide precursors in this work were prepared by Prof. Brigitte Guérin and her team at the Université de Sherbrooke. My working relationship with Brigitte began when I was a research assistant at TRIUMF, and has continued throughout my PhD. I have always appreciated the way she chose to engage me in a true collaborative spirit, while at the same time teaching me about the sometimes maddening world of radiobioconjugate chemistry.

I cannot truly convey the respect and gratitude I have for my supervisors- Tim, Tom and Paul. The knowledge I've gained through their expertise and training has proven invaluable. Just as important to me though, are the lessons I have learned by watching how they carry themselves as academics, as group leaders, and as men of character.

Financial support was provided by a Canadian Institutes of Health Research Operating Grant.

Table of Contents

List of Tables

List of Figures

List of Acronyms

υ	Neutrino
α	Alpha particle and Hammett substituent constant
α-MSH	α-melanocyte-stimulating hormone
β^-	Beta particle (negative electron of nuclear origin)
β^+	Positron (positive electron)
βAla	beta-alanine
γ	Gamma ray
δ	Chemical shift in ppm from tetramethylsilane
ΔE/E	energy resolution
λ	decay constant
ρ	density and Hammet reaction constant
[^{18}F]EF5	[^{18}F]-2-(2-nitro-1[H]-imidazol-1-yl)-N-(2,2,3,3,3-pentafuoropropyl)acetamide
[^{18}F]FBBA	N-(4-[18F]fluorobenzyl)-2-bromoacetimide
[^{18}F]FDG	2-[^{18}F]fluoro-2-deoxy-D-glucose
[^{18}F]FDOPA	6-[^{18}F]fluoro-dihydroxyphenylalanine
[^{18}F]FEP	fluorinated epibatidine
[^{18}F]FLT	3'-deoxy-3'-[^{18}F]fluorothymidine
[^{18}F]FPy5yne	2-[^{18}F]fluoro-3-hex-5-yn-1-yloxypyridine
[^{18}F]FPyBrA	2-bromo-N-[3-(2-[18F]fluoropyridin-3-yloxy)propyl]acetamide
[^{18}F]FPyCYT	fluorinated cystine
[^{18}F]FPyKYNE	2-[^{18}F]fluoro-3-pent-4-yn-1-yloxypyridine
[^{18}F]FPyME	1-[3-(2-[^{18}F]fluoropyridin-3-yloxy)propyl]pyrrole-2,5-dione
[^{18}F]SFB	N-succinimidyl 4-[^{18}F]fluorobenzoate
μPET	small animal PET
Å	Angstrom
A	activity (disintegration rate)
Aba	4-aminobutyric acid
AEBSF	4-(2-aminoethyl) benzenesulfonyl fluoride
AEEA	amino-ethoxy-ethoxy-acetyl
AGE	advanced glycation endproducts
APMSF	(p-amidoinophenyl)methanesulfonyl fluoride
AU	absorbance units
BB2r	gastrin- releasing peptide receptor type 2

BBB	blood-brain barrier
BBN	bombesin
BGO	bismuth germinate
Biolum.	Bioluminesence
Bn	Benzyl
BODIPY	boron-dipyrromethene
BPDS	bathophenanthroline disulfonate
Bq	becquerels
BSA	bovine serum albumin
BVD15	[Pro^{30}, Tyr^{32}, Leu^{34}]NPY(28-36)NH_2
BZH3	PEG2-[D-tyr^{6}, β-Ala^{11}, Thi^{13}, Nle^{14}]BBN(6-14)
BzOH	benzoic acid
c	cyclo
CCK-8	cholesytokinin(26-33)
CCK-Br	cholesytokinin B/gastrin receptor
Ci	curie
CPP	cell penetrating peptide
CT	Computed tomography
CuAAC	copper-catalyzed azide-alkyne cycloaddition
CZT	cadmium zinc telluride
D	Dextrorotatory
DAST	diethylaminosulfur trifluoride
DBU	1,8-Diazabicyclo[5.4.0]undec-7-ene
DC	decay corrected
DIAD	Diisopropyl azodicarboxylate
DIEA	*N, N*-diisopropylethylamine
DMAP	4-Dimethylaminopyridine
DNA	Deoxyribonucleic acid
DO3A	1,4,7-tris(carboxymethylaza)cyclododecane-10-azaacetyl
DOPA	Dihydroxyphenylalanine
DOTA	1,4,7,10-tetraazacyclododecane-1,4,7,10-tetraacetic acid
DTPA	diethylenetriamine pentaacetic acid
e^-	Electron
EC	electron capture
EFR	electrophilic fluorination reagent
EGFRvIII	mutant epidermal growth factor receptor

E_{max}	Maximum energy
E_{mean}	Average energy
EOB	end-of-bombardment
Fluores.	Fluoresence
GFP	green fluoresecent protein
GLUT1	glucose transporter type 1
GRP	gastrin- releasing peptide
GRP2r	gastrin- releasing peptide receptor type 2
HEPES	4-(2-hydroxyethyl)-1-piperazineethanesulfonic acid
HK	hexokinase
HMPAO	hexamethylpropylene amine oxime
HMPT	hexamethylphosphorous triamide
HPLC	high performance liquid chromatography
HPßCD	2-hydroxypropyl-ß-cyclodextrin
HRMS(EI)	High-resolution electron impact mass spectroscopy
HRMS(ESI)	High-resolution electrospray mass spectroscopy
HYNIC	Hydrazinonicotinamide
Hz	Hertz
IC50	half maximal inhibitory concentration
ID/g	injected dose/gram
IGF1	insulin growth factor 1
IR	infrared
iTLC-SG®	Instant Thin-Layer Chromatography silica gel- impregnated glass fibre
i.v.	intravenous
$K_{2.2.2.}$	4,7,13,16,21,24-Hexaoxa-1,10-diazabicyclo[8.8.8]hexacosane (Kryptofix® 2.2.2.)
k_d	equilibrium disassociation constant
K_i	inhibition constant
$k_{obs}/[I]$	second order rate constant of enzyme inhibition
L	Levaorotatory
LD50	median lethal dose
LNA	locked nucleic acid
log *D*	log of the distribution coefficient
LOR	line-of-response
LSO	lutetium oxyothrosilicate
M.P.	melting point

MAb	monoclonal antibody
MAG_3	mercaptoacetyltriglycine
MALDI-TOF	Matrix- assisted laser desorption/ionization time-of-flight mass spectroscopy
MAP	model amphipathic peptide
mdr1	multidrug resistance 1
MIBI	Methoxyisobutylisonitrile
MORF	morpholino phosphoramidate
MRI	magnetic resonance imaging
mRNA	messenger RNA
MTase	methyltransferase
N	Normal and number of atoms
n	Neutron and moles and number
NA	Avogadro's number
NaI(Tl)	thallium- doped sodium iodide
NCA	No-carrier-added
NDC	non-decay corrected
Nle	Norleucine
NMe_3Py5yne	[3-(hex)-5-ynyloxy]pyridine-2-yl]trimethylammonium trifluoromethanesulfonate
NOTA	1,4,7-triazacyclononane-N,N',N''-triacetic acid
NPY	neuropeptide Y
NPY1	Neuropeptide Y receptor type 1
NT	neurotensin
ODN	oligodeoxynucleotide
OTf	Trifluoromethanesulfonate (triflate)
OTs	Tosylate
p	Proton
PBS	phosphate buffered saline
PDAP	polydiamidopropanoyl
PEG	polyethylene glycol
PEG-[^{18}F]FPyKYNE	2-[^{18}F]fluoro-3-(2-(2-(prop-2-ynyloxy)ethoxy)ethoxy)pyridine
PEG-NMe_3-KYNE	[3-(2-(prop-2-ynyloxy)ethoxy)ethoxy)pyridine-2yl] trimethylammonium trifluoromethanesulfonate
Pen	Penetratin
PET	Positron emission tomography

PETT	positron-emission transaxial tomograph
Pgp	P-glycoprotein
pKa	log of the acid distribution constant
PMO	morpholino phosphoramidate
PMSF	phenyl methylsulfonyl fluoride
PNA	peptide nucleic acid
POC	peptide-oligonucleotide conjugate
PO-ODN	phosphodiester oligodeoxynucleotide
PTFE	Polytetrafluoroethylene
pVEC	vascular endothelium cadherin peptide
R^2	square of the correlation coefficient
RBF	round- bottom flask
RCY	radiochemical yield
R_f	retardation factor
RISCs	RNA-induced silencing complexes
RNA	ribonucleic acid
RNAi	RNA interference
RNase H	ribonuclease H
RT	room temperature
R_t	retention time
SA	sprecific activity
SA_{max}	maximum specific activity
SarAr	1-amino-8-(4-aminobenzylamino)-3,6,10,13,16,19-hexaazabicyclo[6.6.6]eicosane-1,8-diamine
SD	standard deviation
SiFA-A	p-(di-tert-butyl[^{18}F]fluorosilyl)benzaldyde
SiFA-Mal	p-(di-tert-butyl[^{18}F]fluorosilyl)phenylmaleimide
SiFA-SH	p-(di-tert-butyl[^{18}F]fluorosilyl)benzenethiol
siRNA	short/small interfering RNA
S_N1	unimolecular nucleophilic substitution
S_N2	bimolecular nucleophilic substitution
S_NAr	addition-elimination nucleophilic aromatic substitution
SOS	start-of-synthesis
SPE	solid phase extraction
SPECT	Single photon emission computed tomography
SST	somatostatin

SUV_{max}	maximum standardized uptake values
$t_{1/2}$	Half-life
Tat	Trans-acting activator of transcription protein
TATE	[Tyr^3]octreotate
$TBAHCO_3$	tetrabutylammonium hydrogencarbonate
TBTA	tris-(benzyltriazolylmethyl)amine
TEAA	triethylammonium acetate
TEG	tetraethylene oxide
TFA	Trifluoroacetic acid
TfR	transferrin receptor
Thi	β-(2-Thienyl)-alanine
THPTA	tris(3-hydroxypropyltriazolemethyl)amine
TLC	thin layer chromatography
T_m	melting temperature
TOCA	[Tyr^3]octreotate
TP	Transportan
Tris	tris(hydroxymethyl)aminomethane
VIP	vasoactive intestinal peptide
Zeff	effective nuclear charge

Introductory Image

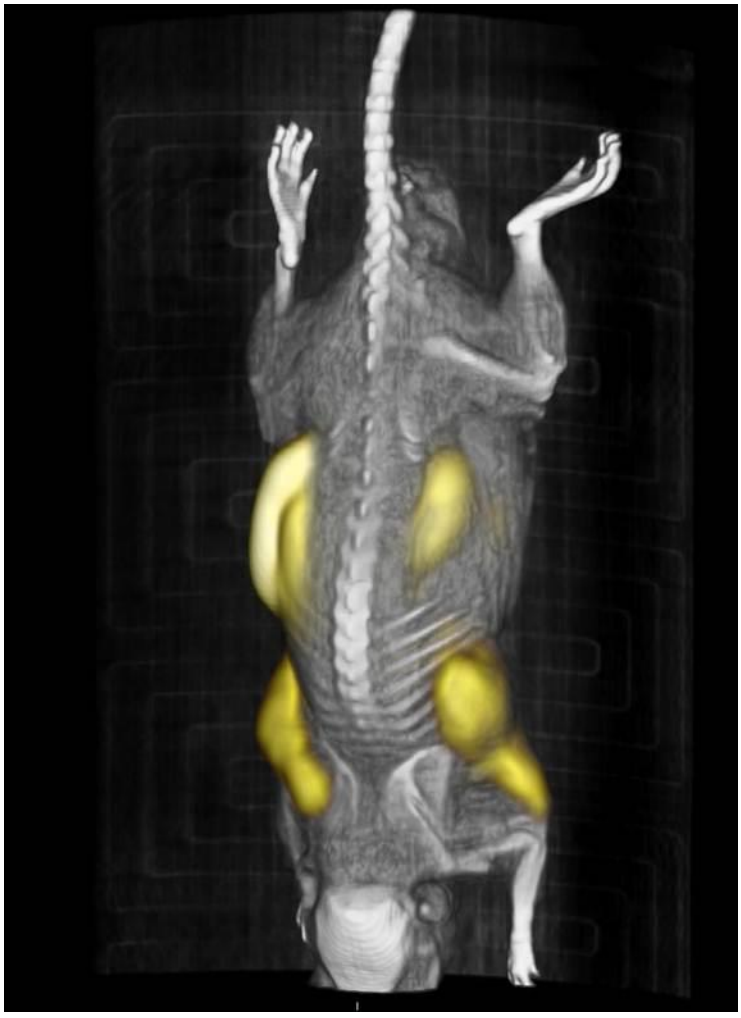

Pictured above is a fused PET/CT 3D image of a prostate cancer- bearing nude mouse, 60 min after injection of ^{18}F- labelled gastrin- releasing peptide receptor ligand **[^{18}F]F-ALK-BBN-PEG**. Tumours can been seen on the right and left flank of the animal, under the forelimbs. (Image appears courtesy of M. Pourghiasian.)

1. Introduction

1.1. Nuclear Imaging

1.1.1. *Early History*

Radionuclides were first used in the study of living systems by the radiochemist and Nobel laureate George de Hevesy in 1923, who measured the uptake of radioactive $Pb(NO_3)_2$ in horse-bean plants and its displacement by other administered nitrates.[1] de Hevesy had already established the notion that a radioactive compound, being chemically identical to its non-radioactive form(s), could be used to elicit the role of that compound in various chemical and biological processes. He later applied his 'radiotracer principle' to the study of phosphate distribution in rats using ^{32}P, which provided evidence for the dynamic 'desorptive/resorptive' process of phosphorus fixation in bones.[2] It is because of these and other discoveries that de Hevesy is considered by many to be the 'Grandfather of Nuclear Medicine.'[3]

The invention of the deuteron cyclotron by E. Lawrence and co-workers in the early 1930s allowed for the reliable production of many new artificial radionuclides.[4] In 1942, the first self-sustained nuclear reaction was produced at the University of Chicago,[5] and the rapid development of nuclear reactors followed. Both technologies were exploited relatively early after their inception for the production of useful quantities of radioisotopes for life science research. In the summer of 1946, representatives from the Manhattan Project announced in *Science* magazine that certain neutron-induced radioisotopes would be made available, on a commercial basis, to trustworthy investigators. Priority went to "publishable researches in the fundamental sciences, including human tracer applications…"[6] This early distribution system contributed significantly to the full development of nuclear diagnostic medicine.

1.1.2. *Early Instrumentation*

Early applications of radioisotopes in diagnostic medicine were limited to *in vitro* measurements such as iron turnover and the volume of distribution of sodium.[3] At the time, researchers lacked a means to efficiently detect penetrating gamma rays. Eventually, the development of photomultiplying technologies allowed for the detection and amplification of the scintillation energy generated from ionization events. The first scintillation counters used to measure the concentration of radioactivity *in vivo* were simple collimated devices. These were eventually replaced by the rectilinear scanner, which was first designed by Cassen, Curtis and Reed to image the distribution of ^{131}I in the thyroid gland.[7] Manually moving the camera laterally across the patient was a tedious and challenging affair, which eventually led to the design of an automated system.[8] In 1956, David Kuhl and colleges made modifications to the Cassen design that significantly improved sensitivity and resolution.[9] A glow lamp with variable output was used to burn images onto photographic film. The lamp was actuated by the output of a thallium- activated sodium iodide scintillator. Sold commercially as the Picker photoscanner, the device was popular with radiologists as it produced a gradient image that could be read on a standard x-ray viewer.[10] Commercialization of the photoscanner did much to advance the field of nuclear imaging during the 50's and early 60's.

Rectilinear scanners can only acquire data line-by-line. Stationary gamma cameras which might be used to map an entire organ at once were envisioned. Early 'pin-hole' designs used a collimator to project activity onto a scintillation crystal, and as with the rectilinear scanner, the scintillation emission was captured on photographic film.[11] Poor sensitivity was the practical issue. However, in 1957, H.O. Anger developed a γ-camera that did not detect scintillation light with film, but instead used an array of photomultiplier tubes.[12] Varying signal strength from the tubes allowed one to determine the X, Y location on the crystal were the γ ray was absorbed, and thus the position of the original emission. Anger's rapid, sensitive, whole-body camera represents a milestone in nuclear medicine. Only recently has the original design been substantially improved upon.[13]

1.1.3. *Single Photon Emission Computed Tomography (SPECT)*

In 1963, Kuhl and Edwards used an Anger camera to obtain a tomographic image, which was computationally reconstructed from a series of planar images ('projections'), obtained while rotating the camera around a subject.[14] The images were very crude, but they inspired a tremendous period of instrumental development during the 60's and 70's, as a number of nuclear emission tomographs were built and tested.[15] Some scanners focused on a single plane of emission (i.e. longitudinal devices), while other transaxial scanners rotated the patient, or used multiple cameras. The groups of Jasczcak[16] and Keyes[17] are usually credited for designing the first practical single photon emission computerized tomographic (SPECT) scanners, for head and whole-body use respectively. Many significant breakthroughs for this technology have come in the form of data filtration and backprojection methods originally developed for x-ray transmission computed tomography (CT). By the mid-80's, these computational advances, along with commercial optimizations in scanner design, helped to establish SPECT as a standard diagnostic tool of the clinical community.

SPECT imaging has greatly benefited from the extensive development of ^{99m}Tc as a radiopharmaceutical agent. ^{99m}Tc possesses many attractive qualities for nuclear imaging.[18] It has a relatively simple decay scheme, which results in the emission of a low energy 140 keV photon for imaging. Its intermediate half-life ($t_{1/2}$ = 6 hrs) and well-established chelation properties simplify development of new targeting agents and can allow for highly efficient radiosynthetic procedures. Finally, ^{99m}Tc can be easily obtained as the primary daughter radionuclide of reactor-produced ^{99}Mo. The long half-life of ^{99}Mo ($t_{1/2}$ = 67 h) allows it to be processed and shipped in the form of a generator, which can be transported over long distances. A typical generator can then be 'milked' (stripped) of ^{99m}Tc over the course of several weeks. Commercial formulation 'kits' and straightforward chelation protocols allow for many established ^{99m}Tc radiopharmaceuticals to be prepared with a minimum of synthetic expertise.[19] Myocardial and brain perfusion imaging represent two of the most recent and important applications of this approach. Even today, a majority of ^{99m}Tc SPECT procedures employ simple lipophilic complexes that are known to absorb, distribute and degrade in various organs of interest. The cardiac procedure uses ^{99m}Tc- methoxyisobutylisonitrile (^{99m}Tc-MIBI) and related complexes to evaluate coronary artery stenosis.[20] ^{99m}Tc-MIBI

is known to distribute in the heart muscle in proportion to blood flow; uptake requires a viable myocardial cell and an intact cell membrane. Thus, imaging of the patient before and after physical or chemical stress allows the identification of ischemic or infarcted areas of the heart. The most popular brain perfusion SPECT agent is ^{99m}Tc-hexamethylpropylene amine oxime (^{99m}Tc-HMPAO). Within functional brain cells, ^{99m}Tc-HMPAO is converted to more hydrophilic complexes by a poorly understood mechanism and becomes trapped.[21] This process of uptake and metabolism is associated with regional blood flow and normal brain function.

1.1.4. *Positron Emission Tomography (PET)*

1.1.4.1. Positron decay

Positrons (β^+) are particles of antimatter that are produced upon decay of a proton to a neutron. This process is also associated with the production of a neutrino, and is described according to the nuclear equation:

$$p \rightarrow n + \beta^+ + \upsilon \quad (Eq.1)$$

Positron emission is common among those unstable nuclei that are considered 'proton rich'- that is, their ratio of neutrons to protons is low relative to that of the next stable nuclide.[22] This type of nuclei can also decay by *electron capture* (EC), a competing process by which a proton combines with an electron from a low energy extranuclear shell to form a neutron:

$$p + e^- \rightarrow n + \upsilon \quad (Eq.2)$$

When positrons (β^+) move through matter, they interact with electrons and gradually lose energy. At the point of near-rest, they collide with an orbital electron and both particles are annihilated. Their rest mass is converted into two 511 keV γ-rays, which are emitted at angles very close to 180° from each other.[23] The production of these annihilation radiations requires that transition energy between the parent and the daughter nuclide is greater than 1022 keV (the combined energy of the two gamma emissions).[22] Otherwise, only electron capture is possible. As one might expect, the probability of β^+ production relative to electron capture increases with increasing transition energy.

1.1.4.2. Historical Development of PET

Considering its current reputation as a state-of-the-art functional imaging technique, it is somewhat remarkable that the first positron imaging devices were built in 1951,[24] prior to the invention of the rectilinear scanner. The first clinical single-pair detector instrument, which collected data in both a coincident and unbalanced fashion, was described a year later by Brownell and Sweet.[25] Research scanners that utilized multiple pairs of detectors did not see extensive development for almost a decade. James Robertson and colleagues at Brookhaven National Laboratory produced a complex spherical scanner that encircled a patient's head, which was used to produce a functional image of cerebral blood flow. Later, the scanner was shipped to Montreal Neurological Institute, where it was reassembled as circular array of detectors.[26] Like SPECT, PET research benefited much from the mathematical reconstruction algorithms that were developed for computed tomography. In 1975, Ter-Pogossian, Phelps, and Hoffman described a circular array scanner that used a filtered backprojection technique to obtain images of dog anatomy with $[^{13}N]NH_3$, $[^{15}O]H_2O$ and $[^{11}C]CO$ that were far superior to any other transmission- based image at the time. They called their device the 'positron-emission transaxial tomograph' (PETT). Later, when it was shown patients could be imaged in the sagittal and coronal planes as well, they shortened the name to 'PET'.

1.1.4.3. The PET Scanner

The modern PET scanner is typically composed of a ring (or ring segments) of scintillation detectors. A subject, who has been dosed with a positron-emitting radiopharmaceutical, is placed inside. Opposing detectors are placed in coincidence, such that if both detect an annihilation photon with a certain pre-defined timing window, a signal is generated.[27] In the same manner as the gamma camera, the light photons produced by scintillation are amplified and converted to electrical pulses by photomultiplier tubes. As the amplitude of the collected pulses are dependent on the energy of the original gamma emission, detections that did not originate from radionuclide decay can be filtered from the stored data set which is ultimately used to reconstruct the tomographic image.[22]

The line connecting positions of the two detection events in space is called the line-of-response (LOR; Figure 1.1). In the ideal case, this line crosses through the site of annihilation; however, other types of false coincidences are possible and these negatively impact the clarity of the PET image.[28, 29] The term 'random coincidence' is used to describe the unproductive detection of two photons from two different annihilations that nevertheless fall within the coincidence timing window. 'Scatter coincidence' describes the scenario in which one or both photons are deflected from their original trajectories through Compton interactions with tissue atoms. Other factors that may convolute the collection and interpretation of PET data include 'multiple coincidences' (two or more photons reaching a detector at the same time, which can result in the true coincidence being ignored) and 'prompt radiations' (detectable photons emitted for the radioisotope that are unassociated with positron emission).

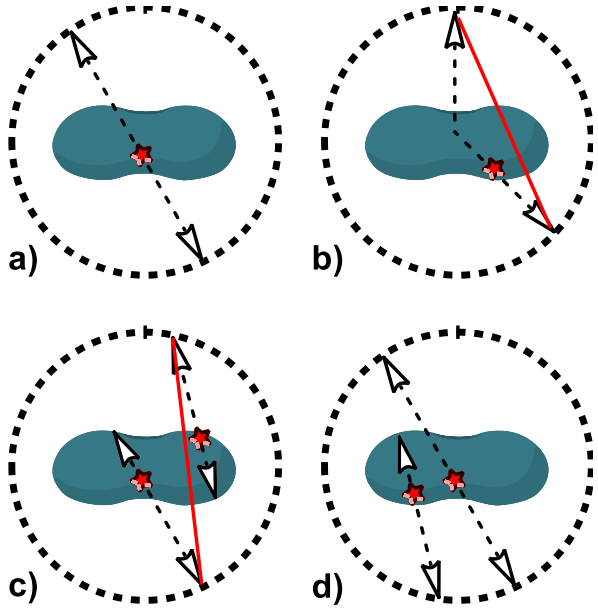

Figure 1.1. Detection events possible when PET imaging

Cross section representations of a) a true coincidence; b) scatter as the result of Compton interactions; c) a random coincidence; d) a multiple (a.k.a. triple) coincidence. Red stars represent points of annihilation, while the dashed arrows represent the path of the resulting photons. False LORs are shown in red. Adapted from *Data Acquisition and Performance Characterization in PET.*[29]

The type and quality of a PET scanner's radiation detection system underlies the success of the entire technology, and thus crystal and photo-detector development

remain active fields of research. In general, the applicability of a scintillation material for PET is judged on four main criteria:[30]

- *Stopping power.* The shorter the mean distance a photon travels in the crystal, the greater chance it will deposit its energy within the material and initiate a detection event. This attenuation length is relative to crystal density and effective atomic number.
- *Signal decay time.* A short decay time allows for the efficient processing of individual detections at high counting rates.
- *High light output.* Good photoelectron generation is one element required for good energy resolution (ΔE/E), which allows for the efficient rejection of scatter coincidences and prompt radiation.
- *Intrinsic energy resolution.* Also relates to overall energy resolution. Intrinsic energy resolution is dependent on the uniformity of the crystal and its light output.

As a popular general scintillation material, thallium- doped sodium iodide [NaI(Tl)] exhibits high light output but possesses low stopping power for 511 keV photons, which makes this crystal matrix sub-optimal for β^+ detection.[31] Thus, most new PET systems employ other materials, with bismuth germinate (BGO) or cerium- laced lutetium oxyothrosilicate (LSO) being the most common. BGO has a slightly higher decay constant than NaI(Tl) and significantly lower light output [15 % of NaI(Tl)]. However, the excellent stopping power of BGO [ρ = 7.13 g/cm^3, Z_{eff} = 74.2 vs. ρ = 3.67 g/cm^3, Z_{eff} = 50.6 for NaI(Tl)] and thus high sensitivity has made it an attractive choice for commercial developers.[30] LSO possess a high light output [75 % of NaI(Tl)] and has similar stopping power to BGO.[32] Unfortunately, due to the intrinsic inhomogeneities of the crystal, LSO systems lack the overall energy resolution of NaI(Tl) scanners. Another impediment to LSO development is that its usefulness as a scintillation matrix outside of PET is limited by the presence of a β^--emitting radioimpurity (^{176}Lu, 2.6 %), which produces convoluting γ photons at 88-400 keV.[33] Gamma detection technologies which eshew scintillation crystals are currently in development for PET, including the use of semiconducting materials [*e.g.* cadmium zinc telluride (CZT)],[34] and scintillating liquids (*e.g.* liquid Xe).[35]

1.1.4.4. Molecular Imaging and PET

Molecular imaging is a relatively new term that was coined to conceptually encompass a seemingly disparate group of imaging modalities. It has been defined as

"the characterization and measurement of biological processes in living animals and humans at the cellular and molecular level using imaging techniques."[36] Modalities that meet this criteria include PET, SPECT, bioluminescence and fluorescence imaging, magnetic resonance imaging (MRI) and ultrasonography. Molecular imaging differentiates itself from structural imaging in the sense that it seeks to image the specific molecular events responsible for a disease, rather than the non-specific macroscopic changes that arise from it.[37] For the nuclear and optical techniques mentioned, the use of targeting vectors is essential, while MRI and ultrasound are inherently structural modalities that can be adapted to produce functional images through the use of targeting contrast agents.

Table 1.1 compares PET with a number of other imaging modalities. In terms of advantages, PET offers a high level of sensitivity (10^{-11}- 10^{-12} M) using a very small amount of radiopharmaceutical (ng quantities). If high specific activity material is used, there is little risk that a PET tracer will perturb the biological system being investigated. As mentioned, radiotracers that mimic authentic compounds exactly are possible. Finally, well established methods are available for quantitative experimentation. The two main disadvantages associated with PET are a) cost and b) a theoretical maximum spatial resolution which is inferior to the structural modalities. The high cost can be attributed to the resources required to safely produce and handle short- lived positron emitters. The spatial resolution of most modern PET scanners that are used for routine clinical work is 4- 6 mm, although the resolution of dedicated brain scanners is slightly higher (~2.5 mm).[38] The resolution of preclinical scanners (*i.e.* small animal, or µPET) is in the range of 1-2 mm.

Table 1.1. Characteristics of various molecular imaging modalities

Modality	Radiation	Max Spatial Resolution (mm)	Max. Depth (cm)	Sensitivity (M)	Probe Amount	Degree of Quant.	Potential for Perturbation	Cost
PET	γ (high E)	1-2	None	10^{-11}-10^{-12}	ng	+++	None	++++
SPECT	γ (low E)	≤1 mm	None	10^{-10}-10^{-11}	ng	++	None	+++
Biolum.	Vis. light	3-5	1-2	~10^{-15}-10^{-17}	µg-mg	+/++	Possible	++

Modality	Radiation	Max Spatial Resolution (mm)	Max. Depth (cm)	Sensitivity (M)	Probe Amount	Degree of Quant.	Potential for Perturbation	Cost
Fluores.	Vis. light or near IR	2-3	<1	~10^{-9}-10^{-12}	µg-mg	+/++	Possible	+/++
MRI	Radio	0.025-0.1	None	10^{-3}-10^{-5}	µg-mg	++	Possible	++++
Ultrasound	Sound	0.050-0.5*	Varies with mode	Varies with mode	µg-mg*	+	Possible	++
CT	x rays	0.050-0.2	None	N/A	N/A	N/A	Possible**	++

Note: Reproduced from the following references.[37, 38] *Very approximate as ultrasound molecular imaging is in its infancy.[39] **By way of high radiation dose.

Computed tomography (CT) uses the differential absorption of x-rays to produce a high- quality structural image. It is not considered a molecular imaging technique, but it has become an important complement to both SPECT and PET imaging. Thus, the nuclear tomographic scan provides the bio-functional image, while the x-ray tomographic scan provides the anatomical frame of reference. The CT scan can also be used to accurately attenuate the positron camera when adjusting for the variances that arise from a patient's size and weight.[40] The first dual modality PET/CT scanners were developed in collaboration with business interests,[41] and over the last 10 years have come to dominate the commercial market.[42] PET/CT is considered particularly valuable in the field of oncology, where the surgical resection of diseased tissue is a desirable treatment option.

1.2. Radionuclides for PET

1.2.1. *Specific Activity*

The most fundamental definition of radionuclide *specific activity* (SA) is the activity (disintegration rate) of a decaying isotope per unit mass of that element present in the sample.[43] In radiochemistry, a moles- related description of specific activity is more valuable:

$$SA = \frac{A}{n} \ (Eq. 3)$$

where *A* is the activity in Becquerels and *n* is the total moles of the element in the sample. The stable isotopes are referred to as *carrier*. Specific activity plays a major role in the development of many nuclear biomarkers because the number of atoms that produce the measured signal is so small. If the process to be imaged relies on a limited number of biological targets, the non-radioactive form of a radiopharmaceutical has the potential to saturate the system and block the uptake and sequesterization of the radioactive form.[44] Furthermore, an excess of carrier- labelled compound may lead to unwanted physiochemical changes in the process being studied, including pharmacological and toxic effects.[45] In these situations, it is desirable to prepare radioisotopes and radiotracers in the highest specific activities possible.

The general equation of the law of radioactive decay states that activity is proportional to the number of radioactive atoms in the sample (*N*) by a decay constant (λ).

$$A = -\frac{dN}{dt} = \lambda N \ (Eq. 4)$$

The integrated form of this law can be used to solve *λ* in terms of half-life:

$$\lambda = \frac{\ln 2}{t_{1/2}} \ (Eq. 5)$$

Merging equations 3, 4 and 5 yields

$$SA = \frac{\left(\frac{\ln 2}{t_{1/2}}\right) N}{n} \ (Eq. 6)$$

If all of the atoms in the sample are radioactive- that is, the sample is truly carrier-free- then $N = N_A * n$, where N_A is Avogadro's number. Equation 6 simplifies to the form

$$SA_{max} = \frac{1.16 \times 10^{20}}{t_{1/2}} \ (Eq. 7)$$

Thus, the maximum possible specific activity of a radioisotope is inversely proportional to its half- life. This is one reason that short- lived radioisotopes are coveted for many nuclear diagnostic procedures. However, in most cases the maximum specific activity is not achievable, due to isotopic exchange with trace levels of carrier present during the radiopharmaceutical production process.[46] Production protocols that seek to exclude carrier are referred to as *no-carrier-added* (NCA) preparations. From a functional imaging standpoint, *any* impurity with physiochemical properties similar to that of the radiotracer will retard its efficacy. This includes the authentic (non-radioactive) compound, but also includes material that has been labelled with non-isotopic carrier, as well as unlabelled precursor. A combined measurement of these factors is described as *apparent* specific activity (Bq/mol). Spectroscopic methods are commonly used to estimate the total mass associated with a tracer after radiochemical production, usually by way of UV-HPLC analysis.

1.2.2. ***PET Isotopes***

Of the ~3800 radioactive isotopes, only 541 include positron emission in their decay schemes.[47] Among these radionuclides, only a handful possess acceptable nuclear and chemical characteristics for PET imaging, namely:

- *A 'short' radioactive half-life ($t_{1/2}$).* In practical terms, this means a range of a few minutes to a few hours. This ensures that patients (and those in their proximity) do not incur an unwarranted radiation burden. However, the $t_{1/2}$ must be long enough to allow for reliable synthesis of the desired molecular probe.* Furthermore, the $t_{1/2}$ must be compatible with the bio-kinetics of the process being studied.
- *A short range in tissue.* One of the core assumptions in PET imaging is that the decaying isotope exists on the line of response of the coincident gamma rays. Discrepancies between the true and perceived line of response ultimately contributes to a blurring of the image.[48] The range of an emitted positron prior to the annihilation event is directly proportional to its energy. Therefore, isotopes with lower positron energy tend to produce images of better spatial resolution.

* In practical terms, this maximum synthesis time is often considered to be three half- lives.[45]

- *High positron abundance.* Isotopes with decay schemes that favour positron emission over electron capture maximize detector sensitivity.
- *Simple decay schemes.* Isotopes that do not produce extraneous emissions minimize unproductive dose to the patient. In addition, prompt gamma radiation within the energy window of the PET scanner can degrade image quality by way of detecting false coincidences.[49]
- *Good availability.* Radionuclides that can be prepared in efficient, clean nuclear reactions are preferred over those that require high bombardment energies for production and/or extensive isotopic purification before use.

Table 1.2 summarizes the most common PET isotopes and their nuclear properties. ^{13}N, ^{15}O and ^{11}C are sometimes described as 'authentic' isotopes because they can be used to prepare exact atomic replicas of biological molecules.[50] ^{13}N and ^{15}O were important isotopes in the early days of PET development; $[^{13}N]NH_4^+$ and $[^{18}O]H_2O$ are still used for cerebral and myocardial perfusion imaging.[51] However, the general utility of the isotopes are limited by their short half- lives. Carbon-11 labelling is available to those radiochemistry laboratories with an on-site cyclotron. Depending on the form of starting ^{14}N and the type of additives present upon bombardment, a host of reactive ^{11}C labelling agents can be synthesized. Optimized protocols exist to make $[^{11}C]CO$, $[^{11}C]CO_2$, $[^{11}C]CH_4$, $[^{11}C]HCN$, $[^{11}C]CH_3OH$, and $[^{11}C]CH_3I$ in high radiochemical purity and specific activity ($SA_{max} = 3.41 \times 10^{11}$ GBq/μmol). These intermediary agents are most commonly employed for the preparation of ^{11}C- labelled small molecule drugs and bioactive compounds. The typical specific activity of a ^{11}C radiopharmaceutical is ~370 GBq/μmol.[46]

The positron- emitting radiohalogens constitute an important class of PET isotopes, if only because they include ^{18}F (*vide infra*). The stable isotopes of chlorine, bromine, iodine and astatine are rarely or never found in human biomolecules. Furthermore, only a relatively small number of small molecule synthetics contain halogens.[52] However, the propensity of halogens to undergo efficient substitution chemistry has ensured their place in the PET chemistry toolkit. Iodine-124 has a viable half-life and can be used to produce positron-emitting analogues of established SPECT compounds.[53] However, the positron abundance of this isotope is low (25 %), and its decay scheme contains interfering high- energy gamma emissions.[51] The radiobromines ^{75}Br, ^{76}Br and ^{77}Br are all positron- emitters; ^{75}Br and ^{76}Br have half-lives amendable to various PET applications. However, their unfavourable decay

characteristics have limited their use. They have been utilized in the radiosynthesis of bromine- containing dopamine D1 receptor[54] and nicotinic acetylcholine receptor[55] ligands, as well as competition molecules to measure the pharmacodynamic parameters of non-radioactive drugs.[52]

Table 1.2. A List of Common PET isotopes

Nuclide	Half-life	Decay mode (%)	β^+ E_{max} (keV)	Production Method*
^{11}C	20.4 min	β^+ (99.8), EC (0.2)	960	$^{14}N(p, \alpha)$
^{13}N	10.0 min	β^+ (100)	1190	$^{16}O(p, \alpha)$
^{15}O	2.03 min	β^+ (99.9), EC (0.1)	1720	$^{15}N(p, n)$
^{18}F	110 min	β^+ (97), EC (3)	635	$^{18}O(p, n)$
^{75}Br	98 min	β^+ (76), EC (24)	1740	$^{78}Kr(p, \alpha)$
^{76}Br	16.1 h	β^+ (57), EC (43)	3900	$^{76}Se(p,n)$)
^{124}I	4.18 days	β^+ (25), EC (75)	2140	$^{124}Te(p, n)$
^{64}Cu	12.7 h	β^+ (18), β^- (37), EC (45)	656	$^{64}Ni(p, n)$
^{68}Ga	68.3 min	β^+ (90), EC (10)	1900	^{68}Ge ($t_{1/2}$ = 270 days) generator
^{82}Rb	1.25 min	β^+ (96), EC (4)	3150	^{82}Sr ($t_{1/2}$ = 25.6 days) generator
^{86}Y	14.7 h	β^+ (33), EC (67)	1545	$^{86}Sr(p,n)$

Note: Adapted from Mason and Mathis[56] and McQuade *et al.*[57] EC = electron capture. *Unless noted, describes the method of production using a H^+ beam cyclotron.

Use of radiometals in PET chemistry has emerged alongside the increasing prevalence of biomolecular imaging agents because these vectors can better tolerate chelator modifications and still retain their targeting affinity. Copper has three viable PET isotopes- ^{60}Cu, ^{61}Cu and ^{64}Cu- of which ^{64}Cu is the most promising.[58] Copper-64 has a relatively low energy positron emission and can be distributed from an off-site cyclotron. As copper is susceptible to *in vivo* reduction and uptake from copper transport proteins, many early ^{64}Cu functionalized radiopharmaceuticals were prone to metal disassociation *in vivo*. However, the development of the 'diaminosarcophagine' chelator core for PET chemistry (see SarAr, Figure 1.11)[59] has permitted the synthesis of ^{64}Cu- labelled peptides[60] and antibodies[61] with attractive biological half-lives. ^{68}Ga can be obtained as the principle decay product from reactor- produced ^{68}Ge. As such, the optimization of generator design and radioprotocols for this isotope are areas of considerable commercial interest. Ga^{3+} ions bear many atomic similarities to Fe^{3+} in

aqueous media, and are thus susceptible to hydrolysis at physiological pH. Furthermore, the serum blood protein transferrin exibits a high affinity for Ga^{3+}.[57] Fortunately, a number of chelators have been shown to exhibit sufficient thermodynamic and kinetic stability to be considered for clinical use.[62] Coincidence detection of ^{86}Y annihilation decay is significantly convoluted by the presence of prompt gamma radiation,[49] thus, ^{86}Y is typically only used as a surrogate isotope for the development of ^{90}Y- bearing therapeutic compounds.[63] ^{82}Rb (in the form [^{82}Rb]RbCl) is used almost exclusively as a myocardial imaging agent[64] and to measure blood-brain-barrier failure caused by brain tumours.[65] Due to its extremely short half- life, [^{82}Rb]RbCl extraction, purification, formulation and injection into patients is entirely computer- controlled.

1.2.3. *The Cyclotron*

A cyclotron is a particle accelerator and as such its basic operation involves the attraction of charged particles to an oppositely charged electrode. In this case, two electrode cavities called *dees*- in reference to their original 'D' shapes- are placed side-by-side and coupled by way of a radio frequency oscillator (RF) such that their polarities can be rapidly inverted (Figure 1.2).[66] The dees are placed in an evacuated environment and 'sandwiched' between the poles of a magnet. Thus any particle introduced into the centre of the cyclotron will tend to rotate in a circular pattern around the magnetic moment, which projects out perpendicular to the dees. When a charged particle crosses the gap between the dees, it sees a small measure of acceleration and its trajectory takes it farther away from the injection point.[67] After numerous periods of acceleration, the spiraling particle can be deflected out of the chamber and used to bombard a 'target' element and initiate the desired nuclear reaction. The cyclotron process can be used to create high- energy protons, neutrons, deuterons, α particles and hydride ions.[22] However, a vast majority of today's cyclotrons are built to generate proton beams of less than 30 MeV for the production of medical isotopes.

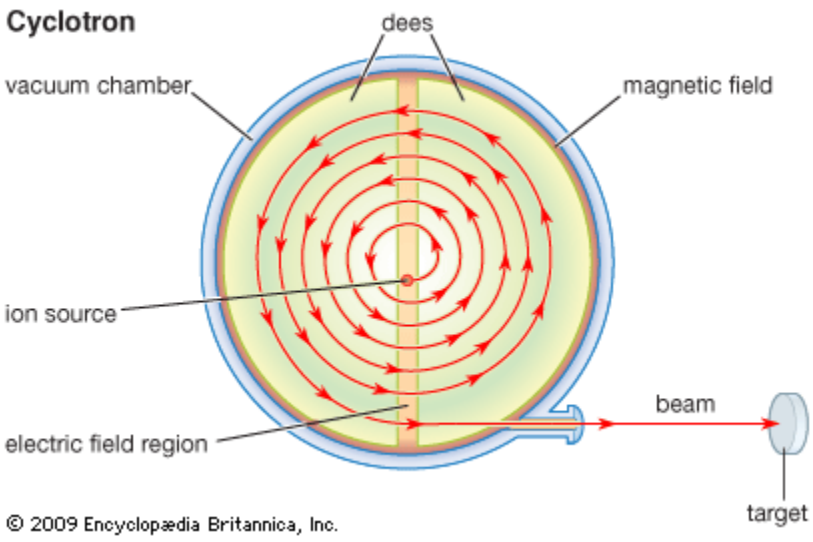

Figure 1.2. Basic design of the classical cyclotron.

Image retrieved from *Encyclopædia Britannica Online* and used with permission.[68]

The first cyclotrons were built by Lawrence and Livingston to accelerate protons which interacted with targets placed inside the cyclotron vacuum tank.[69] Later designs involved the deflection of the beam out of the tank, with the expected losses in efficiency (30- 40 %).[66] Today, the acceleration of H^- ions, followed by their oxidation to H^+ particles, is the standard method for the generation of proton beams. This is accomplished by passing the hydride ions through a thin foil of carbon which strips the particle of electrons. The beam, now positively charged, changes direction in the presence of the magnetic field and can be easily extracted out of the chamber. By changing the distance between the foil and the central injection port, different ranges in beam energy may be selected.[51] In addition, the negative ion source approach allows for the extraction of different beam energies simultaneously by the placement of extraction foils in linear sequence, where the first foil only converts part of the beam.

1.2.4. *Production of ^{18}F*

^{18}F has grown in prominence over the last twenty years to become the single most important isotope for PET. It can be produced in good yields using a relatively low energy proton beam (<16 MeV)[44] *via* the $^{18}O(p,n)^{18}F$ reaction.[301] A growing number of sites worldwide can regularly produce multi-Curie amounts of $[^{18}F]F^-$ or $[^{18}F]F_2$ using compact, dedicated, so-called 'medical' cyclotrons.[70] The radioisotope exhibits many

attractive nuclear properties for *in vivo* imaging, including a low positron kinetic energy (E_{max} = 635 keV, E_{mean} = 250 keV) and thus a short range in water (2.4 mm).[30] It has an intermediate half-life which allows for complex multistep synthesis and shipment of ^{18}F to sites that do not possess a cyclotron.

Although a few reaction pathways have been discovered for the production of ^{18}F,[56] only two are commonly used today. H[^{18}F]F can be produced through the irradiation of a liquid target containing ^{18}O- enriched water. Using this approach, the [^{18}F]F^- can be collected and used in a 'no-carrier-added' (NCA) fashion, and thus the preparation of high specific activity radiotracers is possible. The theoretical maximum SA of carrier-free ^{18}F is 63,000 GBq/µmol.[56] However, the ubiquitous presence of perfluorinated materials (*e.g.* Teflon®) in cyclotron and chemistry environments[71] ensures that most sites worldwide produce [^{18}F]F^- with SAs in the range of 300- 600 GBq/µmol.[70] In contrast, those methods used to produce elemental [^{18}F]F_2 gas by way of $^{18}O_2$ bombardment typically results in batches of much lower specific activity (SAs = 0.35- 0.6 GBq/µmol).[72] This is because the [^{18}F]F_2 produced from the initial bombardment cannot be efficiently purged from the target without the addition of a small amount of $^{19}F_2$ carrier, followed by a secondary irradiation. The radioactive species present after the first irradiation and the mechanism by which it adheres to the interior of the target is not yet understood.[73]

1.2.5. *^{18}F Tracers: General Considerations*

Fluorine is not significantly abundant within living systems, and thus successful ^{18}F tracers tend to fall into three broad categories:

- Established synthetic drugs that already include fluorine within their pharmacores.
- Analogue compounds whereby a functionality (usually a hydride or hydroxyl moiety) is replaced with ^{18}F. ^{18}F is considered sterically similar to the hydroxyl group, with a van der Waals radius of 1.47 Å compared to 1.40 Å for –OH.[74] The significant electronegative character of ^{18}F has the potential to perturb the biological behavior of many tracers; however, in some cases this change can be advantageous.[75]
- Compounds that are ^{18}F- labelled by way of coupling to a pendant small molecule that contains the radioisotope. Because of the potential for this type of modification to alter the distribution, recognition and/or metabolism of many

small molecular weight tracers, this *prosthetic group* approach is typically only used for the labelling of biological targeting agents such as peptides, proteins and oligonucleotides.

Carbon-fluorine bond formation for the production of ^{18}F tracers and intermediary agents is generally achieved by either electrophilic or nucleophilic substitution. A description of these approaches as they relate to ^{18}F chemistry is given below.

1.2.6. *Electrophilic labelling with $[^{18}F]F_2$*

Electrophilic substitution with elemental $[^{18}F]F_2$ results in tracers of low specific activity is thus limited to the preparation of relatively non-toxic compounds that do not significantly perturb normal biological function in micromolar quantities. Furthermore, $[^{18}F]$fluorination yields cannot intrinsically exceed 50 %, because the reacting species contains only one radioactive atom per fluorine molecule. (By convention, radioactive elemental fluorine is usually written as '$[^{18}F]F_2$'; however, the true chemical species is $[^{18}F]$F-F.) From a practical perspective, $[^{18}F]F_2$ production requires specialized equipment owing to its gaseous form and reactive nature. This reactivity can often result in unselective ^{18}F incorporation. Despite these drawbacks, electrophilic fluorination from $[^{18}F]F_2$ gas has remained a vital PET protocol, because until only recently (*vide infra*) no other means was available to ^{18}F label highly electron- rich functionalities. In an effort to reduce the reactivity of $[^{18}F]F_2$, it is sometimes converted into an intermediary fluorination agent prior to ^{18}F labelling. Common synthons include acetylhypo$[^{18}F]$fluorite[76] or xenon di$[^{18}F]$fluoride.[77] Significant regioselectivity can be conferred to many electrophilic aromatic $[^{18}F]$fluorinations by the use of demetallation reactions, with trimethyltin or mercury acetate as the leaving group.[78]

Electrophilic aliphatic $[^{18}F]$fluorinations of carbanions and alkenes are rare. The most significant ^{18}F tracer prepared in this manner is perfluorinated hypoxia sensitizer $[^{18}F]$-2-(2-nitro-1[H]-imidazol-1-yl)-*N*-(2,2,3,3,3-pentafuoropropyl)acetamide ($[^{18}F]$EF5).[79] With regard to electrophilic aromatic $[^{18}F]$fluorinations, the preparation of ^{18}F labelled amino acids is an important area of study. Some phenylalanine- and tyrosine- derived molecules serve as neurotransmitters, and as such, ^{18}F analogues of these compounds can be used to image nervous system function in the heart[80] and brain.[81] Also, in their capacity as metabolic precursors, some ^{18}F- labelled amino acids are preferentially

taken up by neuroendocrine tumours,[82] which typically have higher rates of amino acid transport. In both oncology and neurology, 6-[^{18}F]fluoro-dihydroxyphenylalanine ([^{18}F]FDOPA; Figure 1.3) has served as a valuable ^{18}F tracer. Dihydroxyphenylalanine (DOPA) is the biosynthetic precursor of the neurotransmitter dopamine, and the dysfunctional production, release and storage of dopamine in the brain is responsible for a host of Parkinsonian disorders.[83] [^{18}F]FDOPA is decarboxylated (to [^{18}F]flurodopamine) *in vivo* in a manner identical to its authentic compound, and thus [^{18}F]FDOPA can be used to assess the extent of dopamine synthesis and metabolism in presynaptic nerve terminals.[84] The radiosynthesis of [^{18}F]FDOPA is complicated by the free carboxylic acid, catechol and amino moieties that must be protected prior [^{18}F]fluorination. The synthesis of [^{18}F]FDOPA by of regioselective fluorodestannylation is summarized in Figure 1.3.[85] Decay- corrected radiochemical yield (DC-RCY) by this route was an impressive 25 % from end-of-bombardment (EOB).

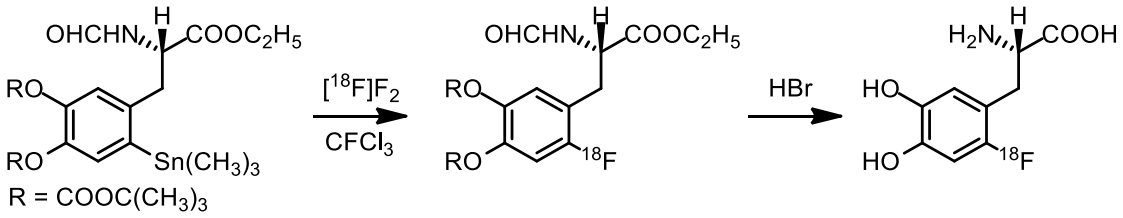

Figure 1.3. A popular route to [^{18}F]FDOPA.

Some investigators have sought to circumvent the problem of low [^{18}F]F_2 specific activity by deriving electrophilic reagents from fluoride ion. Researchers at The Turku PET Centre have devised a means to form [^{18}F]F_2 from [^{18}F]F^-.[86] The process involves the initial production of CH_3[^{18}F]F, which is then admixed with carrier F_2. Upon electrical discharge excitation, isotopic exchange occurs, resulting in material with specific activities as high as 55 GBq/µmol. The process is complex, but the Turku group has used this method for many years to reliably prepare a number of neurological PET tracers for clinical use, including 4-dihydroxyboryl-2-[^{18}F]fluorophenylalanine ([^{18}F]FBPA)[87] and [^{18}F]FDOPA.[88] Another potentially groundbreaking approach utilizes a unique Pd(IV)-fluoride complex, prepared from NCA [^{18}F]F^-, to initiate the oxidative transfer [Pd(II)→Pd(IV)] of ^{18}F to Pd(II)-aryl precursors (Figure 1.4).[89] Subsequent reductive decomposition of the reactive intermediate creates a new aryl-^{18}F bond. Using this new electrophilic fluorination reagent, a small number of established ^{18}F PET tracers

bearing electron- rich rings have been synthesized in moderate decay- corrected (DC) yields (10- 33 %).

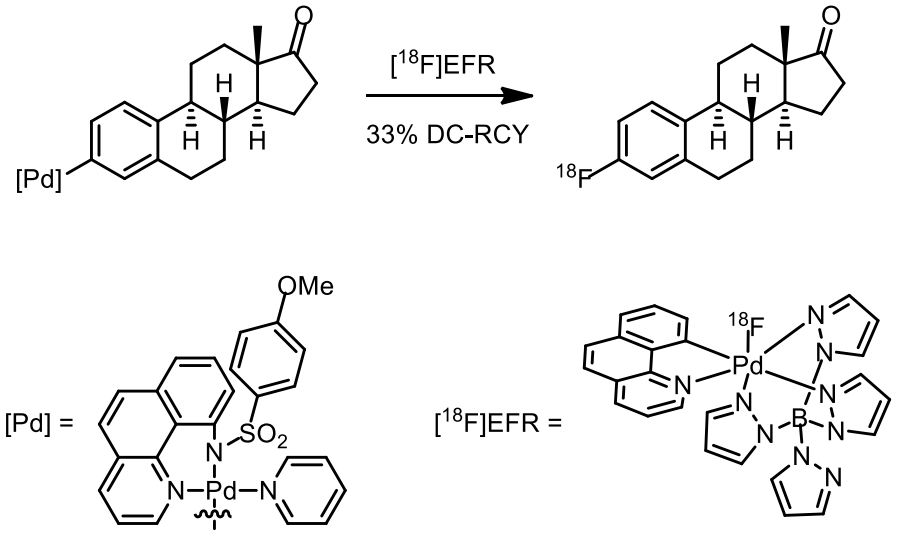

Figure 1.4. [^{18}F]Fluorination of electron-rich Pd(II)-aryl precursors.

EFR = electrophilic fluorination reagent.

1.2.7. *Nucleophilic labelling with [^{18}F]F$^-$*

In accordance with the tracer principle, [^{18}F]F$^-$ possesses the same nucleophilic properties as its stable isomer. Thus, the full complement of chemical transformations known for ^{19}F$^-$ should, in principle, be available for [^{18}F]F$^-$ incorporations. In practice however, there are additional factors that must be considered when working with NCA [^{18}F]F$^-$. First, it is critical that the chemical pathway employed does not allow for the isotopic exchange of [^{18}F]F$^-$ with another fluoride source. The second issue pertains to the very low molar concentration of [^{18}F]F$^-$ relative to reacting precursor in a typical NCA reaction mixture. Indeed, it is this large excess of precursor that greatly enhances the practical viability of the [^{18}F]fluorination reaction through the establishment of pseudo-first order kinetics (where RCY increases exponentially with respect to time).[70] However, under these conditions, reactions that rely on a reactive intermediate for completion can be retarded, as the probability that a free [^{18}F]F$^-$ ion will interact with the intermediate within its lifetime is small. A good example of both these phenomena at work can be found in the application of the Balz-Schiemann reaction to ^{18}F chemistry (Figure 1.5). This reaction has been occasionally used for the preparation of ^{18}F amino

acids, but yields are always low.[90] In this two-step reaction, a reactive diazonium tetrafluoroborate is generated by treatment of an aniline with tetrafluoroboronic acid, which is supplanted by fluoride ion upon heating. However, BF_4^- is a labile anion that has been shown to redistribute ^{18}F for ^{19}F,[91] to the determent of specific activity and radiochemical yields. Furthermore, the salt has the tendency to react with water and other trace nucleophiles, which in the NCA case can be found in higher concentrations than $[^{18}F]F^-$.[44]

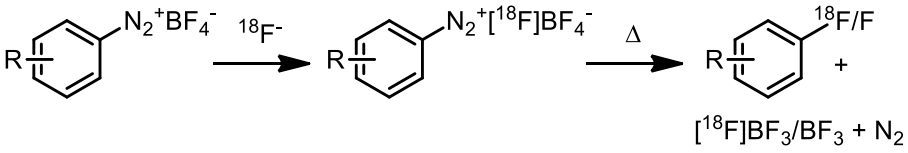

Figure 1.5. The Balz-Schiemann reaction in ^{18}F chemistry.

The preparation of nucleophilic $[^{18}F]F^-$ from irradiated ^{18}O-enriched target water constitutes a critical phase in any ^{18}F labelling procedure. Over the last three decades, a semi-standardized protocol has emerged (Figure 1.6). After remote transfer of the aqueous $[^{18}F]F^-$ solution (1-2 mL) to an appropriate radiosynthetic workspace, the $[^{18}F]F^-$ is efficiently trapped on a strong anion exchange resin. This serves to concentrate the radioactivity and also remove long-lived metallic radio-impurities that are ubiquitously formed upon proton bombardment of the $[^{18}O]H_2O$ target.[92] Unfortunately, the concentration of $[^{18}F]F^-$ in this fashion requires a basic anion to elute the radioactivity; K_2CO_3 is the most regularly used exchange salt. In aqueous solutions, the highly electronegative $[^{18}F]F^-$ is poorly nucleophilic, owing to its high degree of hydration (ΔH_{hyd} = -506 kJ/mol).[93] Thus, the scrupulous removal of the water must be carried out by way of repeated azeotropic distillation from acetonitrile. The boiling point of the H_2O/CH_3CN azeotrope is 76.1 ºC, but this 'drydown' step is usually carried out at 100- 120 ºC while the reaction vessel is flushed with inert gas to ensure removal of water. However, it has been shown that $[^{18}F]$fluorination yields can be retarded by excessive or prolonged heating during drydown,[94] presumably because $[^{18}F]F^-$ adsorbs strongly to the sides of the reaction vessel and makes it unavailable for reaction. As such, azeotropic drydowns introduce significant degree of variability to many radiosynthetic protocols, as the final water content in the reaction mixture can be difficult to regulate. Furthermore, the

overall drydown process can take some time (~20 min), which ultimately affects the overall efficiency and specific activity of the ^{18}F- labelled PET tracer.

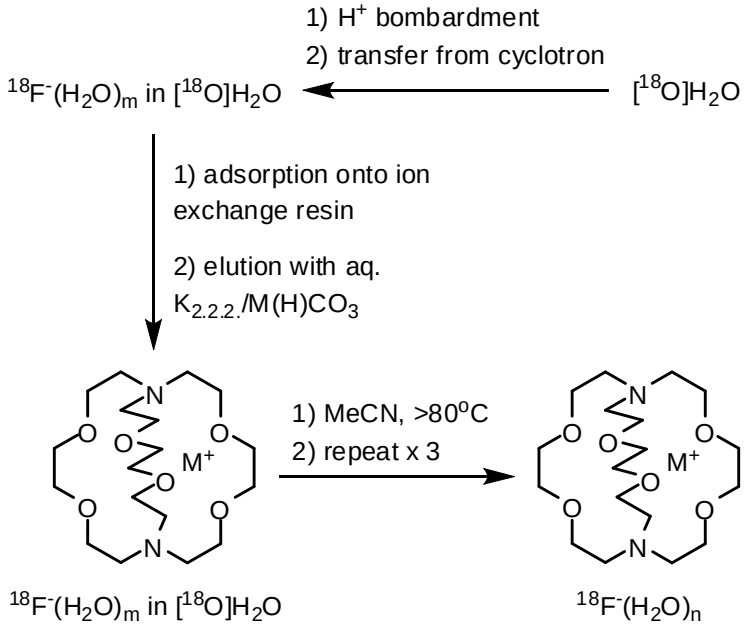

Figure 1.6. The standardized procedure for preparing reactive [^{18}F]F$^-$.

Where *n* is expected to be less than *m*. In this figure, Kryptofix® 2.2.2. phase transfer catalyst is shown.

Most successful nucleophilic [^{18}F]fluorinations also rely on the presence of a phase transfer catalyst to enhance the solubility and nucleophilicity of the alkali metal [^{18}F]fluoride in organic solvent.[44] Tetralkylammonium (hydrogen) carbonates[95] or crown ethers[96] can be used, but in terms of anion activation, aminopolyether Kryptofix® 2.2.2. ($K_{2.2.2.}$) is usually considered the optimal choice (Figure 1.6). This cryptand is added to the [^{18}F]F$^-$ solution before concentration and the resulting $K_{2.2.2.}$/M[^{18}F]F complex enhances the solubility and nucleophilicity of alkali metal [^{18}F]fluorides in organic solvents.[44] However, this activating agent is also highly basic and thus often incompatible with unprotected hydroxy and amino functional groups. Furthermore, $K_{2.2.2.}$ is toxic [LD_{50}(rat) = 35±2 mg/kg (i.v.)][97] and must be carefully removed prior to *in vivo* use of the radiotracer.

With potential problems inherent with S_N1 fluoride substitutions, it is not surprising that S_N2- type reactions dominate [^{18}F]F$^-$ chemistry. Nucleophilic aliphatic [^{18}F]fluorinations are extremely common and can be carried out using the usual cadre of

leaving groups (*i.e.* tosylate, mesylate, nosylate, bromide). As in the non-radioactive case,[98] [^{18}F]fluorination is easier at primary and/or inductively activated α-carbons. Although uncommon, a few strained heterocyclic ring opening reactions have been employed; for instance, [^{18}F]F$^-$ can be selectively incorporated onto the terminal carbon of the epoxide[99, 100] or aziridine.[101] Polar aprotic solvents are the typical solvents of choice for S_N2 [^{18}F]fluorination reactions, with DMSO and acetonitrile being the most commonly used. Recently however, in contrast with popular wisdom, hindered protic solvents were identified as excellent media for S_N2 [^{18}F]fluorination reactions. As proof-of-principle, a number of clinical ^{18}F radiopharmaceuticals were prepared using *t*-BuOH as solvent, in yields much higher than those reported by their standard methods.[102] The improved synthesis of tumour proliferation tracer 3'-deoxy-3'-[^{18}F]fluorothymidine ([^{18}F]FLT) is shown here as example (Figure 1.7). It was surmised that branched protic solvents enhance anhydrous [^{18}F]F$^-$ substitution chemistry by reducing the charge association between the alkali metal and [^{18}F]F$^-$ by hydrogen bonding to the salt, in addition to improving the solvation of the free fluoride ion.[103] It was further hypothesized that the enhanced rate of nucleophilic aliphatic [^{18}F]fluorinations using mesylate precursor relative to bromo and iodo leaving groups may be the result of additional hydrogen bonding of *t*-BuOH solvent to the sulfonyl moiety. As we shall see in Chapter 5, these phenomena may have an important role to play in the S_N1- type syntheses of sulfonyl [^{18}F]fluorides from sulfonyl chlorides.

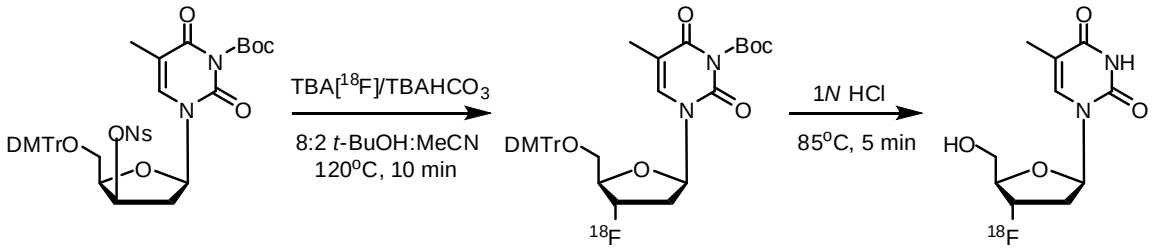

Figure 1.7. Improved synthesis of [^{18}F]FLT in protic solvents.

TBA = *t*-butylammonium. DC-RCY= 65 %. Precursor mass= 20 mg. Conventional synthesis (40 mg precursor, MeCN, 150ºC) affords [^{18}F]FLT in 15 % DC-RCY.[104]

Equally important in the area of [^{18}F]F$^-$ chemistry are nucleophilic aromatic substitution reactions. As observed under non-radioactive conditions, good [^{18}F]fluoride incorporation into benzene rings only occurs when an electron- deficient arene is utilized. Thus, many precursors are activated with electronegative functionalities (*eg.* -

NO_2, -CHO, -CN) *ortho*- and *para*- to the leaving group. Nevertheless, most reactions require significant heating (90- 150ºC) under the classical conditions to obtain acceptable yields. As with aliphatic [^{18}F]fluorinations, the use of anhydrous polar aprotic solvents are the norm. Substitutions can be realized by way of the halex process, or fluorodenitrations, but trimethylammonium trifluoromethane sulphonate [-$N(Me)_3OTf$, TMA] is considered the best leaving group and is used whenever possible.[74] Apart from its strong electron-withdrawing character, one perceived advantage of using a -$N(Me)_3OTf$ leaving group relates to its catonic nature. The difference in lipophilicity between precursor salt and ^{18}F product sometimes allows for simple (*i.e.* non-HPLC) separation of the two materials.[105] In some cases, however, competitive fluorodemethylation of the trimethylammonium group can lead to a mitigation of [^{18}F]fluoroarene radiochemical yields and the production of small but significant quantities of dimethylamino- substituted impurity.[106] Less activating *para*- substituents with low Hammett constants (α) are known to exacerbate this effect.[107]

The need for electron-deficient aromatic [^{18}F]fluorination precursors represents a significant limitation to the field of ^{18}F PET, particularly in regard to small molecule design. Thus, new chemistries for the incorporation of [^{18}F]F^- into unactivated systems are continuously and vigorously being investigated. One of the most promising approaches involves the reaction of diaryliodonium salts with fluoride ion. These potential PET precursors can be readily prepared from arylboronic acids.[108] The reaction was first reported in 1953,[109] but was not applied to ^{18}F radiochemistry until much later.[110] A curious and synthetically valuable feature of this reaction is the fact that *ortho*-substitution on one of the rings directs the nucleophile to that ring.[111] Selectivity can also be generated by utilizing an electron- rich aromatic moiety to act as a leaving group, such as *p*-methoxyphenyl[112] or 2-thienyl[113] (Figure 1.8). In this case, [^{18}F]F^- will be added to the other ring system.[114] This technique has proved particularly useful for the synthesis of *meta*-substituted [^{18}F]fluoroarenes.[115]

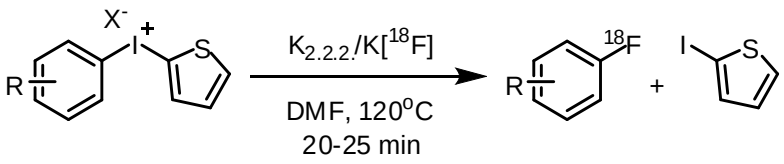

Figure 1.8. Nucleophillic fluorination of electron-poor arenes from aryl(2-thienyl)iodonium salts.[113]

R = H, 4-Me, 2-OMe, 3-OMe, 4-OMe, 4-OBn, 4-I, 4-Br, 4-Cl. X – Br, I, OTs, OTf. Radiochemical yields by TLC were 29- 70 %.

A final comment should be made regarding the relative stability of fluoroorganic molecules *in vivo.* Some aliphatic F- bearing compounds are susceptible to metabolic defluorination. The most common mode of degradation involves enzymatic hydroxylation at the carbon centre adjacent to the C-F bond, followed by subsequent elimination of hydrofluoric acid to yield a ketone.[75] Cytochrome P450 subtype 2E1 is generally thought to be the primary catalytic agent.[116] Fluorobenzenes tend to show increased resistance towards metabolism, but oxidative defluorinations through epoxidation/rearrangement and benzoquinone formation/reduction have been observed as well.[117]

1.2.8. *2-[^{18}F]fluoro-2-deoxy-D-glucose*

2-[^{18}F]fluoro-2-deoxy-D-glucose ([^{18}F]FDG; Figure 1.9) is an analogue of 2-deoxy-D-glucose, with a ^{18}F in place of a hydroxyl group at the C-2 position. Metabolically, [^{18}F]FDG is treated in a manner similar to the natural sugar, in the sense that is transported into cellular compartments and phosphorylated by hexokinase (HK). However, the next enzyme in the metabolic cascade, phosphohexose isomerase, does not recognize 2-[^{18}F]fluoro-2-deoxy-D-glucose-6-phosphate.[118] Thus, the HK reaction is essentially isolated, and radioactivity accumulates in the cell at a rate proportional to glucose need.[119] As many tumours exhibit elevated metabolic rates due to their increased levels of proliferation, [^{18}F]FDG has become an important tool for diagnosis and assessment of cancer. Its general mechanism of action allows the visualization of a variety of tumour types. One can scarcely overestimate the impact that this single radiopharmaceutical has had on the development of nuclear imaging. The success of [^{18}F]FDG has justified the establishment of expensive PET infrastructures (*i.e.* cyclotrons, scanners, radiochemical facilities) worldwide. Today, it is estimated that 9 of

10 clinical PET scans employ [^{18}F]FDG,[119] although this percentage is decreasing as the pace of new tracer research increases.[120] However, despite its importance, [^{18}F]FDG is not a universal cancer imaging agent. In areas of the body where glucose uptake is normally high (such as the brain), tumours can be masked. Furthermore, some tumours do not show significant [^{18}F]FDG uptake, such as bone metastases from prostate cancer.[121] Genetic polymorphisms can also have an impact on overall uptake; for instance, a single A-for-T polymorphism on the glucose transporter type 1 (*GLUT1*) gene was correlated with statistically lower maximum standardized uptake values (SUV_{max}) in patients with non-small cell lung cancer.[122]

[^{18}F]FDG was first designed for the imaging of metabolic rate in the brain. The original radiochemical synthesis involved direct [^{18}F]F_2 fluorination of 3,4,6-tri-O-acetyl-D-glucal.[123] Improved syntheses utilizing acetylhypo[^{18}F]fluorite[124] and xenon di[^{18}F]fluoride[125] were later described. However, in addition to the usual disadvantages related to the use of [^{18}F]F_2, these electrophilic reactions produced varying degrees of 2-[^{18}F]fluoro-2-deoxy-D-mannose, a diasterotopic impurity that was shown to lead to an underestimation of glucose metabolic rate.[126] A major breakthrough came in 1986, when Hamacher *et al.* reported the first high-yielding nucleophilic synthesis of [^{18}F]FDG (Figure 1.9).[127] The key innovation in this approach was the enhancement of [^{18}F]fluoride reactivity using Kryptofix® 2.2.2..

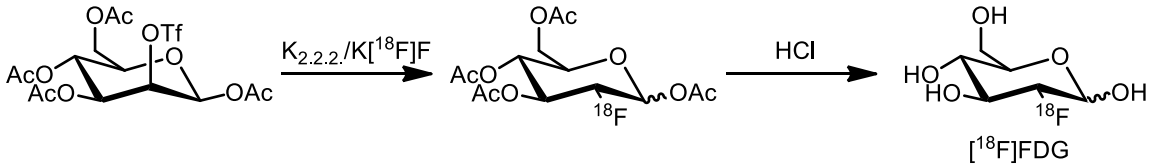

Figure 1.9. A popular route to [^{18}F]FDG.
As developed by Hamacher et al.[127]

1.2.9. *2-[^{18}F]Fluoropyridines*

Although a vast majority of reported nucleophilic aromatic fluorinations utilize a benzene ring, these reactions have been successfully extended to the pyridine series. The S_NAr substitution of 2-chloro- and 2-bromopyridine with CsF in dimethylsulfone at high temperature was first reported in 1963 (<50 % yield).[128] A slightly higher yield (60 %) was achieved from 2-nitropyridine in HMPT (160 ºC, 24 h).[129] The preparation of 3-

and 4- fluoropyridine in this fashion lacks precedent. The synthesis of a handful 2-fluoropyridines bearing additional electron withdrawing functionalities have also been described, in every case by way of fluorodechlorination.[130] In general however, these types of *hetero*aromatic substitutions are uncommon because many fluoropyridines can be accessed by way of the Balz-Scheiman reaction.[131]

The first radioactive [^{18}F]fluoropyridine compounds reported were 2- and 6-[^{18}F]fluoronicotinonic acid diethylamide[132] and 2- and 6-[^{18}F]fluoronicotine,[133] which were generated by reaction of their requisite chlorinated precursors with unactivated Cs[^{18}F]F (>200 ºC, <50 % DC-RCY). An initial investigation of the scope of the reaction determined that acceptable yields of 2-[^{18}F]fluoropyridine could be achieved by conventional heating of 2-nitro (82 %) and 2-trimethyl ammonium triflate (91 %) precursors ($K_{2.2.2.}$/K[^{18}F]F, 120 ºC, 10 min, DMSO).[134] As expected, radiochemical yields increased with time and temperature, and the order of leaving group reactivity was NMe_3^+> NO_2> Br> Cl>>>I. A later methodological experiment using nitropyridine precursors confirmed that [^{18}F]fluorination was easiest at the *ortho*- position, followed by the *para*-position, while the *meta* position of this compound was unreactive.[135] To date, the introduction of [^{18}F]F^- at this position has been limited to those radiopharmaceuticals with additional electron- withdrawing groups.[136] However, it was recently shown that 3-[^{18}F]fluoropyridines can be prepared by way of diaryliodoium salt,[137] which should initiate the development of more 3-[^{18}F]fluoropyridinyl- based tracers.

Heteroaromatic [^{18}F]fluorination chemistry for PET was developed extensively by the group at Service Hospitalier Frédéric Joliot in Orsay, in their efforts to image the nicotinic acetylcholine receptor. To this end, they have prepared and tested 2-[^{18}F]fluoropyridine analogues of a number of bioactive natural products targeting the $\alpha_4\beta_2$ subtype, including cytisine ([^{18}F]FPyCYT)[138] and epibatidine ([^{18}F]FEP) and related compounds (Figure 1.10).[139] Another important $\alpha_4\beta_2$ ligand developed at Orsay is drug derivative 2-[^{18}F]F-A-85380.[140] Finally, the laboratory introduced [^{18}F]F-WAY-100635 for the imaging of serotoninergic 5-HT_{1A} receptors.[141] In all these cases, a benzene ring in the native structure has been replaced by a pyridinyl moiety for ease of [^{18}F]fluorination. This same design strategy has been also used to prepare tumour imaging agents (Figure 1.10). 2-Amino-6-(2-[^{18}F]fluoropyridine-4-ylmethoxy)-9-(ocyl-β-D-

glucosyl)-purine[142] and [^{18}F]MEL050[143] were developed for the targeting of O^6-methyguanine-DNA methyl transferase and melanin respectively.

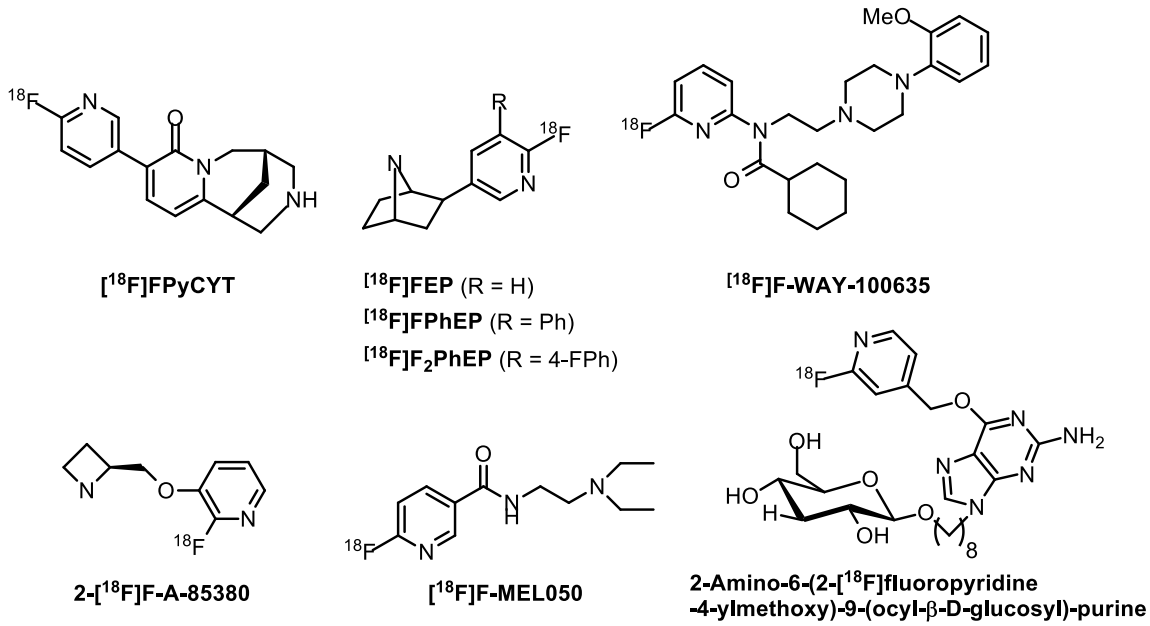

Figure 1.10. Some small molecule PET tracers bearing the 2-[^{18}F]fluoropyridnyl moiety.

1.3. Biological Radiopharmaceuticals for Nuclear Imaging

1.3.1. *General Considerations*

Biological radiopharmaceuticals offer an opportunity to elucidate molecular events associated with disease etiology and progression with an unparalleled degree of specificity. Concentrations of cellular receptors, enzymes, and structural proteins- along with their genetic progenitors- can vary significantly based on disease phenotype and thus are attractive targets for biomolecular targeting agents. Specific information regarding functional (or dysfunctional) physiochemical events not only aids diagnosis of the disease at its earliest stages, but in some cases may allow for a personalized response to treatment.[144] However, successful molecular imaging with peptidic-, antibody-, and nucleic acid- based molecular probes requires consideration of aspects both within and beyond the general field. High specific activity is an important criterion for those radiobioconjugates that target cellular receptors or RNA, as protein expression levels and genetic copy numbers represent finite limits to the functional concentration of

radioactivity. In these cases, efficient separation of the labelled and unlabelled material is critical, a complication often made more serious by the fact that differences between precursor and tracer must necessarily remain small. It is also important that the requisite labelling chemistry can be carried out at low concentrations, as the macromolecular precursors used are often costly and/or difficult to prepare. Finally, the physical characteristics of any potential medical isotope should be compatible with the biological half-life and fate of the intended targeting agent. For example, the time required to achieve adequate contrast for ^{18}F PET imaging using larger monoclonal antibody (MAb) fragments is longer than the working lifetime of this radioisotope.[145] Thus longer- lived metallic isotopes are often considered more appropriate choices for these types of applications.

Three general strategies exist for the incorporation of radioisotopes into biological molecules. The first, and by far the least utilized, is radiolabelling by natural association. Probably the most famous example of the phenomenon is the uptake of certain radiometals by the iron- binding protein transferrin. ^{67}Ga-labelled transferrin will accumulate in some soft tissue tumours, and it has been used in this capacity for many years.[146] The second and third options are basically prosthetic group approaches- that is, the attachment of the radioisotope to the biomolecule by way of a small bifunctional ligand. In this regard, the coupling of the bifunctional molecule to the targeting agent, followed by introduction of the radioisotope is called a *post-labelling* strategy.[147] Similarly, a *pre-labelling* approach involves radiolabelling the prosthetic group first, then conjugating it to the biomolecule. Typically, metal- bearing radiopharmaceuticals are post-labelled, with a metal chelator serving as the tethering functionality, while the attachment of a radiohalogen usually requires the initial preparation of a radiolabelled prosthetic group. Unfortunately, the preparation, purification and bioconjugation of any pre-labelled bifunctional molecule typically adds considerable time and complexity to the overall radiosynthetic protocol. Concerning [^{18}F]fluoride specifically, criteria associated with [^{18}F]F^- production and activation make direct labelling of many biomolecules unfeasible, namely:

- High reaction temperatures.
- Anhydrous conditions.

- Basic environments. The presence of carbonate anion and $K_{2.2.2.}$ cryptand can result in abstraction of protons from the precursor, the generation of H[^{18}F]F and the denaturing or cleavage of precursor and product.[148]

1.3.2. *Receptor Imaging with Peptides*

A number of peptidergic signaling molecules have been discovered that are used by the body to regulate physiologic function. *Neuropeptides*, so called because they allow communication between neurons, constitute a large and diverse class of these biomolecules. In addition to the central nervous system, many neuropeptides are found throughout the greater neuroendocrine system, including the gut, the pituitary gland and the pancreas.[149] Downstream signaling is activated by way of efficient binding of the peptide hormone to one or more membrane- associated G- protein coupled receptors. This is commonly followed by peptide internalization and lysosomal degradation, and possibly the loss of receptor signaling function or complete removal of the receptor from the cell surface.[150] The upregulation of certain neuropeptide receptors is a pathophysiological hallmark of many cancers. As such, radiolabelled peptides can be used to non-invasively delineate lesion size and shape, as well garner valuable diagnostic information related to tumour angiogenesis and growth factor biology.[151] A selected list of neuropeptides that have been labelled with ^{18}F can be found in Table 1.3.

Table 1.3. Neuropeptides for cancer imaging

Peptide	Receptor(s)	Sequence	Native Bioaction
Somatostatin-14	SSTr	AGCKNFFWKTFTSC	Growth hormone inhibiton
Octreotide	Primarily SSTr	DFCFDWKTCT(OL)	----
c(RGD)	$\alpha_v\beta_3$ integrin	RGDfX where X = V, Y or K	Angiogenesis
GRP	GRPr	VPLPAGGGTVLTKMYPRGNHWAVG HLM(NH_2)	Gut hormone release
BBN	GRP2r	pEQRLGNQWAVGHLM(NH_2)	----
CCK-8	CCK-Br	DY(SO_2H)MGWMDF	Vasodilation & many others
VIP	VIPr	HSDAVFTDNYTRLRKQMAVKKYLNSI LN(NH_2)	Gallbladder contraction, pancreatic secretion
α-MSH	α-MSHr	Ac-SYSMEHFRWGKPV(NH_2)	Melanogenesis*

Peptide	Receptor(s)	Sequence	Native Bioaction
NT	NTr	pELYENKPRRPYIL	Hypotensin, analgesia & many others
NPY	NPYr	pYPSKPDNPGEDAPAEDLARYYSALR HYINLITRQRY(NH_2)	Food intake, anxiety inhibition
BVD15	Primarily NPY1r	INPIYRQRY(NH_2)	----

Note: SST = somatostatin. GRP = gastrin releasing peptide. CCK-B = cholesytokinin B. VIP = vasoactive intestinal peptide. α-MSH = α-melanocyte-stimulating hormone. NT = neurotensin. NPY = neuropeptide Y. BBN = bombesin. CCK-8 = cholesytokinin(26-33). * α-MSHr is not expressed in normal tissues.

Peptides exhibit a number of characteristics that make them attractive targeting agents for molecular imaging. First, their relatively small size permits rapid diffusion into target tissues, as well as rapid clearance from the blood and non-target tissues.[149] Thus, high tumour-to-background ratios are possible in a short period of time. Furthermore, most regulatory peptides show low toxicity and low immunogenicity compared to antibody tracers.[152] Many bioactive peptides or peptide fragments are small enough to permit their separation from unlabelled precursor by way of HPLC, thus permiting the production of high apparent specific activity material. A specific activity of >37 GBq/μmol (1 Ci/μmol) are often cited as the minimum required to avoid peptidergic receptor saturation effects in mice;[153, 154] however, a comprehensive validation of this dogma in multiple systems does not yet exist. At the same time however, peptides are usually large enough to tolerate bulky pendant modifications and still retain their affinity for receptor targets. Unlike radiolabelled proteins, these modifications can usually be added in a discreet fashion, such that the final radiopharmaceutical formulation is composed of a single chemical species. In short, peptides can be thought of as being "as large as necessary, and as small as possible."[155]

Disadvantages associated with peptide imaging agents include their sensitivity towards labelling conditions (*vide supra*) and biodegrading enzymes, as well as their sometimes limited bioavailability. In many cases, stability towards peptidase activity can be significantly enhanced by way of cyclization; the introduction of unnatural amino acids (in particular, D- amino acids); peptidomimetic bridges; and/or modification of the C- and N- termini.[156] However, the electrostatic changes brought on by peptide modification can sometimes result in undesirable alterations to a targeting vector's pharmacokinetic

profile. In general, hydrophilic peptides clear from the blood *via* the kidneys, while lipophilic peptides clear through the hepatobiliary tract.[152] This latter clearance profile can obfuscate tumours of the abdomen and thus renal excretion is usually preferred for the imaging of many types of cancers. The introduction of radiohalogens through the use of stable aryl- or alkyl- based tethers can enhance peptide lipophilicity and thus negatively impact tracer biodistribution.[148] On the other hand, excessive kidney uptake can be an undesirable quality in cases when the radioisotope produces a high radiation dose.[155] This scenario is usually associated with radio-metallated peptides, which commonly see changes to their charge or charge distribution upon chelation.

The introduction of hydrophilic amino acids is one possible means to modulate the overall lipophilicity of radiolabelled peptides. In this regard, serine[157] and aspartic acid[158] have both been used with some success. In a related approach, simple sugar moieties have also been employed.[159] Of particular interest to our group is the use of polyethylene glycol (PEG) modifications to improve radio-peptide biodistribution patterns. In its polymeric format, PEG is non-toxic, non-immunogenic and highly water soluble. The conjugation of PEG chains to protein drugs is a well- established method of increasing drug circulation times, decreasing immunogenicity, and improving metabolic stability.[160] However, long PEG chains are not always required to positively affect the pharmacokinetic patterns of peptide radiopharmaceuticals. For example, Zhang *et al.* tethered ^{68}Ga- and ^{177}Lu-1,4,7,10-tetraazacyclododecane-1,4,7,10-tetraacetic acid (DOTA; see Figure 1.11) complexes to BBN(7-14) by means of a four-ethylene glycol spacer (PEG4) and observed high tumour uptake and rapid washout from blood and non-target tissues.[161] Concerning ^{18}F peptides specifically, Wu *et al.* showed that an ^{18}F-PEG3-*c*(RGD) dimer showed significantly improved tumour uptake and blood clearance relative to its non-PEGylated analogue.[162]

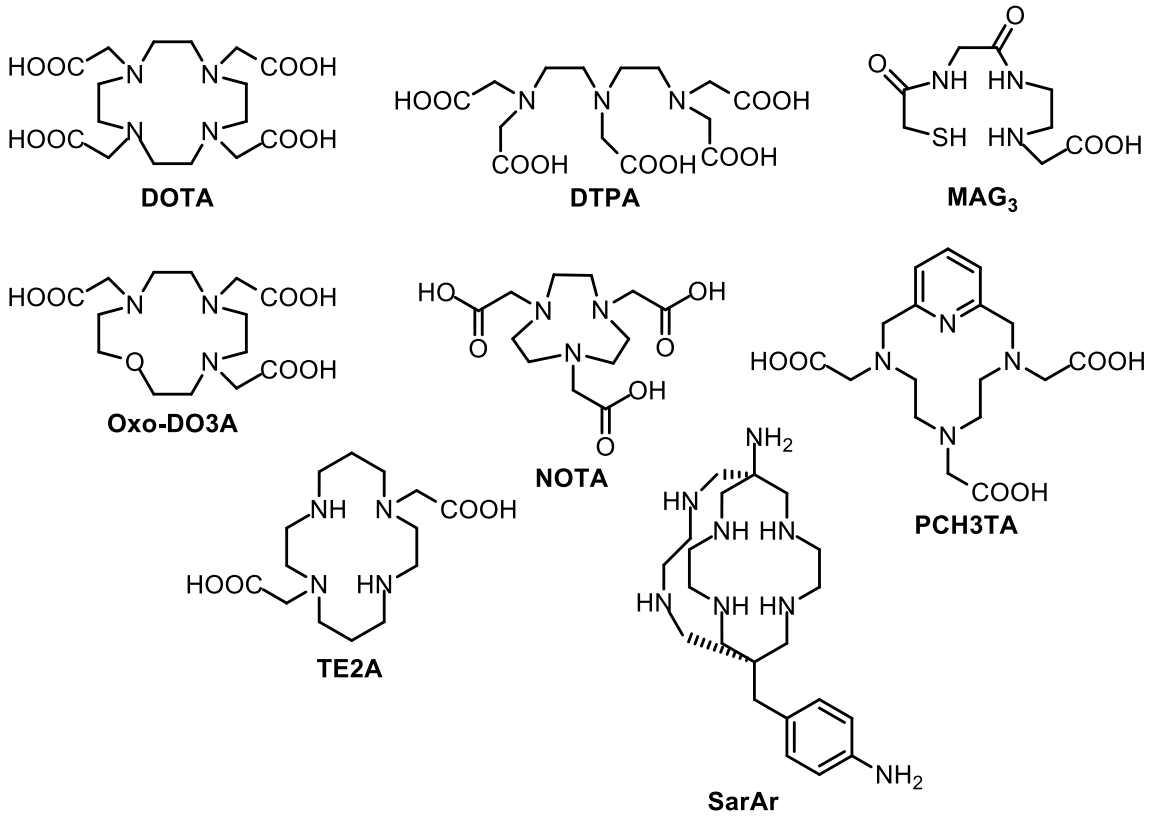

Figure 1.11. Chelators for the labelling of biomolecules with metallic radioisotopes.

1.3.3. *The Antisense Effect*

The exquisitely selective pairing of complementary nucleobase oligomers represents the most fundamental form of molecular communication in living systems. In this fashion, genetic information is converted from DNA to RNA (transcription) and then used to guide protein synthesis (translation). Complementary nucleobase recognition is also the basis for mRNA regulation and the ablation of foreign RNA. These events involve a short DNA polymer binding to the RNA of interest (*i.e.* mRNA, pre-mRNA or viral RNA) and inhibiting the translation or splicing of the encoded material. Inhibition can arise out of simple translational arrest, or may involve the activation of the ribonuclease H (RNase H) enzyme, which recognizes and destroys the DNA-mRNA duplex (Figure 1.12).[163] The encoding RNA is referred to as the 'sense' strand and thus the DNA inhibitor is the 'antisense' strand. A number of antisense therapeutics have been investigated as a means to regulate the aberrant expression of disease-associated genes. The potential to selectively treat genetic ailments in what is

essentially a prophylactic fashion- that is, before the onset of a disease state- has been the driving force for research in this field.[164] However, a litany of challenges has surrounded antisense technology since its initial conception. Some problems, such as *in vivo* stability, cellular uptake and non-specific binding have at least partially been addressed through chemical design (*vide infra*). To date, only one antisense- based drug has been approved for clinical use. Vitravene® (fomivirsen) was a phosphorothiolate oligodeoxynucleotide (PS-ODN) 21mer used to treat cytomegalovirus, an infection associated with HIV.[165] Owing to a marked decrease in these types of complications, Vitravene® is no longer produced.

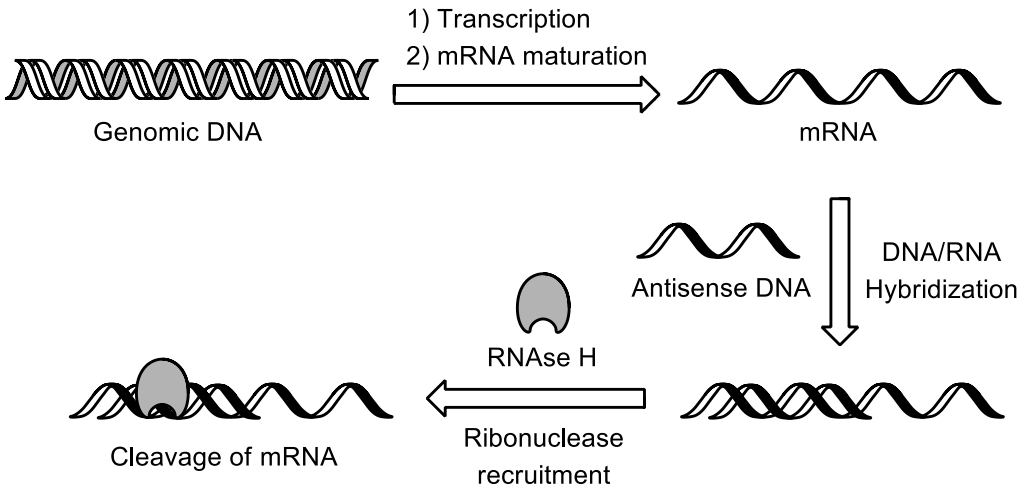

Figure 1.12. RNAse H- based mechanism of antisense inhibition.

Both the affinity and specificity of oligonucleotide therapeutics are highly dependent on oligomer length and sequence. Binding affinity is characterized by melting temperature (T_m, the point at which half the duplex has disassociated) and equilibrium disassociation constants (K_D). A single mismatch can reduce binding affinities by at least 300-fold.[166] Candidate molecules are typically created 15 to 22 bases in length, as DNA strands shorter than 11 units are considered non-specific towards mammalian cellular mRNA,[167] while longer strands (>25 bases) would be expected to exhibit retarded cellular uptake.[168]

1.3.4. *DNA Analogues*

Native DNA and RNA have exceedingly short half-lives in serum (minutes and seconds respectively), while the $t_{1/2}$ of unmodified oligodeoxyribose sequences is >90 min.[169] The primary metabolic culprits are 3'- and 5'- exonuclease enzymes, with the 3'-class predominant in the liver[170] and blood.[171] In a bid to improve *in vivo* stability, a large number of DNA analogues with modified backbones have been successfully developed (Figure 1.13). Phosphorothiolate oligodeoxynucleotides (PS-ODNs) represent the most studied of the early, '1st generation' derivatives. In this analogue, significant nuclease resistance is conferred by replacing the non-bridging oxygen on the phosphorodisester (PO) bond with a sulfur atom. Despite this change, PS-ODNs will recruit RNase H. Furthermore, PS-ODNs also possess many satisfactory drug-like qualities, including good absorption from parenteral sites, broad diffusion into various tissues and a slow but reliable metabolism.[172] However, PS-ODNs bind non-specifically to certain proteins, and this can result in cellular toxicity and immune system activation at higher doses.[173] Furthermore, PS-ODNs show a somewhat reduced affinity for mRNAs relative to their corresponding PO-ODN sequences; the observed decrease in T_m is ~0.5 ºC per nucleotide.[174]

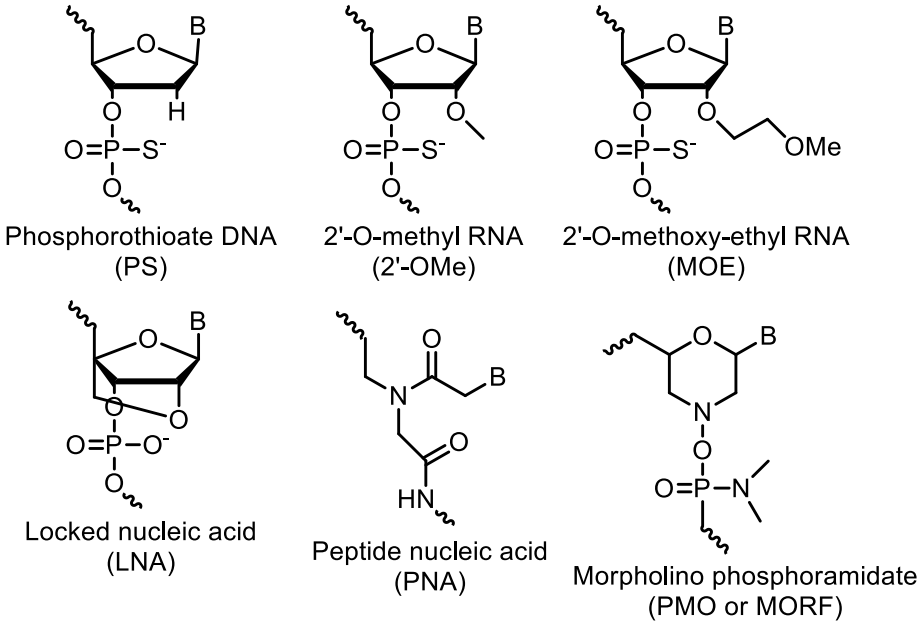

Figure 1.13. DNA/RNA analogues.

B = nucleobase.

So-called '2nd generation' antisense molecules can mainly be characterized by an alteration on the 2'- position of the furanose ring. Thus 2'-*O*-methyl- and 2'-*O*-methoxyethyl- modified RNAs have been designed that exhibit improved nuclease resistance and increased Watson-Crick pairing relative to PO-ODNs (Figure 1.13).[175, 176] This strategy was further improved upon by connecting the 2'- and 4'- position of the ribose with an methyloxy chain. The resulting conformationally rigid, 'locked' nucleic acids (LNAs) possess excellent hybridization properties (T_m increases 5-10 ºC per nucleotide).[177] These 2'- modified analogues are RNase H incompetent and thus are undesirable for therapeutic use; however, if a portion of the internal sequence is kept as PO- (or PS-) ODN (a.k.a 'gapmers'), degradative activity can be maintained.[175] In many of the '3rd generation' of DNA analogues, stability and hybridization affinity have been improved through the use of non-sugar backbones. Thus, morpholino phosphoroamidate (MORF)- based antisense agents have been derived which are completely resistant to biological degredation (Figure 1.13).[178] Unlike first and second generation antisense molecules, MORFs inhibit gene expression by way of translational arrest.[179] Their mRNA binding affinity is higher than that of PO-ODNs.[180] The synthesis of MORF precursor subunits and their subsequent assembly is considered very simple and inexpensive compared to other DNA analogues.[181] Because of their low toxicity and non- degradative properties, MORF technology has been used extensively for the study of gene function in animal embryos.[182]

Arguably the most popular '3rd generation' backbone modification involves abandonment of heterocyclics entirely in favour of a polymeric chain of *N*-(2-aminoethyl)glycine subunits.[183] Peptide nucleic acids (a.k.a polyamide nucleic acids or PNAs; Figure 1.13) hybridize with DNA, RNA or other PNAs *via* standard Watson-Crick/Hoogsteen interactions, with the amino end reflecting the 3'- end of a nucleic acid. Conformational flexibility allows for excellent hybridization affinities and non-standard binding motifs such as invasive triplexes and double duplexes, which permits the use of PNA for anti-gene and anti-pre-mRNA applications.[181] High T_m values have also been attributed to the lack of charge repulsion in PNA-nucleic acid hybids; however, this charge- neutral character is also responsible for its generally poor water solubility and cellular uptake.[184] Consequently, PNAs used in living systems must be further functionalized to improve bioavailability (*vide infra*).

1.3.5. *Antisense- Related Applications*

In the context of DNA- based molecular imaging, other processes ancillary to antisense inhibition are worth mentioning. *RNA interference* (RNAi) is an mRNA degradation pathway that involves a double stranded RNA (dsRNA) sequence of intermediate length (~100 bases).[185] The duplex is ably transfected into cells, where it is cleaved into smaller units (19-21) by an RNase III enzyme called 'Dicer'. These sequences, called siRNA (short/small interfering RNA), can recruit otherwise non-functional multi-protein complexes called RISCs (RNA-induced silencing complexes).[186] The resulting chimeric species then unwinds its siRNA component and uses the ribozyme strand to recognize and cleave complementary mRNA.

Aptamers ('adaptable oligomers') are oligonucleotides of 10-15 kDa which bind to protein targets.[187] As this form of molecular recognition is essentially non-natural, aptamers are designed by the irrational challenge of partially random DNA sequences versus a protein of interest. Tight binding sequences are amplified and the process is repeated multiple times, at which point the enriched library of high affinity ligands is cloned and sequenced. It is possible to raise natural DNA strands against synthetically prepared D-proteins, and by this process discover biologically stable enantiomeric sequences that can efficiently bind the native (L-) protein.[188] These 'mirror-image' aptamers have been dubbed 'Spiegelmers'. Aptamers rival antibodies in terms of binding affinity,[163] and like antibodies, their mode of targeting does not necessarily require cellular penetration. However, unlike antibodies, they are relatively inexpensive and easy to develop.

1.3.6. *Modes of Cellular Internalization*

While the problem of stability has been largely met, the limited cellular uptake of antisense agents *in vivo* remains a major challenge. DNA and negatively charged DNA analogues do not naturally associate with the negatively charged cell surface, and even uncharged species such as PNA do not passively diffuse into the cystosolic space at significant rates.[186] Endocytosis requires the activation of cell surface receptors through processes that are complex, non-general and poorly understood. The small fraction of oligonucleotides that are internalized must then survive compartmentalization into endosomal vesicles (pH 5-6) and trafficking into other cellular compartments.[164]

Potential antisense molecules must then escape the vesicle during trafficking through non-bilayer areas created during the 'pinching off' or fusion phases.[189] If not, lysosomal degradation is their likely fate. Despite evidence to indicate that the unassisted administration of DNA can sometimes produce meaningful results *in vivo*, there is consensus that this approach is sub-optimal.

A number of strategies designed to enhance the bioavailability of oligonucleotide therapeutics have been introduced, and most have been applied to antisense imaging (*vide infra*) in one capacity or another. Non-targeted methods of delivery include the encapsulation of the ODN in a cationic liposome, such as those used to deliver plasmid DNA, which can both improve *in vivo* translocation and lengthen circulation times. Targeted delivery agents for ODNS (and siRNAs) include both bioconjugates and ligand-targeted nanoparticles (*i.e.* functionalized cationic polymers and liposomes).[190] In regard to small molecule delivery vectors, cholesterol has been shown to enhance cellular uptake of siRNA by way of its association with low- and high- density lipoprotein.[191] Folate-ODNs[192] and folate- decorated liposomes[193] show increased *in vitro* accumulation and gene knockdown into tumour cell lines which overexpress the folate receptor (*i.e.* ovarian, breast, colorectal cancers). Among protein vectors, both transferrin and anti-transferrin receptor antibodies have been used to initiate TfR-mediated endocytosis of nucleic acid- based drugs into tumours, endothelial cells, and the brain cavity.[194] Many other antibodies, monoclonal antibodies, and antibody fragments have been explored for the purposes of antisense and siRNA delivery.[190] Finally, a very promising receptor- targeted approach to siRNA delivery involves the use of aptamer-siRNA chimeras. Such therapeutics targeting PMSA receptor and prostate cancer survival genes *Plk1* and *Bcl2* have been shown to elicit substantial gene knockdown *in vitro*[195] and have shown antitumour activity when administered systemically.[196]

Cell penetrating peptides (CPPs) represent a popular means to translocate antisense pharmaceuticals and in the context of antisense imaging this class of vectors is very important. CPPs do not possess any universal structures or qualities, although many possess cationic residues (Table 1.4). Highly cationic peptides are thought to interact with acidic proteoglycans on the cell surface, but whether or not this association event is required for internalization remains a contentious issue.[197] Today, it is

generally accepted that CPPs (whatever their electrostatic character) use endocytoic pathways to enter cells.[198] However, a general mechanism of CPP translocation has not emerged.[189] Previously, peptide-oligonucleotide conjugates (POCs) labelled with fluorescent molecules have been used to estimate CPP ability and postulate mechanisms of internalization. However, fluorescent tags often alter the *in vitro* distribution of POCs and can limit their bioactivity. *Furthermore, in many cases the degree of cellular penetration as determined by fluorescence microscopy does not correlate with extent of gene knockdown.*[199] However, recent efforts to identify superior CPPs for antisense applications have been greatly assisted by the development of *functional* splice correction assays. For example, HeLa cells can be stably transfected with a luciferase- coding sequence which has been interrupted by an intron from β-globin pre-mRNA.[200] The intron contains both cryptic and aberrant splicing regions such that normal processing of the mRNA results in the production of non-fluorescing luciferase. However, upon blocking of the aberrant site with an antisense ODN, the cryptic site is activated and functioning luciferase is translated and detected. This system was used compare seven different peptide-PNA chimeras in the presence or absence of reagents which inhibit specific routes of internilization.[201] For each peptide, the hypothesized mode of uptake could be predicted on the basis of peptide character (*i.e.* cationic vs. amphipathic). However, little correlation was observed between either splice correction and uptake or splice correction and peptide character. The relative degree of splice correction was found to be M918>TP-10>TP>Pen>>Tat_{48-60}>MAP>pVEC (Table 1.4).

Table 1.4. Cell penetrating peptides to assist the general cellular uptake of antisense molecules.

Abbreviation	Peptide Name	Sequence
M918	M918	MVTVLFRRLRIRRASGPPRVRV-NH_2
Pen	Penetratin	RQIKIWFQNRRMKWKK-NH_2
Tat_{48-60}	Trans-acting activator of transcription protein	GRKKRRQRRRPPQ-NH_2
TP-10	Transportan 10	AGYLLGKINLKALAALAKKIL-NH_2
TP	Transportan	GWTLNSAGYLLGKINLKALAALAKKIL-NH_2
pVEC	vascular endothelium cadherin peptide	LLIILRRRIRKQAHAHSK-NH_2
MAP	model amphipathic peptide	KLALKLALKALKAALKLA-NH_2
JB3	JB3	D(CSKC)-NH_2

CPPs can be covalently conjugated to antisense molecules through a number of different methods. Many strategies make use of nucleophilic cysteine residues which can be easily added to the terminus of the CPP. In this fashion, iodoacetamide-modified ODNs were reacted with free thiol- bearing nuclear signal peptides to form thioether linkages.[202] Similarly, thiol-maleimide coupling chemistry has been used to prepare hybridization probes.[203] Citing a need for chemospecificity in these types of reactions, the Dumy group has been a strong advocate for the use of oxime- based tethering in the formation of POCs.[204-206] They have shown that either biomolecule can accommodate the oxyamino moiety,[204] and that the oligonucleotides can be sequentially modified at both ends with a targeting peptide and a reporter probe without significant losses in hybridization affinity.[206] The underlying goal in all the above strategies is the creation of robust chimeras; however, some researchers have argued that the optimal POC is one where the antisense molecule is guided through the cellular membrane, then *released* to act alone. To this end, many recent antisense-carrier bioconjugates (POCs included) have been designed with disulfide linkages. It is assumed that this tether is essentially bio-reversible in the low pH (5-6), thiol- rich environment of the endosomal compartment.[207] As an alternative to covalent coupling strategies, some highly positively charged CPPs can be non-covalently complexed with anionic ODNs to form a cell- permeating nanoparticle.[198] Today, therapeutics of this nature are considered cheaper and more potent than POCs, and thus will likely supplant POCs development as the standard means to deliver siRNAs and plasmid DNA going forward. In the context of molecular imaging however, which has found much success with uncharged PNAs and morpholinos (*vide infra*), covalently-linked bioconjugates should remain popular. CPPs have traditionally been chosen based on their ability to generally distribute cargo into cells, but some recent efforts have focused on the development of peptide carriers that actively target specific transmembrane receptors. For example, Alam *et al.* conjugated 2'-*O*-Me PS-ODN to two *c*(RGD) peptides and showed that this bioconjugate could initiate splice correction in a $\alpha_v\beta_3$- expressing melanoma cell line which had been transfected with an improperly coded luciferase gene.[208] Of further interest to this work, the same group produced a splice switching bombesin- 2'-*O*-Me PS-ODN chimera that exhibited receptor- mediated uptake into PC3 (prostate cancer) cells, along with improved antisense function.[209]

1.4. ^{18}F Radiobioconjugate Strategies

1.4.1. *^{18}F Prosthetic Compounds*

Synthons for the ^{18}F- labelling of biomolecules can be grouped into three broad categories:

- those that target primary amino functionalities, such as proteolytic *N*-termini or internal lysine residues.
- those that label free thiols (*i.e.* cysteines).
- those that target unnatural modifications.

The acylation of polypeptide ε-NH_2 groups yields stable amide linkages. A number of ^{18}F- bearing activated esters have been introduced for this purpose.[210] This bioconjugate chemistry can be carried out in water and under mild conditions, and thus activated esters have proven important for the labelling of highly sensitive protein targeting agents. However, the modification of proteins in this fashion rarely yields a single compound because of the relative abundance of ε-NH_2 groups in protein structures. The most successful ^{18}F prosthetic in this class is unquestionably *N*-succinimidyl 4-[^{18}F]fluorobenzoate ([^{18}F]SFB; Figure 1.14).[211] [^{18}F]SFB has been employed for the production of a large number of demonstrated ^{18}F polypeptide tracers, including bombesin (BBN),[212] *c*(RGD),[213] α-melanocyte stimulating hormone (α-MSH)[214] and the apoptosis- targeting protein Annexin V.[215] In regard to DNA- based molecules, [^{18}F]SFB has been used to modify terminal hexylamine linkers on guanine-rich[216] and cytosine- rich[217] PS-ODNs. In many ways, the preparation of [^{18}F]SFB highlights the synthetic challenges associated with many biocompatible ^{18}F labelling agents, namely: harsh [^{18}F]fluorination conditions, the requirement of (two) additional steps to install bifunctionality, and HPLC purification as a requirement for high apparent specific activity material.[218] Another major disadvantage associated with this prosthetic molecule is its tendency to confer significant lipophilicity to the targeting agent. Extensive efforts have been undertaken to optimize the radiosynthesis of [^{18}F]SFB; the highest reported preparative yield is 44±5 % DC (n=10) over 60 min using automated assistance.[219]

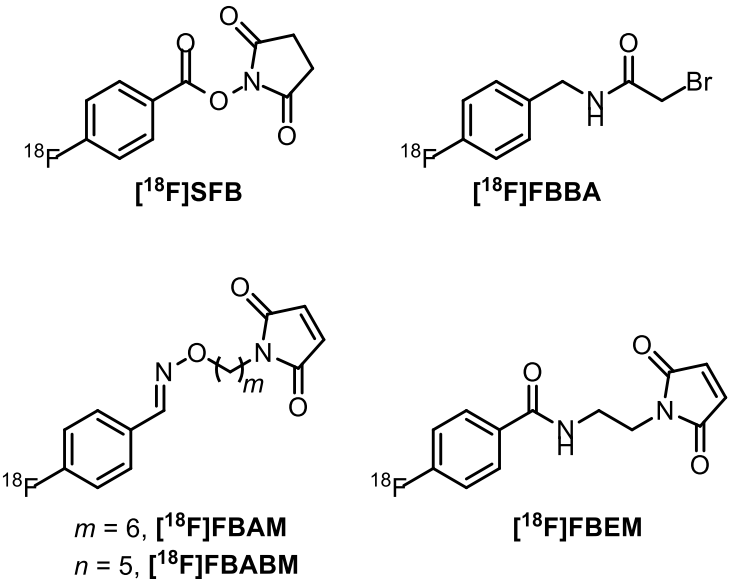

Figure 1.14. Some ^{18}F prosthetic groups for the labelling of biomolecules (non-CuAAC).

The alkylation of sulfhydryl- bearing biomolecules through the maleimide moiety has also seen significant application to ^{18}F labelling chemistry. In 1998, the synthesis of *N*-*p*-[^{18}F]fluorophenylmaleimide and some related prosthetics for the labelling of monoclonal antibodies was described in a conference abstract, but details were never fully reported.[220] The efficient production of 4-[^{18}F]fluorobenzaldehyde constitutes the first step in the radiosyntheses of closely related prosthetics [^{18}F]FBABM[221] and [^{18}F]FBAM[222-224] (Figure 1.14). In the case of both compounds, the alkylating functionality must be introduced in subsequent steps, owing to the occurrence of base-mediated maleimide ring opening under standard $K_{2.2.2}$.[^{18}F]F/K_2CO_3 [^{18}F]fluorination conditions.[222, 225] [^{18}F]FBABM and [^{18}F]FBAM were prepared in DC-RCYs of 35 %[221] and 30 %[222] respectively after HPLC purification. As proof-of-principle, both compounds were conjugated to tripeptide glutathione in good yields; however, bioconjugation of [^{18}F]FBAM to human low-density lipoprotein was not efficient (20 % by HPLC).[224] [^{18}F]FBABM was also used to ^{18}F- label an oligonucleotide bearing a terminal phosphorothiolate group, albeit in very low yields (5 %, 60 min).[225] In a related approach, Cai *et al*. produced [^{18}F]FBEM in three radiochemical steps, starting with the preparation of 4-[^{18}F]fluoroethylbenzoate and followed by hydrolysis, esterification and amidation to install the maleimide functionality.[226] Owing to a complex synthesis,

preparative small molecule yields were low (5 % NDC), but further bioconjugation to sulhydryl-RGD multimers was efficient (85 % by HPLC).

Another important thiol- targeting group for ^{18}F radiobioconjugate chemistry is the bromoacetamide group. In particular, oligonucleotide protocols have benefitted from the chemospecificity and water- tolerance that this functionality offers. Alkylation of an external 3'-phosphorothiolate monoester moiety allowed for the ^{18}F- labelling of 3' -phosphodiester[227] and 3'- phosphorothiolate[228] ODNs using *N*-(4-[^{18}F]fluorobenzyl)-2-bromoacetimide ([^{18}F]FBBA, Figure 1.14). One significant drawback of this approach is the complex, three- step synthesis of the prosthetic group, starting from 4-cyano-*N,N,N*-trimethylanilinium triflate. DC-RCYs of a model ^{18}F- labelled PS-ODN were 40- 45 % over 220 min. An automated synthesis was reported later with a shorter reaction time (1 h) but lower DC-RCYs (3- 18 %).[229] [^{18}F]FBBA has since been used for the ^{18}F-labelling of Spiegelmers,[230, 231] PNAs,[232] and 5'-phosphorothiolate-2'-*O*-methyl-modified RNA.[233]

1.4.2. *Click for Radiobioconjugate Chemistry*

In a bid to confer chemoselectivity and improve labelling yields, the use of modified peptide and oligonucleotide starting materials has come to dominate radiobioconjugate chemistry. In this regard, the field has become an important extension of the 'click' philosophy.[234] Early examples of the 'click' reactions as envisioned by Kolb and Sharpless[235] include:

- Cycloaddition reactions, including 1,3- dipolar cycloadditions (*vide infra*) and *hetero*-Diels Alder reactions.[236]
- Nucleophilic ring-opening reactions of strained heterocyclic electrophiles, including epoxides[99, 100] or aziridines.[101]
- Certain carbonyl addition-elimination reactions. In particular, oxime (*vide infra*) and hydrazone[237] formation.
- Certain additions across double bonds, including oxidations and some Micheal additions.

Excluding the final category, these chemistries have all been utilized for the synthesis of ^{18}F PET tracers. (See the accompanying references for examples.) An important addition to this original list is the water- tolerant, catalyst- free reaction of

organic azides and phosphanes to form an amide linkage (*i.e.* traceless Staudinger ligations). To date, this chemistry has only been used to incorporate a [^{18}F]fluoroalkyl group to a few small molecules;[238] however, the mild, biocompatible characteristics of the Staudinger reaction should see its inclusion into the macromolecular sphere eventually. In fact, a pre-targeting experiment was recently reported whereby antibody-decorated tumours in living mice were targeted by phosphane- modified chelators labelled with ^{89}Zr, $^{67/68}$Ga, ^{177}Lu, and ^{123}I.[239] However, results suggest that this type of ambitious *in vivo* radiobioconjugate chemistry may not be feasible.

Oxime ligations and copper-catalyzed azide-alkyne cycloaddition (CuAAC) reactions are the two most studied 'click' radiobioconjugate approaches, and their role in ^{18}F chemistry will be discussed further.

Carboxyaldehydes readily serve as electrophiles towards nucleophilic attack by oxyamino moieties.[240] These chemoselective reactions can proceed at low temperatures and under aqueous conditions. The resulting oxime linkage is considered stable at biological pH and suitable for *in vivo* use. This approach has been used extensively in the preparation of a diverse range of macromolecular chimeras, including peptide dendrimers[241] and POCs.[242] Furthermore, oxime bioconjugations have been extended to nuclear imaging. Many protocols employing oxime- based tethers for ^{18}F labelling exist, a scenario no doubt facilitated by the ease of synthesis of 4-[^{18}F]fluorobenzaldehyde, which can then be easily coupled to oxyamino- modified biomolecules (Figure 1.15). This constitutes a highly desirable '1+1' labelling strategy, whereby the prosthetic and the bioconjugate can both be prepared in only one step.[148] Poethko *et al.* were the first to prepare ^{18}F peptides in this manner, producing a number of multimeric *c*(RGD) analogues from their corresponding oxyamino- precursors in good coupling yields (70- 90 %), short total synthesis times (60 min) and low peptide concentrations (0.5 mM).[243] However, a low reaction pH (2.5) and elevated temperature (60 ºC) was required to attain these results. The same approach was later used to generate ^{18}F- labelled glucuronidated [Tyr^3]octreotate (TATE) analogs (65- 85 % coupling yields).[244] Aliphatic [^{18}F]fluoride prosthetics have also been reported. A CHO-PEG_4-^{18}F tag was synthesized in two radiochemical steps *via* mesylate displacement followed by deacetylation (Figure 1.16).[245] At 160 ºC in DMSO, [^{18}F]F^- incorporation was near quantitative and preparative yields were 62 % DC. However, bioconjugation

yield to a *c*(RGD) analogue was only 24±6 % DC (*n*=10) and total radiosynthetic yield was 14±6 % DC (*n*=10) from EOB. A recent hybrid approach utilizes a bifunctional arene bearing aldehyde and terminal epoxide moieties (Figure 1.15).[100] After [^{18}F]fluoride- mediated ring opening (80- 95 %), the formylated portion was coupled to oxyamino- modified TATE (60- 70 %) in the usual fashion; DC-RCYs were 28- 32 % after 65- 70 min total synthesis time. An interesting example of ^{18}F labelling *via* oxime linkage utilizes [^{18}F]FDG as a prosthetic group. The approach takes advantage of the fact that [^{18}F]FDG exists in both cyclic and straight- chained forms in aqueous solutions at high temperature, with the open form of the sugar containing an aldehyde functionality (Figure 1.15). Thus, conjugation of [^{18}F]FDG to NH_2O-*c*(RGD) was performed in DC preparative yields of 41 %, starting from [^{18}F]FDG.[246] The authors acknowledge that the harsh reaction conditions required (100 ºC, 0.4 % TFA) may limit the generality of this technique. However, the low lipophilicity of [^{18}F]FDG- coupled with the fact that it is available at most PET centres worldwide- suggests that this protocol may see widespread application in the near future.

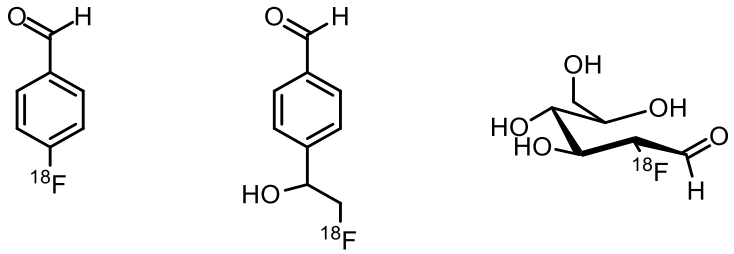

Figure 1.15. Some aldehyde- bearing prosthetic groups for the ^{18}F- labelling of peptides through oxime ligation.

See also Figure 1.16.

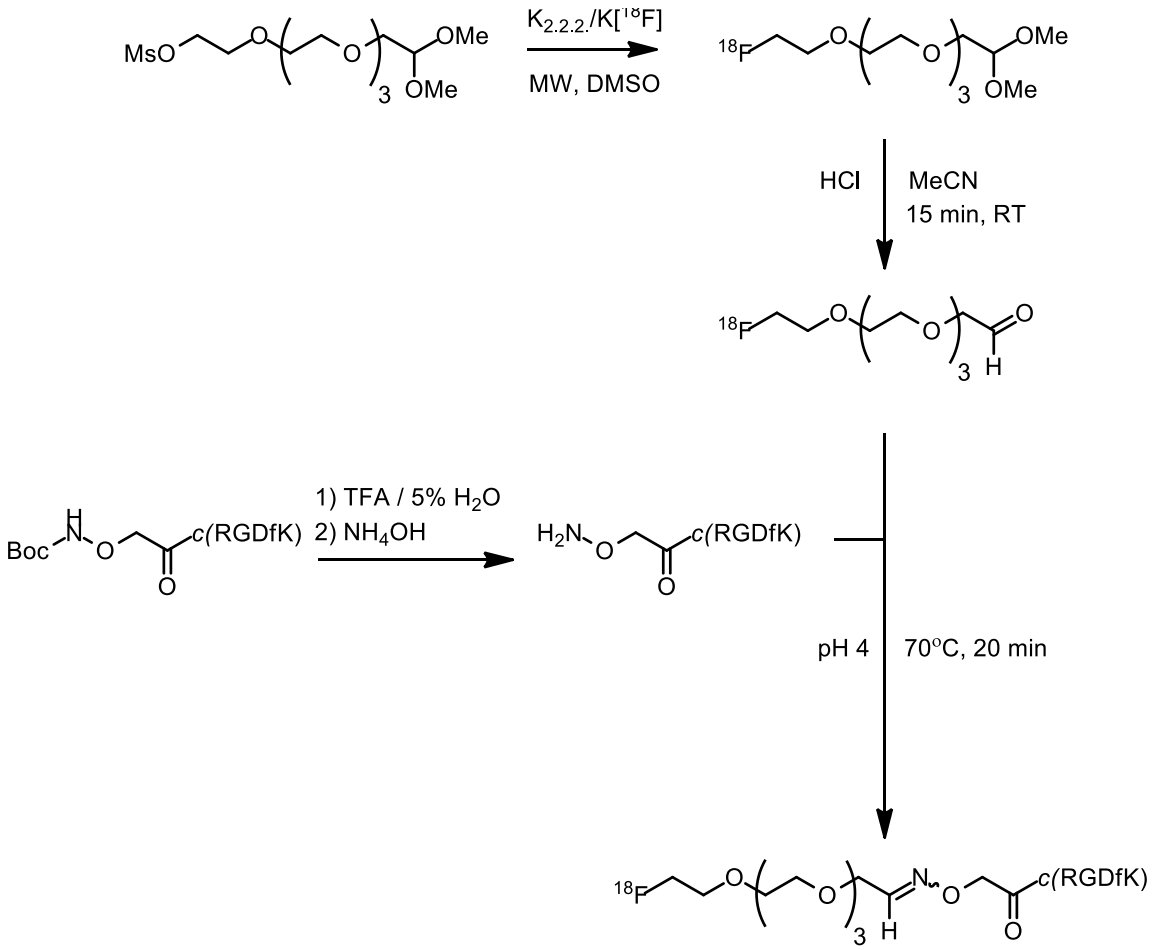

Figure 1.16. Synthesis of ^{18}F peptide via oxime ligation of a TEGylated prosthetic group.

From Glaser et al.[245] TEG = tetraethylene glycol.

The copper- catalyzed variant of Huisgen's 1,3- dipolar cycloaddition reaction (CuAAC) involves the chemoselective coupling of organic azides with alkyne dipolarophiles to form 1,2,3- triazoles.[247] Since its independent discovery by the Sharpless[248] and Meldal[249] groups in 2002, this chemistry has had a profound effect on design of new medicinal and material chemical agents.[250] The Cu^{I} catalyst greatly enhances the rate of triazole formation (~10^7 x),[251] and also confers 1,4- regioselectivity to the heterocycle.[249] However, the greatest impact of the CuAAC reaction has arguably been felt in biological chemistry, as this bio-orthogonal mode of ligation usually proceeds readily in aqueous solutions and at ambient temperatures. Over the last 10 years, a vast array of biomolecular chimeras have been successfully invented, including

chemically modified peptides,[252] proteins,[253] and nucleic acid- based molcules.[254] Indeed, even highly complex architectures can be synthetically or genetically decorated with azides or alkynes for CuAAC couplings. The successful labelling of viral particles,[255] bacterial cell surfaces[256, 257] and even living animals[258, 259] speak much towards the rapid proliferation of the reaction. Despite these successes, it has become clear that the presence of Cu^{I}, even in catalytic amounts, can have a deleterious effect on certain sensitive biomolecules. For example, DNA degrades rapidly in the presence of Cu^{I} and dioxygen,[260] presumably as the result of nucleobase oxidation by hydroxyl radical produced *in situ*.[261] Furthermore, straightforward use of the Cu^{II}/sodium ascorbate redox pair- by far the dominant means of generating Cu^{I} for small molecule applications- is unsuitable for many polypeptide ligations. This is because copper-mediated O_2 oxidation of ascorbate (to dehydroascorbate) can initiate the production of reactive species, including H_2O_2,[262] L-threose,[263] and glyoxal.[264] One means to circumvent these problems is to eliminate the use of copper altogether. To this end, precursor compounds consisting of strained cyclooctyne rings have been developed.[258, 265] These dipolaraphiles were initially developed for those *in vivo* bioconjugations where cytotoxic copper could not be used.

Another approach for the successful marrying of biomolecules and CuAAC chemistry involves the use of copper- complexing additives (Figure 1.17). The first and thus far most popular chelator is *tris*-(benzyltriazolylmethyl)amine (TBTA). TBTA was specifically designed to aid CuAAC reactions by enhancing catalysis through nitrogen lone pair donation to the metal center and blocking interactions that might oxidize the essential Cu^{I} species.[266] The authors hypothesized that the triazole functionalities might chelate the copper when unchallenged, but become temporarily displaced to allow formation of the Cu^{I}-acetylide complex that is thought to initiate the catalytic cycle.[267] TBTA has been extensively employed for CuAAC labellings of the viral and bacterial membrane proteins (as referenced above). In another notable example, TBTA assisted in the florescent modification of an entire proteome for activity- based enzyme profiling.[268] Among DNA- based strategies, the introduction of TBTA permitted the CuAAC coupling of oligonucleotides to self- assembled monolayers.[269] The major disadvantage associated with TBTA is its poor water solubility, which sometimes necessitates the use of high concentrations (mM range) of substrates and copper in the

bioconjugation reaction. Thus, a few water- soluble alternatives have been reported, including a disulfonated bathophenanthroline ligand (BPDS) and carboxylate-, sulfonate- and hydroxy- modified TBTA analogues (Figure 1.17). Unfortunately, the carboxylated and sulfonated compounds show limited catalytic efficiency in the absence of sodium ascorbate and BPDS exhibits acute oxygen sensitivity.[270] However, *tris*-alcohol THPTA [tris(3-hydroxypropyltriazolemethyl)amine] is a stable catalyst which has been proven effective for the preparation of fluorescent Qβ bacteriophages and siRNAs.[271]

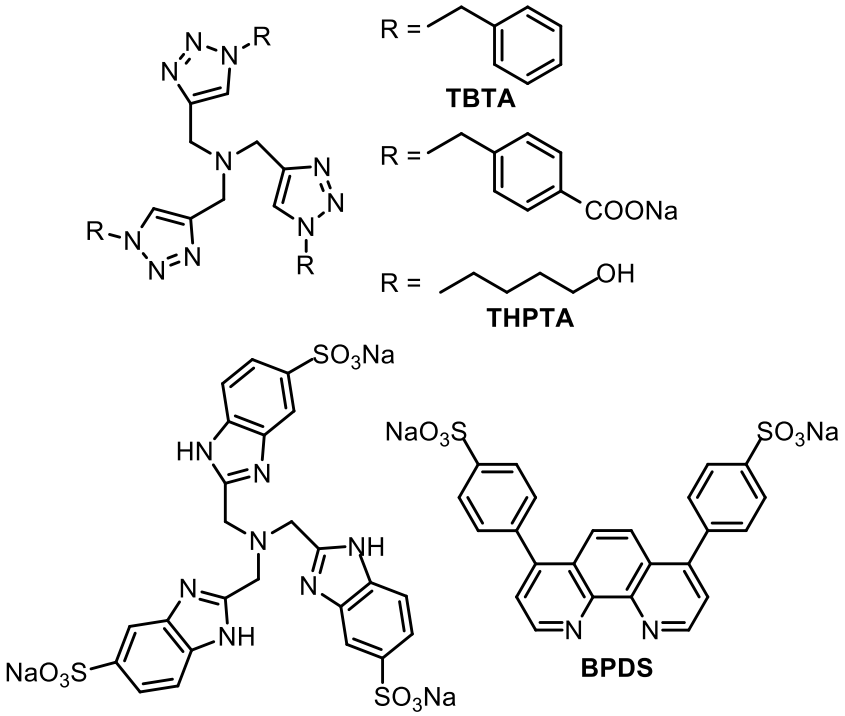

Figure 1.17. CuAAC catalysts.

1.4.3. *CuAAC for ^{18}F Peptides*

The first use of the CuAAC reaction for the ^{18}F- labelling of bioactive peptides (and indeed, for PET chemistry in general) was reported by Marik and Sutcliffe.[272] In this important work, 4- and 8- amino acid *N*-(3-azidopropionyl)peptides were ^{18}F-labelled in acetonitrile using [^{18}F]fluorobutyne, [^{18}F]fluoropentyne and [^{18}F]fluorohexyne (Figure 1.18). The catalyst system was CuI and sodium ascorbate. Interestingly, a large excess of Cu^{I} (40 equivalents relative peptide) was required to elicit significant conversion. Another important observation was that addition of nitrogen base [*N, N*-diisopropylethylamine (DIEA), pyridine or 2,6-lutidine; 400 equivalents] could be used to

improve radiochemical purities. Bioconjugation yields were in the range of 54- 99 %, though no preparative yield was reported. Total synthesis time was a remarkable 30 min, in large part because the small [^{18}F]fluoroalkynes could be both purified and removed from ^{18}F peptide by distillation. Soon afterwards, the reverse strategy was also investigated- that is, the preparation of [^{18}F]fluoroethylazide for conjugation to acetylene-modified peptides (Figure 1.18).[273] Excellent incorporation into a model 5 amino acid peptide was achieved at RT over 15 min (92 %). In this case, the ^{18}F prosthetic could not be removed by distillation and thus HPLC purification was required. This approach was later applied to the labelling of a biologically relevant peptide, namely [Tyr^3]octreotate (TATE, a.k.a. TOCA).[274] Thus a series of somatostatin receptor ligands were synthesized with varying types of linker chains separating the [^{18}F]fluoroethyltriazole moiety. Simple Gly and β-Ala-Gly chains afforded the lowest inhibitory concentrations relative to ^{111}In-DTPA-octreotide in pancreatic cancer cells, while the use of PEG tethers actually increased IC_{50} values. Copper-stabilizing BPDS ligand was used. In recent preclinical study, the labelled peptides ([^{18}F]FET-G-TOCA and ([^{18}F]FET-βAG-TOCA) both showed excellent uptake into pancreatic cancer xenografts in mice and clearly delineated the tumours in associated μPET images.[275] In a bid to decrease ^{18}F prosthetic volatility and increase ^{18}F peptide water- solubility, [^{18}F]fluoroaliphatic labelling agents have been designed that use ethyleneglycol rather than alkyl chains. Thus [^{18}F]fluoroalkynes derived from tri[276]- and tetra[277]-ethylene glycol have been introduced for peptide receptor imaging (Figure 1.18). The former compound was used to ^{18}F- label a *c*(RGDyK) dimer. Good NDC preparative yields of small molecule and peptide were obtained (65 % and 52 % respectively) and the dimer saw improved renal clearance in a mouse model of glioblastoma cancer relative to its [^{18}F]SFB- modified counterpart. However, absolute tumour uptake was diminished and the ^{18}F peptide showed some metabolic degradation over 1 h.

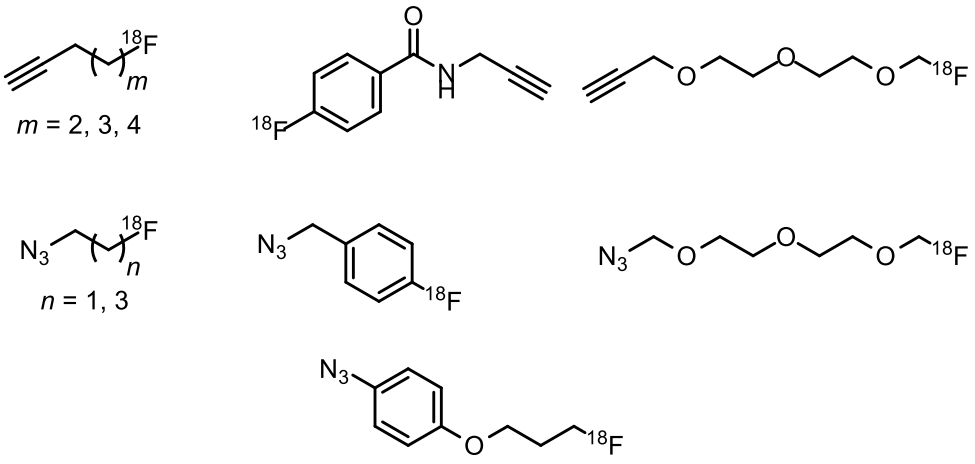

Figure 1.18. Some CuAAC- based ^{18}F prosthetic groups.

[^{18}F]Fluoroarenes bearing azides and acetylene groups have also been utilized for labelling peptides. The Wuest group synthesized [^{18}F]fluoro-*N*-(prop-2-ynyl)benzamide by way of amidation of [^{18}F]SFB with propargyl amine (Figure 1.18).[278] The product was separated from chemical and radiochemical precursor by successive SPE purification. Radiochemical purity of the alkyne- bearing prosthetic after SPE was described as >90 %. Meaningful assessment of this five- step radiobioconjugate protocol is difficult owing to a lack of reported information. For instance, the preparative yield of [^{18}F]fluoro-*N*-(prop-2-ynyl)benzamide was only reported from [^{18}F]SFB (72 % DC, 30 min). In addition, the bioconjugation yield to azide- modified NT(8-13) was given as 66 % by HPLC, but the preparative yield was not reported. Another approach utilizing nucleophilic aromatic [^{18}F]fluorination chemistry involved the synthesis of 4-[^{18}F]fluorobenzyl azide (Figure 1.18).[279] Initial synthesis of this ^{18}F prosthetic was laborious (3 radiochemical steps from 4-[^{18}F]fluorobenzaldehyde), but DC yields of 34 % could be achieved in 75 min with an automated synthesis unit. The final step involves bromo displacement by a solid phase- supported azide nucleophile. A short model peptide sequence was preparatively labelled in 90 % yield (DC) from [^{18}F]fluorobenzyl azide; no total preparative yield was reported. The CuAAC reaction mixture included CuI, DIEA, and sodium ascorbate in DMF (15 min, RT). Despite the drawbacks associated with this complex protocol, it is notable that excellent cycloaddition yields could be achieved using a very low concentration of precursor peptide (3 µM).

Recently, copper- free CuAAC techniques have been applied to the ^{18}F- labelling of bombesin analogues.[280] The dipolarophiles used were 'spring-loaded' cyclooctyne rings, such as those employed for *in vivo* CuAAC ligations. An ^{18}F- bearing triethyleneglycolylated azide, along with [^{18}F]fluoroazidobutane and [^{18}F]fluorobenzyl azide (Figure 1.18) were each coupled to cyclooctyne- modified BBN(7-14) in radio-TLC yields of 19 %, 31 %, and 37 % respectively. Unfortunately, in the absence of copper, 1,2,3- triazole formation is not regiospecific. Furthermore, the heterocyclic linkages produced are rather large and lipophilic. The ^{19}F peptide standards prepared in this fashion exhibited 50 % inhibitory concentrations relative to [^{125}I]Tyr^4-BBN in the 29-40 nM range in PC3 cells.[280]

1.4.4. *CuAAC for Nucleic Acid- Based Probes*

Compared to polyamides, the use of the CuAAC coupling strategy for the labelling of nucleic acid polymers is not widespread. Presumably, this fact stems from concerns regarding Cu^{I}-catalyzed nucleobase oxidation, as described above.[261] Nevertheless, a small number of fluorescent oligonucleotides have been prepared in this fashion, including large duplex MTase substrates,[281] end-sealed DNA duplexes,[282] densely modified PCR fragments,[283] primers for DNA sequencing,[284] and bioconjugates from arylacetylene- modified sequences.[260] In addition, a microwave- assisted coupling of galactosyl azide derivatives with alkyne- functionalized T_{12} on solid support has been reported.[285] With regards to nuclear imaging, glucose[286] and thymidine[287] analogues were labelled with azide- and alkyne- bearing alkyl [^{18}F]fluorides, despite the small size of these targeting molecules.

A manuscript[288] describing the first published radiolabelling of an oligonucleotide molecular probe by way of CuAAC bioconjugation makes up part of this thesis document. Subsequently, other procedures of this type have been reported. Shiraishi *et al.* prepared arylacetylene- modified RNA analogues amendable to the CuAAC coupling of 4-fluorobenzyl azide.[289] However, radiochemical versions of these bioconjugates have not yet been prepared. In a similar approach, 4-[^{18}F]fluorobenzyl azide and 1-azido-4-(3-[^{18}F]fluoropropoxy)benzene (Figure 1.18) were synthesized in DC yields of 41 % (3 steps) and 35 % (1 step) respectively for conjugation to propargyl amide- modified siRNA.[290] The alkyl[^{18}F]fluoride prosthetic afforded ^{18}F- labelled siRNA in DC-RCYs of

15±5 (*n*=3) over 2 h. Preparative yields of the [^{18}]fluoroarene- bearing bioconjugate were not reported. Finally, 4-[^{18}F]fluorobenzyl azide was also the chosen prosthetic for a study that attempted to label a relatively small amount of ODN precursor (20 nmol; Figure 1.19).[291] Prosthetic group preparation and conjugation to a 5'-alkynylated nucleoside moiety at the 5'- terminus could be achieved in good yields (96 % and 90 % respectively). Strangely, the apparent specific activity of the product oligonucleotide was reported to be much higher than the ^{18}F prosthetic (2.12 GBq/µmol vs. 1809 GBq/µmol respectively). The total preparative yield was 7 % DC (4 % NDC) before desalting of the final product. Murine PET scans showed extensive bone uptake after >30 min, suggesting that this ^{18}F bioconjugate is rapidly metabolized *in vivo*.

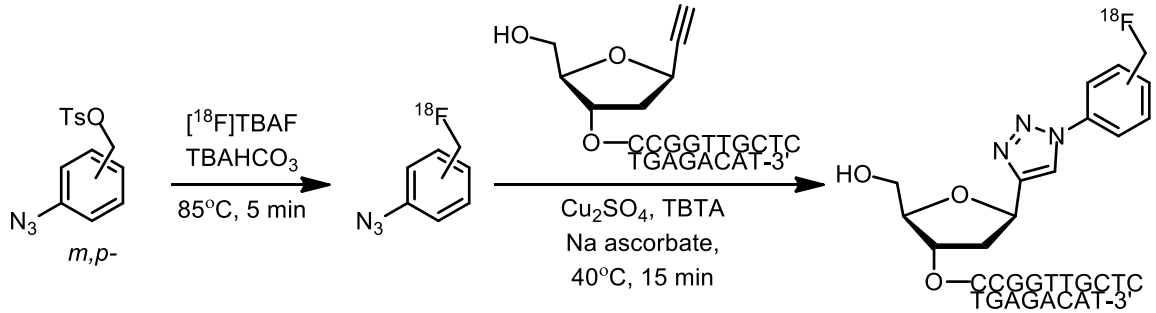

Figure 1.19. Radiosynthesis of ^{18}F- labelled ODN via CuAAC conjugation of 4-[^{18}F]fluorobenzyl azide and 5'-alknylated DNA.

From Kuboyama et al.[291]

1.5. 2-[^{18}F]Fluoropyridines in Bioconjugate Chemistry

2-[^{18}F]Fluoropyridines have been utilized for the preparation of ^{18}F- labelled bifunctional molecules. The first prosthetic bearing this functionality was 2-[^{18}F]fluoroisonicotonic acid hydrazine, developed by the Amartey group for the labelling of folate derivatives (Figure 1.20).[292] However, the strongest advocates of this approach have been investigators at Service Hospitalier Frédéric Joliot. First, a 2-[^{18}F]fluoropyridine pendant to a bromoacetamide group ([^{18}F]FPyBrA; Figure 1.20) was introduced for the chemospecific ^{18}F labelling of short, sulfhydryl- modified DNA analogues.[293] This compound was prepared in 18- 20 % NDC yields over three radiochemical steps, including [^{18}F]fluorination, Boc deprotection and condensation with 2-bromoacetyl bromide. After regioselective alkylation to an ODN bearing a PS

monoester terminus (20- 30 % yield), the final radiosynthesis time was 140- 160 min using a Zymate automated synthesis system. (Thus, the inferred overall NDC yield is 4 %.) Originally designed to radiolabel antisense sequences, [^{18}F]FPyBrA has been subsequently used to ^{18}F- label a variety of potential nucleic acid- based drugs and imaging agents, including Speigelmers,[230] siRNAs,[294, 295] and PNAs.[296] An alternative automated synthesis of [^{18}F]FPyBrA was recently published by another group.[297] In this case radiobioconjugate yields were very high (>90 %), but specific activity was low, owing to incomplete HPLC separation of precursor and ^{18}F- labelled material. A maleimide- functionalized 2-[^{18}F]fluoropyridine compound, [^{18}F]FPyME, was designed for conjugation to sulfhydryl- bearing peptides and proteins (Figure 1.20).[225] Small molecule synthesis was achieved in a manner similar to [^{18}F]FPyBrA, except for the third step which involves installation of a maleimido group using maleic anhydride in basic dioxane. NDC yields of the ^{18}F prosthetic were 28- 37 % and the synthesis time was 110 min with automated assistance. Model targeting molecules included cysteine-bearing (*N*-Ac)KAAAAC peptide, apoptosis- targeting miniprotein AFIM-0, and *c*-STxB, a Shiga toxin analogue targeting the glycosphingolipid globotriaosyl ceramide receptor. All conjugations were achieved in excellent yields (>90 %), with total synthesis times in the range of 130- 140 min. The proteins were separated from [^{18}F]FPyME using Sephedex© SPE cartridges, while HPLC was used obtain chemically and radiochemically pure peptide. In a recent application of this technology, [^{18}F]FPyME was used to label a small library of new peptides (31- 52 % coupling yields) targeting a cancer- specific mutation on the epidermal growth factor receptor (EGFRvIII).[298]

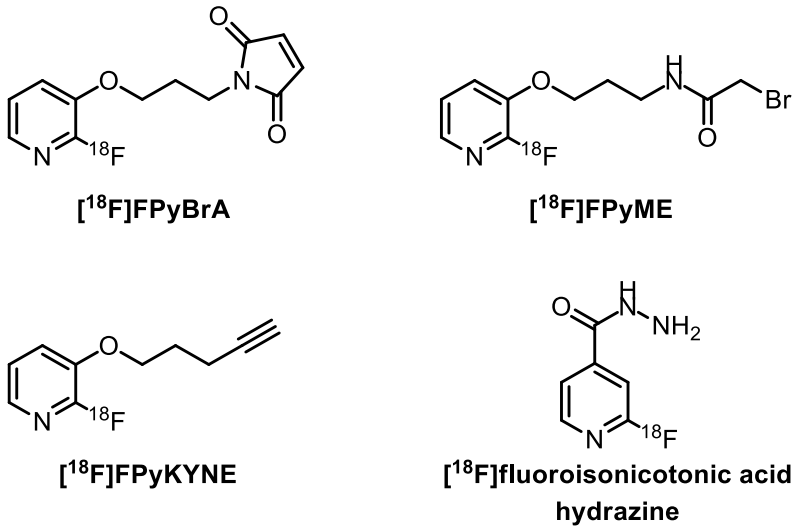

Figure 1.20. ^{18}F prosthetic groups bearing the 2-[^{18}F]fluoropyridnyl moiety.

See also Figure 1.21.

Acetylene- bearing 2-[^{18}F]fluoropyridines have been developed for the labelling of azide- modified biomolecules. 2-[^{18}F]Fluoro-3-pent-4-yn-1-yloxypyridine ([^{18}F]FPyKYNE; Figure 1.20) was prepared from the corresponding 2-trimethylammonium triflate and 2-nitro precursors (30 µmol) in >90 % RCYs using classical $K_{2.2.2}$.[^{18}F]F/K_2CO_3 conditions (DMSO, 165ºC).[299] Purification involved dilution with water, C_{18} cartridge trapping to isolate the ^{18}F prosthetic from DMSO and free [^{18}F]F, and finally normal phase HPLC purification on silica gel. Further concentration and bioconjugation steps were not reported. Overall preparative radiochemical yield was 30- 35 % DC in a procedure time of 60- 70 min. Very recently, a fully automated procedure for the ^{18}F labelling of *c*(RGDyK) with [^{18}F]FPyKYNE was reported.[300] The prosthetic was rapidly separated from 2-nitro-3-pent-4-yn-1-yloxypyridine precursor by way of silica gel SPE (20- 25 min), albeit in moderate 20- 35 % DC RCYs. Preparative ^{18}F peptide syntheses ($CuSO_4$/Na ascorbate, DMSO:H_2O, 60 ºC) could be achieved in 12- 18 % DC-RCYs. A closely related molecule- 2-[^{18}F]fluoro-3-hex-5-yn-1-yloxypyridine ([^{18}F]FPy5yne, [^{18}F]-**1**; Figure 1.21) was developed independently by Inkster *et al*.[379] Incorporation of ^{18}F into the

corresponding 2-nitro (**2**) and 2-trimethylammonium triflate (**3**) precursors was optimized for time, temperature and solvent (Figure 1.21). The ^{18}F prosthetic group was isolated from the reaction mixture using a C_{18} Sep-pak® prior to reverse phase HPLC purification.* The best NDC preparative yield of [^{18}F]-**1** from **3** was 24 % (42 % DC). The specific activity of [^{18}F]-**1** was estimated to be 61 GBq/μmol. The collected radioproduct was trapped on another C_{18} cartridge, eluted with methylene chloride, and the elution solvent was removed at 50 ºC under a stream of helium. CuAAC coupling of [^{18}F]-**1** to a model peptide (N_3-$(CH_2)_4$-CO-YKRI-OH; **N_3-BG142**; Figure 1.21) was achieved in an average bioconjugation yield of 89±9 % (*n*=4). After another HPLC purification, Sep-pak® concentration and eluent evaporation, the ^{18}F peptide (**^{18}F-BG142**) was obtained in a final NDC yield of 6 % (19 % DC) after 160 min. Apart from the fact that this protocol included HPLC purification, trapping, and drydown steps for both the prosthetic group and ^{18}F peptide, procedural efficiency suffered from the fact that a significant amount of the [^{18}F]-**1** was lost during the evaporation step.

* HPLC was required even when TMA salt **3** was used, as 2-methylamino- substituted impurity accumulates during the [^{18}F]fluorination reaction, presumably by way of competitive demethylation of the precursor.

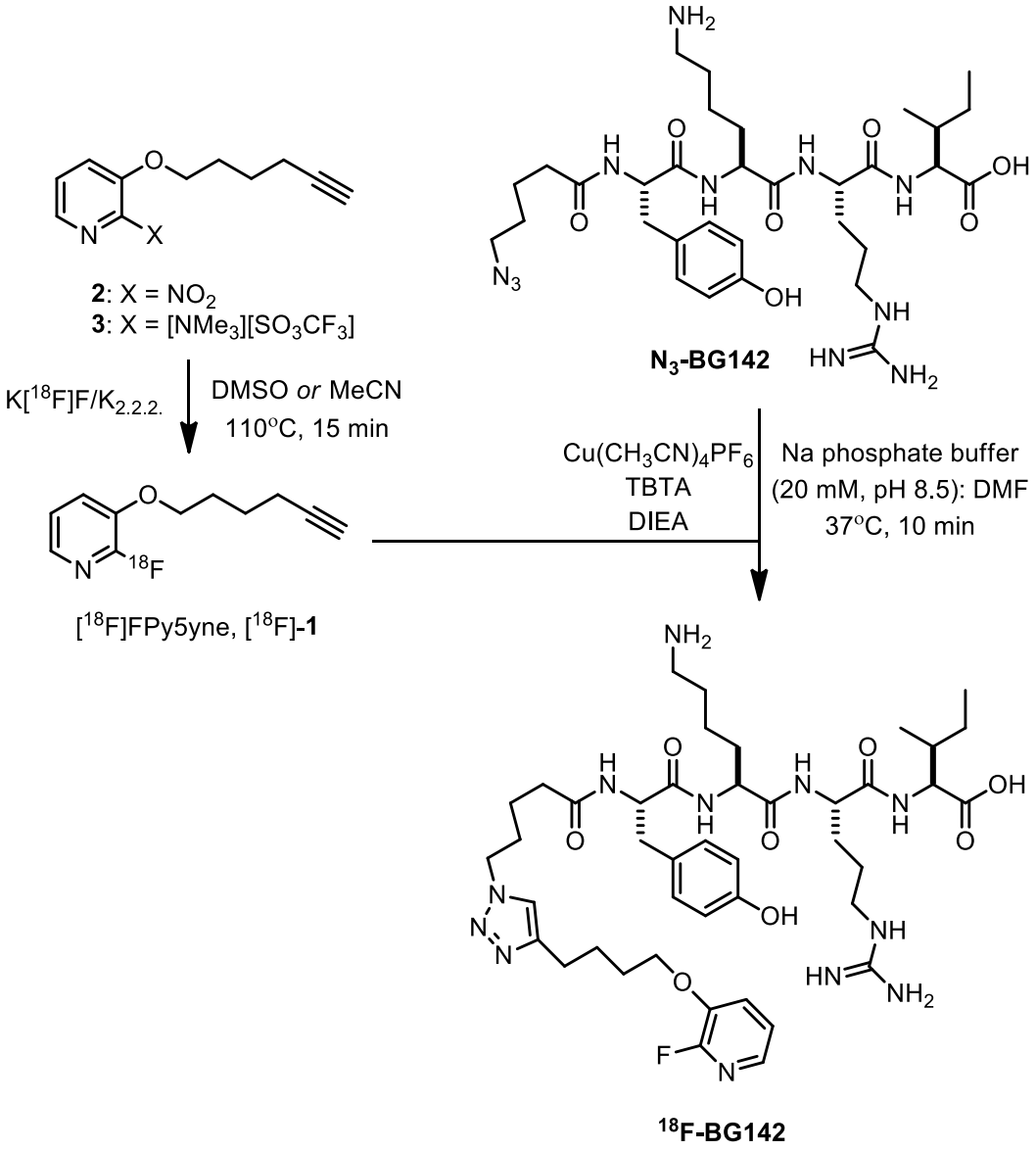

Figure 1.21. Synthesis and radio-bioconjugation of [^{18}F]FPy5yne.

From Inkster et al.[379] Radiochemical yields by TLC of [^{18}F]-**1** were >86 % regardless of solvent or precursor used. Only [^{18}F]-**1** derived from **3** was employed in subsequent bioconjugations.

1.6. Sulfonyl [^{18}F]Fluorides

1.6.1. *Beyond C-^{18}F Bond Chemistry*

The inherent challenges associated with traditional nucleophilic aromatic and nucleophilic aliphatic [^{18}F]fluorination chemistry (see Section 1.2) have prompted

researchers to seek novel strategies for ^{18}F incorporation that employ atoms other than carbon.[302] For example, aryltri[^{18}F]fluoroborate pendant groups have been used by the Perrin group and others to ^{18}F- label a number of small bioactive molecules. With regard to this post-labelling approach, initial investigations involved the direct, aqueous fluorination of pinacolyl phenylboronate diesters with carrier- added KH[^{18}F]F_2. These early tri[^{18}F]fluoroarylborate prosthetics reported lacked additional functionalities on the benzene ring. Although initially deemed stable towards aqueous solvolysis,[303] autoradiographic assay after a more rigorous TLC protocol proved otherwise.[153, 304] However, it was found that the presence of electron- withdrawing groups on the aryl ring significantly enhanced the solvolytic stability of the Ar-BF_3 functionality in buffered solution.[153] In particular, the rate constant for the solvolysis of a BODIPY fluorophore conjugated to a 2,4,6- trifluoro- bearing benzenetrifluoroborate pendant group was estimated to be $1.2\pm0.4 \times 10^{-4}$ min^{-1}, which corresponds to a $t_{1/2}$ of 92.5±29 h.[304]

Furthermore, the *in vivo* stability of certain tri[^{18}F]fluoroarylborated targeting vectors has been established by way of PET imaging. A biotin analogue of this type was synthesized from its tetraphenylpinacolyl arylboronate precursor and found to be stable in normal mice.[305] Oncological applications of this technology have included the synthesis of Ar-B[$^{18/19}F$]F_3- modified Lymphoseek® (tilmanocept)[306] and marimastat.[307] These radiopharmaceuticals enabled μPET visualization of sentinel lymph nodes and matrix metalloproteinase upregulation, respectively. Tilmanocept is a dextran polymer composed of repeating mannose and DTPA units (for incorporating ^{99m}Tc); in this case, a dual modality PET/near infrared fluorescence tag ([^{18}F]-BOMB) was inserted between the side chains. Unfortunately, syntheses described above require low pH (<3, HCl), long reaction times (45- 160 min) and the addition of ^{19}F carrier in order to achieve even moderate radiochemical yields. The above aryltri[^{18}F]fluoroborates are shown in Figure 1.22.

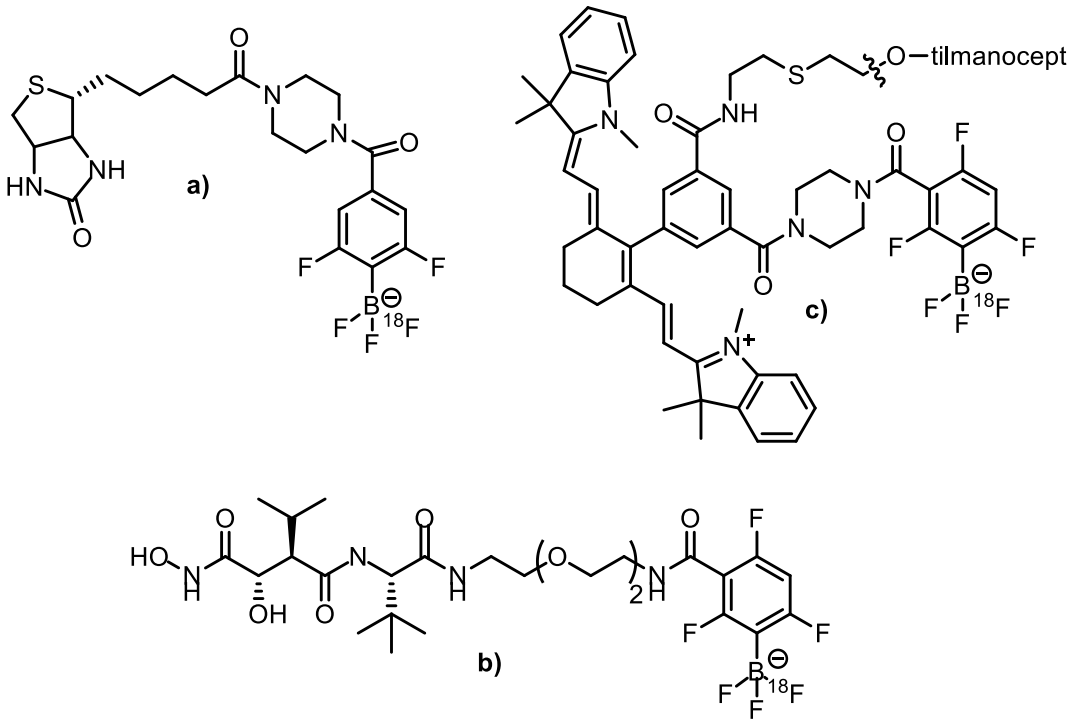

Figure 1.22. Structures of some aryltri[^{18}F]fluoroborate- based PET tracers.

a) B[$^{18/19}$F]F_3-biotin.[305] b) B[$^{18/19}$F]F_3-marimastat.[307] c) [^{18}F]-BOMB.[306]

Another novel inorganic approach to ^{18}F- labelling exploits the strong association of Al^{III} with fluoride ion (ΔH = >670 kJ/mol).[308] It was shown that $AlCl_3$ could be labelled in acetate buffer with [^{18}F]F^- and this $(Al^{18}F)^{2+}$ complex was then conjugated to peptide targeting agents using a bifunctional chelator (pH 4, >100 ºC, 15 min).[309] A number of established radiometal chelation platforms were tested, but only the NOTA-Al-^{18}F complex showed sufficient stability in human serum. This novel post-synthetic [^{18}F]fluorination system was used to prepare an ^{18}F octreotide analog for μPET imaging of pancreatic cancer in mice, with no sign of *in vivo* defluorination.[310] Challenges associated with the technology include:

- the relatively high temperatures required for adequate $(Al^{18}F)^{2+}$ incorporation
- the non-productive binding of non-fluorinated aluminum, which limits specific activity
- the production of diastereomers upon chelation.

Recently, attempts to optimize $(Al^{18}F)^{2+}$ incorporation yields by tuning reagent concentration, pH, and tethering group resulted in a NOTA derivative that could be

labelled in yields as high as 87 % and specific activities as high as 115 GBq/µmol over 5 min.[311] Although the mass of peptide (20 nmol) and metal (10 nmol) required for labelling was significantly reduced, a high temperature was still required (100 ºC). Finally, it was shown that the ^{18}F- labelled peptide could be adequately separated from [^{18}F]F^{-} and $(AlF)^{2+}$ using a SPE purification step, thus obviating the need for HPLC and greatly decreasing the overall radiosynthesis time (30 min).

The *in vivo* stability of the Si-^{18}F bond was first investigated in 1985. [^{18}F]Fluorotrimethylsilane was synthesized in 65 % DC-RCY and deemed to be hydrolytically unstable in normal mice.[312] Much later, the use of amphipathic tetra[^{18}F]fluorosilicate salts were examined, but found to be only moderately stable in carbonate buffer ($k_{hydrolysis}$ = 0.01 min^{-1}).[303] However, soon afterwards the Schirrmacher group discovered that bulkyl lipophilic alkylarylfluorosilanes were hydrolytically stable under physiological conditions. In their initial report, di-*tert*-butyl-phenylfluorosilane was radiolabelled by way of ^{19}F-to-^{18}F exchange in near- quantitative yields in MeCN using K[^{18}F]F/$K_{2.2.2.}$ over 15 min.[313] This labelling strategy has been dubbed 'SiFA' (**Si**licon-**F**luoride **A**cceptor) chemistry. The bifunctional derivative *p*-(di-*tert*-butyl[^{18}F]fluorosilyl)benzaldyde (SiFA-A) was used to ^{18}F- label a series of oxyamino-modified peptides, including *c*(RGDfK), [Tyr^{3}]octreotate and a PEG2 bombesin analogue (BZH3; Figure 1.23).[313, 314] Because the isotopic exchange reaction proceeds efficiently using very low amounts of peptide (1 µg), remarkably high specific activities can be achieved (225- 680 Gq/µmol). Another SiFA compound, *p*-(di-*tert*-butyl[^{18}F]fluorosilyl)phenylmaleimide (SiFA-Mal) was designed by the same group for conjugation to protein sulhydryl residues.[315] Similarily, *p*-(di-*tert*-butyl[^{18}F]fluorosilyl)benzenethiol (SiFA-SH) was synthesized and used to ^{18}F- label maleimide- modified bovine serum albumin for use as a blood pool imaging agent.[316]

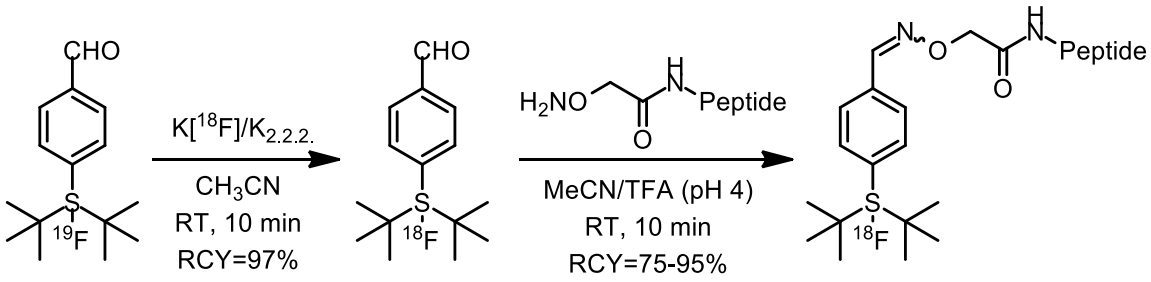

Figure 1.23. Si-F bond-making for the synthesis of ^{18}F- labelled peptides (SiFA chemistry).

From Schirrmacher *et al.*[314] Peptide = *c*(RGDfK), BZH3, TATE. Overall DC preparative yield was 50- 55 % over 40 min.

Inspired by the SiFA approach, Mu *et al.* modified a series of peptide ligands with di-isopropylaryl silanes for direct radio-bioconjugations in 1 % AcOH in DMSO.[317] In this case, hydroxy or hydride leaving groups were employed. A small tetrapeptide was shown to be stable in human plasma over 2 h. However, when this post-labelling approach was extended to the synthesis of ^{18}F bombesin analogues, the di-isopropylfluorosilyl moeity was unstable in 2:1 MeCN:H_2O.[318] In contrast, di-*tert*-butylfluorosilyl-BBN was stable under the same conditions, and thus this alternate pendant group was examined further. The aforementioned ^{18}F peptide, which contains an isolated lysine residue to improve water- solubility, showed poor and non-specific uptake into PC3 tumour xenografts (0.63±0.13 % ID/g,* 0.5 h) but high and specific uptake into GPRr-rich murine pancreatic tissue (5.41±0.12 % ID/g, 0.5 h).[319] Notably, the log *D* value of the peptide was high (1.3±0.1, *n* =5), which suggests that the compound was still rather lipophilic. Finally, the use of 'click'-able di-*tert*-butylsilyl pendant groups for the post-synthetic labelling of nucleosides and oligonucleotides has recently been introduced. First reported steps involved the preparation of 3'- silylated thymidine precursor by way of CuAAC reaction with *p*-(di-*tert*-butylsilyl)benzyl azide.[320] Later, a 5'-azidothymidine precursor was also prepared for conjugation to its *O*-propargyl- bearing counterpart .[321] Typical K[^{18}F]F/$K_{2.2.2.}$ [^{18}F]fluorinations of the modified thymidines in 1 % AcOH in DMSO yielded ^{18}F nucleosides in NDC yields of 43

* % ID/g = percent injected dose per gram of tissue.

% and 34 % respectively (60 ºC, 15 min). Furthermore, the 5'-silylated precursor was phosphoroamidated and incorporated into the model oligonucleotide 10mer, where fluorination under similar conditions yielded NDC preparative yields of 36±2 % after HPLC purification. While this represents the first direct ^{18}F labelling strategy for DNA-based PET probes, the use of high temperatures (100 ºC) and anhydrous organic solvents may limit the generality of this approach.

1.6.2. *Sulfonyl Fluorides: Basic Characteristics*

The reactivites of sulfonyl fluorides are analogous to their more ubiquitous sulfonyl chloride counterparts. Notably, they have the potential to react with amine,[322] aniline,[323] morpholine,[324] and acetate[322] groups, which results in the displacement of fluoride ion. Compared to arylsulfonyl chlorides, however, arylsulfonyl fluorides are far more resistant toward nucleophilic attack, including attack by water.[325] For example, it was shown that benzenesulfonyl chloride hydrolyzes at a rate >4800 faster than the corresponding sulfonyl fluoride (1:1 acetone:water, 25 ºC).[325] A high reaction constant (ρ= +1.8) was found for the hydrolysis of benzenesulfonyl fluorides (40:60 dioxane:water, 65.5 ºC), suggesting that electronic effects play a significant role in the hydrolysis of these compounds.[326] Further support for this hypothesis can be drawn from the fact that *o*-nitrobenzenesulfonyl fluoride is significantly *less* stable under these conditions than *o*-nitrobenzenesulfonyl chloride. Kinetic features of the coupling of substituted sulfonyl fluorides and sulfonyl chlorides with various anilines have been studied (MeOH/MeCN, 35- 45 ºC).[323, 327] For both functionalities, electron- donating substituents on the nucleophile ($\sigma_{Nuc} < 0$) and electron- withdrawing substituents on the substrate ($\sigma_{Sub} > 0$) yield faster reaction rates. However, observed rates were ~10^3 times slower for the fluoride series. Unlike arylsulfonyl chlorides, arylsulfonyl fluorides are stable in acid, boiling water, boiling ethanol and pyridine[328]- features that are important to this work.

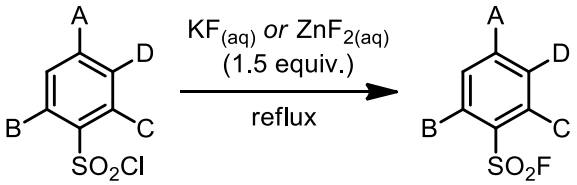

Figure 1.24. The Davies-Dick route to benzenesulfonyl fluorides from benzenesulfonyl chlorides.

See Table 1.5.

Table 1.5. Some benzenesulfonyl fluorides prepared by Davies and Dick.

Functionalities				Fluoride source	Time (h)	% Yield
A	**B**	**C**	**D**			
H	H	H	H	KF	1	83
H	CH_3	H	H	ZnF_2	1	60
CH_3	H	H	H	KF	1	80
CH_3	CH_3	H	H	KF	1	54
Cl	H	H	H	ZnF_2	1	73
H	CH_3	Cl	H	KF	1	76
SO_2F	H	H	H	KF	0.5	68
SO_2F	Cl	H	H	KF	0.42	72
OCH_3	OCH_3	H	SO_2F	KF	4.5	63

Note: From Davies and Dick.[329]

Arylsulfonyl fluorides will readily form from arylsulfonyl chlorides in mixtures of water and organic co-solvent at room temperature, and this is how they were first obtained in useful yields (Figure 1.24 and Table 1.5).[329] Halogen exchange in THF or acetonitrile remains the most common route to these compounds, with alkali metal or quaternary alkylamine fluorides used as fluorinating agents. Of potential relevance to ^{18}F chemistry, 18-crown-6 phase transfer catalyst has been shown to assist sulfonyl fluoride formation in acetonitrile solutions of KF.[330] Furthermore, small quantities of arylsulfonyl fluorides have been easily prepared in good yields by slowly passing the corresponding sulfonyl chloride through a fluoride- impregnated basic quaternary amine anion exchange resin.[331] Recently, Kim and Jang[332] prepared a series of arylsulfonyl fluorides in a one-pot procedure with *t*-butylammonium tetra(*t*-butyl alcohol) fluoride,[333]

where sulfonic acid was first converted *in situ* to sulfonyl chloride using Cl_3CCN and triphenylphosphine. As for approaches utilizing electrophilic aromatic substitution, the fluorosulfonation of benzaldehydes with HSO_3F-SbF_5 superacid has also been reported.[334] Aliphatic sulfonyl fluorides can be prepared in a straightforward fashion by way of chloro-for-fluoro conversion, albeit under anhydrous conditions because these functionalities are considered water- sensitive. The fluorination of arylsulfonic acids with diethylaminosulfur trifluoride (DAST) has been described once in the literature; toluenesulfonyl fluoride (TsF) was obtained from toluenesulfonic acid (TsOH) upon heating (80ºC).[335] More recently, DAST was used to fluorinate aliphatic sulfonates at room temperature (Figure 1.25).[336] The fluorination of aromatic and aliphatic (benzylic) disulfides with large excess of Selectfluor™ in refluxing acetonitrile:water (10:1) was shown to produce the corresponding sulfonyl fluorides in good yields.[337]

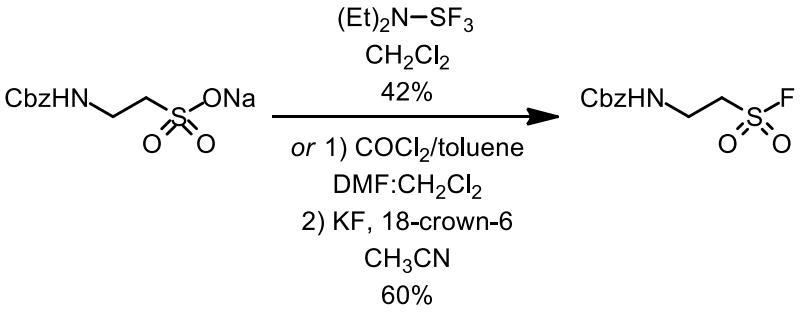

Figure 1.25. Two synthetic routes to protected taurine sulfonyl fluoride.

From Brouwer *et al.*[336]

1.6.3. *Serine Protease Inhibitors*

Serine proteases are the most widely distributed class of proteolytic enzymes.[338] A vast majority of serine proteases fall into three main categories based on their substrate preference: chymotrypsin-like, elastase-like, and trypsin-like.[339] Chymotrypsin-like enzymes normally cleave peptide bonds where the amino acid residue on the carbonyl side of the split bond is aromatic or lipophilic (i.e. Trp, Tyr, Phe, Met, Leu). In contrast, elastase-like enzymes tend to cleave at small side chain residues (Ala, Val, Ser, Leu). In most cases, extensive secondary enzyme specificity exists that recognizes amino acids removed from the site of cleavage. Chymotrypsin-like and elastase-like enzymes are found in many cell types and fluids, including leukocytes

(white blood cells), mast cells, and pancreatic juice. Most bacteria, yeast, viruses and parasites will also produce serine proteases as part of their survival strategy.

Small molecule sulfonyl fluoride- bearing compounds have the capacity to irreversibly inhibit serine protease catalysis.[340] Their mode of activity involves sulfonylation of the active site serine residue (Ser^{195}) to give a stable sulfonyl-enzyme derivative (Figure 1.27).[341, 342] In this regard, sulfonyl fluorides are widely used in biomedical research to help identify newly discovered proteolytic enzymes and prevent undesired proteolysis of polyamides during their production, isolation, purification, transport and storage. Two of the most commonly used anti-serine protease reagents are phenyl methylsulfonyl fluoride (PMSF) and 4-(2-aminoethyl) benzenesulfonyl fluoride (AEBSF; Figure 1.26).

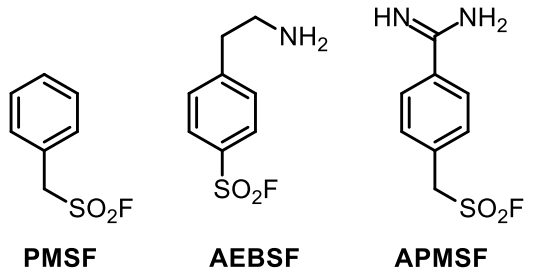

PMSF **AEBSF** **APMSF**

Figure 1.26. Some sulfonyl fluoride- based serine protease inhibitors.

Sulfonyl fluorides have also been investigated as potential therapeutics. However, many sulfonyl fluoride inhibitors exhibit fairly broad anti-serine protease activity, which currently limits their viability as drugs. Thus, research in this area has focussed on improving substrate specificity. Structure-activity studies have demonstrated that further functionalization of the aryl ring can significantly attenuate the reactivity of arylsulfonyl fluorides towards serine proteases.[343-345] Lively and Powers showed that the specificity of certain sulfonyl fluorides toward elastase, cathepsin G and chymotrypsin could be improved with structural changes in the inhibitor (Figure 1.27).[343] While significant differences in rate could be achieved among the inhibitors (up to 26,000 times), none of the compounds could be considered markedly potent. Inhibitory data for a few of the inhibitors is shown on Table 1.6. The instability of the *o*-substituted compounds was attributed to anchimeric assistance of the acylamido group in hydrolysis, a phenomenon that has been observed by other researchers.[326] In a related

experiment, *p*-amidinophenyl)methanesulfonyl fluoride (APMSF, Figure 1.26) was shown to inactivate bovine trypsin and human thrombin in equimolar quantities, and four other serine proteases when placed in 5- 10 molar excess.[345] Inhibition constants (*K*i) were between 1 and 2 µmol for each of these proteases. However, even large molar excesses of APMSF could not inactivate chymotrypsin or acetylcholinesterase. The authors conclude that despite a large degree of sequence homology between serine proteases, the design of certain selective sulfonyl fluoride inhibitors may be possible.

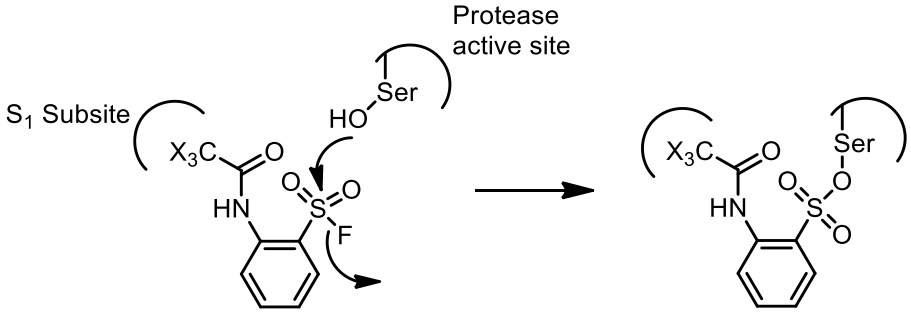

Figure 1.27. Potential mode of selectivity of sulfonyl fluoride- based serine protease inhibitors.

See Table 1.6. X = H or F.

Table 1.6. Inhibition of serine proteases with amidated benzene sulfonyl fluorides (see Figure 1.27).

SO_2F functionality	**Hydrolysis Rate (x 10^3 s^{-1})**	**Second order rate constant (k_{obs}/[I])**			
		HL elastase	**PP elastase**	**Cathepsin G**	**Chymotrypsin A_α**
o-(CF_3CONH)-	2.3	590	2300	12	48
m-(CF_3CONH)-	0	8.8	1.9	1.8	6.0
p-(CF_3CONH)-	0	4.8	0.28	2.3	4.7
o-(CH_3CONH)-	1.5	6.6	N.I.	N.I.	N.I.

Note: Adapted from Lively and Powers.[343] HL = human leukosyte; PP = pig porcine; N.I. = no inhibition after 1 h.

1.7. Thesis Objectives

The following thesis document outlines three avenues of radiosynthetic enquiry; each relate, in a general way, to improving the chemical and procedural means by which biological molecules are labelled with the positron- emitting radioisotope ^{18}F for PET imaging. The first two projects utilize the efficiently- prepared 2-[^{18}F]fluoropyridine prosthetic [^{18}F]FPy5yne ([^{18}F]-**1**) for the CuAAC pre-synthetic labelling of azide- modified biomolecules. Thus far [^{18}F]-**1** has only been used to ^{18}F- label a short, biologically irrelevant peptide sequence. Chapter 3 describes the successful conjugation of [^{18}F]-**1** to an antisense sequence of interest in cancer biology. In Chapter 4, [^{18}F]FPy5yne, along with mini-PEGylated derivative PEG-[^{18}F]PyKYNE, is coupled to bioactive peptide analogues targeting peptide receptors found overexpressed in certain cancers. This work was in support of small animal biodistribution and PET imaging trials by our biological collaborators. The final project (Chapter 5) details exploratory efforts to establish efficient protocols for the synthesis and bioconjugation of bifunctional arylsulfonyl [^{18}F]fluoride prosthetic molecules in aqueous mixtures and ambient temperatures. The stability of these compounds in buffered solutions and biological media is examined and discussed.

2. General Experimental Methods

2.1. Chemicals and Media

^{18}O-enriched water ([^{18}O]H_2O, >97 % pure) was purchased from Rotem Industries (Beer Sheva, Israel). Unless noted, reagents were purchased from Sigma-Aldrich (Oakville, ON, Canada) or Alfa Aesar (Ward Hill, MA, USA) in their standard purities. All organic solvents used in radiochemical synthesis were designated anhydrous. HPLC solvents were filtered prior to use. All reverse phase solid phase extraction (SPE) columns were purchased from Waters (Sep-pak®, Mississauga, ON, Canada). Anion exchange '^{18}F Trap & Release' columns were obtained from ORTG, Inc. (Oakdale, TN, USA). Clarity® brand size exclusion columns were obtained from Phenomenex (Torrance, CA, USA), while NAP-5 and NAP-10 columns were purchased from GE Healthcare (Mississauga, ON, Canada). Most TLC and radio-TLC was performed on 60F_{254} silica gel plates purchased from Sorbent Technologies (Atlanta, GA, USA). However, Instant Thin-Layer Chromatography silica gel- impregnated glass fibre (iTLC-SG) plates (Gelman Sciences, Ann Arbor, MI, USA) were used for the serum stability study in Chapter 5.

Desalted 5'-amino-C6-modified oligodeoxyribonucleotide bearing the sequence 5'-CCA TCC CGA CCT CGC GCT CC-3' (**NH_2-ODN**) was purchased from IDT (Coralville, IA, USA). The syntheses of peptides **N_3-BVD**, **N_3-BBN**, **N_3-BBN-PEG** and **H_2NO-BBN** was carried in the Guérin lab at Université de Sherbrooke.

For all radiochemical experiments, no-carrier-added [^{18}F]F^- was produced by cyclotron- produced proton bombardment of [^{18}O]H_2O water [^{18}O(p,n)^{18}F reaction].[346]

2.2. Analytical Methods

2.2.1. *Equipment*

Acrodisc® HT Tuffryn filters (PTFE, 0.45 µm) were purchased from Pall-Gelman (Ville St. Laurent, QB, Canada). Millex-HV filters (PVDF, 0.45 µm) were purchased from EMD Millipore (Billerica, MA, USA).

Radio-TLCs were obtained using a Bioscan System 200 Imaging scanner. Unless noted otherwise, ethyl acetate was used as eluent.

^{1}H NMR and ^{13}C NMR were recorded on either a Bruker AV 400 MHz apparatus or Bruker AV 600 MHz apparatus with cryoprobe attachment. Chemical shifts are reported relative to the hydrogenated residue of the deuterated solvents. ^{19}F NMR was collected on a Bruker AV 300 MHz device using $CFCl_3$ as internal standard.

Elemental analyses were performed on a Carlo Erba Elemental Analyzer EA 1108. High-resolution electron impact mass spectroscopy [HRMS(EI)] was performed on a Kratos MS50 apparatus. High-resolution electrospray ionization mass spectroscopy [HRMS(ESI)] was performed on a Micromass LCT time-of-flight mass spectroscope. Matrix- assisted laser desorption/ionization time-of-flight mass spectroscopy (MALDI-TOF) of modified oligonucleotides was performed on an Applied Biosystems Voyager-DE STR instrument with 3-hydroxypicolinic acid as matrix. MALDI-TOF of modified peptide sequences was carried out on an Applied Biosystems Voyager System 4311 with α-cyano-4-hydroxycinnamic acid as matrix.

2.2.2. *HPLC Parameters*

- System A Controller: Waters 600; Detectors: Waters 2487 Dual λ (absorbance) and Bioscan Flow-Count NaI (radioactivity).
- System B Controller: Agilent 35900E; Detectors: Agilent G1314B Variable λ (absorbance) and Bioscan Flow-Count NaI (radioactivity).
- Column A Phenomenex Luna PFP(2) C_{18} (250 × 10 mm, 5µm).
- Column B Phenomenex Clarity Oligo-RP (100 × 10 mm, 5 µm).
- Column C Phenomenex Jupiter Proteo C_{12} 90 Å (250 × 10 mm, 10 µm).
- Column D Phenomenex Luna PFP(2) C_{18} (150 × 4.6 mm, 3 µm).

- HPLC 1 System A, Column A. UV Detector: 260, 214 nm; Program: isocratic elution, flow = 4 mL/min, 50:50 MeCN:0.1 % TFA.
- HPLC 2 System A, Column B. UV Detector: 260, 214 nm; Program: gradient elution, flow = 4.75 ml/min, 10 % to 60 % MeOH in 5 % MeCN in triethylammonium acetate (TEAA) buffer (pH 7.0) over 20 min, then hold for 5 min.
- HPLC 3 System A, Column A. UV Detector: 280, 214 nm; Program: gradient elution, flow = 4 mL/min, 10 % to 100 % MeCN in 0.1 % TFA over 25 min, then hold for 5 min.
- HPLC 4 System A, Column C. UV Detector: 280, 214 nm; Program: gradient elution, flow, 4 mL/min, 0 % to 60 % MeCN in 0.1 % TFA over 25 min, hold for 10 min.
- HPLC 5 System B, Column C. UV Detector: 260 nm; Program: isocratic elution, flow = 4 mL/min, 55:45 MeCN:0.1 % TFA.
- HPLC 6 System B, Column C. UV Detector: 260; Program: isocratic elution, flow = 4 mL/min, 45:55 MeCN:0.1 % TFA.
- HPLC 7 System A, Column A. UV Detector: 280, 214 nm; Program: gradient elution, flow, 4 mL/min, 0 % to 60 % MeCN in 0.1 % TFA over 25 min, hold for 10 min.
- HPLC 8 System B, Column A. UV Detector: 280 nm; Program: gradient elution, flow = 4 mL/min, 0 % to 60 % MeCN in 0.1 % TFA over 25 min, 60 % to 100 % MeCN in 0.1 % TFA over 5 min.
- HPLC 9 System B, Column A. UV Detector: 280 nm; Program: gradient elution, flow = 4 mL/min, 10 % to 100 % MeCN in 0.1 % TFA over 25 min, hold for 5 min.
- HPLC 10 System B, Column D. UV Detector: 280 nm; Program: gradient elution, flow = 1 mL/min, 10 % to 100 % MeCN in 0.1 % TFA over 25 min.
- HPLC 11 System B, Column D. UV Detector: 280 nm; Program: gradient elution, flow = 1 mL/min, 0 % to 60 % MeCN in 0.1 % TFA over 25 min, 60 % to 100 % MeCN in 0.1 % TFA over 5 min.
- HPLC 12 System A, Column A. UV Detector: 260 nm; Program: isocratic elution, flow = 4.25 mL/min, 70:30 MeOH:H_2O.
- HPLC 13 System A, Column A. UV Detector: 260 nm; Program: isocratic elution, flow = 4.25 mL/min, 60:40 MeOH:H_2O.
- HPLC 14 System A, Column A. UV Detector: 260 nm; Program: isocratic elution, flow = 4.25 mL/min, 70:30 MeCN:H_2O.
- HPLC 15 System A, Column A. UV Detector: 260 nm; Program: isocratic elution, flow = 4.25 mL/min, 70:30 MeCN: 0.1 % TFA.
- HPLC 16 System A, Column A. UV Detector: 260 nm; Program: isocratic elution, flow = 3 mL/min, 70:30 MeCN: 0.1 % TFA.

- HPLC 17 System A, Column: C. UV Detector: 280, 214 nm; Program: gradient elution, 10 % to 100 % MeCN in 0.1 % TFA over 25 min, hold for 5 min, flow = 4 mL/min.
- HPLC 18 System A, Column C. UV Detector: 260 nm; Program: isocratic elution, flow = 3 mL/min, 70:30 MeCN: 0.1 % TFA.
- HPLC 19 System B, Column C. UV Detector: 280 nm; Program: gradient elution, flow, 4 mL/min, 0 % to 100 % MeCN in 0.1 % TFA over 25 min, hold for 5 min.

3. ^{18}F- labelling of oligonucleotides with [^{18}F]FPy5yne

The chemical synthesis and radiochemistry described in this chapter was carried out by James Inkster. This chapter was published in *Nucleosides, Nucleotides and Nucleic Acids.*[288]

3.1. Nuclear Antisense Imaging

Molecular imaging of radiolabelled DNA analogues prepared complementary to disease- upregulated or disease- specific nucleic acids offers an inimitable means to study the genetic origins of these conditions in living systems. Apart from the obvious diagnostic advantage to be gained through the detection of early paraphysiologic markers (even, presumably, before the onset of symptoms), DNA- and RNA- targeting radioprobes might allow for the determination of early cellular response to treatment, the assessment of nucleic acid- based therapeutics, and the differentiation between disease phenotypes. Yet for all its realized potential, the general application of antisense technologies for the imaging of endogenous gene expression has not been achieved. In regard to stability, cellular uptake and biodistribution, antisense imaging agents and therapeutics share common challenges (as discussed in Sections 1.3.3- 1.3.6). However, concerns related to insufficient mRNA expression levels are unique to imaging applications. At any given time, a cell may contain mRNA in concentrations of 1- 1000 pM. One might expect a many-fold increase in mRNA copy number as the result of viral or cancerous gene overexpression. Lendvai *et al.* noted even a cell bearing 500,000 total mRNA (100 pM) would possess ~250 copies of a unique sequence and this is within the range thought imagable by PET (100- 1000 copies);[347] however, the authors concede that this is an insufficient argument given the large degree of uncertainty associated with counting cellular mRNAs. Nevertheless, some have argued that mRNA transcription rate should be considered a more important indicator of success than copy

numbers. This is based on the observation that antisense ODNs accumulate in specific tissues in orders-of-magnitude higher concentrations than what could be expected from estimated steady state mRNA levels.[348] Furthermore, antisense molecules have been found at higher levels in the nucleus than in the cytoplasm, suggesting that pre-mRNA serves as an additional target for antisense probes.[349]

Attempts to validate the concept of antisense imaging *in vitro* have largely been successful. To this end, multiple groups have shown that a variety of radiolabelled DNAs will accumulate in different cell types in greater concentrations relative to control sequences. The Hnatowich group was instrumental in these first crucial radio-experiments, showing that ^{99m}Tc-MAG_3- labelled phosphorothiolate DNA accumulated in kidney cancer cells bearing protein kinase RIα mRNA in statistically greater amounts than sense and random probes.[348] Furthermore, it was shown that this process was inhibited by unlabelled PS-DNA, and that radioactivity did not accumulate in a non- RIα cancer cell line. A similar result was observed by the same group using a ^{99m}Tc-HYNIC-labelled sequence antisense to the *c-myc* oncogene in breast cancer cells.[350] A third seminal investigation involving ^{99m}Tc- labelled ODNs involved the *in vivo* targeting of mRNA transcribed from *mdr1*, which encodes the multidrug resistance protein P-glycoprotein (Pgp). Transcriptional suppression of *mdr1* by antisense phosphorothioate oligonucleotides has shown to effectively inhibit expression of Pgp in human tumour xenografts.[351] Thus, a ^{99m}Tc- labelled PS-ODN antisense to *mdr1* was shown to accumulate in KB-G2 (*mdr1*++) epidermoid tumours in mice at statistically higher levels relative to labelled sense controls.[352] Accumulated radioactivity was much lower in the KB-31 cell line, where *mdr1* is endogenous but not overexpressed. This model system has been used extensively to test the efficacy of novel modifications and delivery agents intended to improve the tumour- targeting capabilities of other radiolabelled nucleic acid-based molecular imaging agents.[352-354] The transcription rate of *mdr1* in KB-32 cells was measured using a novel radio-method whereby the concentration of functional cellular mRNA was first zeroed using an unlabelled complementary strand, then the rate of new mRNA was monitored using a ^{99m}Tc- labelled antisense probe.[349] In this fashion, the transcription rate for this system was estimated to be ~2000 copies per min per cell, enough to explain the observed accumulation of radio-probe (10^6 copies over 10 h).

Theoretically, the ideal means of transmembrane delivery for an DNA- based radiopharmaceutical is a non-targeted approach, such that the sequesterization of radiation is based unambiguously on the antisense effect. Nevertheless, the use of non-selective cationic complexes to aid antisense imaging remains underdeveloped compared to the use of CPPs and proteomic targeting vectors (Section 1.3.6). However, the Hnatowich group found significantly increased ^{99m}Tc-PS-ODN accumulation and hybridization to *c-myc* mRNA in tumour cell cultures when the radioprobe was encapsulated into a cationic liposome.[350] Later, Zheng and Tan showed that the same tracer could be used to image colon cancer xenografts *in vivo*.[355] The ^{99m}Tc-PS-ODN accumulated well into target tissue after 7 h (13.5±0.2 %) and the tumour was visible at 2 h, but tumour-to-contralateral tissue ratios (max = 1.7±0.3 %, 2 h) were low.

While numerous reports detailing *in vitro* hybridization and *in vivo* biodistribution of antisense radio-probes exist, examples of *in vivo* antisense imaging remain few.[347] Dewangee *et al.* were the first to image *c-myc* oncogene mRNA in tumour- bearing mice with an ^{111}In-labelled PS-ODN 15mer.[356] Although this group saw more success with other isotopes and sequences,[357] this unverified protocol remained the state-of-the-art for many years. Roivainen *et al.* showed that ^{68}Ga(DOTA)- labelled PS- and OMe-17mers antisense to a codon 12 mutant of the *KRAS* oncogene (*KRAS G12D*) could be used to image the A549 lung carcinoma in rats.[358] Apart from verifying the functional integrity of the experiment with labelled control sequences, the authors also showed that the antisense probes were not taken up into a different tumour type harbouring wild-type *K-ras*. The Pardridge group published a remarkable series of experiments showing that mRNA expressed in rat *brains* could be targeted and (invasively) imaged using *ex vivo* autoradiography. In the first experiment, the target was glial tumours which were stably transfected with the luciferase gene.[359] The antisense construct contained ^{125}I-labelled PNA conjugated *via* biotin/streptavidin tether to a blood-brain-barrier (BBB)- penetrating monoclonal antibody (OX26). The second experiment showed that a similar approach could be used to image Huntington's disease in a transgenic mouse model.[360] Finally, endogenous oncogene expression was imaged using an ^{111}In-PNA-OX26 chimera targeting upregulated *CAV* mRNA.[361] Impressively, a similar construct possessing PNA antisense to a native, yet underexpressed, oncogene did not accumulate in the tumours. Sun *et al.* challenged four newly- rationalized antisense sequences [^{64}Cu(DOTA)-PNA-

K_4] against human *unr* mRNA which is uniquely expressed in MCF7 breast cancer tumours in mice. Although all the sequences exhibited high *in vitro* affinity for the same mRNA,[362] two sequences showed similar biodistribution patterns yet significantly different levels of contrast in PET images, while the other two exhibited unique biodistributions and were not significantly taken up into tumours.[363] This experiment showcases the ongoing questions and challenges facing researchers seeking a general antisense imaging strategy.

In recent years, the Wickstom group has been at the forefront of nuclear antisense imaging. Their preferred targeting agent is PNA that has been coupled to a translocating peptidergic agent. Early experiments from these researchers utilized chimeras consisting of GDAGG-Aba peptide (for ^{99m}Tc chelation), PNA 12mer (for targeting *CCND1*[364] or *MYC*[365] mRNA in MCF7 tumours) and D-inverso cyclic analogue of insulin growth factor 1 (IGF1) for cellular penetration and cell specificity (Figure 3.1). The complete synthesis of these complex peptide-PNA-peptide species, including cyclization of the D-inverso IGF1 disulfide bond, was performed on solid phase support.[366] Cell surface IGF1 receptors are overexpressed in MCF7 breast cancer, and thus these POCs can be thought of *dual specificity* molecular probes. For both *CCND1* and *MYC* targeting, tumour-to-muscle ratios (% ID/g:% ID/g) for the antisense and mismatch compounds are very similar, but at 12 h only the antisense tracers visualized the tumours. The authors suggest that this seemingly inconsistent result arises from the fact that in both cases the tumours contain necrotic cores which cause their masses to be overestimated upon resection. Later, the *CCND1* mRNA/MCF7 system served as a testing ground for a ^{64}Cu-labelled PNA-IGF1 antisense probe.[367] In this case, the authors used an effective macrocyclic ^{64}Cu chelator (DO3A, see Figure 1.11)[368] to minimize *in vivo* decupration. *KRAS G12D* (vs. *KRAS* wild-type) mRNA in pancreatic cancer xenografts were also imaged in this fashion.[369] In both cases, image contrast of tumour vs. contralateral tissue was very high (7.9±2.0 and 8.6±1.4 respectively). The most recent report from this group involves attempts to place multiple imaging metals to a single antisense strand. To this end, PNA-IGF1 bioconjugates antisense to *KRAS G12D* mRNA were affixed *via* two amino-ethoxy-ethoxy-acetyl (AEEA) spacers to polydiamidopropanoyl (PDAP) dendrimers. The dendrimers were previously modified with DOTA chelators at their primary amines (four DOTA chelators per dendrimer),

which were used to conjugate up to 16 ^{111}In isotopes per probe. It should be noted that the primary goal of this experiment was to assess the validity of this approach for use in functional MRI imaging with Gd^{3+}. Nevertheless, scintigraphic tumour-to-muscle ratios in pancreatic cancer xenografts for fully matched [^{111}In]$_n$-PDAP$_m$- AEEA2-*KRAS G12D*-AEEA-IGF1 chimeras increased from 3.1±0.2 where *n*=2, *m*=1, to 4.1±0.3 where *n*=8, *m*=3, to 6.2±0.4 at *n*=16, *m*=4. The more functionalized compounds exhibited longer clearance times and less renal excretion. This is a fine example of how radiometals can serve as surrogates for other isotopes that are less easy to detect.

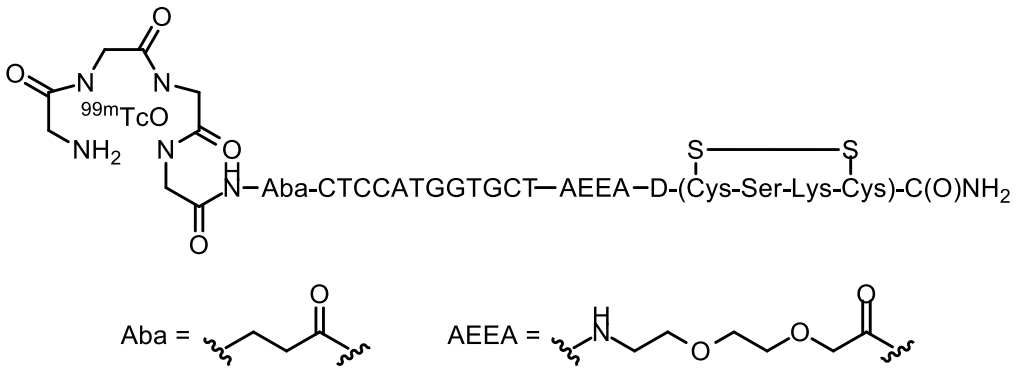

Figure 3.1. Representation of a ^{99m}Tc- labelled peptide-PNA chimera for the dual specificity SPECT imaging of cancer- associated CCND1 mRNA.

As described in Tian *et al.*[364]

3.2. Antisense- Related Imaging

For those pursuing nuclear antisense imaging, the synthesis of nucleic acid-based probes for non-antisense applications is of general interest. With regard to aptamer technologies, a thrombin- targeting sequence bearing a stannylated 2'-deoxyuridine residue was labelled with ^{123}I for SPECT imaging.[470] Later, a ^{99m}Tc-(MAG_2)-labelled aptamer was used to image extracellular matrix protein tenascin-C in a variety of tumour types *in vivo*.[370] The ^{99m}Tc-chelate significantly altered aptamer pharmacokinetics, but the introduction of a long PEG tether (PEG3400) restored renal and bladder clearance to the radioligand. Because the aptamer is rapidly degraded in the blood but not the tumour, excellent tumour-to-blood ratios could be achieved at longer time points (50 at 3 h). At 20 h, only the tumour is visible by gamma camera scintillography.

Few radiolabelled siRNAs have so far been prepared. Thusfar, the primary role for these bioconjugates has been the evaluation of the therapeutic potential of RNAi. The cellular uptake and biodistribution of ^{99m}Tc[371]- and ^{111}In[372]- labelled siRNAs has been examined, as has the stability of ^{111}In-siRNA-poly(ethyleneimine) constructs.[373] ^{64}Cu(DOTA)- labelled siRNA was used to compare the efficacy of non-targeted and transferrin-targeted polycation delivery agents.[373] Finally, siRNAs labelled with [^{18}F]FPyBrA (Figure 1.20 and Section 1.5) were used to probe the effect of stabilizing nucleobase modifications on the RNAi mechanism.[295] It was discovered that 2'-F-modified siRNA showed improved bioavailability over 2'-OMe and 2'-OH species but that this did not translate to better gene knockdown.

3.3. Objectives

As described in Section 1.3.5, a host of nucleic acid- based therapeutics and their associated delivery systems have been explored.[164] In parallel, a small number of radiolabelled antisense sequences have been developed for the non-invasive visualization of mRNA *in vivo* (Section 3.1). The successful and general application of this strategy might eventually allow for the clinical diagnosis and staging of cancer and other pathological processes that upregulate gene expression.[354, 361, 363, 374] Additionally, tracer analogues of antisense drugs might be used to assess the bioavailability of these compounds in living systems.[230, 295, 375] Taken overall, the impressive characteristics of PET make it an attractive modality for these purposes. However, in the case of a short-lived radionuclide such as ^{18}F, highly optimized radiosynthetic procedures are essential to the successful development of the molecular imaging platform. Synthetic challenge is further compounded when the targeting agent is a sensitive, functionally complex macromolecule. In regard to antisense ^{18}F PET agents specifically, a number of labelling strategies have already been developed for the synthesis of these radiotracers (see Section 1.4). However, despite the fact that the first reported synthesis of a ^{18}F-labelled oligonucleotide dates back to 1995,[376] *not one PET image of gene expression using ^{18}F antisense probes has yet emerged.* This marked lack of progress can at least in part be attributed to the persistent complexity of ^{18}F ODN development.

The alkyne- bearing 2-[^{18}F]fluoropyridine prosthetic group [^{18}F]FPy5yne ([^{18}F]-**1**]) has proven an effective means to ^{18}F- label bioactive peptides *via* CuAAC bioconjugation (Section 1.5).[379] It was hypothesized that this easy-to-synthesize ^{18}F prosthetic might also be useful for the preparation of nucleic acid- based probes for antisense imaging. Thus, the aim of Chapter 3 was to establish a chemical protocol for the synthesis and radiolabelling of a 5'-azide- modified antisense oligodeoxyribonucleotide (**N_3-ODN**) with [^{18}F]-**1**. The radiosynthesis should be robust and efficient enough to be realistically amendable to the preparation of CPP-antisense chimeras for preclinical PET study. Although only a model compound, the DNA sequence chosen for ^{18}F- labelling is antisense to multidrug resistance 1 (*mdr1*) mRNA. It has been used previously to assess the validity of other potential antisense imaging agents and transfection techniques in the KB-G2 (Pgp++) cell line.[377]

3.4. Non-Radioactive Small Molecule Syntheses

Important note! This chapter includes the details for the preperation of azide-bearing molecules. The synthesis, purifiction and handling of all azides should be done with care as these compounds are known to explode when subject to heat or concussive force. Organic azides with low carbon and oxygen content relative to nitrogen content are particularly dangerous. In practice, molecules in which the ratio of C + O atoms/ total N atoms is ≤3 should be kept impure or in solutions and stored at <0 ºC. Compounds with ratios ≤1 should only be prepared as a limiting reaction intermediate, if at all. The use of chlorinated solvents may result in the production di- and tri-azidomethane and should be avoided.

3.4.1. *N-Succinimidyl 5-azidovalerate (4)*

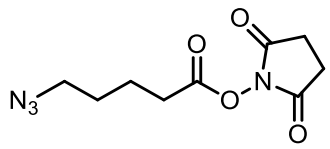

This synthesis was based on reported methods.[284, 378] *N*-Succinimidyl 5-azidovalerate (**4**) was prepared in a three-step process (Figure 3.2). 5-Bromo-1-ethylvalerate (**5**, 5.01 g, 23.9 mmol) was dissolved in DMSO (40 mL). Sodium azide (2.33 g, 35.9 mmol) was added with stirring and the reaction was heated (50- 60 ºC) for 20 h. The reaction was quenched with water (200 mL) and extracted with diethyl ether (3 x 300 mL). The organic portions were pooled, washed with brine (25 mL), and dried over Na_2SO_4 to afford crude 5-azido-1-ethylvalerate (**6**, 3.94 g, 96 %). After concentration, this compound was dissolved in THF (20 mL) and cooled to 0 ºC. $LiOH_{(aq)}$ (2 M, 20 mL) was added and the reaction was allowed to warm to room temperature over 90 min. The reaction was poured into ether (100 mL) and water (50 mL) and the two phases were separated. The aqueous portion was acidified to pH = 0 with conc. HCl and extracted into ethyl acetate (3 x 100 mL). The extract was dried overnight over Na_2SO_4 to yield 3.28 g (99 %) of crude 5-azidovaleric acid (**7**). After concentration and drying *in vacuo*, **7** was dissolved in dry CH_2Cl_2 (45 mL) under N_2 and *N*- hydroxysuccinimide (2.76 g, 24.0 mmol) was added, followed by 1-(3-dimethylaminopropyl)-3-ethylcarbodiimide hydrochloride (EDC, 4.62 g, 24.1 mmol). The reaction was left to stir for 26 h, after which it was quenched with water and the product extracted three times into CH_2Cl_2, then washed once with water and once with brine. Concentration afforded pure oil *N*-succinimidyl 5-azidovalerate (**4**, 5.29 g, 92 % over three steps) as determined by TLC and NMR.[284] ^{1}H NMR(400 MHz, $CDCl_3$): δ: 1.52-1.77 (m, 2H); 1.77-1.96 (m, 2H); 2.65 (t, *J* = 7.1 Hz, 2H); 2.83 (br s, 4H); 3.33 (t, *J* = 6.5 Hz, 2H). HRMS(EI) calcd. for $C_9H_{13}N_4O_4$ $[M+H]^+$: 241.0937. Found: 241.0933. Anal. Calcd. for $C_9H_{12}N_4O_4$: C, 45.00; H, 5.03; N, 23.32. Found: C, 44.77; H, 5.06; N, 23.58. *Caution! Azides such as **8, 9, 7** can explosively decompose when subject to heat or shock. If replicating the above procedure, future workers are strongly advised to substitute CH_2Cl_2 for another reaction solvent.*

3.4.2. *Tris[(1-benzyl-1H-1,2,3-triazol-4-yl)methyl]amine (10, TBTA)*

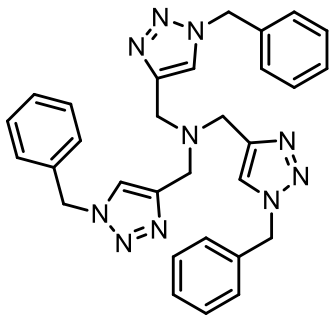

This synthesis is based on a reported method.[266] To a solution of tripropargylamine (1.16 g, 8.81 mmol) in MeCN (15 mL) was added benzyl azide (5.27 g, 39.6 mmol), followed by 2,6- lutidine (1.0 mL, 8.81 mmol). After cooling to 0 ºC, $Cu(CH_3CN)_4PF_6$ (0.13 g, 0.34 mmol) catalyst was added and the reaction was allowed to warm to RT over 24 h. The reaction mixture was concentrated, dissolved in a minimum of acetone, and water was added until a precipitate was first observed. The mixture was left overnight, then filtered and washed with ice-cold water to afford 1.47 g (63 %) of TBTA (**10**) as an off- colour white powder. M.P. = 137-141 ºC (Lit.[266] 138-139 ºC). ^{1}H NMR (600 MHz, CD_3OD): δ 3.69 (s, 6H), 5.54 (s, 6H), 7.30–7.25 (m, 6H), 7.37- 7.30 (m, 9H), 7.90 (s, 3H). ^{13}C NMR (151 MHz, CD_3OD): δ 54.89 [3 x CH_2, 3 x CH_2]; 125.46 [3 x CH]; 129.05 [CH]; 129.55 [6 x CH]; 130.03 [6 x CH]; 136.84 [C]; 145.75 [C]. MS(EI): 530, 531. Anal. Calcd. for $C_{30}H_{30}N_{10}$: C, 67.90; H, 5.70; N, 26.40. Found: C, 67.90; H, 5.74; N, 26.36.

3.5. Non-radioactive Bioconjugate Syntheses

3.5.1. *5'-Azide- modified oligonucleotide (N_3-ODN)*

Desalted 5'-amino-C6-modified oligodeoxyribonucleotide (**NH_2-ODN**, 226 nmol) was dissolved in phosphate buffered saline (PBS, 100 µL, 150 mM, pH 7.2). An aliquot (50 µL) of 53 mg/mL *N*-succinimidyl 5-azidovalerate (**4**, 11 µmol) in DMF was added. The reaction was shaken vigorously for 3.5 h, then diluted with TEAA buffer (1.5 mL, 5 mM, pH 7.0), purified on a Clarity® desalting column (3 µm, 200 mg), and concentrated by centrifugal evaporation to afford **N_3-ODN**. This material was subsequently used in a

CuAAC ligation as is; however, analytically pure material could be obtained by further HPLC purification (HPLC 2, R_t = 10.2 min), followed by vacuum concentration and desalting on an NAP-10 size exclusion column. MALDI-TOF (*m/z*): calcd. 6241.2 $[M+H]^+$. Found. 6241.6.

3.5.2. *5'-^{19}F-modified oligonucleotide (^{19}F-ODN).*

A sample of **N_3-ODN** (62.5 nmol) in a 2 mL microcentrifuge tube was dissolved in 100 µL PBS (150 µM, pH 7.2) and 240 µg (1.2 µmol) of FPy5yne (**1**) in DMF (25 µL) was added, followed by DIEA (2.2 µL, 1.2 µmol). To this mixture was added a freshly prepared solution (25 µL) of $Cu(CH_3CN)_4PF_6$ (19.2 mg/mL) and TBTA (20.8 mg/mL) in DMF. The sample was shaken vigorously for 48 h, diluted with water (200 µL) then passed through a Millex-HV filter (0.45 µm) to remove insoluble material. The product oligonucleotide **^{19}F-ODN** was then purified by HPLC (HPLC 2, R_t = 12.4 min). The collected eluent was concentrated *in vacuo* and desalted on a NAP-10 size exclusion column. MALDI-TOF (*m/z*): calcd. 6433.4 $[M+H]^+$. Found. 6438.9.

3.6. Radiochemical Syntheses

Radiosyntheses were carried out at the TRIUMF Chemistry Annex. Typical production of $[^{18}F]F^-$ was 65- 100 mCi at EOB after a 10 µA, 5 min irradiation.

3.6.1. *[^{18}F]FPy5yne, [^{18}F]-1*

The radiosynthesis of [^{18}F]-**1** for oligonucleotide labelling was based on a previously described protocol, with some modifictions.[379] $[^{18}F]F^-$ in $[^{18}O]H_2O$ was concentrated on an '^{18}F trap-and-release' column (ORTG, Inc.), which was activated with water (5 mL). $[^{18}F]F^-$ was eluted with a mixture of $K_{2.2.2.}$ (3.4 mg) and K_2CO_3 (14.1 mg) in MeCN:H_2O (1 mL:0.3 mL). The mixture was dried in a 5 mL screw-cap vial at 110 ºC under a stream of He. After concentration, another portion of MeCN (1 mL) was added and the reaction was heated to dryness. This step was repeated once more. The vial was removed from heat and cooled in tap water, then trimethylammonium triflate precursor **3** (3.5 mg) in DMSO (500 µL) was added. The vial was resealed and heated to 110 ºC for 15 min. After heating, [^{18}F]-**1** was cooled in tap water and transferred into

H_2O (17 mL). The ^{18}F prosthetic compound was trapped on a tC_{18} SPE column [activated previously with MeOH (3 mL) and water (10 mL)], washed with water (5 mL), and eluted from the column with MeCN (1 mL).] [^{18}F]-**1** was separated from precursor molecule **3** and [^{18}F]fluorodemethylation[106] contaminant 2-dimethylamino-3-(hex-5-ynyloxy)pyridine (**11**; Figure 4.3) by semi-preparative HPLC (HPLC 1). [^{18}F]-**1** was extracted from HPLC eluent using another tC_{18} column, eluted off the column with CH_2Cl_2 (2 mL), and *carefully* concentrated to ~100- 150 µL (residual H_2O) in a 5 mL conical glass vial under a stream of He at RT over 10 min.

3.6.2. *5'-^{18}F-modified oligonucleotide (^{18}F-ODN).*

Dimethylformamide (100 µL) was added to an aqueous solution of [^{18}F]-**1** (~150 µL, 20.4 mCi) and the prosthetic molecule was transferred to a microcentrifuge tube (84 % efficiency) containing **N_3-ODN** (200 nmol) in PBS (100 µL, 150 mM, pH 7.2). To this mixture was added a solution of Cu^{I}-TBTA complex (50 µL), followed by 2,6-lutidine (4 µL, 17.3 µmol). The Cu^{I}-TBTA slurry was prepared immediately beforehand by addition of TBTA (15.8 mg, 29.8 µmol) in DMF (250 µL) to CuBr powder (99.9999 %, 2.7 mg, 18.8 µmol), followed by the addition of water (250 µL). The reaction was heated at 75 ºC for 20 min, then diluted to 1 mL with PBS (150 mM, pH 7.2), centrifuged for 2 min (15,668 × *g*) and purified by HPLC (HPLC 2). The transfer efficiency in this step was 84%. The collected portion (~6 mL) was concentrated to ~100 µL at 110 ºC under a stream of He, diluted with H_2O (400 µL), and desalted on a NAP-5 size exclusion column. The final formulation (1 mL) contained 4.03 mCi of **^{18}F-ODN**.

3.7. Results and Discussion

3.7.1. *Non-Radioactive Chemistry*

N-Succinimidyl 5-azidovalerate (**4**) has been used previously as a means to modify ODNs for CuAAC coupling with fluorescent pendant groups.[284] The activated NHS ester was efficiently synthesized from 5-bromo-ethylvalerate (**5**) in three steps (92 % overall yield; Figure 3.2). Simple extraction of the final product into CH_2Cl_2, followed by aqueous washing, afforded pure material.

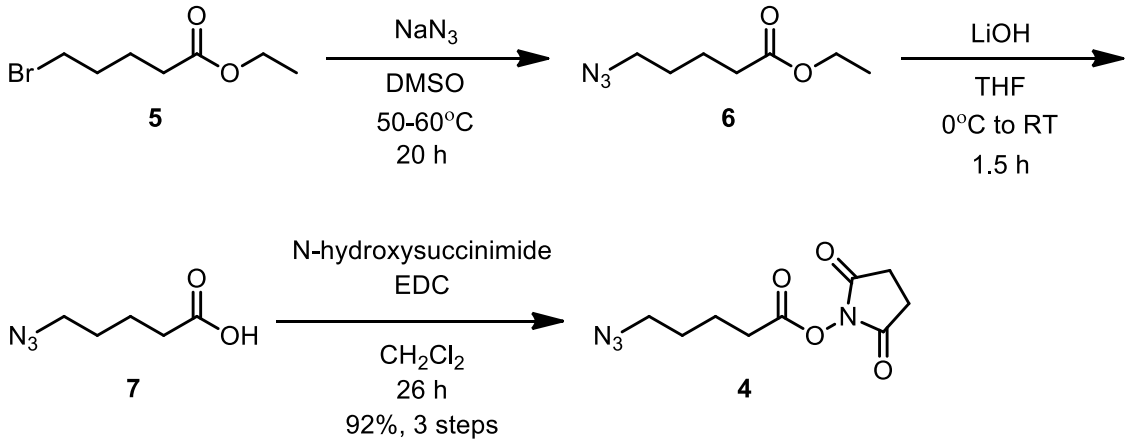

Figure 3.2. Synthesis of N_3- bearing prosthetic 4 for the modification of aminated oligonucleotides.

For the purposes labelling ODN with ^{18}F by way of Cu^{I}-catalyzed azide/alkyne cycloaddition, commercially available 5'- aminohexyl oligonucleotide 20mer **NH_2-ODN** was converted to 5'-azide modified **N_3-ODN** *via* acylation with **4**. Analytical standard **^{19}F-ODN** was obtained *via* bioconjugation of **N_3-ODN** and [^{18}F]-**1** in the presence of TBTA, tetrakis(acetonitrilo)copper(I) hexfluorophosphate [$Cu(CH_3CN)_4PF_6$] and *N, N*-diisopropylethylamine (DIEA). The choice of Cu catalyst was based on its solubility in DMF. The expected MALDI-TOF mass spectra of modified oligonucleotides **N_3-ODN** and **^{19}F-ODN** were obtained (see A1. 1 and A1. 2 of Appendix, respectively).

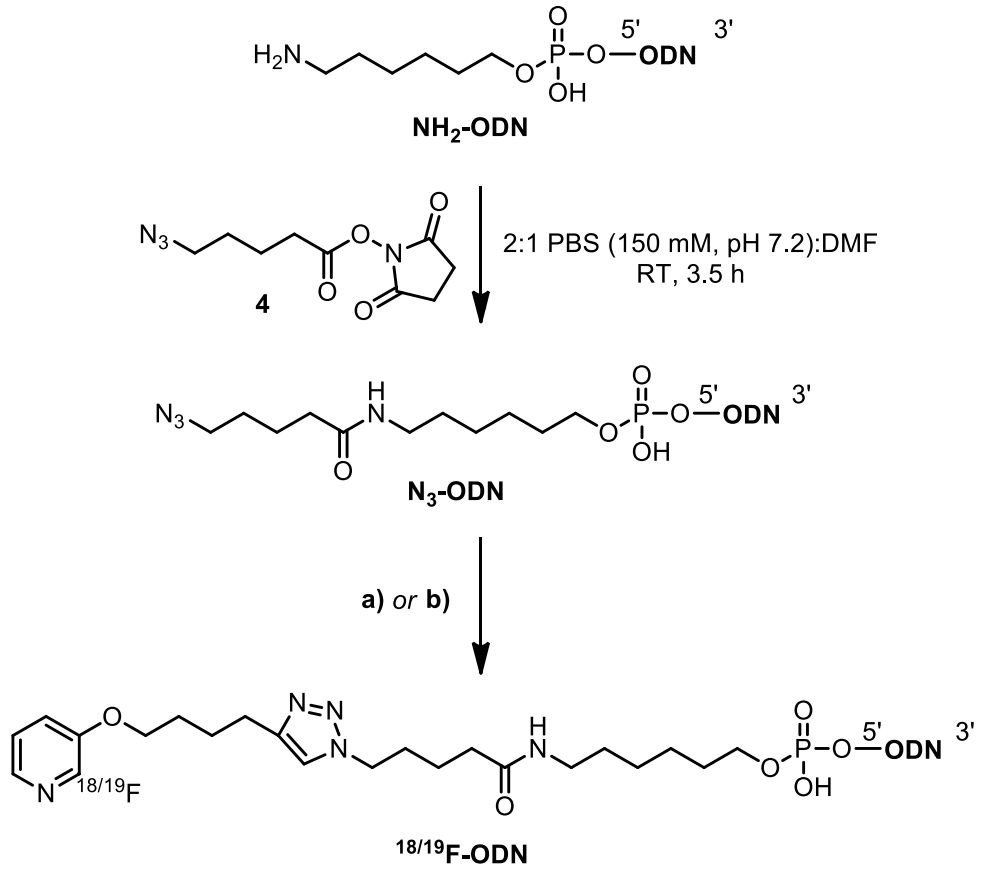

Figure 3.3. Bioconjugate synthesis of N_3-ODN and $^{18/19}$F-ODNs.

a) **1**, $Cu(CH_3CN)_4PF_6$, TBTA, DIEA in 4:1 PBS:DMF, RT, 48 h. b) [^{18}F]-**1**, CuBr, TBTA, 2,6-lutidine in ~2:1 PBS:DMF, 75 ^{o}C, 20 min.

An earlier synthetic protocol for CuAAC- based PO-ODN ligations reported oligonucleotide strand scission when Cu^{I} salt was used as catalyst alone, without TBTA chelate.[283] We confirmed this to be the case for PS-ODNs as well. As mentioned earlier, it has been hypothesized that the [1,2,3]-triazole functionalities of the TBTA tetradentate ligand protect the metal center from unwanted oxidation and subsequent destructive radical formation, disassociating only to allow the formation of the catalytic Cu^{I}-acetylide/ligand complex.[266] As for the addition of DIEA during non-radioactive coupling reactions, this nitrogen base has been reported to inhibit side product formation in peptide-based CuAAC radiobioconjugations.[272] Later, during radiochemical preparations, we found 2,6-lutidine to be equally efficient.

3.7.2. *Radiochemistry*

[^{18}F]FPy5yne ([^{18}F]-**1**) was synthesized from its 2-trimethylammonium triflate pyridine precursor (**3**) using reported K[^{18}F]F-$K_{2.2.2}$/K_2CO_3 conditions (DMSO, 110 ºC, 15 min; Figure 1.21).[379] Two minor modifications were made to the described protocol. First, the amount of DMSO used in the [^{18}F]fluorination reaction was reduced from 0.7 mL to 0.5 mL. Second, in order to minimize product loss of [^{18}F]-**1** due to evaporation, concentration of the purified prosthetic group from methylene chloride was performed at RT (instead of 50 ºC) over 10 min. As such, the eluent was concentrated to ~100- 150 µL, the bulk of which is presumably residual water. Average radiochemical incorporation of [^{18}F]fluoride was 90±2 % (*n*=4) as determined by radio-TLC (Figure 3.4). Although this nucleophilic substitution proceeds adequately in acetonitrile, a small radio-impurity (denoted **α** in Figure 3.4) was observed when this solvent was employed. Thus, preparative radiosyntheses of [^{18}F]-**1** for this project was carried out exclusively in DMSO. The NDC, collected yield of [^{18}F]-**1** from **3** (30±2 %; *n*=4) is consistent with the yield previously reported (24 %).[379] Typical preparation time was 90 min from start-of-synthesis (SOS).

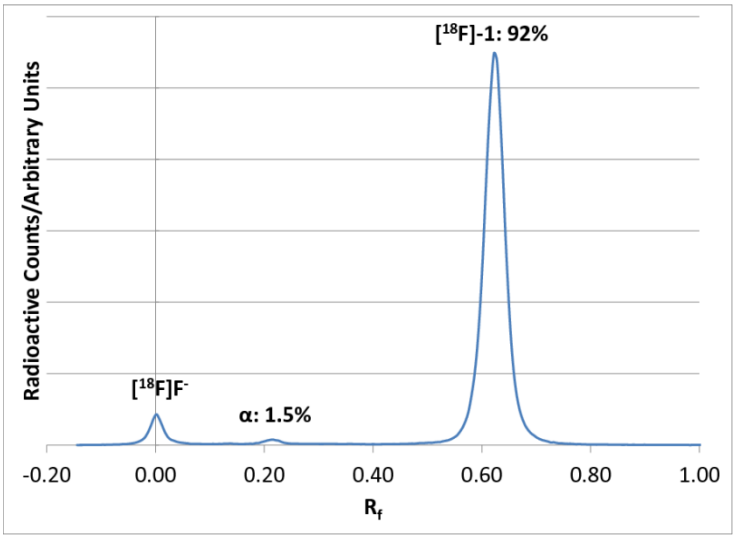

Figure 3.4. Representative radio-TLC of a [^{18}F]FPy5yne reaction mixture.

Reaction conditions: K[^{18}F]/$K_{2.2.2}$/K_2CO_3, MeCN, 110 ºC, 15 min.

^{18}F-labelled antisense oligonucleotide **^{18}F-ODN** was prepared by mixing the azide-modified **N_3-ODN** with [^{18}F]-**1** in the presence of CuBr (10 equiv.) and TBTA (15

equiv.) for 15 min at 75 ºC (Figure 3.3). We found that 99.9999 % CuBr afforded products of higher radiochemical purity compared to the use of $Cu(CH_3CN)_4PF_6$, which was employed for the non-radioactive preparation of **^{19}F-ODN** standard. This is consistent with a previous report describing CuAAC ligations to an azide-modified cell surface protein of *E.Coli*, where the purity of the copper catalyst had a marked effect on reaction yield.[257] The solvent matrix was a mixture of PBS and DMF (~2:1 including the residual water remaining after [^{18}F]-**1** concentration). An analytical HPLC trace of the preparative reaction mixture is shown in Figure 3.5. In this case, the efficiency of the bioconjugation reaction could not be estimated with good certainty by HPLC, as the hydrophobic prosthetic group is only partially soluble in strong buffer, which was used to quench the reaction prior to HPLC purification. Indeed, upon transfer of the mixture to HPLC, 16 % of the total radioactivity remained in the microcentrifuge tube. However, the collected, non-decay corrected bioconjugate yield, which is ultimately a more meaningful value, was found to be 18±3 % (*n*=3). After HPLC purification and desalting by size exclusion chromatography, the non-decay corrected, collected yield of **^{18}F-ODN** was 4±1 % (*n*=3) from EOB (25±1 % DC). The chemical nature of **^{18}F-ODN** was confirmed by way of HPLC co-injection with its ^{19}F standard (Figure 3.6). Shortest total preparation time was 276 min from SOS.

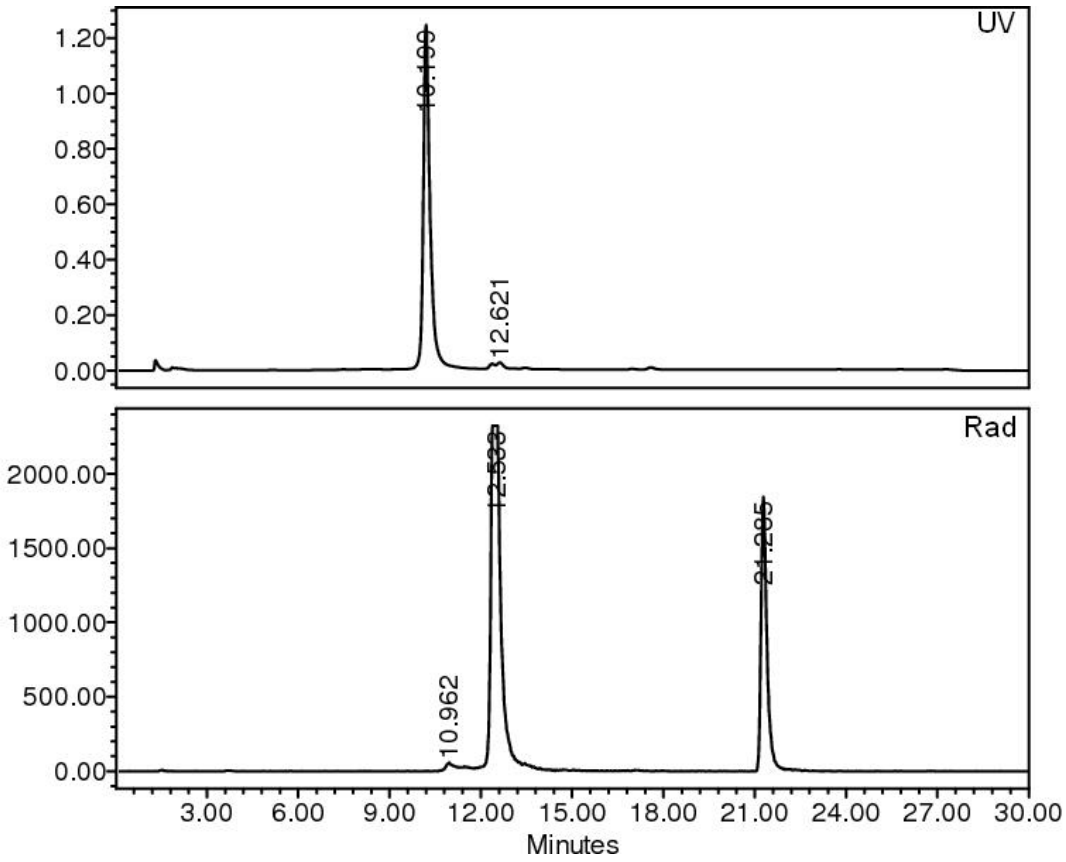

Figure 3.5. Preparative radio-HPLC of the ^{18}F-ODN reaction mixture.

HPLC 2.Top: UV trace (absorbance units), 260 nm. Bottom: Radioactive trace (meV). Reaction conditions: CuBr, TBTA, 2,6-lutidine in ~2:1 PBS:DMF, 75 ^{o}C, 20 min. **N_3-ODN**: R_t = 10.2 min: **^{18}F-ODN**: R_t = 12.5 min. [^{18}F]-**1**: R_t = 21.3 min.

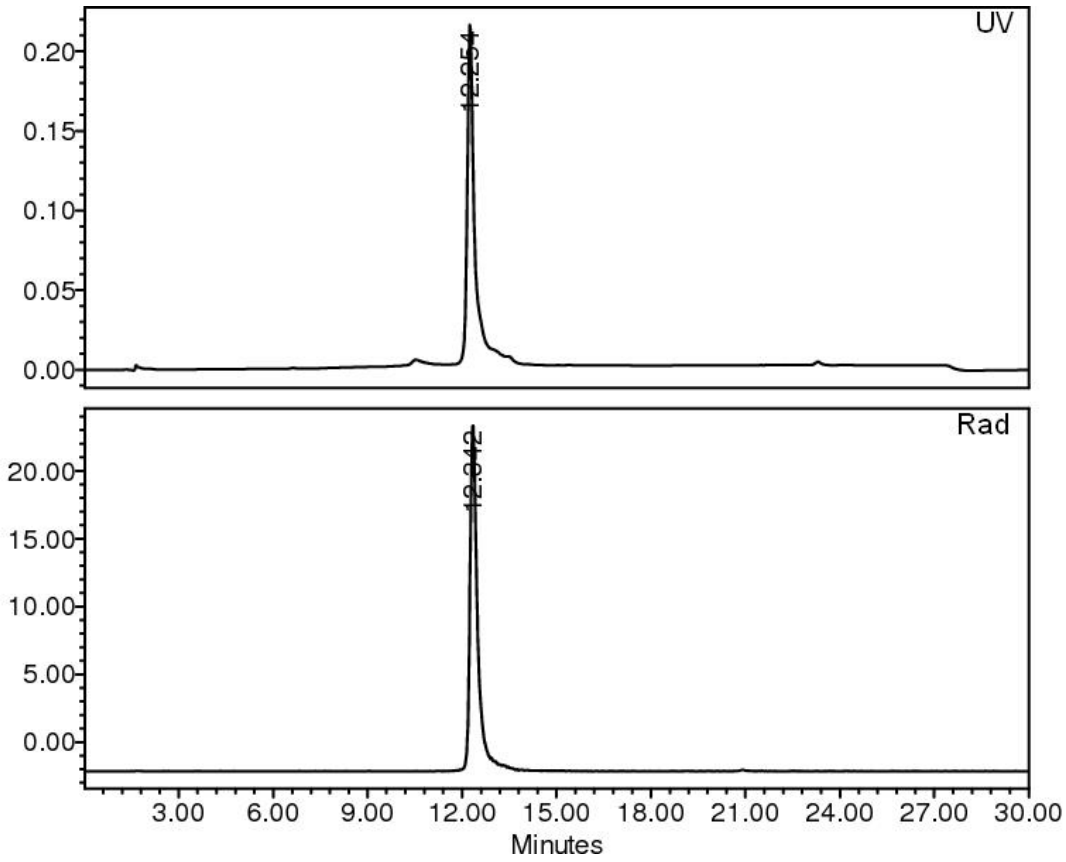

Figure 3.6. Radio-HPLC of ^{18}F-ODN admixed with synthetic standard ^{19}F-ODN.

HPLC 2. Top: UV trace (absorbance units), 260 nm. Bottom: Radioactive trace (meV).

3.8. Conclusion

[^{18}F]FPy5yne ([^{18}F]-**1**) is highly amendable to the ^{18}F- labelling of complex biomolecules owing to the straightforward and high- yielding synthesis of this prosthetic molecule. In this work, [^{18}F]-**1** was prepared and HPLC- purified in NDC, collected yields of 30±2 % (*n* = 4) from SOS. Total synthesis time of the ^{18}F- bearing small molecule was 90 min. [^{18}F]-**1** was used to radiolabel a 5'-azide-modified oligodeoxyribonucleotide with ^{18}F by way of a Cu^{I}-mediated azide/alkyne cycloaddition reaction. [^{18}F]-**1** was ligated to a DNA sequence antisense to *mdr1* mRNA in the presence of Cu^{I}- stabilizing ligand TBTA and 2,6-lutidine. This pre-labelling approach represents the first synthesis of an ^{18}F- labelled DNA analogue by way of CuAAC chemistry. More importantly, this method should be considered as 'proof-of-principle' for the radiosynthesis of other nucleic acid- based ^{18}F PET imaging agents, including biologically stable antisense

PNAs and morpholinos, aptamers, and siRNAs. This technology compares favorably to the current 'state-of-the-art' route for the ^{18}F labelling of ODNs, namely sulfhydryl-targeting compound [^{18}F]FPyBrA (Figure 1.20). While NDC preparative yields are identical within error (4%), radiochemistry in this work was carried out without the aid of a computer- controlled robot system. Furthermore, unlike [^{18}F]FPyBrA, [^{18}F]-**1** is compatible with all potential antisense-CPP targeting vectors, irrespective of the presence of cysteine residues in the peptide sequence.

Others in the TRIUMF PET group are now leading efforts towards the conjugation of [^{18}F]-**1** to azide- modified PNA molecules antisense to mRNA encoding for the green fluorescent protein (GFP).* We anticipate that the chemical and radiochemical groundwork that has been laid here should be invaluable to these efforts. The new antisense probes have been coupled to Tat peptide to improve their cell penetration. The stable transfection of the *GFP* gene into a breast cancer cell line should allow for the complementary PET/fluorometric *ex vivo* assessment of [^{18}F]FPy5yne-PNA-CPP chimeras for the targeting of high levels of uniquely expressed mRNA.

A final word should be said about the failure of ^{18}F antisense probes thus far to allow for the non-invasive visualization of gene expression. Molecular imaging data using other antisense probes typically affords images of highest contrast at time points in excess of 2 hours. This has been attributed to the fact that image quality depends not only on probe distribution and endocytosis, but on the capacity of non-hybridized sequences to efflux from cells and excrete from the target region.[380] Thus it could be argued that because of its intermediate half- life ^{18}F is not the most appropriate radionuclide for the specific *in vivo* imaging of mRNAs. It remains clear however, that the comprehensive pre-clinical testing of this hypothesis remains wholly dependent on the development of efficient radiochemical protocols.

* Hua Yang, Qing Miao and Paul Schaffer, personal communication.

4. 2-[^{18}F]Fluoropyridines for the peptide receptor imaging of cancer *in vivo*

The chemical synthesis, radiochemistry, and experimental protocols described in this chapter were carried out by James Inkster, with the exception of compound **14**, which was synthesized by Simon Gosslein (TRIUMF/Université de Sherbrooke). Samia Ait-Mohand from Prof. Brigitte Guérin's lab (Université de Sherbrooke) prepared the azide- modified peptide precursors described herein. All murine biodistribution assays and µPET experiments were carried out by Maral Pourghiasian (UBC/BC Cancer). Navjit Hundal assisted during µPET scans.

4.1. Neuropeptide Y and BVD-15

Neuropeptide Y (NPY) is a 36 amino acid peptide modulator of a variety of normal mammalian functions, including appetite, anxiety, memory and blood pressure.[381] NPY is found to mediate the action of five different G- protein receptor subtypes in humans (NPY1r- NPY5r). Of interest to oncologists, NPY1r was found expressed in 58 %[382] and 85 %[383] of resected breast tumours in two separate experiments. In contrast, the NPY2 subtype is preferentially expressed in normal breast.[383] Furthermore, activation of the NPY1 receptor has been shown to increase or decrease the proliferation of prostate cancer cells depending on their androgen dependency.[384] Like many neuropeptides, NPY exhibits only local action because of its susceptibility to proteolysis (biological $t_{1/2}$ in human = ~4 min).[385] Owing much to its ability to curb feeding behaviour and regulate blood pressure, a number of small molecule and peptidergic NPY1r antagonists have been investigated as therapeutic agents.[386] However, relatively few NPY analogs have been radiolabelled for nuclear imaging. A truncated analogue of NPY [Ac-YPSK-[Ala^{26}]NPY(25-36)] was labelled with ^{99m}Tc and ^{185}Re *via* a 2-pocolylamine-N,N-diacetic acid- modified lysine residue.[387] This radio-peptide retained a high affinity for NPY1r (IC_{50} = 16 nM) and was shown to be 6

times more stable in human plasma than the natural ligand. The same group also introduced an ^{111}In- labelled peptide, [Lys(^{111}In-DOTA)^4, Phe^7, Pro^{34}]NPY, which exhibited good binding affinity for the MCF-7 breast cancer cell line but exhibited only moderate uptake into tumour xenografts (mouse, max. % ID/g = 1.7 %, 30 min). Most uptake and clearance occurred through the kidneys (max. % ID/g = 86.8 %, 4 h). The sub-optimal performance of this radio-peptide was attributed to both its instability *in vivo* and its low effective specific activity. (The authors could not completely separate the labelled and unlabelled peptides by HPLC.)

Interest in the NPY fragment BVD-15 ([Pro^{30}, Tyr^{32}, Leu^{34}]NPY(28-36)) was initiated by its subnanomolar affinity for NPY1r.[388] BVD15 is unsuitable as a therapeutic however, due to its potent agonism of NPY4r.[389] Guérin *et al.* sought to modify BVD15 to allow for incorporation of a radiometal.[390] Thus, the Ile^4 position of BVD15 was replaced with a Lys residue to allow for the installation of DOTA. [Lys(DOTA)^4]BVD15 retained its affinity for NPY1r in MCF7 cells (K_i = 63 nM vs. 39 nM for BVD15). A conference abstract described the labelling of this chelated peptide with ^{64}Cu for µPET imaging.[391] In this case however, tumour uptake could not be blocked with co-injected non-radioactive peptide, suggesting that the sequesterization of radiometal was not mediated by NPY1r.

4.2. Gastrin-Releasing Peptide and Bombesin

The gastrin- releasing peptide (GRP) is the native ligand of the gastrin- releasing peptide receptor (GRPr, a.k.a. BB2r), which is distributed predominantly throughout the mammalian brain and gut. GRPr is one of four receptor subtypes which make up the bombesin receptor superfamily (BB1r- BB4r).[392] The GRP/GRPr neurotransmission/ neuromodulation system helps to regulate a broad range of physiological functions, including gastric and pancreatic secretion, pain transmission, smooth muscle contraction, hunger, body temperature and blood pressure.[393] GRP also acts as a mitogen, morphogen, and proangiogenic factor of receptive tissues,[394] and as such GRP receptors are found overexpressed in a variety of cancer types.[149] In particular, Reubi and co-workers found GRPr expressed in 65 % of a total of 77 exorcised breast tumours[382] as well as 100 % (30/30) of a population of invasive prostatic neoplasms.[395]

Bombesin (BBN) is a shortened 14 amino acid analogue of GRP which was first discovered in the skin of the European fire-bellied toad, *Bombina bombina*.[396] Bombesin shares a homologous C terminus with GRP [WAVGHLM(NH_2)], and the two peptides display similar biologic function. Bombesin was first radiolabelled with ^{125}I *via* Tyr^4- modification;[397] this peptide is still used to estimate receptor densities and binding affinities for related sequences through competitive assays. A BBN(7-13) bioconjugate labelled with ^{125}I-*m*-iodobenzoate prosthetic was introduced with increased stability and improved uptake into ovarian tumours relative to [Tyr^4]bombesin. However, the majority of GRP imaging research has employed radiometallated bioconjugates. For SPECT, a variety of BBN derivatives have been labelled with ^{99m}Tc[398]; attempted optimizations have focused on the diminution of the hepatobiliary clearance that is common to ^{99m}Tc-labelled peptides. For PET, DOTA- modified [β-Ala^{11}, Thi^{13}, Nle^{14}]BBN(6-14) peptide was labelled with ^{68}Ga.[399] The efficacy of this compound was evaluated for the delineation of gastrointestinal stromal tumours in humans.[400] The ^{68}Ga peptide fared poorly when compared [^{18}F]FDG, with 8 of 30 lesions detected versus 25 of 30 for [^{18}F]FDG (17 patients total). However, the peptide tracer did detect one [^{18}F]FDG-negative tumour, suggesting that there is a patient subgroup that might benefit from this technique. In addition, a sizable number of ^{64}Cu- labelled bombesin analogues have been introduced. Most thus far have employed DOTA as chelator,[401] although the observed decupration this complex *in vivo* has instigated the use of NOTA,[402] TE2A,[403] DO3A and PCTA as well (Figure 1.11). A recent comparison of these chelators with respect to bombesin(6-14) found PCTA and NOTA to be stable in mice over 20 h, while Oxo-DO3A and DOTA were not (37 % and 0 % remaining after 20 h respectively).[404]

The successful *direct* ^{18}F labelling of bombesin fragments for PET imaging has been reported.[405-407] Scientists at ETH Zurich were able to prepare modified peptide precursors with TMA- bearing benzonitrile pendant groups on solid support (Figure 4.1). These compounds were then pre-labelled using classical [^{18}F]fluorination conditions (Cs[^{18}F]F/$K_{2.2.2.}$, 150- 300 µL DMSO, 70- 90 ºC, 10- 15 min). ^{18}F incorporation could be achieved in the range of 74- 89 %. However, DC preparative yields were only 14- 20 %. The discrepancy in these values was attributed to the absorption of free [^{18}F]F$^-$ onto the surface of the reaction vial after drydown.[405] Another disadvantage of this approach is the need for relatively large amounts of peptide precursor (2 mg) to achieve acceptable

radiochemical yields. Nevertheless, the remarkable simplicity of the radiosynthetic protocol has undoubtedly accelerated the preclinical evaluation of these ^{18}F peptides. A similar ^{18}F-BBN fragment which was modified with L-cysteric acid to improve hydrophilicity showed high tumour uptake (6.4 % ID/g vs. 2.4 % for [^{18}F]FDG) and rapid excretion in a mouse model of prostate cancer (PC3).[407] Very recently, a related strategy was applied to the direct ^{18}F labelling of dimeric [*c*(RGDfK)]$_2$ analogues.[408] The peptides were coupled by way of amidation of the lysine residues. In this case, a nitro-for-[^{18}F]fluoro substitution was achieved using a *o*-CF_3 moiety as the electron-withdrawing activator (Figure 4.1). Maximum decay- corrected preparative yield was 23 %. It should be noted that the peptides described above are relatively small, robust biomolecules that do not contain acidic amines or hydroxy groups. In fact, in the preceding study it was found that the analogous tyrosine- bearing precursor ([*c*(RGDyK)]$_2$) could not be successfully ^{18}F- labelled in this fashion.

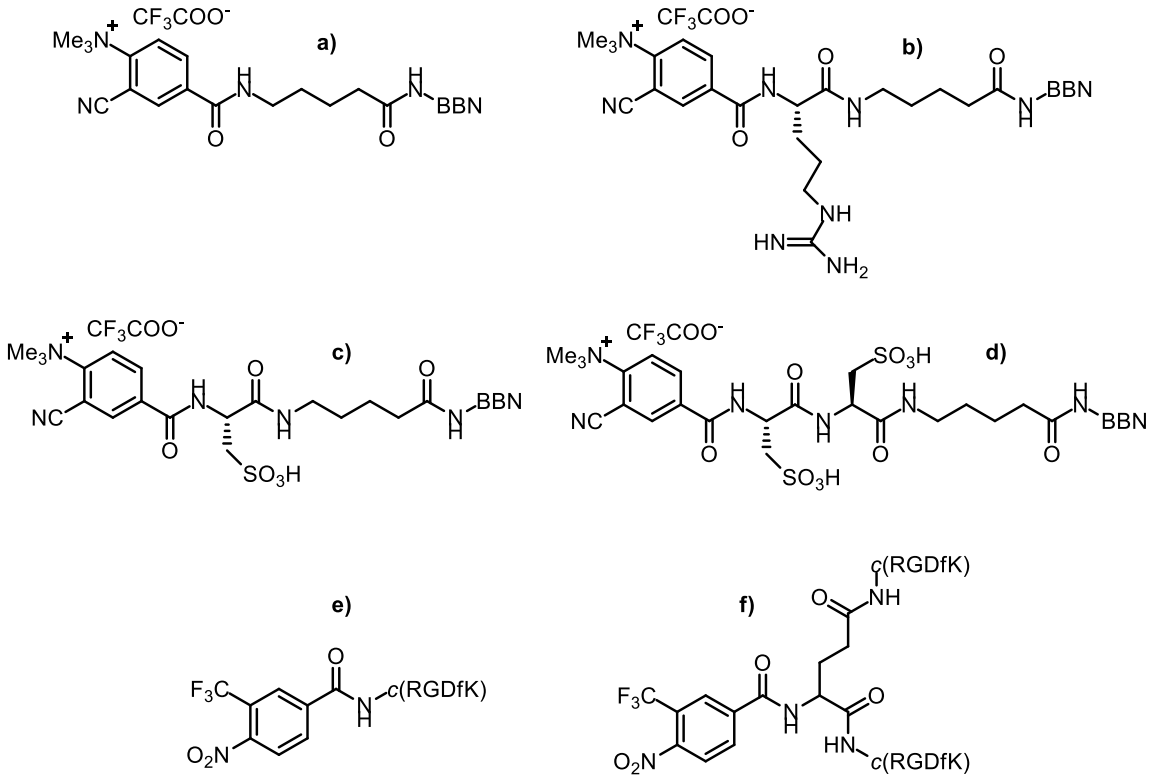

Figure 4.1. Pendant groups for the direct ^{18}F labelling of peptide analogues.

a) and b) Becaud *et al.*[405] c) Mu *et al.*[406] d) Honer *et al.*[407] e) and f) Jacobson *et al.*[408] In the case of the RGD-based peptides, the prosthetic portion is connected to Lys.

Bombesin has proven to be a targeting agent of choice for those exploring the potential for multi-receptor PET imaging. In this approach, multimeric heteropeptides are radiolabelled to produce imaging agents that have the potential to target specific cancers in a truly diagnostic fashion.[382] To this end, BBN-RGD peptides have been labelled with *N*-succinimidyl 4-[^{18}F]fluorobenzoate ([^{18}F]SFB; see Figure 1.14 and Section 1.4.1) for PET imaging of cancer. In a prostate cancer study, an ^{18}F-labelled BBN-RGD heterodimer showed improved uptake into PC3 cells (GRPr+/$\alpha_v\beta_3$+) and exhibited a superior pharmacokinetic profile relative to its monomeric counterparts.[409] In a later study, ^{18}F-, ^{64}Cu- and ^{68}Ga- labelled BBN-RGD peptides were challenged by GRPr+/low $\alpha_v\beta_3$ and GRPr-/$\alpha_v\beta_3$+ breast tumours.[410] The ^{18}F-BBN-RGD peptide imaged both tumour types with high contrast, thus proving the validity of this technique.

4.3. Objectives

This chapter describes the application of the [^{18}F]FPy5yne- labelling approach toward the PET imaging of breast, prostate and brain cancer in a murine model. The first neuropeptide ligand selected for this transitionary work was BBN(6-14). BBN(6-14), as the name implies, is a truncated version of bombesin composed of the last 9 amino acids of the bombesin C terminus. Simple truncation yields a less potent peptide than bombesin, but additional modifications can restore binding affinity for GRP2r.[411] In this case, the alterations (relative to bombesin) are: D-Tyr^6, βAla^{11}, Thi^{13} and Nle^{14} (see Table 1.3). It is assumed that these changes also serve to enhance the stability of the peptide *in vivo.* Our collaborators at the Université de Sherbrooke synthesized this peptide with an N_3-$CH_2C(O)$- residue at its N terminus (**N_3-BBN**; Figure 4.2) for CuAAC coupling with [^{18}F]-**1**. A mini-PEGylated derivative of **N_3-BBN** was also prepared (**N_3-BBN-PEG**). The utility of GRPr- based tumour- targeting strategies *in vivo* have been relatively well established, and ^{18}F- labelled bombesin analogs have shown promise for the delineation of certain breast and prostate xenografts using μPET. Thus it was hypothesized that this peptide ligand-receptor pair might well serve as a model system for the preclinical assessment of [^{18}F]-**1**- labelled peptide targeting agents. To this end, we committed to repeated syntheses of **[^{18}F]F-ALK-BBN** and **[^{18}F]F-ALK-BBN-PEG** (Figure 4.2) for the determination of certain key molecular imaging parameters of these radio-peptides in PC3 (prostate cancer)- bearing mice by our collaborators in the Bénard lab at the BC

Cancer Research Centre. Planned work included *in vitro* (*i.e.* cell permeation, plasma stability), *ex vivo* (biodistribution), and *in vivo* (PET) experiments. In light of the successes in this case (*vide infra*), we chose another, less established bioactive peptide for labelling with [^{18}F]-**1**: BVD15 ([Pro^{30}, Tyr^{32}, Leu^{34}]NPY(28-36)NH$_2$). An azide-modified version of this neuropeptide Y1 analogue was recently designed in the Guérin lab. Thus, Chapter 4 also details attempts to synthesize [^{18}F]-**1**- labelled BVD15 (**[^{18}F]-ALK-BVD**; Figure 4.2) for similar experiments using the MCF7 (breast cancer) and SK-N-MC (neuroblastoma) cell lines. Our motivation for choosing a NPY analogue was two-fold; first, because no peptidergic ligand of the NPY receptor has thus far been labelled with ^{18}F; and second, because no molecular images have thus far been obtained with an NPY analogue.

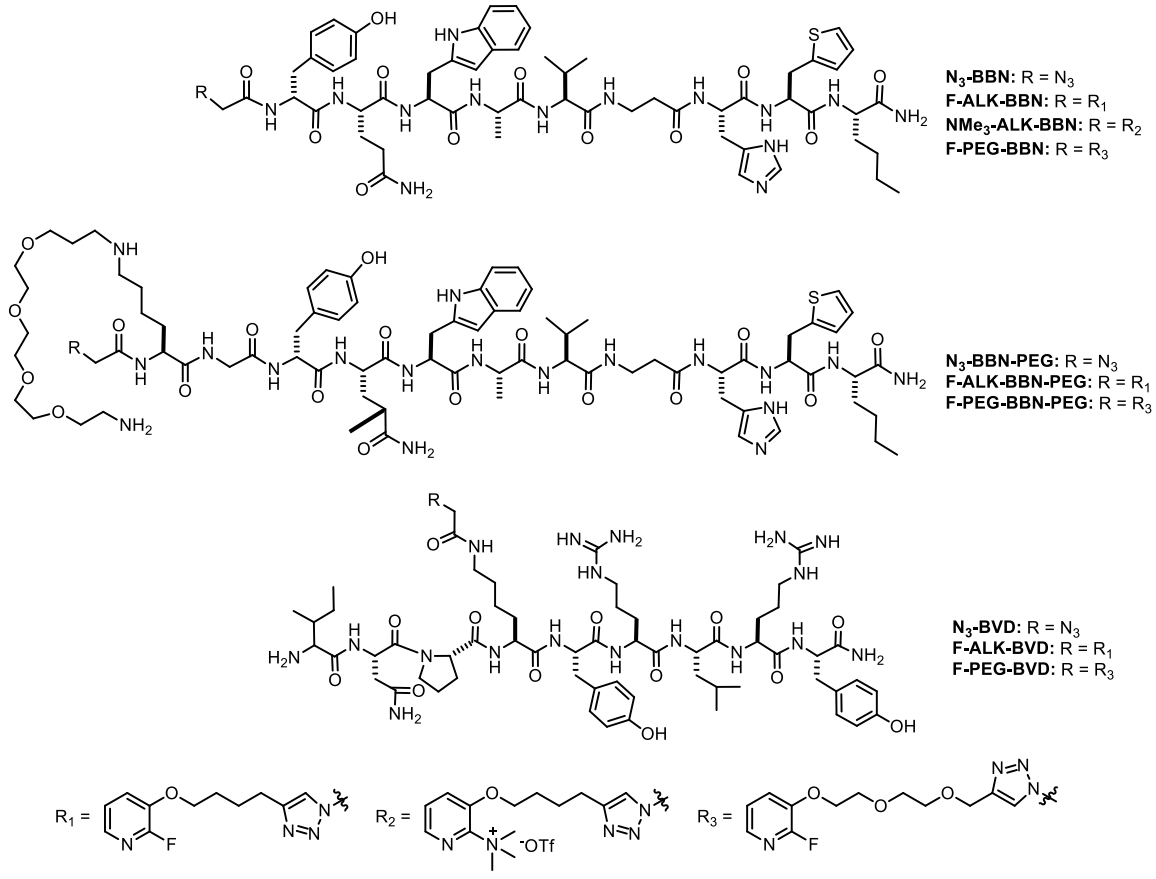

Figure 4.2. Peptides referenced in this work.

F = ^{19}F and ^{18}F.

4.4. Non-radioactive Small Molecule Syntheses

Important note! This chapter includes the details for the preperation of azide-bearing molecules. The synthesis, purifiction and handling of all azides should be done with care as these compounds are known to explode when subject to heat or concussive force. Organic azides with low carbon and oxygen content relative to nitrogen content are particularly dangerous. In practice, molecules in which the ratio of C + O atoms/ total N atoms is ≤3 should be kept impure or in solutions and stored at <0 ºC. Compounds with ratios ≤1 should only be prepared as a limiting reaction intermediate, if at all. The use of chlorinated solvents may result in the production di- and tri-azidomethane and should be avoided.

4.4.1. *2-Fluoro-3-hydroxypyridine (12)*

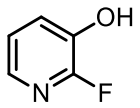

This synthesis is based on a reported method.[412] A round- bottom flask (RBF) containing 2-amino-3-hydroxypyridine (2.01g, 18.2 mmol) in 48 % tetrafluoroboric acid (50 mL) was cooled to 0 °C. Sodium nitrite (10.1 g, 145 mmol) was *carefully* added, in small portions. The reaction mixture was stirred and cooled at 0 °C for 2.5 h, then basified slowly, in portions, with NaOH powder (~10 g). The solution was extracted into EtOAc three times. The pooled organic portions were washed twice with water, once with brine and dried over Na_2SO_4. Concentration to dryness yielded 1.34 g (65 %) of **12** as a brown solid, which was deemed pure enough for further use after ^{1}H NMR and melting point analysis. M.P. = 131ºC (Lit.[140] = 131ºC). ^{1}H NMR (600 MHz, CD_2Cl_2): δ 5.86 (s, 1H), 7.12 (ddd, J = 7.7, 4.9, 0.6 Hz, 1H), 7.42–7.33 (m, 1H), 7.71 (dd, J = 3.2, 1.6 Hz, 1H). ^{13}C NMR (100 MHz, CD_2Cl_2): δ 123.14 [CH, d, $J_{F\text{-}C}$ = 3.9 Hz], 126.68 [CH, d, $J_{F\text{-}C}$ = 4.6 Hz), 138.06 [CH, d, $J_{F\text{-}C}$ = 13.0 Hz], 139.49 [C, d, J = 29.7 Hz], 153.29 [CF, d, J = 229.3 Hz]. ^{19}F NMR (300 MHz, CD_2Cl_2): δ: -92.01. HRMS (EI) calcd. for C_5H_4NOF: 113.02769. Found: 113.02757.

4.4.2. *2-Fluoro-3-(hex-5-yn-1-yloxy)pyridine (FPy5yne, 1)*

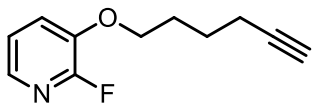

To a solution of 5-hexyn-1-ol (0.96 mL, 8.84 mmol) in CH_2Cl_2 (33 mL) under Ar was added 2-fluoro-3-hydroxypyridine (**12**, 1.02 g, 9.06 mmol) followed by triphenylphosphine (3.05 g, 11.6 mmol). The reaction mixture was stirred for 35 min and diisopropyl azodicarboxylate (2.28 mL, 11.5 mmol) was added slowly under argon. An additional portion 5-hexyn-1-ol (100 µL, 0.92 mmol) was added after 4.5 h and the reaction was stirred at RT overnight. The product was concentrated to dryness and the residue was purified by flash chromatography (3:1 hexanes:ether) to give **1** as a light yellow oil (0.872 g, 51 %). R_f (1:1 ethyl acetate:hexane): 0.61. ^{1}H NMR (600 MHz, CD_2Cl_2) δ 1.77 – 1.67 (m, 2H), 1.99 – 1.90 (m, 2H), 2.01 (t, J = 2.7 Hz, 1H), 2.28 (td, J = 7.1, 2.7 Hz, 2H), 4.06 (t, J = 6.3 Hz, 2H), 7.12 (dd, J = 7.8, 4.9 Hz, 1H), 7.33 – 7.26 (m, 1H), 7.70 (dd, J = 3.3, 1.5 Hz, 1H). ^{19}F NMR (300 MHz, CD_2Cl_2) δ -85.83. ^{13}C NMR (150 MHz, CD_2Cl_2): δ 18.55 [CH_2]; 25.44 [CH_2]; 28.54 [CH_2]; 69.04 [CH_2]; 69.25 [CH]; 84.43 [C]; 122.38 [CH, d, $J_{F\text{-}C}$ = 4.1 Hz]; 123.04 [CH, d, $J_{F\text{-}C}$ = 4.4 Hz], 137.51 [CH, d, $J_{F\text{-}C}$ = 13.6 Hz]; 142.86 [C, d, $J_{F\text{-}C}$ = 25.9 Hz], 154.26 [CF, d, $J_{F\text{-}C}$ = 237.0 Hz]. HRMS (EI) calcd. for $C_{11}H_{12}NOF$: 193.09029. Found: 193.09023.

4.4.3. *2-Dimethyl-3-hex-5-yn-1-yloxypyridine (11)*

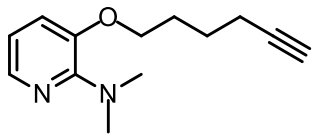

FPy5yne (**1**, 310 mg, 1.60 mmol) was dissolved in EtOH (20 mL), then a solution of Me_2NH was added (20 mL, 40 % wt in water). A condenser was attached, and the reaction mixture was heated to 50 °C for 3 h, then at 80 °C- 90 °C overnight. The reaction was cooled to RT and quenched with sat. $NaHCO_3$. The product was extracted twice into EtOAc (180 mL), then washed once with water, once with brine, and dried over Na_2SO_4. The concentrated residue was purified by flash chromatography on silica

gel (1:1 hexanes: ether) to afford **11** as a light yellow oil (288 mg, 82 %). R_f (1:1 ether:hexanes): 0.32. ^{1}H NMR (400 MHz, CD_2Cl_2) δ 1.73 (m, 2H), 1.95 (m, 2H), 2.00 (t, *J* = 2.6 Hz, 1H), 2.29 (td, *J* = 7.0, 2.6 Hz, 2H), 2.98 (s, 6H), 3.98 (t, *J* = 6.3 Hz, 2H), 6.70 (dd, *J* = 7.8, 4.9 Hz, 1H), 7.00 (dd, *J* = 7.8, 1.1 Hz, 1H), 7.77 (dd, *J* = 4.9, 1.4 Hz, 1H). ^{13}C NMR (101 MHz, CD_2Cl_2): δ 18.64 [CH_2], 25.89 [CH_2], 28.90 [CH_2], 41.19 [CH_3], 68.33 [CH_2], 68.98 [CH], 84.56 [C], 115.66 [CH], 118.74 [CH], 138.88 [CH], 146.25 [C], 153.56 [C]. HRMS (EI) calcd. for $C_{13}H_{18}N_2O$: 218.14191. Found: 218.14217.

4.4.4. *[3-(Hex)-5-ynyloxy]pyridine-2-yl]trimethylammonium trifluoromethanesulfonate (NMe$_3$Py5yne, 3)*

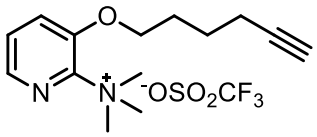

Compound **11** (223 mg, 1.02 mmol) in a conical vial was dissolved in dry toluene (2 mL) and the solution was cooled to 0 °C. Methyl triflate (151 µL, 1.33 mmol, 1.3 equiv.) was added *via* syringe, and the reaction was stirred at 0 °C for 1 h. During this time a white precipitate formed, which was quickly filtered and washed with diethyl ether (7 mL). Drying *in vacuo* afforded trimethylammonium triflate **3** (361 mg, 92 %) as a hygroscopic white powder. M.P. = 69 °C (Lit.[379] = 66- 67 °C). ^{1}H NMR (400 MHz, DMSO-d) δ 1.76 – 1.53 (m, 2H); 2.07 – 1.85 (m, 2H); 2.28 (td, *J* = 7.0, 2.6 Hz, 2H); 2.82 (t, *J* = 2.6 Hz, 1H); 3.61 (s, 10H); 4.32 (t, *J* = 6.4 Hz, 2H); 7.73 (dd, *J* = 8.3, 4.5 Hz, 1H); 7.96 (dd, *J* = 8.4, 1.1 Hz, 1H); 8.17 (dd, *J* = 4.5, 1.2 Hz, 1H). ^{13}C NMR (100 MHz, DMSO) δ 17.37 [CH_2]; 24.66 [CH_2]; 27.30 [CH_2]; 53.40 [3 x CH_3]; 69.29 [CH_2]; 71.60 [CH]; 84.14 [C]; 120.67 [CF_3, q, J_{F-C} = 322.4 Hz); 125.04 [CH]; 128.38 [CH]; 138.24 [CH]; 142.52 [C]; 147.11 [C]. HRMS (ESI+) calcd. for $C_{14}H_{21}N_2O$ [M^+-$^-$OTf]: 233.1654. Found: 233.1648.

4.4.5. *3-Azido-1-propanol (13)*

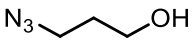

This synthesis was based on a reported method.[270] 3-Bromo-1-propanol (13.3 g, 95.4 mmol) was dissolved in H_2O (100 mL) and to this solution, NaN_3 (12.4 g, 191 mmol, 2 equiv.) was added. The reaction mixture was stirred at 40 °C overnight, extracted into CH_2Cl_2 (3 × 50mL). The product was dried over Na_2SO_4 and *carefully* concentrated by rotary evaporation to yield **13** as pale yellow oil (7.28 g). The compound was 89 % pure by NMR and used without further purification. ^{1}H NMR (600 MHz, CD_2Cl_2): δ 1.61 (s, 1H), 1.80 (m, 2H), 3.42 (t, *J* = 6.7 Hz, 2H), 3.70 (t, *J* = 6.1 Hz, 2H). ^{13}C NMR (151 MHz, CD_2Cl_2): δ 32.08 [CH_2], 49.05 [CH_2], 60.28 [CH_2]. *Caution! Azides such as **13** can explosively decompose when subject to heat or shock. When replicating this procedure, future workers are strongly advised to scale down the reaction and substitute CH_2Cl_2 for another reaction solvent. Owing to the low (C+O)/N ratio of **13** (see section 4.4.),* ***the isolation of this compound is not advised.***

4.4.6. *Tris(3-hydroxypropyltriazolemethyl)amine (THPTA) (14)*

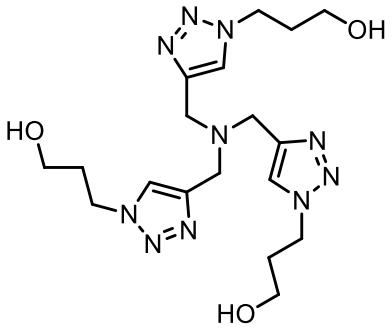

3-Azido-1-propanol (**13**, 6.08 g, 60.1 mmol) was dissolved in 1:1 CH_2Cl_2: H_2O (40 mL). To this solution, $CuSO_4 \cdot 5H_2O$ (753 mg, 3.01 mmol) and sodium ascorbate (1.79 g, 9.02 mmol) were added. The resulting solution was stirred at RT for 18 h. The reaction mixture was separated and the aqueous portion was concentrated to dryness. The residue was purified by flash chromatography on silica gel (25 % MeOH in CH_2Cl_2+2 % TFA). The collected material was further recrystallized twice (acetonitrile, then isopropanol) to yield a white solid, THPTA (**14**, 960 mg, 11 %). ^{1}H NMR (400 MHz, CD_3OD): δ 2.11 (m, 6H), 3.57 (t, *J* = 6.1 Hz, 6H), 3.75 (s, 6H), 4.51 (t, *J* = 7.0 Hz, 6H), 7.98 (s, 3H). ^{13}C NMR (100 MHz, CD_3OD) δ 33.96 [3 x CH_2], 48.29 [3 x CH_2], 48.74 [3 x CH_2], 59.32 [3 x CH_2], 125.69 [3 x CH], 145.33 [3 x C]. M.P.= 103-104°C (Lit.[413] = 104-

106°C). Anal. calcd. for $C_{18}H_{30}N_{10}O_3$: C, 49.76; H, 6.96; N, 32.24. Found: C, 49.66; H, 6.96; N, 31.89.

4.4.7. *2-(2-(Prop-2-ynyloxy)ethoxy)ethanol (15)*

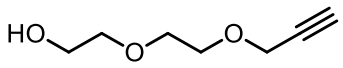

In a RBF charged with argon and cooled to 0 ºC, 95 % NaH (1.64 g, 65 mmol) was suspended in anhydrous THF and di(ethylene)glycol (9.5 mL, 100 mmol) was added dropwise. After 30 min of stirring at 0 °C, propargyl bromide (5.5 mL, 50 mmol, 80 % in toluene) was added slowly. The reaction was kept at 0 °C for another 2 h, then allowed to warm to RT overnight. The reaction was slowly quenched with water (30 mL) and the compound was extracted into CH_2Cl_2 (3 x 50 mL). The organic portions were combined and washed with H_2O (1 x 30 mL), dried over Na_2SO_4, and concentrated *in vacuo.* Flash chromatography on a silica column (3:2 ethyl acetate:hexanes) afforded alkyne **15** (3.66 g, 51 %) as a yellow oil. ^{1}H NMR (400 Hz, $CDCl_3$): δ 2.43 (t, 1H, *J* = 2.4 Hz); 2.84-2.88 (br s, 1H), 3.58 (dt, 2H, *J* = 4.6 Hz, 5.3 Hz); 3.63-3.76 (m, 6H); 4.18 (d, 2H, *J* = 2.8 Hz). ^{13}C NMR (100 MHz, $CDCl_3$) : δ 58.5 [CH_2]; 61.8 [CH_2]; 69.2 [CH_2]; 70.3 [CH_2]; 72.7 [CH_2]; 74.9 [CH]; 79.6 [C]. HRMS (ESI+) calcd. for $C_7H_{12}O_3Na$ [M^++Na]: 167.0684. Found: 167.0680.

4.4.8. *2-Fluoro-3-(2-(2-(prop-2-ynyloxy)ethoxy)ethoxy)pyridine (PEG-FPyKYNE, 16)*

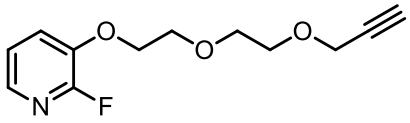

2-(2-(Prop-2-ynyloxy)ethoxy)ethanol (**15**, 797 mg, 5.53 mmol) was dissolved in dry THF (50 mL) and the flask was charged with argon and cooled to 0 ºC. To this solution, triphenylphosphine (1.45 g, 5.53 mmol), 2-fluoro-3-hydroxypyridine (**12**, 500 mg, 4.43 mmol) and diisopropylazodicarboxylate (DIAD, 1.5 mL, 7.63 mmol, dropwise) were added sequentially. The reaction was allowed to stir for 48 h and then concentrated

to dryness. The crude mixture was purified by flash chomatography on silica gel (1:1 hexanes:ethyl acetate) to afford PEG-FPyKYNE (**16**, 695 mg, 66 %) as a yellow light oil. ^{1}H NMR (600 MHz, CD_2Cl_2): δ 2.48 (t, *J* = 2.4 Hz, 1H), 3.69 – 3.65 (m, 2H), 3.73 – 3.69 (m, 2H), 3.86 (t, *J* = 4.7 Hz, 2H), 4.17 (d, *J* = 2.4 Hz, 2H), 4.19 (t, *J* = 4.7 Hz, 2H), 7.13 (dd, *J* = 7.9, 4.9 Hz, 1H), 7.38 – 7.32 (m, 1H), 7.72 (dt, *J* = 4.6, 1.4 Hz, 1H). ^{19}F NMR (282 MHz, CD_2Cl_2): δ -85.50. ^{13}C NMR (151 MHz, CD_2Cl_2): δ 58.80 [CH_2]; 69.44 [CH_2]; 69.72 [CH_2]; 69.90 [CH_2]; 71.17 [CH_2]; 74.70 [CH]; 80.26 [C]; 122.40 [CH, d, $J_{F\text{-}C}$ = 4.2 Hz], 123.61 [CH, d, $J_{F\text{-}C}$ = 4.3 Hz); 137.93 [CH, d, $J_{F\text{-}C}$ = 13.6 Hz]; 142.72 [C, d, $J_{F\text{-}C}$ = 25.9 Hz], 154.27 [CF, d, $J_{F\text{-}C}$ = 236.9 Hz]. HRMS (ESI+) calcd. for $C_{12}H_{14}NO_3F$: 239.09577. Found: 239.09583.

4.4.9. *2-Dimethylamino-3-(2-(2-(prop-2-ynyloxy)ethoxy)ethoxy)pyridine (17)*

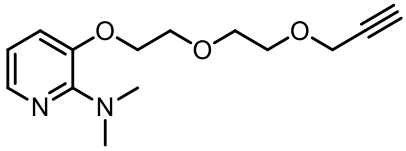

PEG-FPyKYNE (**16**, 64.4 mg, 0.27 µmol) was dissolved in aqueous dimethylamine (40 % w/w, 3.38 mL, 27 µmol). The reaction vessel was sealed and the reaction heated at 70 ºC for 4 h. After cooling to RT, MeCN (~7 mL) was added and the reaction mixture was *carefully* concentrated by rotary evaporation. The crude product was purified on a flash column of silica gel (3:2 hexanes:ethyl acetate) to afford 2-dimethylaminopyridine **17** (65.0 mg, 91%) as a clear oil. ^{1}H NMR (400 MHz, CD_2Cl_2) δ 2.47 (t, *J* = 2.4 Hz, 1H), 2.97 (s, 6H), 3.68 (m, 2H), 3.85 (dd, *J* = 5.4, 4.0 Hz, 2H), 4.13 – 4.05 (m, 2H), 4.18 (d, *J* = 2.4 Hz, 2H), 6.70 (dd, *J* = 7.8, 4.9 Hz, 1H), 7.02 (dd, *J* = 7.8, 1.2 Hz, 1H), 7.79 (dd, *J* = 4.9, 1.4 Hz, 1H). ^{13}C NMR (101 MHz, CD_2Cl_2) δ 41.15 [2 × CH_3], 58.82 [CH_2], 68.35 [CH_2], 69.80 [CH_2], 70.14 [CH_2], 71.04 [CH_2], 74.67 [CH], 80.32 [C], 115.59 [CH], 119.49 [CH], 139.23 [CH], 146.00 [C], 153.67 [C]. HRMS (EI) calcd. for $C_{14}H_{20}O_3N_2$: 264.14739. Found: 264.14756.

4.4.10. *[3-(2-(Prop-2-ynyloxy)ethoxy)ethoxy)pyridine-2yl] trimethylammonium trifluoromethanesulfonate (18)*

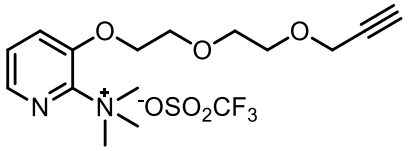

2-Dimethylamino-3-(2-(2-(prop-2-ynyloxy)ethoxy)ethoxy)pyridine (**17**, 207 mg, 0.78 mmol) was dissolved in dry CH_2Cl_2 and the flask was charged with argon and cooled to 0 ºC. Methyl triflate (610 µL, 5.40 mmol) was added *via* syringe, and the reaction was stirred at 0 ºC for 2 h. The reaction was quenched with diethyl ether (25 mL) and concentrated to dryness. The resulting solid was triturated with diethyl ether (25 mL), then filtered, washing generously with ether, then dried to afford 286 mg (85 %) of **19**. M.P. = 62-63 °C. ^{1}H NMR (600 MHz, CD_3OD): δ 2.88 (t, *J* = 2.2 Hz, 1H), 3.69 – 3.65 (m, 2H), 3.71 (m, 11H), 3.98 – 3.92 (m, 2H), 4.16 (d, *J* = 2.3 Hz, 2H), 4.51 – 4.45 (m, 2H), 7.68 (dd, *J* = 8.3, 4.5 Hz, 1H), 7.90 (d, *J* = 8.3 Hz, 1H), 8.15 (d, *J* = 4.4 Hz, 1H). ^{13}C NMR (151 MHz, CD_3OD): δ 54.85 [3 x CH_3], 58.98 [CH_2], 69.59 [CH_2], 70.17 [CH_2], 70.44 [CH_2], 71.11 [CH_2], 76.10 [CH], 80.67 [C], 122.86 [CF_3], 126.38 [CH], 129.65 [CH], 140.10 [CH], 144.58 [C], 148.83 [C]. HRMS (ESI+) calcd. for $C_{15}H_{23}O_3N_2^+$: 279.1709. Found: 279.1699.

4.5. Non-Radioactive Bioconjugate Syntheses

4.5.1. *F-ALK-BBN*

N_3-BBN peptide (2.0 mg) was dissolved in DMF (50 µL) and added to a microcentrifuge tube containing **1** (3.2 mg, 10.1 equiv.). PBS (200 µL, 150 mM, pH 7.2) was added, followed by a freshly prepared solution of TBTA (9.1 mg, 10.5 equiv.) and $Cu(CH_3CN)_4PF_6$ (6.1 mg, 10.0 equiv.) in DMF (50 µL). The reaction was shaken vigorously for 3.5 h, quenched with 1:1 MeCN:0.1 % TFA (400 µL), and purified by HPLC (HPLC 7, R_t = 22.5 min). The collected eluent was concentrated by way of centrifugal evaporation to afford the title peptide. MALDI-TOF (*m/z*) calcd.: 1415.65 $[M+H]^+$. Found: 1415.12.

4.5.2. *F-ALK-BVD*

FPy5yne (**1**, 5.9 mg, 10.8 equiv.) was dissolved in DMSO (50 µL) and transferred into a microcentrifuge tube containing **N_3-BVD** peptide (2.0 mg). PBS (25 µL, 150 mM, pH 7.2) was added. A freshly prepared solution of $Cu(CH_3CN)_4PF_6$ (5.7 mg, 10.0 equiv.) and TBTA (8.2 mg, 10.1 equiv.) in DMSO (50 µL) was added. The reaction was shaken vigorously for 3.5 h, then diluted with a mixture of 1:1 MeOH:H_2O (600 µL) and purified by HPLC (HPLC 3, R_t = 11.5 min). The collected eluent was concentrated by way of centrifugal evaporation to afford the title peptide. MALDI-TOF (*m/z*) calcd.: 1497.82 $[M+H]^+$. Found: 1497.62.

4.5.3. *F-PEG-BVD*

PEG-FPyKYNE (**16**, 11.0 mg, 20.0 equiv.) was dissolved in DMSO (50 µL) and transferred into a microcentrifuge tube containing **N_3-BVD** peptide (3.0 mg). PBS (25 µL, 150 mM, pH 7.2) was added. A freshly prepared solution of $Cu(CH_3CN)_4PF_6$ (8.5 mg, 9.9 equiv.) and TBTA (12.2 mg, 10.0 equiv.) in DMSO (50 µL) was added, and the reaction was shaken vigorously for 3.5 h. The reaction was quenched with 600 µL of 1:1 MeOH:H_2O solution and purified by HPLC (HPLC 3, R_t = 12.2 min). The collected eluent was concentrated by way of centrifugal evaporation (2.0 mg). Analysis by MALDI-TOF confirmed the presence of a Cu/**F-PEG-BVD** complex. MALDI-TOF (*m/z*) calcd.: 1606.76 $[M+^{63}Cu]^+$, 1543.83 $[M+H]^+$. Found: 1606.03 (10 %), 1544.10 (100 %).

4.5.4. *F-PEG-BBN*

PEG-FPyKYNE (**16**, 11.7 mg, 29.9 equiv.) was dissolved in DMSO (50 µL) and transferred into a microcentrifuge tube containing **N_3-BBN** (3.0 mg). PBS (25 µL, 150 mM, pH 7.2) was added. A freshly prepared solution of $Cu(CH_3CN)_4PF_6$ (9.1 mg, 9.9 equiv.) and TBTA (12.9 mg, 9.9 equiv.) in DMSO (50 µL) was added, and the reaction was shaken vigorously for 5.5 h. The reaction was quenched with a mixture of 1:1 MeOH:H_2O (800 µL) and purified by HPLC (HPLC 3). The collected eluent was a mixture of two closely eluting peaks (R_t = 14.2 and 14.3 min). The eluent was concentrated by centrifugal evaporation and assayed by MALDI-TOF, which confirmed the presence of a Cu/**F-PEG-BBN** complex. MALDI-TOF (*m/z*) calcd.: 1523.58 $[M+^{63}Cu]^+$, 1461.65 $[M+H]^+$. Found: 1523.79 (19 %), 1461.93 (100 %).

4.5.5. *F-ALK-BBN-PEG*

FPy5yne (**1**, 2.5 mg, 7.1 equiv.) was dissolved in DMSO (100 µL) and transferred into a microcentrifuge tube containing **N_3-BBN-PEG** peptide (2.1 mg). A freshly prepared solution of $Cu(CH_3CN)_4PF_6$ (7.2 mg, 15.2 equiv.) and TBTA (10.3 mg, 15.3 equiv.) in DMSO (200 µL) was added to this mixture. The reaction was shaken vigorously at RT for 1 h 20 min, then quenched with PBS (300 µL, 150 mM, pH 7.2) and purified by HPLC (HPLC 4, R_t = 19.9 min). The collected fraction was concentrated by way of centrifugal evaporation to afford the title peptide. MALDI-TOF (*m/z*) calcd.: 1869.93 $[M+Na]^+$, 1847.94 $[M+H]^+$. Found: 1870. 65 (100 %), 1848.95 (69 %).

4.5.6. *F-PEG-BBN-PEG*

PEG-FPyKYNE (**16**, 5.8 mg, 20.1 equiv.) was dissolved in DMSO (100 µL) and transferred into a microcentrifuge tube containing **N_3-BBN-PEG** peptide (2 mg). A freshly prepared solution of $Cu(CH_3CN)_4PF_6$ (4.3 mg, 9.5 equiv.) and TBTA (6.7 mg, 10.4 equiv.) in DMSO (200 µL) was added to this mixture. The reaction was shaken vigorously at room temperature for 2 h, then quenched with 0.1 % TFA (600 µL) and purified by HPLC (HPLC 19, R_t = 13.6 min). The collected fraction was concentrated by way of lyophilization to afford the title peptide. MALDI-TOF (*m/z*) calcd.: 1893.95 $[M+H]^+$. Found: 1894.40 (100 %).

4.5.7. *NMe_3-ALK-BBN*

NMe_3Py5yne (**13**, 6.4 mg, 10.8 equiv.) was dissolved in DMF (50 µL) and transferred into a microcentrifuge tube containing **N_3-BBN** (1.9 mg). A freshly prepared solution of $Cu(CH_3CN)_4PF_6$ (6.3 mg, 10.9 equiv.) and THPTA (**15**, 10.9 mg, 16.1 equiv.) in DMF (150 µL) was added, and the reaction was shaken vigorously for 3 h 40 min. The reaction was quenched with H_2O (700 µL) and **NMe_3-ALK-BBN** was purified by HPLC (HPLC 17). The collected eluent was removed from the peptide by lyophilization. MALDI-TOF (*m/z*) calcd.: 1454.72 $[M]^+$. Found: 1454.65.

4.6. Radiochemical Syntheses

The following representative syntheses were conducted at the BC Cancer Radiopharmaceutical Laboratory, with the exception of **[^{18}F]F-ALK-BBN**, which was prepared at the TRIUMF Radiochemistry Annex. Proton bombardment at TRIUMF was carried out on a 13 MeV cyclotron; [^{18}F]F$^-$ production ranged between 59- 190 mCi (at EOB) for a 50- 170 µA*min irradiation. Proton bombardment at BC Cancer was carried out on a 19 MeV cyclotron; [^{18}F]F$^-$ production ranged between 76- 645 mCi (at EOB) for a 100- 250 µA*min irradiation.

4.6.1. *[^{18}F]FPy5yne ([^{18}F]-1)*

The following synthesis of [^{18}F]-**1** is based on the protocol described in Section 3.6.1, with some key modifications. [^{18}F]F$^-$ in [^{18}O]H_2O was remotely transferred from the cyclotron directly onto a '^{18}F trap-and-release' column. [^{18}F]F-**1** (179.1 mCi) was eluted from the column with a solution of $K_{2.2.2.}$ (11.9 mg) and K_2CO_3 (2.5 mg) in MeCN:H_2O (1 mL:0.3 mL) into a 5 mL conical vial. Solvent was removed by way of azeotropic distillation at 110 ºC under a stream of He. Another aliquot of MeCN (1 mL) was added and the reaction mixture was concentrated to dryness again. This process was repeated once more. The reaction vessel was removed from heat and cooled in tap water, then precursor **3** (3.4 mg) in DMSO (500 µL) was added. The vial was resealed and heated to 110 ºC for 15 min. The closed reaction vessel was cooled in tap water, then the reaction mixture was transferred to another screw-cap vial containing H_2O (500 µL). This mixture was purified by HPLC (HPLC 5) (R_t = 11.7 min). The collected eluent (60.9 mCi) was diluted with H_2O (50 mL) and trapped on a tC_{18} light column [pre-activated with MeOH (2 mL) and water (6 mL) water]. The sorbent was washed with water (5 mL) and purged with air (10 mL), then the product ([^{18}F]-**1**) was eluted from the column (47.4 mCi, 44% DC yield from SOS) with DMF (200 µL). Synthesis time for this step was 82 min.

4.6.2. *PEG-[^{18}F]FPyKYNE ([^{18}F]F-16)*

[^{18}F]F$^-$ in [^{18}O]H_2O was remotely transferred from the cyclotron directly onto a '^{18}F trap-and-release' column. [^{18}F]F$^-$ (398.9 mCi) was eluted from the column with a mixture of $K_{2.2.2.}$ (13.3 mg) and K_2CO_3 (3.8 mg) in 2:1 MeCN:H_2O (1 mL). Solvent was removed

by way of azeotropic distillation at 110 ºC under a stream of He. Another aliquot of MeCN was added (1 mL) and the reaction mixture was concentrated to dryness again. This process was repeated once more. The reaction vial was removed from heat and cooled in tap water, then precursor **18** (3.6 mg) in DMSO (500 µL) was added. The vial was resealed and heated to 110 ºC for 15 min. After heating, the sealed reaction vessel was cooled in tap water, then the reaction mixture was transferred into H_2O (500 µL). [^{18}F]-**16** was separated from precursor using semi-preparative HPLC (HPLC 6, R_t = 10.0 min). The collected eluent (162.3 mCi, 63 % DC) was immobilized on *two* tC_{18} Plus® SPE cartridges [activated previously with MeOH (10 mL) and water (10 mL), then concentrated under a stream of He at 90 ºC over 24 min. Over this time, 2 x 1 mL portions of MeCN were added. The efficiency of this concentration step was 73 % DC. 102.0 mCi of [^{18}F]-**16** (48 % DC from SOS) remained after drydown. Synthesis time for this step was 103 min.

4.6.3. *[^{18}F]F-ALK-BBN*

Prepared immediately beforehand was Cu^{I}-TBTA catalyst. TBTA (5.3 mg, 9.4 equiv. relative to peptide) was dissolved in DMSO (960 µL) and transferred to a microcentrifuge tube containing $Cu(CH_3CN)_4PF_6$ (3.1 mg, 7.8 equiv.). To this mixture, 2-6-lutidine was added (40 µL, 325 equiv.).

To a sealable test tube containing dried [^{18}F]-**1** (17.0 mCi) in ~100 µL residual water was added DMSO (100 µL) and the solution was transferred to a microcentrifuge tube containing **N_3-BBN** (1.3 mg). The efficiency of this transfer step was 85 % DC. The mixture of Cu^{I}/TBTA/2,6-lutidine (100 µL) was added, and the reaction was heated at 37 °C for 20 min. The reaction was diluted with 2:1 MeOH:H_2O (600 µL) and the slightly cloudy solution was passed through a Millex-HV filter (0.45 µm). The efficiency of this transfer step was 98 % DC. Filtered material was purified by HPLC (HPLC 7, R_t = 22.8 min), then the collected eluent was diluted with water (21 mL). The solution was trapped on a tC_{18} cartridge (4.34 mCi), washed with water (5 mL), and eluted with MeOH (2 mL). DMSO (100 µL) was added to the eluent and the mixture dried to ~100 µL at 80 ºC. A solution of 10 % 2-hydroxypropyl-ß-cyclodextrin (HPßCD) in PBS (900 µL) was added and the final formulation was filtered through a Millex-HV filter (0.45 µm) at afford

2.84 mCi of **[^{18}F]F-ALK-BBN** (35 % DC yield from start of bioconjugate synthesis). Synthesis time for this step was 85 min.

4.6.4. *[^{18}F]F-ALK-BVD*

[^{18}F]-**1** (44.7 mCi) was eluted off a tC_{18} column with DMSO (300 µL) in a microcentrifuge tube containing **N_3-BVD** (0.73 mg). A freshly prepared solution of $Cu(CH_3CN)_4PF_6$ (2.12 mg, 10.2 equiv. relative to peptide) and TBTA (4.47 mg, 15.1 equiv.) in DMSO (100 µL) was added, and the reaction was shaken thoroughly and left to react at RT. After 15 min, the reaction was diluted with water (400 µL) and centrifuged for 3 min (13,000 cm^{-1}), then the supernatant was purified by HPLC (HPLC 8, R_t = 22.8 min). The collected eluent (6.12 mCi in ~4 mL) was diluted to 50 mL with water, then trapped on a tC_{18} light cartridge [activated previously with EtOH (1 mL) and water (5 mL)]. After washing with H_2O (5 mL), the ^{18}F peptide was eluted off the column with EtOH (300 µL), followed by saline (2.7 mL) and filtered through a HT Tuffryn syringe filter (0.2 µm). The final formulation (10 % EtOH in saline) contained 4.39 mCi of **[^{18}F]F-ALK-BVD** (26 % DC yield from start of bioconjugate synthesis). Synthesis time for this step was 60 min.

4.6.5. *[^{18}F]F-ALK-BBN-PEG*

Prepared immediately beforehand was mixture of Cu^{I}-TBTA catalyst. TBTA (2.3 mg, 14.3 equiv. relative to peptide) was dissolved in DMF (200 µL) and transferred to a microcentrifuge tube containing $Cu(CH_3CN)_4PF_6$ (1.2 mg, 10.7 equiv.). 2,6-Lutidine (35 µL, 1000.3 equiv.) was added to this solution, followed by aqueous sodium ascorbate (25 µL of a 36 mg/mL solution, 15.0 equiv.).

[^{18}F]-**1** (7.48 mCi) was eluted with DMF (300 µL) directly into a microcentrifuge tube containing **N_3-BBN-PEG** (0.5 mg). The Cu^{I}/TBTA/2,6-lutidine/Na ascorbate solution was then added, and the reaction was shaken thoroughly and left to react at room temperature for 30 min. After this time, the mixture was diluted with water (400 µL), filtered through a HT Tuffryn syringe filter (0.45 µm), and purified by HPLC (HPLC 9, R_t = 13.3 min). The collected eluent (3.62 mCi, ~6 mL) was diluted to 50 mL with water and trapped on a tC_{18} light column [activated previously with EtOH (3 mL) and H_2O (6 mL)]. After washing with H_2O (5 mL), the ^{18}F peptide was eluted off the column with

EtOH (150 µL), followed by saline (1.35 mL) and filtered through a HT Tuffryn syringe filter (0.2 µm). The final formulation (10 % EtOH in saline) contained 2.45 mCi of **[^{18}F]F-ALK-BBN-PEG** (58 % DC yield from start of bioconjugate synthesis). Synthesis time for this step was 73 min.

4.6.6. *[^{18}F]F-PEG-BBN-PEG*

In a 5 mL conical vial, [^{18}F]-**17** (17.3 mCi) was dissolved in DMSO (300 µL). To this vessel **N_3-BBN-PEG** (0.5 mg) in DMSO (100 µL) was added. A freshly prepared solution of $Cu(CH_3CN)_4PF_6$ (1.2 mg, 11.7 equiv. relative to peptide) and TBTA (2.6 mg, 17.6 equiv.) in DMSO (100 µL) was added, and the reaction was shaken thoroughly and left to react at RT for 30 min. After this time, the mixture was diluted with an aqueous solution of 0.1 % TFA (600 µL), centrifuged for 3 min (11337 × *g*), and purified by HPLC (HPLC 19, R_t = 13.8 min.) The collected eluent (2.98 mCi, ~5 mL) was diluted to 50 mL with water and trapped on a tC_{18} light column [activated previously with MeOH (3 mL) and H_2O (6 mL)]. After washing with H_2O (5 mL), the ^{18}F peptide was eluted off the column with EtOH (300 µL), followed by saline (2.7 mL), then filtered through a HT Tuffryn syringe filter (0.2 µm). The final formulation (10 % EtOH in saline) contained 2.39 mCi of **[^{18}F]F-PEG-BBN-PEG** (23 % DC yield from start of bioconjugate synthesis). Synthesis time for this step was 83 min.

4.7. Experimental Procedures

4.7.1. *Determination of Apparent Specific Activities of ^{18}F Peptides*

^{19}F peptide (0.5- 1.0 mg) was dissolved in EtOH (200 µL) and diluted with 0.9 % saline (1.8 mL). The stock solution was serially diluted by 5 into four separate containers using 10 % EtOH in saline, and 100 µL or 200 µL of these standards (depending on the starting concentration of peptide) were assayed by analytical UV-HPLC at 280 nm. Each standard was injected three times and the average measure of UV- absorbing material associated with the ^{19}F peptide at each concentration was used to generate a straight line representing absorbance with respect to peptide moles (R^2 > 0.9998). Upon completion of an ^{18}F peptide radiosynthesis, an aliquot of known activity from the final formulation was assayed using identical HPLC conditions and the amount

of UV- absorbing material co-eluting with the radio-peptide signal was estimated relative to the mass standard curve. Apparent specific activities were reported in GBq of injected activity per μmol of associated peptide. **[^{18}F]F-ALK-BBN-PEG:** R_t = 10.3 min. (HPLC 10). **[^{18}F]F-ALK-BVD:** R_t = 16.1 min. (HPLC 11). **[^{18}F]F-PEG-BBN-PEG:** R_t = 13.6 min. (HPLC 19).

4.7.2. *Determination of log D of ^{18}F- labelled BBN analogues at pH 7.4*

Four aliquots of ^{18}F peptide (200 μL in 10 % EtOH in saline*) were added to a 1:1 mixture of 1-octanol and phosphate buffer (10 mL, 20 mM, pH 7.4) in a centrifuge tube. After vortexing for 3 min at RT, the mixture was centrifuged (11337 × *g*, 3 min). An aliquot (1 mL) of each phase was removed from each tube and counted with a dose calibrator. The distribution coefficient was determined by calculating the logarithms of ratios of cpm per mL of 1-octanol to that of phosphate buffer: log $D_{[7.4]} = \log_{10}$[(counts/mL octanol)/(counts/mL buffer)]. The experiment was done in quadruplicate. **[^{18}F]F-ALK-BBN**: 1.40±0.01. **[^{18}F]F-ALK-BBN-PEG**: -0.92±0.03. **[^{18}F]F-PEG-BBN-PEG**: -1.12±0.01.

4.7.3. *Determination of Apparent Specific Activity of PEG-[^{18}F]FPyKYNE (16)*

Non-radioactive **16** was dissolved in 1:1 DMSO:0.1 % TFA (1 mM). This stock solution was serially diluted by 10 into four separate containers using MeCN and an aliquot of each (100 μL) was assayed by analytical UV-HPLC (HPLC 6, R_t = 9.7 min). Each sample was injected three times and the average measure of UV- absorbing material associated with the ^{19}F bifunctional molecule at each concentration was used to generate a straight line representing absorbance at 260 nm with respect to compound moles ($R^2 > 0.9998$). After purification of the radioactive version, an aliquot of known

* Except **[^{18}F]F-ALK-BBN**, which is insoluble in this solvent matrix. In this case, 10 % MeOH in saline was used. The solubility of **[^{18}F]F-ALK-BBN** in this solvent system was confirmed (80 % transfer efficiency, DC).

activity in MeCN was assayed using identical HPLC conditions and the amount of UV-absorbing material co-eluting with the radio-detection signal was estimated relative to the mass standard curve. Apparent specific activity was reported in GBq of injected activity per µmol of associated non-radioactive material.

4.8. Results and Discussion

4.8.1. *Non-Radioactive Small Molecule Chemistry*

A summary of the established synthesis of FPy5yne (**1**) as reported by Inkster *et al.*[379] is shown in Figure 4.3. In this approach, standard compound **1** was prepared from the fluorodenitration of 3-(hex-5-ynyloxy)-2-nitropyridine (**2**). In a separate synthesis, the reductive dimethylation of 2-amino-3-hydroxypyridine afforded 2-dimethylamino-3-hydroxypyridine (Error! Bookmark not defined.), which was then alkynylated *via* Williamson ether synthesis to yield 2-dimethylamino-3-(hex-5-ynyloxy)pyridine (**11**). Finally, the trimethylammonium triflate salt (**3**) was furnished in good yield by treatment of **11** with methyl triflate.

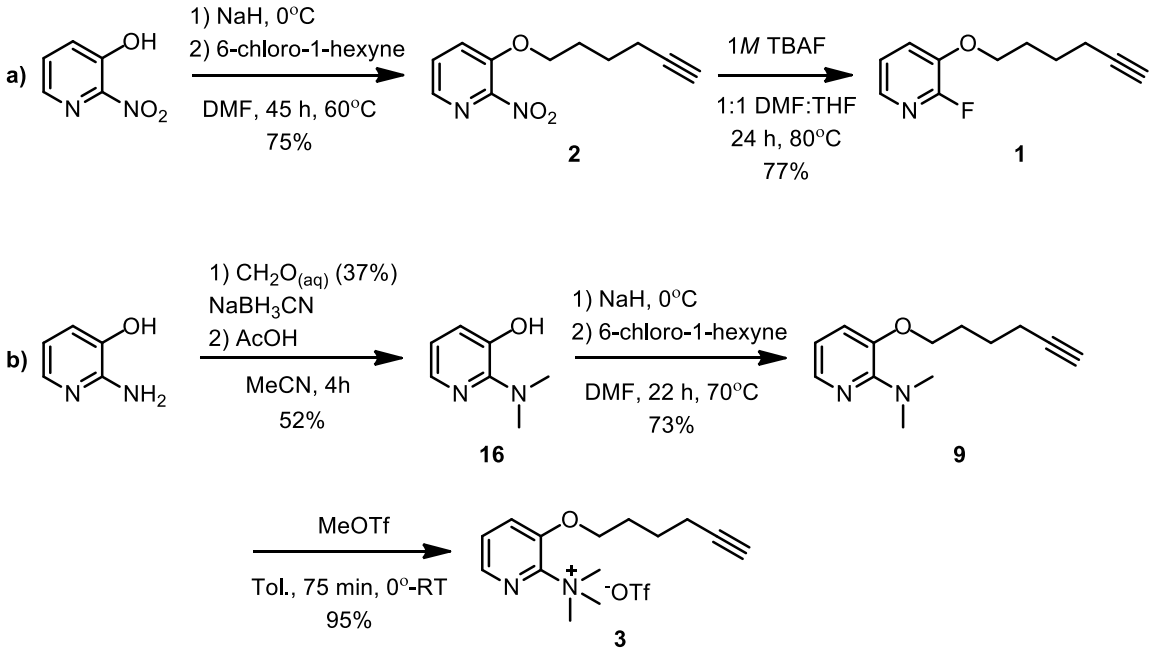

Figure 4.3. Reported synthesis of [^{18}F]FPy5yne- related compounds.

Adapted from Inkster *et al.*[379] a) Synthesis of precursor **2** and synthetic standard **1**. b) Synthesis of precursor **3**.

An attempt was made to improve the non-radioactive chemistry associated with the preparation of [^{18}F]-**1**. Owing to the superior ^{18}F labelling qualities of **3** over **2**, along with its ease of removal from the fluorination reaction mixture, we focused our attention on the improved synthesis of precursor **3** only. However, 2-fluoro standard **1** was still desired, and thus a route was devised where **1** and **3** could be prepared in the same convergent synthesis (Figure 4.4). Paramount to our new strategy was the desire to eliminate the need for 2-dimethylamino-3-hydroxypyridine (Error! Bookmark not defined.), because the original reported yield could not be replicated by others in our group and yields of 10- 25 % were the norm. This was at least partially attributed to the observed sublimation of Error! Bookmark not defined. upon concentration *in vacuo*.

The alternative route starts with the synthesis of 2-fluoro-3-hydroxypyridine (**12**) from 2-amino-3-hydroxypyridine *via* Balz-Schiemann reaction (47 %). 2-Amino-3-hydroxypyridine has been used previously to prepare **12** in crude yields of 63 %[412] and 57 %.[299] Alkylation of the pyridin-3-ol moiety under Mitsunobu conditions afforded FPy5yne (**1**). A portion of the ^{19}F standard then served as starting material for the synthesis of 2-dimethylaminopyridine derivative **11** by way of heating in aqueous dimethylamine. Excess volatile amine nucleophile and ethanol co-solvent were required to complete the reaction. The total synthetic efficiency of this route is 18 %, which compares favorability to the method in Figure 4.3, considering that a) both **1** and **3** can be obtained in a single, convergent 4-step protocol and b) the unreliable synthesis of Error! Bookmark not defined. has been obviated.

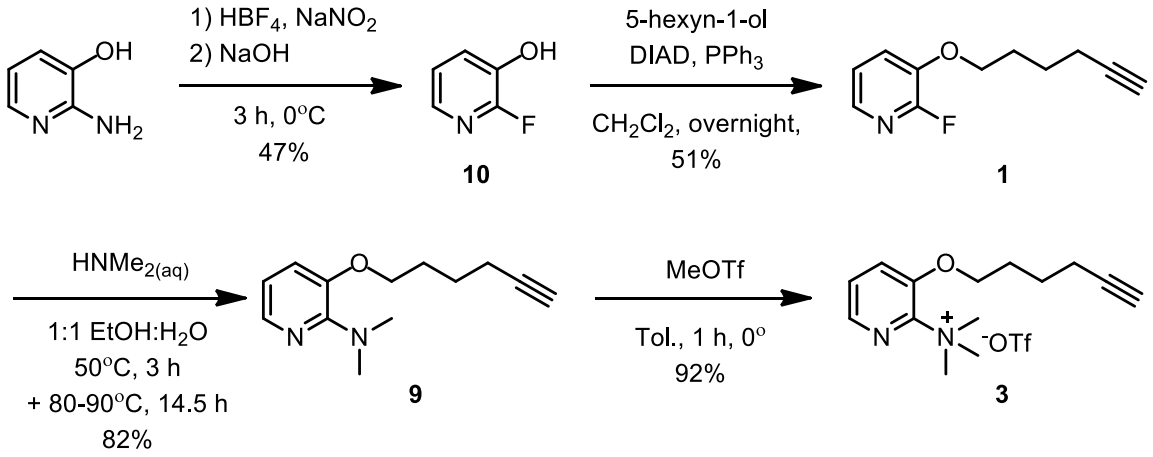

Figure 4.4. Revised synthesis of [^{18}F]FPy5yne precursor 3 and non-radioactive FPy5yne.

With the desire to utilize a water- soluble CuAAC catalyst that might be more amendable to bioconjugate ligations, crude 3-azido-1-propanol (**13**) was reacted with tripropargylamine in the presence of $Cu(CH_3CN)_4PF_6$ (1.7 % with respect to total alkyne units) to form THPTA (**14**). THPTA has been previously synthesized in analytically pure form from acetate-protected **13** (32 % efficiency after deprotection).[271] In addition, a crude THPTA yield of 72 % was reported using polymer- supported Cu^I; the authors found some copper, presumably leached from the solid support, in the final product.[413] Finally, a crude yield of 76 % was achieved after the direct coupling of **13** and tripropargylamine with $Cu(CH_3CN)_4PF_6$, followed precipitation of the chelator from a methanolic solution with acetonitrile.[414] We took a similar synthetic approach, but found that analytically pure material could only be obtained after silica gel chromatography and two recrystallizations. As might be expected after three purification steps, the preparative yield was low (11 %).

As described in Section 1.3.2, PEG spacers can serve as a means to enhance the hydrophilicity of peptidic molecular imaging agents which might otherwise exhibit undesirable hepatobiliary clearance as a result of chemical modification (*i.e*. truncation, amino acid replacement, and/or introduction of pendant groups). Incorporation of the PEG functionality directly into the prosthetic molecule (as in Figure 1.16) enhances the simplicity and utility of the overall synthetic strategy because, in effect, two modifications are being carried out at one time. To this end, we envisioned a ^{18}F prosthetic compound similar to [^{18}F]-**1** in which the butyl chain is replaced with diethylene glycol spacer (PEG-

[^{18}F]FPyKYNE, [^{18}F]-**16**). We predicted that, like [^{18}F]-**1**, high radiochemical yields could be achieved through the [^{18}F]fluorination of a 2- trimethylammonium triflate precursor (**18**). The synthesis of precursor **18** and non-radioactive standard **16** is shown in Figure 4.5. Mitsunobu coupling[415] of 2-fluoro-3-hydroxypyridine (**12**) and alcohol **15** was used to afford PEG-FPyKYNE (**16**). Then, in light of the successful conversion of ^{19}F standard **1** to 2-dimethylamino pyridine **11** with $HNMe_{2(aq)}$, a similar nucleophilic substitution was used to furnish **17** from **16**. Owing to the increased hydrosolubility of **17** relative to **1**, the addition of organic co-solvent was not required in this case. Finally, the mixing of **17** with one equivalent of methyl triflate yielded PEG-NMe_3-KYNE (**18**) precursor salt.

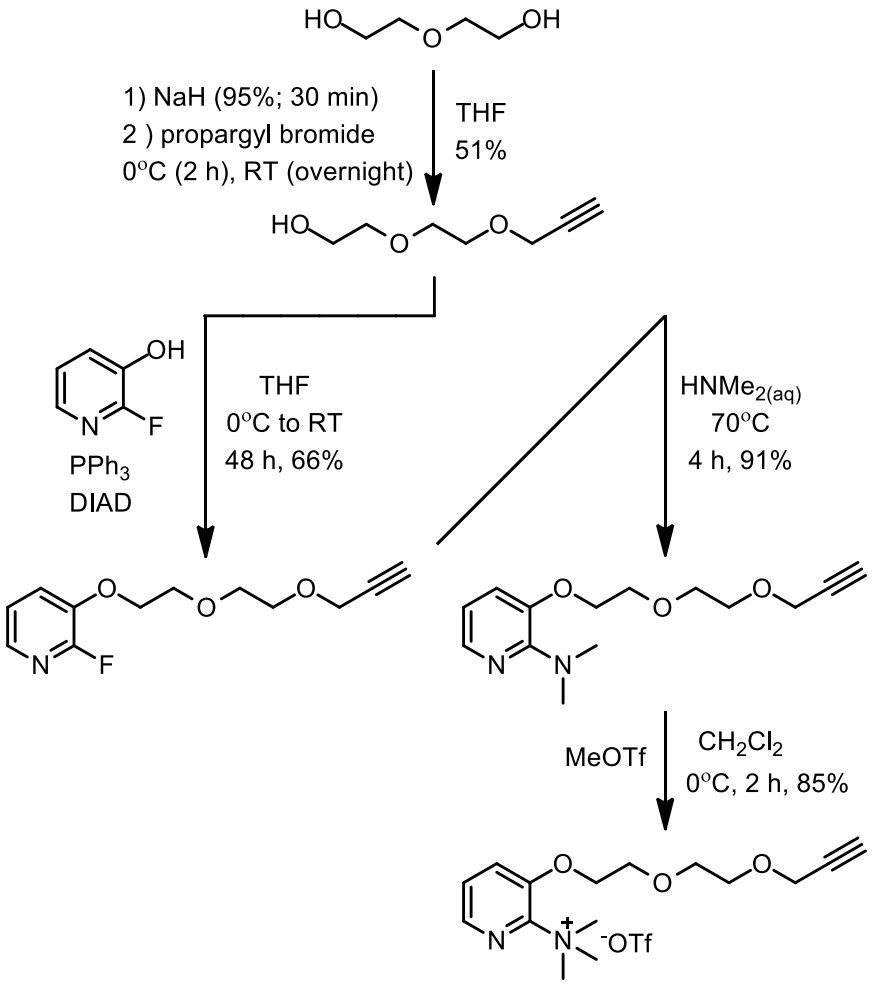

Figure 4.5. Non-radioactive synthesis of PEG-FPyKYNE and PEG-NMe_3-KYNE.

While looking for means to predict the outcomes of nucleophilic aromatic [^{18}F]fluorination reactions, Ding *et al.* observed a correlation between the ^{13}C NMR

chemical shifts of certain electron- rich formylated nitrobenzene precursors and measured radiochemical yields.[416] In particular, higher RCYs were positively and linearily correlated with larger shifts at the carbon adjacent to the nitro leaving group. Thus, for five structurally similar compounds with δ ranging from 142.24-149.58 ppm, RCYs of 5- 78 % were observed (Figure 4.6). This point considered, a strictly electrostatic comparison of the C_1 carbon in NMe_3Py5yne (**3**, δ 148.85 in MeOD, 600 MHz) and PEG-NMe_3-KYNE (δ 148.83) suggested that the new mini-PEGylated precursor **18** would be at least as effective as **3** for the incorporation of $[^{18}F]F^-$.

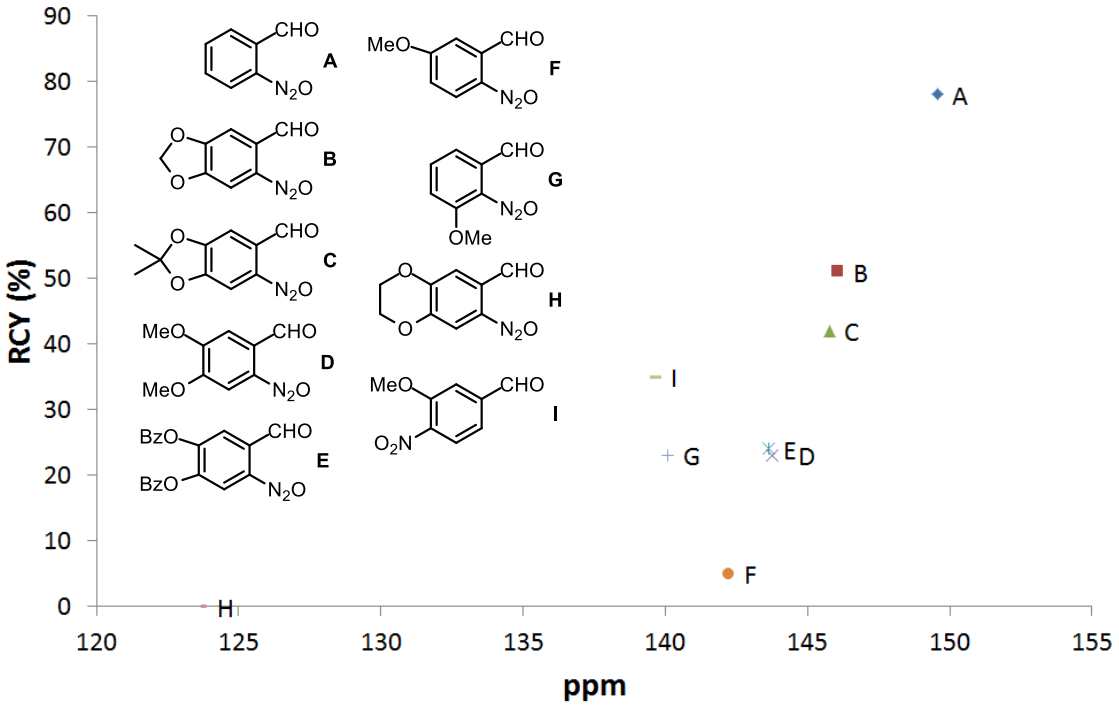

Figure 4.6. Plot of ^{13}C chemical shift (δ) of reaction centres vs. nuclear aromatic $[^{18}F]$fluorination radiochemical yields for a series of electron-rich C6 rings.

Adapted from Ding *et al.*[416] Radiochemical yields using precursors **A**-**F** increase with chemical shift of the carbon adjacent to NO_2 leaving group; the yields fit well onto a straight line. Compounds **G** and **I** are structurally dissimilar and their radiochemical yields are not well-correlated. The α carbon of compound **H** is significantly shielded relative to the others (δ 123.70 ppm); no $[^{18}F]$fluorination of this precursor was observed.

4.8.2. *Non-Radioactive Bioconjugate Chemistry*

Non-radioactive acetylene- bearing pendant molecules were conjugated to azide-modified bombesin and neuropeptide Y1 analogues by way of post-synthetic CuAAC bioconjugation reactions. Details of these bioconjugate syntheses are given in Table 4.2, and structures of the resulting modified peptides are shown in Figure 4.2. In most cases, $Cu(CH_3CN)_4PF_6$ and TBTA were used as the catalytic components. After purification by HPLC and structural confirmation by MALDI-TOF, the non-radioactive peptides were used as synthetic standards during radiochemical preparations and for the generation of mass standard curves. As observed with other peptide- based CuAAC bioconjugations, the presence of chemical impurities in the reaction mixture were the norm. However, unless noted below, the labelled peptides were separated from other UV- absorbing species as judged by HPLC.

^{19}F peptides **F-ALK-BBN** and **F-ALK-BVD** were assayed by our collaborators for their ability to inhibit the retention of ^{125}I- labelled peptide receptor ligands from the surface of human cancer cells (Table 4.1). Based on these assays, **F-ALK-BBN** and **F-ALK-BVD** were selected for future radiofluorination experiments. It was noted at this time that **F-ALK-BBN** was not soluble in water, suggesting that this peptide is rather lipophilic. Thus, two strategies were envisioned to enhance the water- solubility of **F-ALK-BBN** and perhaps improve its receptor binding affinity, biodistribution and clearance pattern *in vivo*. The first approach involves the synthesis of a modified BBN(6-14) fragment with a longer pendant group that includes a triethyleneglycol diamine moiety. Thus, **N_3-BBN-PEG** was post-synthetically conjugated to **1** to afford a synthetic standard of **F-ALK-BBN-PEG** (Figure 4.2). This water- soluble peptide exhibited excellent inhibitory capabilities (Table 4.1). The second approach involves the conjugation of F-PEG-KYNE (**16**) to **N_3-BBN** to yield **F-PEG-BBN** and to **N_3-BBN-PEG** to afford **F-PEG-BBN-PEG** (Figure 4.2). Although **F-ALK-BVD** proved to be water-soluble, we also explored the preparation of **F-PEG-BVD** (Figure 4.2).

Table 4.1. Inhibitor constants for peptide ligands of interest.

Peptide	Competing Peptide	Receptor Target	Cell Line	K_i (nM)
BBN(6-14)	[^{125}I]Tyr^3-BBN	GRPr	PC3	~1*
F-ALK-BBN	[^{125}I]Tyr^3-BBN	GRPr	PC3	21±8

Peptide	Competing Peptide	Receptor Target	Cell Line	K_i (nM)
F-ALK-BBN-PEG	[^{125}I]Tyr^3-BBN	GRPr	PC3	0.4±0.2
F-PEG-BBN-PEG	[^{125}I]Tyr^3-BBN	GRPr	PC3	0.4±0.2
BVD15	[^{125}I]PYY	NPY1r	MCF7	18±13
F-ALK-BVD	[^{125}I]PYY	NPY1r	MCF7	31±18
F-ALK-BVD	[^{125}I]PYY	NPY1r	SK-N-MC	15±6

Note: *Brigitte Guérin, personal communication. PC3 = human prostate cancer cell line. MCF7 = human breast cancer cell line. PYY = peptide YY, a pan-NPYr ligand. SK-N-MC = human neuroblastoma cell line.

CuAAC bioconjugations of mini-PEGylated **16** to obtain **F-PEG-BBN** and **F-PEG-BVD** were not straightforward. During the non-radioactive synthesis of **F-PEG-BVD**, consumption of **N_3-BVD** starting material was accompanied by appearance of a new chemical species, which appeared as a single peak during semi-preparative HPLC (HPLC 3). When concentrated and assayed by MALDI-TOF, the product exhibited a base peak of the expected mass. However, also observed in the spectra was a signal corresponding to [M^++^{63}Cu] (A1. 3, Appendix). Evidence of a Cu-peptide adduct was also observed during the attempted synthesis of **F-PEG-BBN**. In this case however, the product formed during CuAAC reaction was found to be two fractionally resolved chemical species (Figure 4.7).* Furthermore, the closest of the two product peaks ran close to the N_3 precursor peptide (ΔR_t = 0.5 min, HPLC 3). This suggests that [^{18}F]-**16** may not be amendable to the ^{18}F labelling of longer peptides, because it does not confer a significant change in charge localization upon ligation such that the N_3 and ^{18}F peptides may be separated by HPLC. As the advancement of pre-clinical objectives was considered paramount to this project, concerns about the potentially low achievable radiochemical purity and specific activity of **F-PEG-BVD** and **F-PEG-BBN** led to a cessation of their further study. Further discussion related to the presence of Cu-peptide adducts in this work can be found in Section 5.7.7.

* For MALDI-TOF analysis, both peaks were collected and concentrated together.

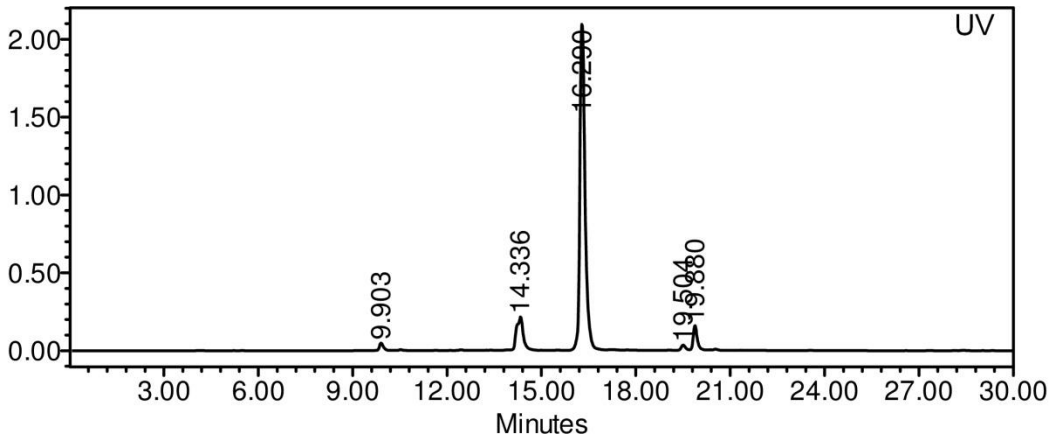

Figure 4.7. Analytical HPLC trace of F-PEG-BBN reaction mixture.

HPLC 3. Collected product (a composite of two peaks) can be seen at 14.3 min. R_t of **16** = 16.3 min. R_t of precursor peptide **N_3-BBN** = 13.8 min (consumed in this trace).

Not unexpectedly, di-mini-PEGylated peptide ligand **F-PEG-BBN-PEG** (Figure 4.2) eluted closely with its N_3- bearing precursor during HPLC purifications. An alternative C_{12} HPLC sorbent (90Å, Jupiter Proteo®, Phenomenex), which has been optimized for peptide chromatography, was required for even modest resolution (ΔR_t = 0.3 min, HPLC 19). Nevertheless, it was established that radioactive **[^{18}F]F-PEG-BBN-PEG** could, with careful execution, be separated from **N_3-BBN-PEG** precursor using this HPLC system. Furthermore, the collected ^{19}F standard did not exhibit evidence of Cu adduct formation when assayed by MALDI-TOF (A1. 4, Appendix). These results prompted the further development of [^{18}F]-**16** and **[^{18}F]-PEG-BBN-PEG**. (Sections 4.8.3.5 and 4.8.3.6 respectively).

Table 4.2. Non-radioactive synthetic details of peptides for Chapter 4.

Product Peptide	Synthetic Details	R_t (min)	ΔR_t (min)*	HPLC
F-ALK-BBN	TBTA, 2:1 PBS:DMF, RT, 3.5 h	22.5	1.4 (22.5-21.1)	HPLC 7
NMe$_3$-ALK-BBN	THPTA, DMF, RT, 3.7 h	12.1	-1.1 (12.1-13.2)**,†	HPLC 17
F-PEG-BBN	TBTA, ,2:1 DMSO:PBS, RT, 5.5 h	14.2/14.3	0.5 (14.2-13.8)**	HPLC 3
F-ALK-BBN-PEG	TBTA, DMSO, RT, 1.3 h	19.9	1.2 (19.9-18.7)	HPLC 4
F-ALK-BVD	TBTA, 2:1 DMSO:PBS, RT, 3.5 h	12.2	2.0 (12.2-10.8)	HPLC 3
F-PEG-BVD	TBTA, 2:1 DMSO:PBS, RT, 3.5 h	11.5	1.7 (11.5-10.8)	HPLC 3
F-PEG-BBN-PEG	TBTA, DMSO, RT, 2 h	13.6	0.3 (13.6-13.3)	HPLC 19

Note: In all cases, $Cu(CH_3CN)_4PF_6$ was used as catalyst. *Product peptide – N_3 peptide. **From closest peptide- associated peak. †Closest peak was 1.2 min from **13** (17.4 min).

The choice of a relatively robust peptide analogue such as [D-Tyr^6, βAla^{11}, Thi^{13}, Nle^{14}]BBN(6-14) allows for the uncommon opportunity to investigate a *pre-synthetic* strategy for the ^{18}F labelling of this receptor ligand. Specifically, **N_3-BBN** labelling precursor does not contain any moieties that might easily liberate a proton under the standard, basic $K_{2.2.2}$/K[^{18}F]/K_2CO_3 conditions. We were inspired by the work of scientists at ETH Zürich, which showed that bombesin derivatives bearing TMA- and cyano- modified benzene rings could be synthesized and eventually [^{18}F]fluorinated in the classical manner[405-407] (see Figure 4.1 and Section 4.2). Owing to the outstanding capacity of 2-TMA-substituted pyridines to incorporate [^{18}F]F^- in dilute solutions,* a GRPr ligand that bears this functionality might well serve as an excellent precursor for the rapid and high yielding preparation of ^{18}F-BBN analogues. To this end, **NMe_3-ALK-BBN** (Figure 4.2) was synthesized by way of CuAAC reaction with NMe_3Py5yne (**3**) and **N_3-BBN**. In this case, THPTA had recently become available and was used as an alternative to TBTA. Unlike TBTA, THPTA does not precipitate out upon quenching the reaction with aqueous solution, yet its polar character ensures that it is well removed from peptidergic species upon purification with the HPLC conditions used. The collected peptide was well resolved from its N_3 precursor using the HPLC conditions reported (Table 4.2) and the lyophilized product exhibited the desired base peak when assayed by MALDI-TOF (A1. 5, Appendix). However, **NMe_3-ALK-BBN** could only be partially separated from **3** by HPLC, which exhibits significant tailing character due its ampiphatic nature. An attempt to [^{18}F]fluorinate this partially purified peptide analogue is described in Section 4.8.3.7.

* A RCY of 68 % by HPLC was observed for the labelling of [^{18}F]-**1** using a precursor concentration of 1 mM (110 ºC, 15 min). (Hua Yang, personal communication.)

4.8.3. *Radiochemistry*

The time it takes to deliver a PET isotope from its point of origin to an appropriate radiosynthetic workspace (*i.e.* transfer time) is often variable and essentially outside a chemist's control, yet can have a marked effect on the efficiency of a radiochemical synthesis. For instance, the average difference between EOB and EOS at TRIUMF was 35±21 min (*n*=13). This excludes one transfer that took 214 min. In an attempt to better describe the quality of the protocols reported in this section, preparative RCYs are given from start-of-synthesis (SOS).*

4.8.3.1. Radiosynthesis of [^{18}F]FPy5yne ([^{18}F]-1)

Syntheses of [^{18}F]-**1** for the preparation of **[^{18}F]F-ALK-BBN** were initially carried out at the Radiochemical Annex at TRIUMF. These syntheses followed a previously published protocol,[379] with modifications as described in Section 3.6.1. As observed previously, incorporation of [^{18}F]F^- in DMSO solvent (100ºC) was facile and efficient. Furthermore, reaction mixtures were devoid of radiolabelled impurities as confirmed by TLC. One perceived flaw in the preparation of [^{18}F]-**1** as originally reported was the need to concentrate the somewhat volatile prosthetic from solution after HPLC purification and SPE extraction. With this in mind, the concentration of [^{18}F]-**1** from CH_2Cl_2 (2 mL) for **[^{18}F]F-ALK-BBN** syntheses was carried out under a stream of He (180 mL/min) at room temperature (see 2.4 of Figure 4.8). Average drydown efficiency was 77±13 % (*n*=13).† Average DC, preparative yield of [^{18}F]-**1** at TRIUMF was 51±14 % (*n*=14).

* For ^{18}F prosthetic molecules, this refers to the point when the activity adsorbed to the anion exchange column is measured, just prior to elution with $K_2CO_{3(aq)}$. For ^{18}F peptides, this refers to the point when the first CuAAC reactant or reagent is introduced to the N_3 precursor.

† This excludes one radio-experiment in which excessive drying resulted in a drydown efficiency of 26 %.

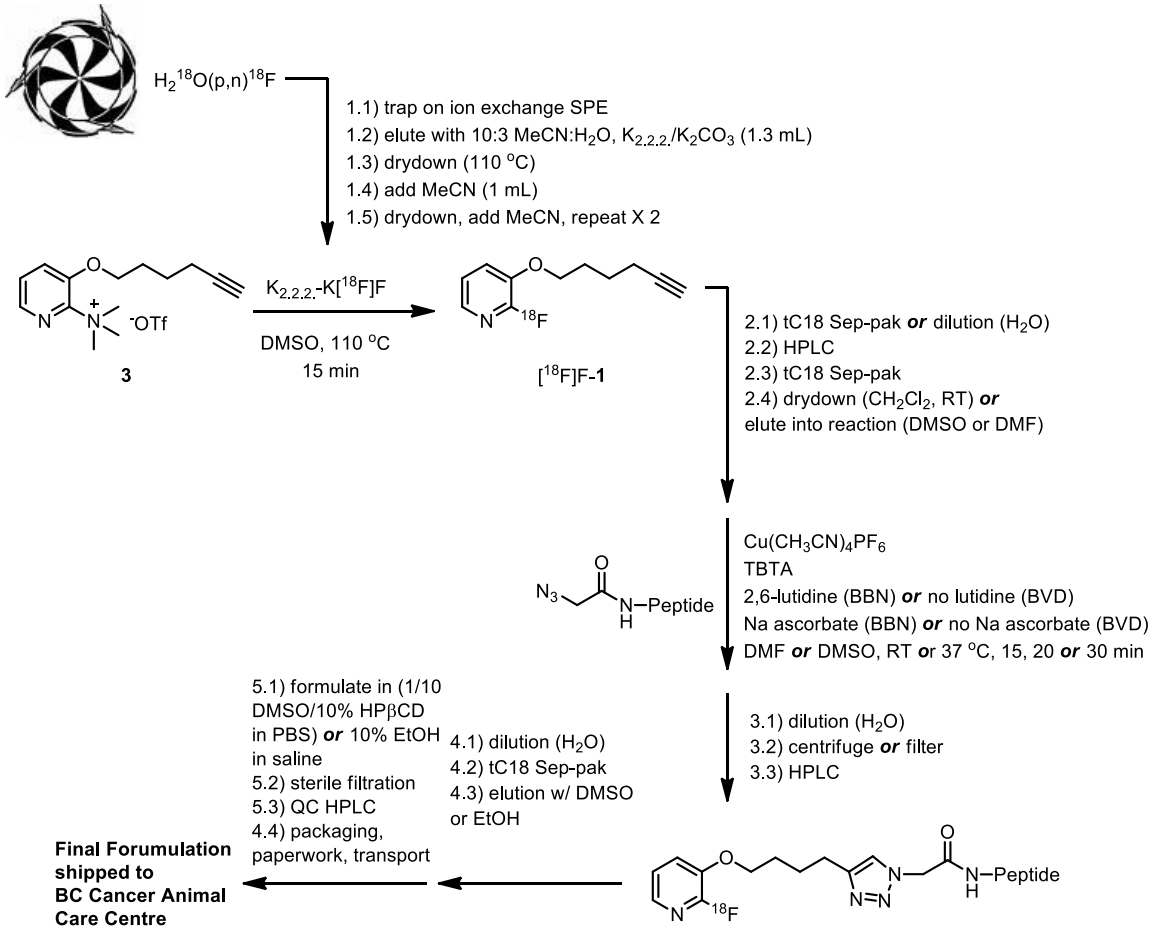

Figure 4.8. Radiosynthesis of ^{18}F peptides labelled with [^{18}F]-1.

Peptide = BBN, BVD or BBN-PEG. [^{18}F]F-**1** at TRIUMF: 2.1) tC_{18} Sep-pak; 2.4) drydown. [^{18}F]F-**1** at BC Cancer: 2.1) dilution; 2.4) elute into reaction. For individual bioconjugation and formulation details, see Sections 4.6.3- 4.6.6.

Preparation of [^{18}F]-**1** at BC Cancer was accompanied by two further improvements. First, it was determined that it was not necessary to extract [^{18}F]-**1** from the reaction mixture before HPLC purification. Instead, the reaction mixture (0.5 mL DMSO) could be diluted with water (0.5 mL) and injected directly onto a semi-preparative HPLC column (See 2.1 of Figure 4.8). Good separations could only be achieved if the reaction mixture was transferred from the original vessel to another one containing dilution solvent (H_2O). Presumably, this step works to partially remove the basic reagents ($K_{2.2.2.}/K_2CO_3/[^{18}F]F^-$) that have adsorbed to sides of the reaction vessel prior to HPLC injection. Second, the deleterious concentration of [^{18}F]-**1** by way of CH_2Cl_2 evaporation (See 2.4 of Figure 4.8) was obviated in favour of elution off the tC_{18}

SPE column with DMF or DMSO directly into a microcentrifuge tube containing N_3 peptide precursor. This constitutes a significant radiosynthetic improvement as reverse-phase SPE trapping adds ~20 min to the synthetic protocol and often increases exposure of the chemist to ionizing radiation.

Despite these gains, radiosynthetic yields of [^{18}F]-**1** were often mitigated by the appearance of persistent and excessive radiochemical impurities (Figure 4.9) which appeared during a majority of [^{18}F]FPy5yne syntheses at BC Cancer. These low-yielding reactions were accompanied by the observation that dried batches of [^{18}F]F$^-$ (which presumably contain only $K_{2.2.2.}$, K_2CO_3 and [^{18}F]F$^-$) appeared rust- coloured, rather than off- white. While [^{18}F]-**1** could still be prepared chemically and radiochemically pure, collected yields were variable and unimpressive (DC-RCY = 24±16 % from SOS, 6-44 % NDC). Efforts to rectify this problem included: a) employing an alternative brand of anion exchange sorbent for [^{18}F]F$^-$ trapping (PS-HCO_3 cartridges, GE Healthcare); b) changing all solvents and reagents; c) utilizing freshly prepared TMA precursor. In the end, radiochemical purities were only restored (Figure 4.9) after another researcher observed brownish contaminant in her ^{11}C reactions and the decision was made to replace the shared He lines which supply the facility. For the runs carried out after this renovation was completed, average NDC yield of [^{18}F]-**1** was 24±4 % (*n*=5) from SOS (47±6% DC), which is similar to [^{18}F]-**1** yields obtained at TRIUMF for the synthesis of **[^{18}F]F-ALK-BBN** (25±9 %, *n*=14) and **^{18}F-ODN** (30±2 %, *n*=4, Section 3.7.2).

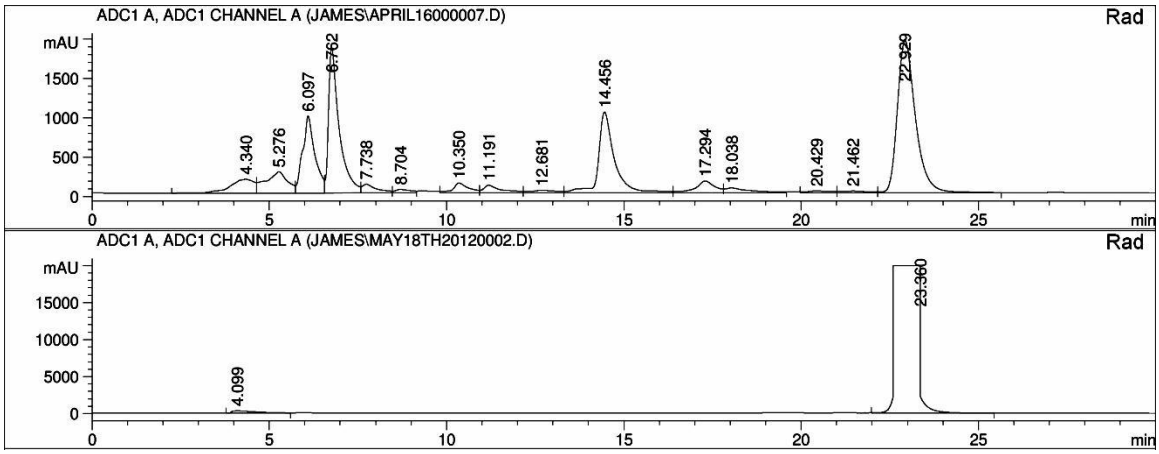

Figure 4.9. Radio-HPLC of two preparations of [^{18}F]FPy5yne at BC Cancer

HPLC 6. Y-axis = radiation detection (arbitrary units). Preparative traces of [^{18}F]-**1** reaction mixtures at BC Cancer on April 16th, 2011 (top) and May 18th, 2012 (bottom).

4.8.3.2. Radiosynthesis of [^{18}F]F-ALK-BBN

^{18}F-ALK-BBN was synthesized exclusively at TRIUMF (Figure 4.8). Early attempts at optimization focused on shortening and simplifying the general protocol for the preparation of [^{18}F]-**1**- labelled peptides as reported in Inkster *et al*[379] (Section 1.5). In the aforementioned report, HPLC- purified ^{18}F peptide was concentrated by azeotropic distillation of the collected eluent (4-8 mL). However, this method typically takes between 25- 40 min and does not assure complete removal of TFA from the final formulation. Thus, this drydown step was avoided in favour of immobilization of the ^{18}F peptide on tC_{18} sorbent (see 4.3 of Figure 4.8). The tracer was then eluted from the SPE column with a solvent amendable for *in vivo* use. The choice of final formulation demanded significant attention because **[^{18}F]F-ALK-BBN** is only sparingly soluble in aqueous solutions. A summary of ^{18}F peptide solubility tests can be found in Table 4.3. Benzoic acid (10 %) in PBS resulted in acceptable levels of solvation, but a signal associated with BzOH co-eluted with **[^{18}F]F-ALK-BBN**, making HPLC assay of the final formulation impossible (Figure 4.10). In the end, a 9:1 mixture of 2-hydroxypropyl-ß-cyclodextrin[417] solution (10 % HPßCD in PBS) and DMSO was employed for *in vivo* use. Collected yield of **[^{18}F]F-ALK-BBN** after bioconjugate synthesis was 34±17 % DC (*n*=8).

Table 4.3. Formulations tested for the solvation of [^{18}F]F-ALK-BBN.

Final Formulation	Final Volume (mL)	% Solvation (DC)
PBS*	0.5	3
9:1 PBS: Intralipid® (20 %)**	1	7
Intralipid® (20 %)	0.5	12
5 % BzOH in water	1	25
10 % BzOH in sodium acetate†	1	63
10 % BzOH in PBS	1	81
9:1 HPßCD (10 % in PBS):DMSO	1	88
9:1 HPßCD (10 % in PBS):DMSO	1	89

Note: *150 mM, pH 7.4. **Commercially available fat emulsion composed of soybean oil, glycerin and egg lecithin.[418] †20 mM, pH 4.6. Percent solvation represents the ratio DC activity removed from the final formulation vessel / total activity × 100. Each entry represents a separate radio-experiment.

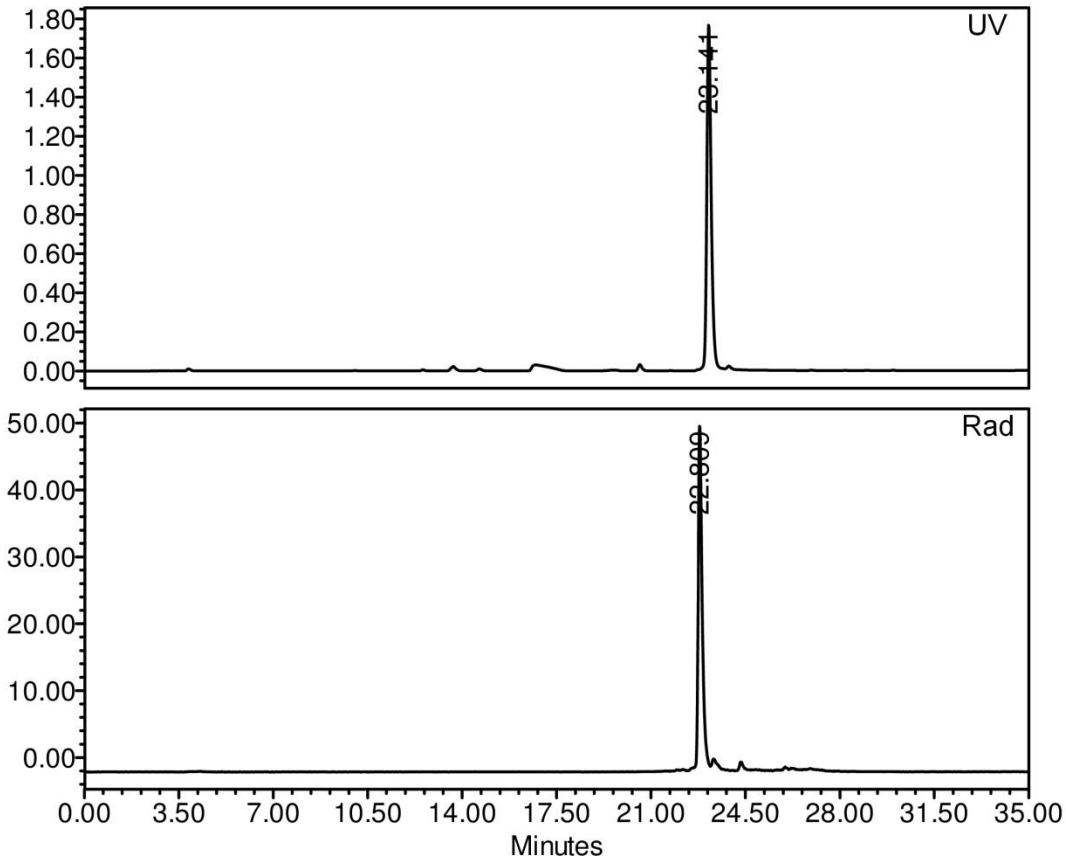

Figure 4.10. HPLC trace of final formulation of [^{18}F]F-ALK-BBN in 10 % BzOH in PBS

HPLC 7. Top: UV absorbance (280 nm, absorbance units). A convoluting peak associated with BzOH formulation solvent can be seen at 23.1 min. Bottom: radioactive detection (mV).

4.8.3.3. Radiosynthesis of [^{18}F]F-ALK-BBN-PEG

[^{18}F]F-ALK-BBN-PEG was synthesized exclusively at BC Cancer, in a manner similar to the synthesis of **[^{18}F]F-ALK-BBN** (Figure 4.8). However, three important improvements to protocol were made at this time. First, the inclusion of sodium ascorbate to the reaction mixture (15 equivalents relative to peptide) was accompanied by a marked increase in radiochemical yield as observed by HPLC, such that complete consumption of [^{18}F]-**1** starting material could be achieved in <30 min at room temperature. Second, the removal of the ^{18}F peptide from HPLC eluent was achieved by way of tC_{18} SPE trapping, rather than evaporation of MeCN/0.1 % TFA at 80 ºC. While the BBN derivatives described here do not seem to be detrimentally affected by heating under these conditions, concentration by evaporation may not be amendable to all

peptide ligands; furthermore, this approach was time-consuming (~25 min) and lacked reproducibility. Third, **F-ALK-BBN-PEG** is soluble in most aqueous systems and- unlike **F-ALK-BBN**- could be formulated in 10 % EtOH in saline, which is a well- established solvent system for peptide- based PET ligands. Collected yields after bioconjugate synthesis was 31±19 % DC (*n*=11).

Overall preparative yields of many ^{18}F radiobioconjugates tend to be highly variable, owing to the length and complexity of the standard pre-synthetic labelling strategy. In addition to the standard complement of challenges associated with short-lived radioisotope chemistry, many of the radiochemical yields of **[^{18}F]F-ALK-BBN-PEG** and **[^{18}F]F-ALK-BVD** were depressed as a result of the inefficient production of [^{18}F]-**1** (see Section 4.8.3.1). Nevertheless, useful quantities of **[^{18}F]F-ALK-BBN-PEG** were repeatedly produced for cellular affinity, *ex vivo* biodistribution, and µPET studies.[*] The apparent specific activity of **[^{18}F]F-ALK-BBN-PEG** in four separate experiments was found to be 14, 39, 43, and 74 GBq/µmol. Not surprisingly, the radio-peptide of lowest specific activity (14 GBq/µmol) failed to image PC3 tumours in a murine PET experiment (*vide infra*).

4.8.3.4. Radiosynthesis of [^{18}F]F-ALK-BVD

The development of **[^{18}F]F-ALK-BVD** was initiated at TRIUMF, then later carried over to BC Cancer. Initial radiosyntheses utilized a reaction mixture of Cu^{I}/TBTA/2,6-lutidine. Complete CuAAC ligations were not achieved at 37 ºC over 20 min in DMSO. The optimization of **[^{18}F]F-ALK-BBN-PEG** yields through the addition of sodium ascorbate prompted us to attempt the same with **[^{18}F]F-ALK-BVD**. While this strategy did lead to the complete consumption of [^{18}F]-**1**, HPLC chromatography suggested that little or no product peptide was formed (Figure 4.12). Instead, a host of closely eluting, polar impurities made up the bulk of the ^{18}F- labelled material. As noted in the Section

[*] Delivered activity ranged from 0.63 mCi- 37.1 mCi. Collaborators at BC Cancer typically used the minimum activity required to obtain quality data: 20 µCi/biodistribution and 100 µCi/µPET scan. The maximum number of scans carried out in one day was four; the maximum number of biodistribution assays was 13. (Maral Pourghiasian, personal communication.)

1.4.2, CuAAC reaction mixtures employing sodium ascorbate may yield reactive carbonyl species *via* formation and hydrolysis of dehydroascorbate. These degradation products have been shown to react with arginine, lysine, and N-terminal cysteine residues[419] through various carbonyl addition- elimination reactions, in a manner conceptually similar to the formation of advanced glycation endproducts (AGEs).[420] Of specific interest to **N_3-BVD**- based CuAAC ligations is the observation that α,β-dicarbonyl glyoxal reacts with arginine residues to form a hydroimidazolone compound (**19**; Figure 4.11).[421, 422] In cell-free assays, the glyoxal generated (19±4 μM) over 2 h when incubated with sodium ascorbate (20 mM) and Cu was quadruple that of mixtures that did not contain Cu.[264] Furthermore, when bovine serum albumin (BSA) was incubated with ascorbate (20 mM) and Cu for 7 days, hydroimidazolone- specific BSA adducts were measured in a >22 fold excess relative to controls. Although the complex mixture of polar peptide degradation products observed in **[^{18}F]F-ALK-BVD** reaction mixtures (Figure 4.12) was not identified, this observation is consistent with the conversion of one or both BVD15 arginines to **19**- and/or **20**- type derivatives (Figure 4.11).

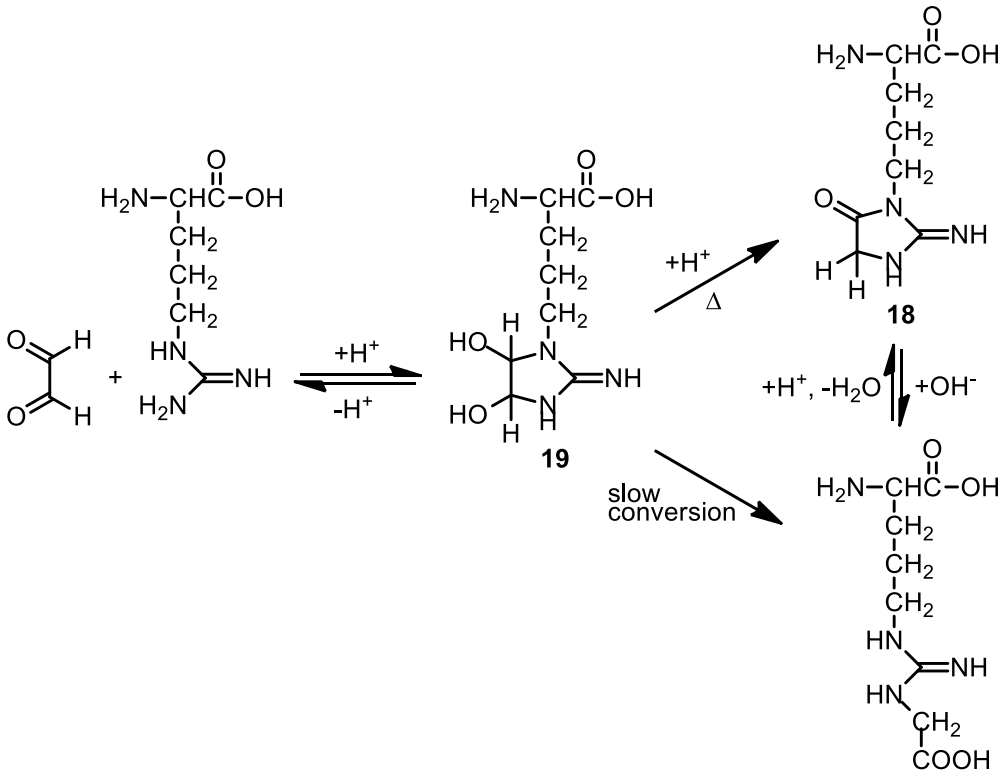

Figure 4.11. Proposed mode of condensation of arginine and ascorbic acid oxidation product glyoxal.

Adapted from Glomb and Lang.[421] Initial condensation product 5-(4,5-dihydroxy-2-imino-1-imidazolidinyl)norvaline (**20**, four isomers) can undergo ring opening followed by intramolecular disproportionation to yield 1-(4-amino-4-carboxybutyl)-2-imino-5-oxo-imidazolidine (**19**). Formation of **19** is greatly enhanced under acid conditions.

In an attempt to mitigate the observed radiochemical impurities, syntheses of **[^{18}F]F-ALK-BVD** for preclinical assay were eventually carried out under the most straightforward conditions possible, *i.e.* no sodium ascorbate or nitrogen base. Reactions were carried out in DMSO at RT over 15 min. In this fashion, high- purity ^{18}F peptide was achievable, albeit at the cost of collected bioconjugation yields (11 % and 26 % DC). A third reaction was carried out in DMF and resulted in an inferior yield (2.7 % DC.) For two of these experiments, specific activity at end-of-synthesis was measured and found to be 42 and 96 GBq/µmol.

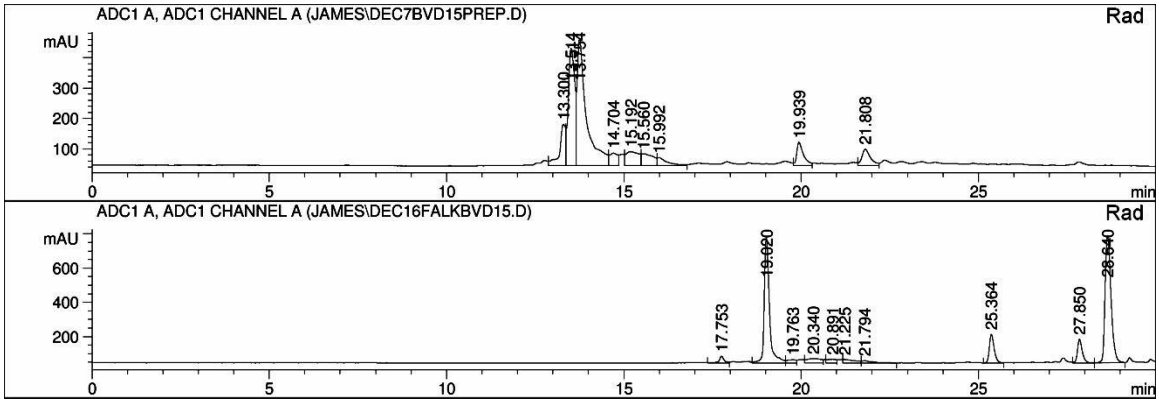

Figure 4.12. Radio-HPLCs of [^{18}F]F-ALK-BVD with and without sodium ascorbate.

HPLC 19. Figure shows two preparative traces of **[^{18}F]F-ALK-BVD** reaction mixture with (top trace) and without (bottom trace) sodium ascorbate (15 equiv. relative to peptide). Y-axes = radioactive detection (arbitrary units). R_t of **[^{18}F]F-ALK-BVD** = 19.0 min. R_t of [^{18}F]-**1** = 28.6 min.

4.8.3.5. Radiosynthesis of PEG-[^{18}F]FPyKYNE ([^{18}F]-16)

During the preparation of this manuscript, the first radiosynthesis of PEG-[^{18}F]FPyKYNE ([^{18}F]-**16**) was reported in abstract form.[423] The authors ^{18}F- labelled 2-bromo and 2-nitro analogues of precursor **18** in radiochemical yields of ≤50 % by radio-TLC (165 °C, 5 min). As described above, the trimethylammonium moiety is the premier leaving group for the K[^{18}F]/$K_{2.2.2.}$ fluorination of homo- and hetero- aromatic systems, both in terms of [^{18}F]F^- incorporation[134] and ease of precursor removal.[105] Thus we anticipated that salt **18** might offer a superior route to [^{18}F]-**16**. The reaction conditions used to prepare [^{18}F]-**16** were similar to those used for synthesis of [^{18}F]-**1** (Figure 4.13). Incorporation of [^{18}F]F^- during three separate experiments was achieved in yields of 69±1 %, 81±2 % and 91±1 % (*n*=3 traces each), as determined by the gamma counting of fractionated radioTLC plates. A graphical plot of the data collected during one of these experiments is shown in Figure 4.14.

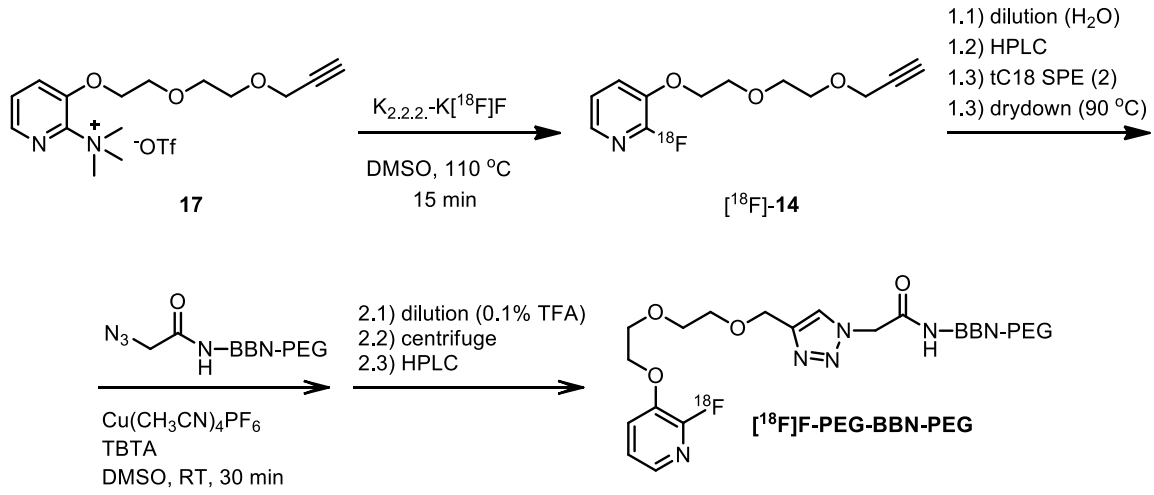

Figure 4.13. Radiosynthesis of PEG-[^{18}F]FPyKYNE and [^{18}F]F-PEG-BBN-PEG.

Additional preparative steps (such as those found in Figure 4.8) have been removed for clarity.

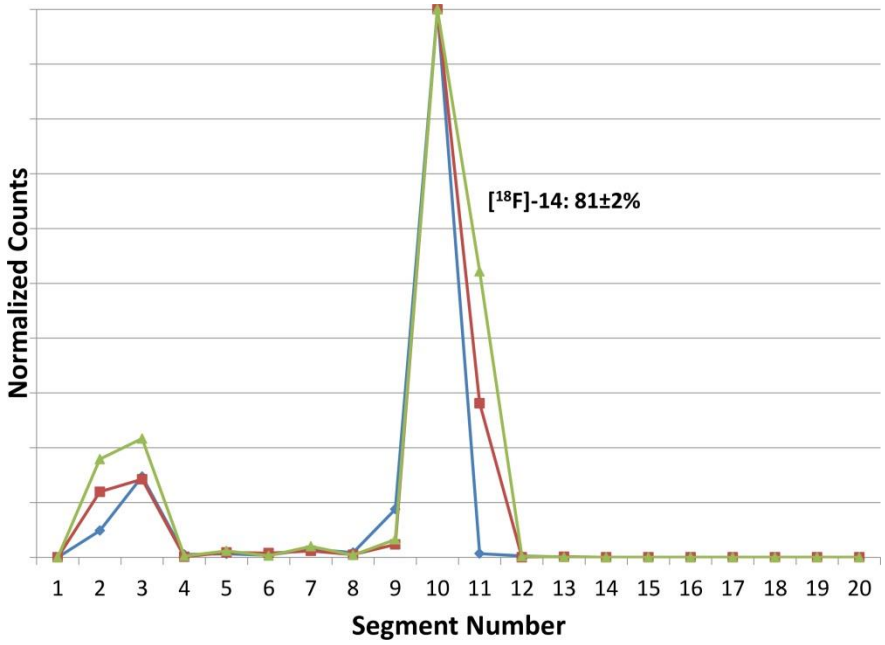

Figure 4.14. Distribution of radioactivity on a radio-TLC plate spotted with [^{18}F]-16 reaction mixture.

Plot includes data from three plates. Each plate (20 cm) was cut into 20 segments; each segment was individually assayed by gamma scintillography.

HPLC purification of the [^{18}F]-**16** was straightforward and collected yields were satisfactory and reproducible (45- 64 % DC, *n*=4). However, in contrast with

[^{18}F]FPy5yne, which could be efficiently extracted from HPLC eluent using tC$_{18}$ SPE sorbent after dilution with 50 mL of water, PEG-[^{18}F]FPyKYNE was not well retained on this sorbent type. The decay- corrected trapping efficiency was 27- 42 % (*n*=4 experiments) when a small ('light') SPE cartridge was used.* Not surprisingly, final preparative radiochemical yields of [^{18}F]-**16** were only 16±2 % DC (*n*=4). Prior to the start of pre-clinical testing in mice, the efficiency of the concentration step was improved by employing two full-size tC$_{18}$ SPE columns, then removing [^{18}F]-**16** from SPE eluent (MeOH) by heating (90 ºC) under a stream of He (73±2 % efficiency, DC, *n*=3). It is worth noting that this strategy would likely not be possible for the radiosynthesis of [^{18}F]-**1**, owing to its low boiling point (69- 70 ºC).[379] Isolation by heating resulted in longer protocol times, but higher collected yields (39±9 % DC, *n*=4) versus tC$_{18}$ 'light' extraction. An attempt to concentrate the solvent mixture at 110 °C resulted in significantly more product loss by evaporation (41 % efficiency, DC). Measured apparent specific activity at end-of-synthesis was 180±9 GBq/µmol (*n*=3).

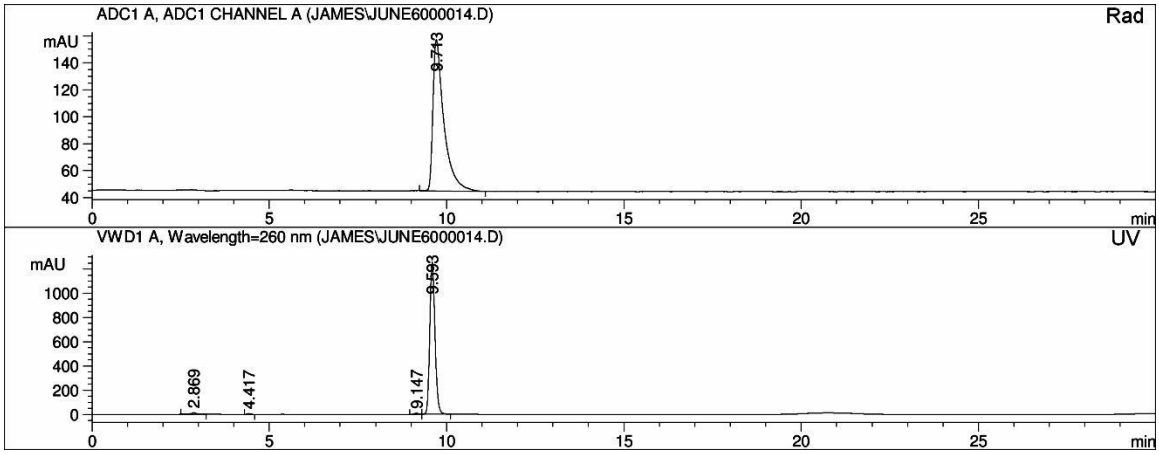

Figure 4.15. Radio-HPLC of PEG-[^{18}F]F-PyKYNE, co-injected with ^{19}F standard.

HPLC 6. Figure shows final formulation of [^{18}F]-**16** admixed with non-radioactive standard. Top: UV absorbance, 260 nm (absorbance units). Bottom: radioactive detection (arbitrary units).

* Trapping the ^{18}F prosthetic molecule on a 'light' SPE column allows for elution with a small volume of organic solvent (as little as 0.3 mL). In this way direct elution into the bioconjugate reaction mixture is possible, without the need for a secondary drydown step.

4.8.3.6. Radiosynthesis of [^{18}F]F-PEG-BBN-PEG

As described in Section 4.8.2, the synthesis of **[^{18}F]F-PEG-BBN-PEG** was initiated after it was established that the non-radioactive version could be obtained in chemically pure form after HPLC purification. Given the challenging separation of **N_3-BBN-PEG** and **[^{18}F]F-PEG-BBN-PEG** required, straightforward CuAAC conditions were employed ($Cu(CH_3CN)_4PF_6$/TBTA, RT, DMSO, 30 min) in a bid to minimize the production of radiochemical impurities. Under these conditions, the radio-bioconjugation did not proceed to completion (Figure 4.16). Nevertheless, collected yields from start of bioconjugation were 25±13 % DC (*n*=4), and chemically and radiochemically pure tracer was obtained in amounts amendable for *in vivo* study. (A maximum of 19.9 mCi was prepared starting from a single batch of [^{18}F]F^-.) The apparent specific activity of **[^{18}F]F-PEG-BBN-PEG** at end-of-synthesis in was found to be 78±38 GBq/μmol (*n*=4).

During HPLC purifications of **[^{18}F]F-PEG-BBN-PEG**, a radio-impurity was consistently observed that was notable in terms of amount (7- 17 % of total radioactivity) and polarity (HPLC 19, R_t = 12.3 min; Figure 4.16). In an effort to establish the origin of this chemical species, a small molecule prosthetic group [^{18}F]-**16** was synthesized and incubated in a similar CuAAC reaction mixture, but without ^{18}F peptide (Figure 4.17). The radio-impurity was observed in this case as well (4 % by HPLC). It is hypothesized that this radio-peak represents Cu- chelated [^{18}F]-**16**. The variability in observed yield during ^{18}F peptide preparations may be the result of small but significant differences in free copper in each reaction mixture. Alternatively, the specific activity of [^{18}F]-**16** could be a factor, as the radiochemical yield of any association between Cu and ^{18}F small molecule should be negatively correlated the amount of non-radioactive chelator present. Furthermore, a dependence on high specific activity conditions does much to explain why this species does not form during non-radioactive syntheses of **F-PEG-BBN-PEG**. Further discussion on the topic of Cu-peptide adducts can be found in Section 5.7.7.

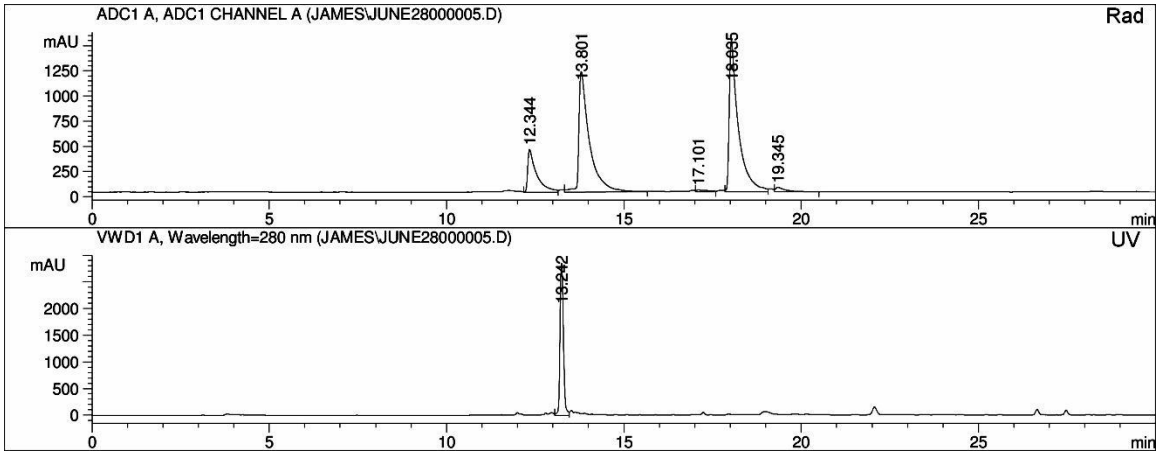

Figure 4.16. Preparative HPLC of [^{18}F]F-PEG-BBN-PEG synthesis.

HPLC 19. Top: radioactive detection (arbitrary units). Bottom: UV, 280 nm (absorbance units). R_t of **N_3-BBN-PEG** = 13.2 min. R_t of **[^{18}F]F-PEG-BBN-PEG** = 13.8 min. R_t of [^{18}F]-**16** = 18.1 min. Note the persistent radiochemical impurity at 12.3 min.

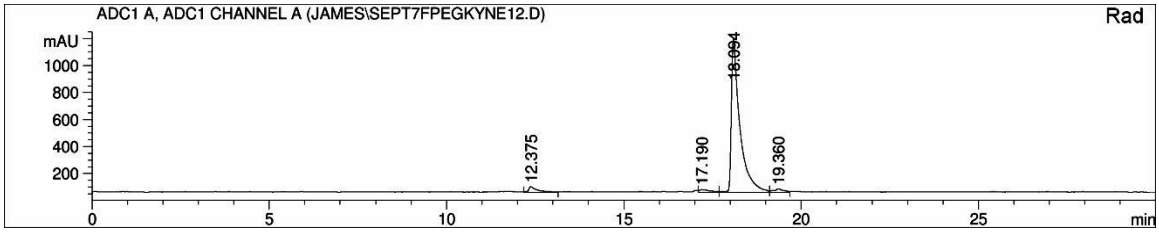

Figure 4.17. [^{18}F]-17 in [^{18}F]F-PEG-BBN-PEG reaction mixture, sans peptide.

HPLC 19. Y-axis: radioactive detection (arbitrary units). Radiotrace of purified [^{18}F]-**16** (18.1 min) after incubation in $Cu(CH_3CN)_4PF_6$/TBTA in DMSO (RT, 30 min). Note the radiochemical impurity at 12.4 min.

4.8.3.7. Attempted synthesis of [^{18}F]F-ALK-BBN from NMe_3-ALK-BBN precursor

Two attempts to *directly* ^{18}F label **NMe_3-ALK-BBN** in the classical fashion were unsuccessful. The reaction conditions were as follows: 4.1 and 3.7 mM peptide precursor, K[^{18}F]F/K_2CO_3, DMSO, 90 ºC, 15 min. Very little radioactivity was transferred from the reaction vessel to the HPLC needle (1.9 % and 0.4 % DC respectively), which

is indicative of significant amounts of free [^{18}F]F$^-$ remaining after heating.* Indeed, analytical radio-HPLC revealed only trace amounts of **[^{18}F]F-ALK-BBN**. The radio-peak associated with [^{18}F]-**1** was only slightly larger, which presumably forms from co-contaminant NMe_3Py5yne in the radiochemical reaction (see Section 4.8.2). In addition to these negative results, HPLC revealed a number of non-radioactive impurities in the reaction mixture, suggesting that **NMe_3-ALK-BBN** precursor is susceptible to degradation under the tested conditions.

4.8.3.8. Lipophilicity of ^{18}F bombesin analogues

The lipophilicity of **[^{18}F]F-ALK-BBN** was assessed relative to its mono- and di-PEGylated derivatives (**[^{18}F]F-ALK-BBN-PEG** and **[^{18}F]F-PEG-BBN-PEG** respectively) by measuring their coefficients of distribution into equal parts octanol and sodium phosphate buffer (20 mM, pH 7.4). As expected, log $D_{[7.4]}$ values decreased with an increase in ethylene oxide (EO) groups in the targeting vectors (1.40, -0.92 and -1.12 respectively). The rather high log *D* found for **[^{18}F]F-ALK-BBN** is consistent with the qualitative observation that this modified peptide is not soluble in purely aqueous solutions. The difference in log *D* values between **[^{18}F]F-ALK-BBN-PEG** and **[^{18}F]F-PEG-BBN-PEG** (0.20) is similar to the observed shift in log *D* between TEGylated and non-TEGylated ^{18}F *c*$(RGD)_2$ peptides (0.18).[162]

4.8.4. *Summary of In Vivo Results*

Significant collaborative efforts with the Bénard group at the BC Cancer Agency has allowed [^{18}F]FPy5yne to see pre-clinical use. A comprehensive description of all biological assays will be published in the PhD. dissertation of Maral Pourghiasian (UBC/BC Cancer). However, PET ligand design is a highly dynamic and multi-disciplinary endeavour which is best understood in the context of *in vivo* and *ex vivo* outcomes. Therefore, some important pre-clinical results are included below.

* In lieu of chemical reaction, the dried [^{18}F]F$^-$ tends to stay adsorbed to the sides of the reaction vial.

[^{18}F]-**1** was first used to ^{18}F- label bioactive derivatives of bombesin(6-14) and neuropeptide Y (**[^{18}F]F-ALK-BBN** and **[^{18}F]F-ALK-BVD** respectively). **[^{18}F]F-ALK-BBN** was designed for the molecular imaging of GRP receptors overexpressed in human prostate cancer (PC3), while **[^{18}F]F-ALK-BVD** (a NPY1r ligand) was tested on MCF7 (breast cancer) and SK-N-MC (neuroblastoma) cell lines. Despite showing retained affinity for their intended receptor targets *in vitro*, both tracers showed insufficient tumour uptake in µPET images and *ex vivo* biodistribution assays (nu/nu mice). Percent ID/g in tumours at 1 h was only 0.14 ±0.04. **[^{18}F]F-ALK-BBN** exhibits unfavourable pharmacokinetic qualities for prostate imaging, including excessively fast blood clearance times, extensive hepatic extraction/biliary excretion and predominantly gut uptake. **[^{18}F]F-ALK-BVD** showed better distribution profiles but % ID/g was only 0.10±0.04 % and 0.7±0.2 % in MCF7 and SK-N-MC models respectively. A murine plasma stability study was carried out with non-radioactive **F-ALK-BVD** and the biological $t_{1/2}$ was found to be 28.2 min. Thus, the poor performance of **[^{18}F]F-ALK-BVD** was attributed to its instability in this biological medium.

[^{18}F]F-ALK-BBN-PEG exhibited an improved biodistribution profile compared to **[^{18}F]F-ALK-BBN**, with less relative uptake into small and large intestine and more into PC3 tumours (% ID/g = 2.8±0.14 % at 15 min post- injection, 1.4±0.13 % at 1h post-injection). Uptake into pancreas, which is an abundantly GRPr- expressing organ, was also observed. Uptake of radioactivity was blocked upon pre-injection of 100 µg BBN acetate salt, thus confirming that an association with GRPr was the source of the images. Furthermore, **[^{18}F]F-ALK-BBN-PEG** permitted the visual delineation of human prostate cancer lesions using µPET. The distribution of di-mini-PEGylated BBN analogue **[^{18}F]F-PEG-BBN-PEG** into tissues was also very rapid and similar to that of **[^{18}F]F-ALK-BBN-PEG**. **[^{18}F]F-PEG-BBN-PEG** showed very high uptake into GRPr-positive tissues (11.9±5 % ID/g at 1 h in pancreas) but slightly inferior uptake into PC3 tumours (1.99±0.1 % at 15 min, 1.31±0.4 % at 1h) relative to **[^{18}F]F-ALK-BBN-PEG**. However, PET images obtained with **[^{18}F]F-PEG-BBN-PEG** were qualitatively superior to those of **[^{18}F]F-ALK-BBN-PEG,** showing clearly delineated tumours. The sequesterization of radiation was blocked by non-radioactive bombesin acetate salt.

4.9. Conclusion

With regard to efficiency and ease of synthesis, the preparation of [^{18}F]-**1** as described in Chapter 4 is clearly an improvement on the methods described in Chapter 3 and by Inkster *et al.*[379] In particular, it was determined that [^{18}F]-**1** need not be extracted out of the reaction solvent prior to HPLC purification, and that removal of HPLC eluent could be achieved by SPE extraction rather than evaporation. When compared with other ^{18}F prosthetic molecules in significant use, the simplicity of this protocol stands out; indeed, it contains the minimum number of radiochemical transformations (two) and the minimum number of SPE concentration steps (two) required to obtain the final radio-bioconjugate. On the other hand, the need for two HPLC purifications to obtain radiobioconjugate of high specific activity remains a significant downside to the use of [^{18}F]FPy5yne. However, other TRIUMF researchers have recently established a protocol whereby [^{18}F]-**1** can be efficiently purified from 2-TMA- pyridine precursor **3** and demethylation product **11** using only C_{18} SPE methods.* This is possible because unusually small amounts of precursor are used during radiosyntheses (100 nmol). Needless to say, it is the excellent capacity of 2-substituted pyridines to incorporate [^{18}F]F^- that makes this approach viable.

Efforts to ^{18}F- label mini-PEGylated precursor peptide **N_3-BBN-PEG** with [^{18}F]-**1** resulted in a ^{18}F- labelled GRPr ligand (**[^{18}F]F-ALK-BBN-PEG**) of enhanced hydrophilicity relative to its non-PEGylated analogue (**[^{18}F]F-ALK-BBN**). Many syntheses of **[^{18}F]F-ALK-BBN-PEG** (and **[^{18}F]F-ALK-BVD15**) were complicated by poor collected yields of [^{18}F]-**1**, but this problem was deemed specific to the BC Cancer radiochemistry workspace and was eventually resolved. Regardless of [^{18}F]F^- incorporation yields, good bioconjugate yields and a cadre of improvements to the overall radiosynthetic protocol permitted the synthesis of **[^{18}F]F-ALK-BBN-PEG** in preparative yields and specific activities amendable for further biological study. During those radiobioconjugations in which [^{18}F]-**1** could be efficiently prepared, the collected

* Hua Yang, personal communication.

DC-RCY of **[^{18}F]F-ALK-BBN-PEG** from EOB was 14±13 % (*n* =4). This work further confirms the notion that problems associated with the addition of lipophilic pendant groups to macromolecules can be mitigated through the use of PEG modifications. Presumably, this solution could positively affect the *in vivo* outcomes of other lipophilic bioconjugates , including [^{18}F]SFB- and di-*tert*-butyl[^{18}F]fluorosilyl- modified bombesin analogues.

The overall preparative yield of **^{18}F]F-ALK-BBN-PEG** described here compares reasonably well with yields obtained through the direct labelling of GRPr ligands which bear SiFA precursors [13±3 % DC (*n* =4), Section 1.6.1][319] and TMA-benzonitrile groups (~15 % DC, Section 4.2).[407] The latter approach is being aggressively pursued by the Ametamey group; a microdosing trial in healthy volunteers was announced in 2011.[407] It is therefore likely that one or both of these simpler ^{18}F labelling strategies will eclipse the use of pre-synthetic ^{18}F prosthetics for the radiofluorination of bombesin analogues. In this regard, the use of post-labelled TMA- bearing pyridines may, in light of their tremendous [^{18}F]fluorinating potential, offer a significant advantage over benzonitriles and other activated C6 aromatic pendant groups. However, preliminary attempts in this work to radiolabel a NMe_3Py5yne (**3**)- modified BBN analogue (**NMe_3-ALK-BBN**) were unsuccessful. Evaluation of the reaction was complicated by the presence of co-contaminant **3** in the reaction mixture. It is possible that **NMe_3-ALK-BBN** could be obtained in pure form if the pendant group was introduced during solid- phase synthesis of the peptide. Finally, it should be noted that the above post-labelling technologies employ classical, anhydrous [^{18}F]fluorination conditions at elevated temperatures, and thus they do not represent general approaches for the ^{18}F- labelling of biological molecules.

While the radiolabelling of a mini-PEGylated peptide with [^{18}F]-**1** proved successful in this case, a mini-PEGylated ^{18}F prosthetic offers an opportunity to introduce two beneficial modifications at the same time (*i.e.* [^{18}F]fluorination and hydro-solubilization). This might prove useful in cases when a potential targeting agent cannot be easily modified- or exhibits diminished bioactivity- with two pendant groups. Thus, encouraging *in vivo* results with **[^{18}F]F-ALK-BBN-PEG** (Section 4.8.4) led to the iterative development of a '2nd generation' FPy5yne derivative (PEG-FPyKYNE; **16**), which bears a PEG tether between its [^{18}F]fluorinated and conjugating functionalities. The CuAAC

conjugation of this hydrophilic molecule to N_3 bombesin analogues **N_3-BBN** and **N_3-BBN-PEG** proved challenging, as only small differences in retention time were observed between the labelled and unlabelled peptides upon HPLC purification. More seriously, two of the **16**- modified peptide ligands (**F-PEG-BVD** and **F-PEG BBN**) exhibited evidence of copper ion association after HPLC purification. In terms of end use, this scenario is unacceptable, owing to the inherent pharmacokinetic and pharmacodynamic complications associated with attempting to utilize a potentially impure or unstable PET agent. Fortunately, the di-mini-PEGylated analogue of **F-PEG BBN** (**F-PEG-BBN-PEG**) could be obtained as a single, non-cuprated chemical species after CuAAC coupling of **16** and **N_3-BBN-PEG**.

The similarity of [^{18}F]-**16** to [^{18}F]-**1** ensured that the radiosynthesis of this prosthetic was straightforward, although an additional evaporative concentration step was required to obtain CuAAC- ready PEG-[^{18}F]FPyKYNE. In this regard, the reduced volatility of [^{18}F]-**16** relative to [^{18}F]-**1** proved advantageous. Radio-peptide **[^{18}F]F-PEG-BBN-PEG** was prepared in yields and specific activities sufficient for *ex vivo* biodistribution experiments and μPET assays in PC3- bearing mice [10±7 % (*n*=4) DC-RCY from EOB]. Log $D_{[7.4]}$ measurements suggests that the peptide is significantly more hydrophilic than **[^{18}F]F-ALK-BBN** and slightly more hydrophilic than **[^{18}F]F-ALK-BBN-PEG**. Initial μPET results suggest a comprehensive pre-clinical evaluation of this novel GRPr ligand is warranted. More importantly, the radio-protocols outlined here make up a viable general strategy for the simultaneous [^{18}F]fluorination/ PEGylation of other, less-established biological targeting vectors.

5. Sulfonyl fluorides for the ^{18}F- labelling of biological PET agents

The chemical synthesis, radiochemistry, and experimental protocols described in this chapter were carried out by James Inkster, although Kate Liu (TRIUMF/UBC) obtained much of the HPLC data that comprises Figure 5.6. Samia Ait-Mohand from Prof. Brigitte Guérin's lab (Université de Sherbrooke) prepared the oxyamino- and azide-modified peptide precursors described herein. This chapter was published in *Chemistry: A European Journal*.[424]

5.1. ^{18}F- labelled sulfonyl fluorides

Reports detailing the synthesis of ^{18}F-labelled sulfonyl fluorides are extremely scarce. In 1975, tosyl [^{18}F]fluoride was synthesized in a carrier- added fashion using reactor- produced K[^{18}F]F as a means to validate the production of ^{18}F by way of neutron bombardment of Li_2CO_3 (Figure 5.1a).[425] In modern ^{18}F research, sulfonyl [^{18}F]fluorides have only been considered in the context of unwanted tosyl [^{18}F]fluoride production during nucleophilic ([^{18}F]F^-) displacement of *p*-toluenesulfonates. The phenomenon is typically considered failed chemistry and thus under-reported. However, Neal *et al*. thoroughly described the production of substantial tosyl [^{18}F]fluoride impurity generated during their synthesis of [^{18}F]fluoromethyl tosylate labelling agent from bis(tosyloxy) methane (Figure 5.1b).[426] It was shown that the ratio of active ester to sulfonyl fluoride could be attenuated by varying the level of residual water in the reaction mixture. Also in this work, tosyl [^{18}F]fluoride was intentionally synthesized from tosyl chloride ($K_{2.2.2.}$/K[^{18}F]F/K_2CO_3, MeCN, 110 °C, 10 min) for use as a radiochemical standard, but no yield was reported. A thesis from the University of Jülich described the radiosynthesis of perfluorobutane-1-sulfonyl[^{18}F]fluoride from *N,N*-bis(perfluorobutane-1-sulfonyl)aniline in the presence of DBU base. High temperatures and an unusual [^{18}F]fluorination solvent (toluene) was utilized. (Figure 5.1c).[427] This perfluorinated ^{18}F

labelling agent could be use to [^{18}F]fluorinate the unnatural hydroxyproline (Hyp) residue of sensitive Z-Pro-Leu-Gly-Hyp-OMe and *Z*-Gly-Leu-Hyp-Gly-Leu-OMe peptides. In this regard, a perfluorinated sulfonate ester is first formed, which is then attacked by the previously displaced [^{18}F]F$^-$ ion. The central flaw in this strategy is that the true labelling precursor (perfluorinated peptide) is produced under low-mass conditions. Thus, for the reaction to proceed, the addition of equimolar amounts of non-radioactive perfluorobutane-1-sulfonyl fluoride was required, resulting in low specific activity radio-peptide.

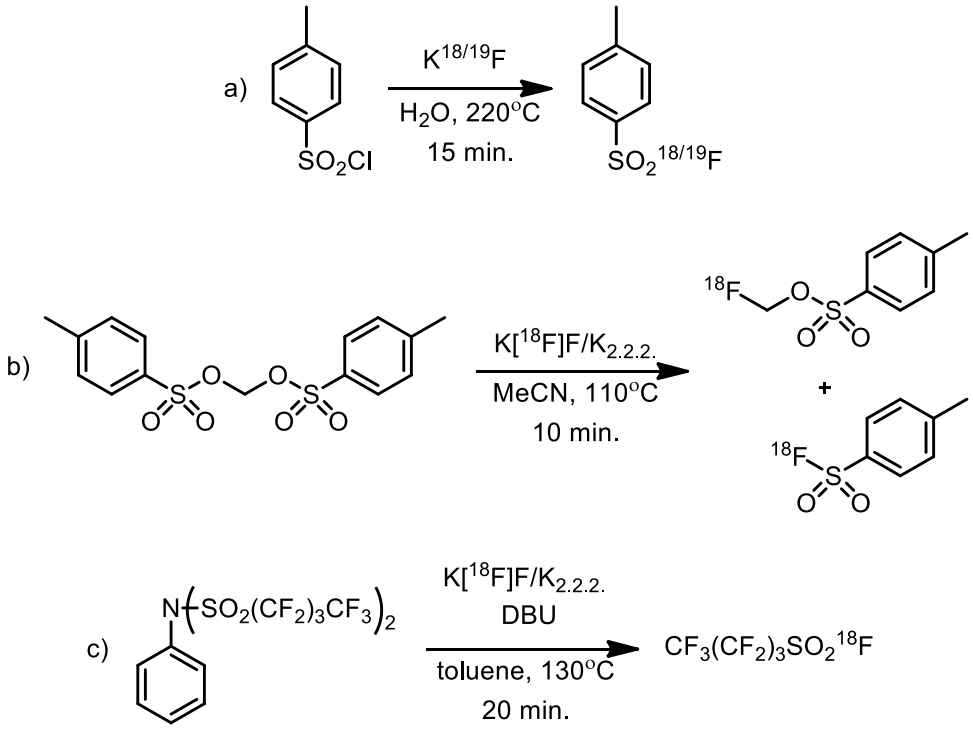

Figure 5.1. Reported syntheses of sulfonyl [^{18}F]fluorides.

a) de Kleijn *et al.*[425] b) Neal *et al.*[426] c) Jelinski, Master's thesis.[427]

To date, the potential utility of sulfonyl fluorides as ^{18}F carriers for PET has been overlooked, no doubt because of issues (both understood and assumed) regarding their stability *in vivo*. However, it is worth noting that under physiological conditions the reaction of benzenesulfonyl fluorides with biological nucleophiles is not typically a straightforward process but requires additional neighboring group interactions to proceed. For example, sulfonyl fluoride- bearing azo dyes have been shown to conjugate to cellulose only if the dye can reversibly complex with the cellulose.[428] With

regard to sulfonyl fluoride reactivity and protein nucleophiles, the principle of 'sulfonylation upon direction' seems to hold. For instance, only chymotrypsin, and not enzyme precursor chymotripsogen, with react with a 20 fold excess of PMSF, and the depletion of PMSF is stoichiometric with respect to enzyme.[341] In another example, Baker *et al.* designed a series of sulfonyl fluoride inhibitors of dihydrofolic reductases and showed that enzyme inhibition did not occur in the absence of a diamino-*s*-triazine ring, the moiety that forms a reversible complex with these enzymes (Figure 5.2).[328] Thus inactivation did not depend simply on a bimolecular reaction but required active-site direction to acylate the enzyme and expel the fluorine atom.

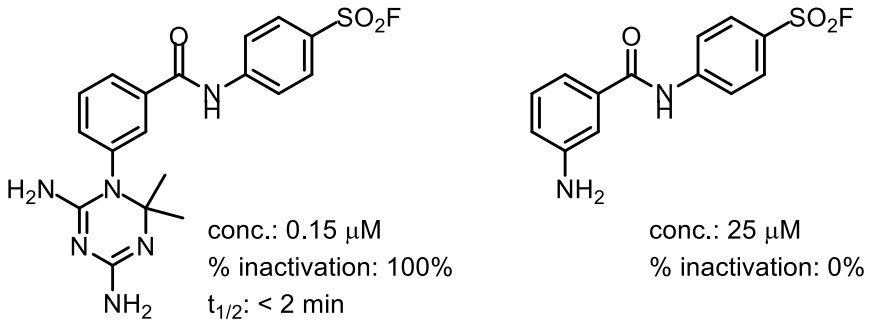

Figure 5.2. An active-site directed serine protease inhibitor of pigeon liver dihydrofolic reductase.

From Baker and Lourens.[429]

5.2. Objectives

In recent years, a desire to circumvent the challenges associated with the established ^{18}F bioconjugate chemistries has led to development of a number of innovative labelling techniques that eschew C-^{18}F bond formation (see Section 1.6.1). However, the potential utility of sulfonyl fluorides for PET chemistry remains unexplored. The ready conversion of sulfonyl fluorides from sulfonyl chlorides in mixtures of water and organic solvent at room temperature might offer an outstanding opportunity to generally improve the simplicity and efficiency of ^{18}F radio-bioconjugations. A strategy was envisioned whereby bifunctional benzenesulfonyl [^{18}F]fluoride prosthetic molecules could synthesized without the need to remove [^{18}F]F^- from [^{18}O]H_2O target water by way of time- consuming azeotropic distillation. Furthermore, the use of highly basic, toxic $K_{2.2.2.}$ cryptand would not be required. Owing to the relative stability of sulfonyl fluorides

over sulfonyl chlorides, it was hypothesized that nitrogen base could be used to selectively degrade the precursor in the presence of the $SO_2[^{18}F]F$ prosthetic group and thus greatly facilitate the ease of tracer purification. Optimization of this general strategy for the preparation of formyl- (**21, 22**), maleimido- (**23**) and oxypropargyl- (**24**) bearing sulfonyl [^{18}F]fluorides (Figure 5.3) in ambient 1:1 mixtures of MeCN, THF, or *t*-BuOH represents the crux of efforts summarized in this chapter. Ancillary to these methodology experiments, we chose to conjugate compounds **22** and **24** to azido- and oxyamino- modified bombesin(6-14) analogues respectively as a means to test the utility of these novel prosthetics for the ^{18}F labelling of functionally complex biomolecules. Finally, given the propensity of some sulfonyl fluorides to react with serine proteases, we deemed it crucial to conduct a preliminary assessment of a novel **22**- bearing GRPr ligand in biological media (*i.e.* mouse serum).

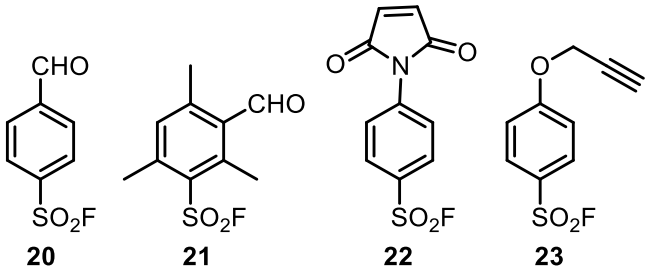

Figure 5.3. Bifunctional sulfonyl fluorides of interest to this work.

5.3. Non-radioactive Small Molecule Syntheses

5.3.1. *4-Formylbenzenesulfonyl fluoride (21):*

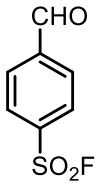

t-Butylammonium fluoride (1M in THF, 4.8 mL) was added dropwise to a solution of 4-formylbenzenesufonyl chloride (Astatech; Bristol, PA; 750 mg, 3.67 mmol) in THF (12 mL) at 0 °C. After 5 min at 0 °C, the reaction was allowed to warm to RT over 45

min. The reaction was poured into sat. ammonium chloride and extracted into diethyl ether. The organic portion was washed once with water and dried over Mg_2SO_4. Purification by silica gel flash chromatography (3:2 hexanes:diethyl ether) afforded 4-formylbenzenesulfonyl fluoride (388 mg, 69 %) as a white powder (**21**). M.P. = 60 °C. ^{1}H NMR (CD_2Cl_2): δ 8.14 (d, J = 8.1 Hz, 2H); 8.20 (d, J = 8.4 Hz, 2H); 10.16 (s, 1H). ^{19}F NMR (CD_2Cl_2): δ 64.765. ^{13}C NMR (CD_2Cl_2): δ 129.79 [2 x CH]; 130.95 [2 x CH]; 137.95 [$J_{C\text{-}F}$ = 25.5 Hz, C]; 141.59 [C]; 190.89 [CHO]. HRMS (EI) calcd. for $C_7H_5O_3FS$: 187.99434. Found: 187.99446. Anal. calcd. for $C_7H_5O_3FS$: C, 44.68; H, 2.68; N, 0. Found: C, 45.07; H, 2.74; N, 0. Compound **21** was also prepared using CsF as fluoride source, in a manner similar to the radiosynthetic protocol (see Section 5.3.15).

5.3.2. ***(E)-4-((Ethoxyimino)methyl)benzenesulfonyl fluoride (25):***

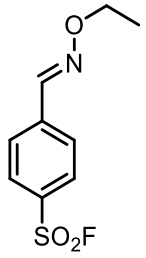

O-Ethylhydroxyamine hydrochloride (63 mg, 0.64 mmol) in EtOH (2 mL) was added to a solution of 4-formylbenzenesulfonyl fluoride (**21**, 100 mg, 0.52 mmol) in EtOH (5 mL) and the reaction was stirred at RT for 90 min. The reaction was quenched with 5 % HCl (10 mL) and extracted into ethyl acetate (3 x 40 mL). The pooled organic portions were washed with water (10 mL) and brine (10 mL) and dried over Na_2SO_4. Purification by silica gel chromatography (9:1 hexanes:ethyl acetate) afforded 83 mg (61 %) of diasterotopically pure *E*-**25**. ^{1}H NMR (400 MHz, CD_2Cl_2): δ 1.33 (t, J = 7.1 Hz, 3H); 4.28 (q, J = 7.1 Hz, 2H); 7.84 (d, J = 8.2 Hz, 2H); 8.00 (d, J = 8.5 Hz, 2H); 8.13 (s, 1H). ^{13}C NMR (400 MHz, CD_2Cl_2): δ 14.71 [CH_3]; 71.09 [CH_2]; 128.04 [CH]; 129.17 [CH]; 133.17 [C, d, $J_{F\text{-}C}$ = 24.6 Hz]; 140.22 [C]; 146.21 [CH]. ^{19}F NMR (300 MHz, CD_2Cl_2): δ 65.082. HRMS (EI) calcd. for $C_9H_{10}N_2O_3FS$: 231.03654. Found: 231.03673.

5.3.3. *Potassium 3-formyl-2,4,6-trimethylbenzenesulfonate (26):*

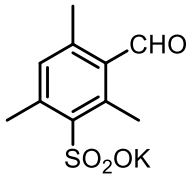

Oleum (20 mL) was added to a RBF, with stirring. Mesitaldehyde (5 mL, 34 mmol) was added *via* syringe. The flask was affixed with a drying tube and heated to 40 °C, during which time the reaction mixture went orange. After 22 h, the reaction was poured onto ice and diluted to 300 mL with water. The reaction was basified to pH 11 with powdered K_2CO_3, with significant evolution of gas and the formation of a precipitate. The precipitate was filtered, and the filtrate diluted with MeCN (300 mL) and filtered again. The filtrate was concentrated to dryness and crystallized from water (35 mL) to afford potassium 3-formyl-2,4,6-trimethylbenzenesulfonate (**26**; 9.03 g, 77 %), a cotton candy-like white solid. M.P. = >260°C. ^{1}H NMR (CH_3OD): δ 2.46 (s, 3H); 2.68 (s, 3H); 2.90 (s, 3H); 7.01 (s, 1H); 10.57 (s, 1H). ^{13}C NMR (CH_3OD): δ 18.22 [CH_3]; 20.58 [CH_3]; 24.23 [CH_3]; 134.53 [C]; 134.64 [C]; 141.60 [C]; 141.72 [C]; 143.20 [C]; 143.51 [C]; 196.23 [C]. HRMS (ESI-) calcd. for $C_{10}H_{11}O_4{}^{32}S$: 227.0378. Found: 227.0377.

5.3.4. *3-Formyl-2,4,6-trimethylbenzenesulfonyl chloride (27):*

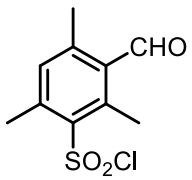

Potassium 3-formyl-2,4,6-trimethylbenzenesulphonate (**26**, 899 mg, 3.38 mmol) and 18-crown-6 (135 mg, 0.51 mmol) were added together as powders and wetted with acetone (12 mL). To this slurry was added cyanuric chloride (623 mg, 3.39 mmol) and the reaction was stirred at 50 °C for 48 h. The reaction was filtered through a plug of Celite, washing with acetone. The resulting filtrate was concentrated and purified on a column of silica gel (4:1 hexanes:diethyl ether) to afford **27** (664 mg, 80 %) as an

amorphous solid. M.P. = 48-50°C. ^{1}H NMR (CD_2Cl_2): δ 2.53 (s, 1H); 2.75 (s, 1H); 2.92 (s, 1H); 7.17 (s, 1H); 10.56 (s, 1H). ^{13}C NMR (CD_2Cl_2): δ 18.16 [CH_3]; 20.96 [CH_3]; 24.11 [CH_3]; 100.18 [CH]; 135.39 [CH]; 135.45 [C]; 142.08 [C]; 142.33 [C]; 143.75 [C]; 146.76 [C]; 193.45 [C]. HRMS (EI) calcd. for $C_{10}H_{11}O_3S^{35}Cl$: 246.01174. Found: 246.01153. Anal. calcd. for $C_{10}H_{11}ClO_3S$: C, 48.68; H, 4.49; N, 0. Found: C, 48.74; H, 4.43; N, 0.

5.3.5. *3-Formyl-2,4,6-trimethylbenzenesulfonyl fluoride (22).*

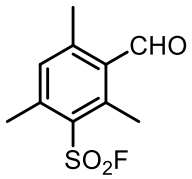

Into a RBF containing 3-formyl-2,4,6-trimethylbenzenesulfonyl chloride (**27**, 1.00 g, 4.05 mmol) in THF (15 mL) was added a solution of TBAF (1 M in THF; 4.9 mL), followed by pyridine (65.3 µL, 0.81 mmol). The reaction was stirred for 5 h at RT, then 24 h at 50 °C. After cooling to RT, the reaction was diluted with 5 % HCl (50 mL) and extracted twice into diethyl ether (150 mL). The pooled organic extracts were washed twice with water (50 mL) and dried over Na_2SO_4. After vacuum concentration, the product was purified on a short column of silica gel (diethyl ether) to afford **22** (816 mg, 87 %) as a yellow oil. ^{1}H NMR (400 MHz, CD_2Cl_2): δ 2.54 (s, 1H); 2.68 (d, J = 1.4 Hz, 1H); 2.83 (d, J = 2.1 Hz, 1H); 7.18 (s, 1H); 10.56 (s, 1H). ^{19}F NMR (300 MHz, $(CD_3)_2CO$): δ 69.205. ^{13}C NMR (400 MHz, CD_2Cl_2): δ 17.49 [CH_3]; 20.71 [CH_3]; 23.35 [CH_3]; 131.92 [C, $J_{C\text{-}F}$ = 20.6 Hz]; 134.72 [C]; 134.89 [CH]; 142.13 [CH_3]; 144.10 [CH_3]; 146.44 [CH_3]; 193.17 [CHO]. HRMS (EI) calcd. for $C_{10}H_{11}O_3SF$: 230.04129. Found: 230.04098 (85 %), 229.03363 (100 %). Anal. calcd. for $C_{10}H_{11}FO_3S$: C, 52.16; H, 4.82; N, 0. Found: C, 52.28; H, 4.96; N, 0. Compound **22** was also prepared using CsF as fluoride source, in a manner similar to the radiosynthetic protocol (Section 5.3.15).

5.3.6. *4-N-Maleimido-benzenesulfonyl chloride (28):*

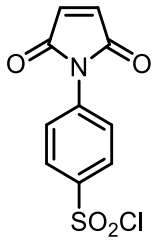

This compound was prepared according to literature procedure,[430] with modifications to the later steps. Into a RBF containing chlorosulfonic acid (6.9 mL, 105.6 mmol) under argon at 0 °C was added *N*-phenylmaleimide (3.06 g, 17.7 mmol) in portions. The reaction was stirred for 3.5 h under argon at RT, during which time the reaction darkened into clear orange-red solution, then lightened again. The reaction was quenched with ice water (250 mL) and extracted into ether (250 mL), then washed with water (50 mL). The organic phase was dried over Na_2SO_4. Purification by way of silica gel chromatography (3:2 hexanes:ethyl acetate) afforded 4-*N*-maleimide-benzenesulfonyl chloride (**28**; 957 mg, 20 %) as a white powder. M.P. = 139-141 °C (Lit.[430]=139-140°C). ^{1}H NMR (400 MHz, CD_2Cl_2): δ 6.94 (s); 7.78 (d, *J* = 9.0 Hz); 8.14 (d, *J* = 11.6 Hz). ^{13}C NMR (400 MHz, CD_2Cl_2): δ 126.12 [CH]; 128.36 [CH]; 135.05[2 x CH]; 138.30 [C];142.40 [C]; 168.87 [2 x C]. Anal. calcd. for $C_{10}H_6ClNO_4S$: C, 44.21; H, 2.23; N, 5.16. Found: C, 44.41; H, 2.28; N, 5.37.

5.3.7. *4-N-Maleimido-benzenesulfonyl fluoride (23).*

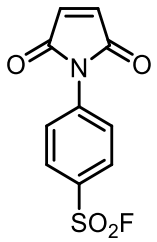

To a slurry of 4-maleimido-benzenesulfonyl chloride (**28**, 11.20 g, 41.2 mmol) in *t*-BuOH (20 mL) was added a 2.27 M solution of $KF_{(aq)}$ (20 mL) and the reaction was heated to reflux for 3.5 h. After this time, pyridine was added (3.33 mL, 41.2 mmol)

added the reaction was allowed to stir at RT for 30 min. The resulting precipitate was filtered and purified on a flash column of silica (1:1 hexanes:ethyl acetate) to afford 4.23 g (40 %) of maleimide **23** as a reddish powder. Analytically pure material was obtained by way of recrystallization from acetonitrile (15 mL). Final yield of **23** was 2.19 g (21 %). M.P. = 172°C. ^{1}H NMR (400 MHz, CD_2Cl_2): δ 6.94 (s); 7.80 (d, *J* = 8.3 Hz); 8.11 (d, *J* = 8.8 Hz). ^{19}F NMR (300 MHz, CD_2Cl_2): δ 65.388. ^{13}C NMR (400 MHz, CD_2Cl_2): δ 126.13 [CH]; 129.78 [CH]; 131.20 [$J_{C\text{-}F}$ = 24.9 Hz, C]; 135.05 [2 x CH]; 138.72 [C]; 168.87 [2 x C]. HRMS (EI) calcd. for $C_{10}H_6O_4FSN$: 255.00016. Found: 254.99992. Anal. calcd. for $C_{10}H_6NO_4SF$: C, 47.06; H, 2.37; N, 5.49. Found: C, 47.25; H, 2.46; N, 5.65. Compound **23** was also prepared using CsF as fluoride source, in a manner similar to the radiosynthetic protocol (Section 5.3.15).

5.3.8. *4-(Prop-2-ynyloxy)benzenesulfonyl chloride (29).*

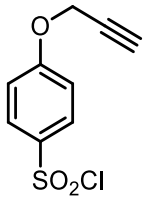

Into a RBF containing dry CH_2Cl_2 under argon at 0 °C was added phenyl propargyl ether (4.0 mL, 31.1 mmol) *via* syringe. A dropping funnel was used to *carefully* add chlorosulfonic acid (4.7 mL, 72.0 mmol) over 5 min. The colour of the reaction immediately went black. The reaction was stirred at 0 °C for 2 h. The reaction was quenched with ice water and extracted three times into $CHCl_3$ (3 × 75 mL), then washed twice with water and once with brine. The pooled organic portions were dried over Na_2SO_4. The product solution was concentrated and purified on a column of silica gel (5:1 hexanes:ethyl acetate) to afford 3.60 g (50 %) of 4-(prop-2-ynyloxy)benzenesulfonyl chloride (**29**) as a yellow oil. ^{1}H NMR (400 MHz, CD_2Cl_2): δ 2.66 (t, *J* = 2.4 Hz, 1H); 4.83 (d, *J* = 2.4 Hz, 2H); 7.17 (d, *J* = 9.1 Hz, 2H); 8.01 (d, *J* = 9.1 Hz, 2H). ^{13}C NMR (400 MHz, CD_2Cl_2): δ 56.82 [CH_2]; 77.05 [CH]; 77.29 [C]; 116.05 [2 x CH]; 129.87 [2 x CH]; 137.13 [C]; 163.18 [C]. HRMS (EI) calcd. for $C_9H_7O_3S^{35}Cl$: 229.98044. Found: 229.98023. Anal. calcd. for $C_9H_7ClO_3S$: C, 46.86; H, 3.06; N, 0. Found: C, 47.14; H, 3.09; N, 0.

5.3.9. *4-(Prop-2-ynyloxy)benzenesulfonyl fluoride (24):*

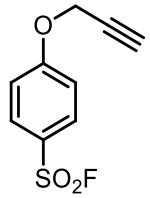

*From **29**.* Sulfonyl chloride **29** (1.92 g, 8.33 mmol) was dissolved in THF (25 mL). A solution of 1 M TBAF in THF (9 mL) was added and the reaction was stirred at RT for 40 min, then heated at 60 °C for 3.5 h. The reaction was quenched with ice water, extracted three times in diethyl ether, washed twice with water and dried over Na_2SO_4. The solution was concentrated to a brown oil and purified on a flash column of silica gel (2:1 hexanes:diethyl ether) to afford benzenesulfonyl fluoride **24** (1.38 g, 81 %) as an oily white solid. M.P. = 33-34.5°C. ^{1}H NMR (400 MHz, CD_2Cl_2): δ 2.66 (t, *J* =2.4 Hz, 1H); 4.83 (d, *J* = 2.4 Hz, 2H); 7.18 (d, *J* = 8.7 Hz, 2H); 7.97 (d, *J* = 8.9 Hz, 2H). ^{9}F NMR (300 MHz, CD_2Cl_2): δ 66.16. ^{13}C NMR (400 MHz, CD_2Cl_2): δ 56.75 [CH_2]; 77.01 [CH]; 77.29 [C]; 116.18 [2 x CH]; 125.18 [C, $J_{C\text{-}F}$ = 24.9 Hz]; 131.17 [2 x CH]; 163.49 [C]. HRMS (EI) calcd. for $C_9H_7O_3FS$: 214.00999. Found: 214.01009. Anal. calcd. for $C_9H_7O_3SF$: C, 50.46; H, 3.30; N, 0. Found: C, 50.53; H, 3.33; N, 0. Compound **24** was also prepared using CsF as fluoride source, in a manner similar to the radiosynthetic protocol (see Section 5.3.15).

*From **30** (Sections 5.3.14 and 5.7.3).* In a conical vial, DMAP salt **30** (300 mg, 0.85 mmol) was wetted with THF (2.5 mL) and mixed with a solution (1.5 mL) of $KF_{(aq)}$ (79 mg/mL) and $Cs_2CO_{3(aq)}$(10 mg/mL). Additional $Cs_2CO_{3(aq)}$ was added (1 mL) and the mixture was stirred for 6 h at RT. The reaction mixture was diluted diethyl ether (70 mL) and extracted once. The organic portion was immediately passed through a short column of silica gel (diethyl ether) and dried over Mg_2SO_4. Filtration and concentration afforded 153 mg (84 %) of **24.** Melting point (32- 32.5 °C), TLC and NMR data were in agreement with synthetic standard.

5.3.10. *N-Methyl-N-(prop-2-ynyl)aniline (31)*

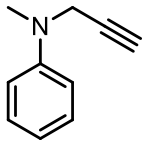

The following synthesis is based on a published method,[431] although analytical data appears here for the first time. Potassium carbonate (3.14 g, 22.7 mmol) was wetted with dry MeCN (20 mL) and the slurry was placed under argon. *N*-methylaniline (2.47 mL, 22.7 mmol) was added *via* syringe, followed by propargyl bromide (80 % in toluene, 5.25 g, 35.3 mmol). The reaction was left to stir for 28 h, during which time the yellow solution darkened. The reaction mixture was filtered through Celite and concentrated. The product was purified on a flash column of silica gel (19:1 hexanes:ethyl acetate) to afford 3.30 g (49 %) of **31**. ^{1}H NMR (400 MHz, CD_2Cl_2): δ 2.22 (t, *J* = 2.4 Hz, 1H), 2.96 (s, 3H), 4.07 (d, *J* = 2.4 Hz, 1H), 6.80 (m, 1H), 6.86 (dd, *J* = 8.8, 0.9 Hz, 2H), 7.26 (dd, *J* = 8.9, 7.3 Hz, 2H). ^{13}C NMR (101 MHz, CD_2Cl_2): δ 38.94 [CH_3], 42.93 [CH_2], 72.18 [CH], 79.89 [C], 114.76 [2 x CH], 118.72 [CH], 129.58 [2 x CH], 149.60 [C]. HRMS (EI) calcd. for $C_{10}H_{11}N$: 145.08915. Found: 145.08916.

5.3.11. *3-(Methyl(phenyl)amino)-2-oxopropane-1-sulfonic acid (32):*

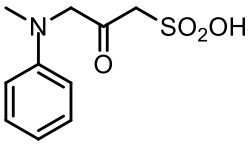

N-Methyl-*N*-(prop-2-ynyl)aniline (**31**, 1.59 g, 10.9 mmol) was dissolved in dry CH_2Cl_2 (20 mL) and cooled to 0 °C under argon. Chlorosulfonic acid (4.4 mL, 66.2 mmol) was added slowly *via* dropping funnel. The reaction was stirred for 4 h at 0 °C, then 22 h at RT, and finally 22 h at 50 °C. The reaction was quenched with 50 mL water (*Caution: violent reaction!*) and poured into $CHCl_3$ and water. The product was extracted three times into water and the water portions were pooled (250 mL total) and washed once with $CHCl_3$. The water was concentrated to ~1/5 of its original volume and let stand. After 4 h, white crystals began to precipitate out of solution, and the liquor was let

stand for another two days. The white precipitate (**32**, 1.75 g, 66 %) was filtered and washed with a minimum of water. M.P. = >159°C (decomposes). ^{1}H NMR (400 MHz, DMSO-d): δ 2.91 (s, 3H); 3.65 (s, 2H); 4.57 (s, 2H); 5.53 (br s, 1H); 6.66 (t, *J* = 7.2, 1H); 6.74 (d, *J* = 8.0, 2H); 7.13 (dd, *J* = 8.8, 7.2, 2H). ^{13}C NMR (400 MHz, DMSO-d): δ 39.45 [CH_3]; 60.82 [CH_2]; 62.69 [CH_2]; 112.51 [2 x CH]; 116.92 [CH]; 128.85 [2 x CH]; 148.50 [C]; 200.00 [C]. HRMS(ESI-) calcd. for $C_{10}H_{12}NO_4{}^{32}S$: 242.0487. Found: 242.0491. Anal. calcd. for $C_{10}H_{13}NO_4S{\cdot}0.75H_2O$: C, 46.77; H, 5.69; N, 5.45. Found: C, 46.94; H, 5.30; N, 5.36.

5.3.12. ***1-Tosylsulfonyl-4-dimethylaminopyridinium chloride (33).***

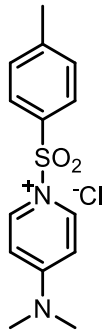

This compound was prepared according to a literature procedure,[432] with some modifications. 4-Dimethylaminopyridine (767 mg, 6.29 mmol) was dissolved in dry EtOAc (40 mL) and placed in a bath of cold tap water. Tosyl chloride (996 mg, 5.22 mmol) in dry EtOAc (12.5 mL; 52.5 mL total solvent) was added *via* syringe. The reaction was left to warm to RT over 22 h, then filtered. The product was washed generously with diethyl ether (3 × 50 mL) and dried *in vacuo* to afford 1.30 g (79 %) of a bright white solid (**33**). M.P. = 128-130°C (Lit.[432] = 124°C) ^{1}H NMR (300 MHz, DMSO-d): δ 2.28 (s, 3H); 3.17 (s, 6H); 6.97 (d, *J* = 7.25 Hz, 2H); 7.12 (d, *J* = 7.90 Hz, 2H); 7.48 (d, *J* = 7.99 Hz, 2H); 8.21 (dd, *J* = 6.06, 6.66 Hz, 2H). ^{13}C NMR (300 MHz, DMSO-d): δ 20.81 [CH_3]; 39.65 [2 x CH_3]; 106.98 [2 x CH]; 128.15 [2 x CH]; 137.84 [2 x CH]; 139.03 [C]; 145.43 [2 x CH]; 156.96 [C]. HRMS (ESI+) calcd. for $C_{14}H_{17}N_2O_2{}^{32}S$: 277.1011. Found: 277.1013. Anal. calcd. for $C_{14}H_{17}ClN_2O_2S{\cdot}0.75H_2O$: C, 51.53; H, 5.71; N, 8.58. Found: C, 51.70; H, 5.78; N, 8.53.

5.3.13. *Toluenesulfonyl fluoride (34):*

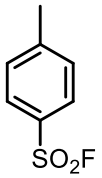

In a conical vial DMAP salt **33** (300 mg, 0.96 mmol) was wetted with THF (2.5 mL) and mixed with an aqueous solution (2.0 mL) of KF (33.4 mg/mL) and Cs_2CO_3 (10 mg/mL). Additional $Cs_2CO_{3(aq)}$ (10 mg/mL) was added (0.5 mL) and the mixture was stirred for 23 h at RT. The reaction was transferred into water (10 mL) and extracted into diethyl ether (70 mL). The organic portion was washed with water (10 mL) and dried for a short time over Mg_2SO_4 (30 min). The product was passed through a short column of silica gel (diethyl ether) and concentrated to afford 61 mg (37 %) of toluenesulfonyl fluoride (**34**). M.P. = 36-36.5°C (Lit.[329]= 41-42°C). ^{1}H NMR spectrum was in agreement with published data.[433]

5.3.14. *1-(Prop-2-ynyloxy)benzenesulfonyl-4-dimethylaminopyridinium chloride (30):*

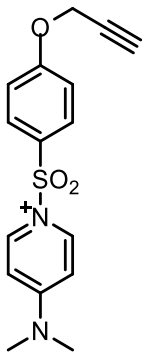

4-Dimethylaminopyridine (637 mg, 5.22 mmol) was dissolved in dry EtOAc (40 mL) and placed in a bath of cold tap water. 4-(Prop-2-ynyloxy)benzenesulfonyl chloride (**29**; 1.00 g, 4.34 mmol) in dry EtOAc (3 mL) was added *via* syringe. The reaction was left to warm to RT over 2.5 h, then filtered. The product was washed generously with ethyl acetate (2 × 50 mL) and dried *in vacuo* to afford 1.51 g (98 %) of a white solid (**30**).

M.P. = 103°C. ^{1}H NMR (400 MHz, DMSO-d): δ 3.17 (s, 3H); 3.56 (t, *J* = 2.38 Hz, 1H); 4.79 (d, *J* = 2.39 Hz, 2H); 6.55 (br s, 1H); 6.90 (dt, *J* = 2.83, 8.84, 2H); 6.97 (d, *J* = 7.44, 2H); 7.53 (d, *J* = 8.83, 2H). ^{13}C NMR (400 MHz, DMSO-d): δ 39.63 [2 x CH3]; 55.45 [CH2]; 78.28 [CH]; 79.14 [C]; 106.96 [2 x CH]; 113.79 [2 x CH]; 126.99 [2 x CH]; 139.01 [2 x CH_2]; 141.45 [C]; 156.95 [C]; 157.19 [C]. HRMS (ESI+) calcd. for $C_{16}H_{17}N_2O_3{}^{32}S$: 317.0960. Found: 317.0967. Anal. calcd. for $C_{16}H_{17}ClN_2O_3S{\cdot}H_2O$: C, 51.82; H, 5.16; N, 7.55. Found: C, 51.90; H, 5.15; N, 7.57.

5.3.15. *General procedure for the synthesis of sulfonyl fluorides 20-23 under conditions similar to radiochemical protocols.*

Benzenesulfonyl chlorides **20**- **23** (250 mg) were dissolved in *t*-BuOH. An aqueous solution composed of Cs_2CO_3 (10 mg/mL) and CsF (1.1 equiv.) was added in equal volume with *t*-BuOH and the reaction was left to stir at RT. The final concentration of sulfonyl chloride was 30 mM. After 30- 90 min, the reaction was quenched and extracted with diethyl ether (125 mL) and washed with water (10 mL), then dried over Mg_2SO_4. After concentration, the sulfonyl fluorides were purified on silica gel (7:3 ethyl acetate hexanes) to afford the following: **21**: 30 min reaction time, 65 %. **22**: 60 min, 73 % **23**: 30 min, 22 %. **24**: 90 min, 79 %. ^{1}H NMR and EI-MS were in agreement with synthetic standard.

5.4. Non-radioactive Bioconjugate Syntheses

5.4.1. ***BBN-OX-MESIT-SO_2F***

3-Formyl-2,4,6-trimethylbenzenesulfonyl fluoride (**22**; 2.5 mg, 10.9 µmol, 5.5 equivalents relative to N_3 peptide) in DMSO (100 µL) was added to **BBN-ONH_2** (2.4 mg, 2 µmol) and the solution was shaken vigorously for 5 h. The reaction was quenched with 1:1 MeOH:H_2O (1 mL) and purified by semi-preparative HPLC (HPLC 3, R_t = 17 min). The collected HPLC eluent was concentrated by centrifugal evaporation to afford the title peptide. MALDI-TOF calcd.: 1424.59 $[M+H]^+$. Found: 1425.09.

5.4.2. *Attempted synthesis of BBN-TRIAZOLE-BENZ-SO_2F*

A mixture of $Cu(CH_3CN)_4BF_4$ (5.3 mg, 16.8 µmol, 10.8 equivalents relative to peptide) and TBTA (13.1 mg, 24.7 µmol, 15.9 equiv.) in DMSO (100 µL) was added to peptide precursor **N_3-BBN** (1.9 mg, 1.6 µmol). Then 4-(prop-2-ynyloxy)benzenesulfonyl fluoride (**24**, 3.7 mg, 17.3 µmol, 11.1 equiv.) in DMSO (100 µL) was added, and the clear, blueish-yellow solution was shaken vigorously for 1 h. The reaction mixture was diluted with PBS (200 µL) and injected into a semi-preparative HPLC (HPLC 4). Two closely eluting peaks (R_t = 23.0 and 23.3 min) were collected together and the eluent was concentrated by centrifugal evaporation. MALDI-TOF (*m/z*) calcd.: 1436.57 $[M+H]^+$, 1498.49 $[M+^{63}Cu]^+$. Found: 1436.63 (100 %), 1498.46 (50 %).

5.5. Radiochemical Syntheses

Radiosyntheses in Chapter 5 were carried out at the TRIUMF Chemistry Annex. Typical production was 1.5- 2.6 GBq of $[^{18}F]F^-$ at end of bombardment for a 10 μA, 5 min irradiation.

5.5.1. *Radio-TLC assay of bifunctional sulfonyl fluoride ($[^{18}F]$-20-$[^{18}F]$-23) reaction mixtures.*

$[^{18}F]$Fluoride in $[^{18}O]H_2O$ was immobilized on an anion exchange ^{18}F 'trap-and-release' column, then eluted into a 5 mL conical vial with a 10 mg/mL solution of cesium carbonate (400 μL). From this bulk solution, smaller aliquots were removed for further use. An aliquot (100 μL or 200 μL) of $[^{18}F]F^-$ in aqueous Cs_2CO_3 was pipetted into a reaction vessel containing precursor sulfonyl chloride or sulfonyl chloride in 100 μL organic solvent (see Table 5.1). Reaction volume was 0.2 mL and precursor concentration was 30 mM. The reaction was shaken and left to stand for 15 min, then the reaction mixture was spotted on 3 or 4 TLC plates. The plates were 20 cm long, with the origin at 2 cm. Pyridine (80 μL) was added and the mixture was shaken and let stand for another 15 min before TLC sampling in the same fashion. The TLC eluent was ethyl acetate. Alternately, pyridine (80 μL) was added immediately after addition of $[^{18}F]F^-$ and the reaction sampled after 15 min (see Table 5.1).

5.5.2. *General procedure for the preparative syntheses of $[^{18}F]$-22 and $[^{18}F]$-24.*

Into a reaction vessel containing sulfonyl chloride **27** or **29** in *t*-BuOH (100 μL), an aliquot of $[^{18}F]F^-$ (100 μL) in aqueous Cs_2CO_3 (10 mg/mL) was added (30 mM final concentration). Immediately afterward, pyridine (80 μL) was added and the mixture was vortexed thoroughly, then let stand for 15 min. The reaction solution was transferred into an open syringe containing water (20 mL) and immobilized on a tC_{18} 'light' SPE column. The column [activated previously with EtOH (2 mL) and water (6 mL)] was washed with water (5 mL), and dried with air (15 mL). 3-Formylmesitylenesulfonyl $[^{18}F]$fluoride ($[^{18}F]$-**22**) or 4-(prop-2-ynyloxy)benzenesulfonyl fluoride ($[^{18}F]$-**24**) was eluted from the column with either DMSO (300 μL) for further bioconjugation experiments or acetonitrile (1 mL) for determination of specific activity by HPLC (HPLC 18, see Section 5.6.2).

5.5.3. ***BBN-OX-MESIT-SO$_2$[^{18}F]F***

Purified [^{18}F]-**22** (9.8 mCi) in DMSO (300 µL) was added to **BBN-ONH$_2$** peptide (0.5 mg) in a microcentrifuge tube and 5 % AcOH (100 µL) was added. The reaction mixture was vortexed, centrifuged briefly, and placed in a bed of heated beads (37 °C) for 30 min. The ^{18}F- labelled peptide was diluted with water (600 µL) and purified by reverse phase HPLC (HPLC 17). The collected portion (R_t = 16 min) was diluted to 20 mL with water and trapped on a tC$_{18}$ light column [activated previously with EtOH (2 mL) and water (6 mL)]. The column was washed with water (5 mL) and dried with air (10 mL). **BBN-OX-MESIT-SO$_2$[^{18}F]F** was eluted from the column with EtOH (300 µL) and diluted with 0.9 % saline solution (2.7 mL). The final formulation contained 2.99 mCi of **BBN-OX-MESIT-SO$_2$[^{18}F]F** (51 % DC yield from start of bioconjugate synthesis). Total bioconjugate synthesis time was 82 min. In cases when **BBN-OX-MESIT-SO$_2$[^{18}F]F** was prepared for serum stability experiments, the ^{18}F peptide was eluted from the column with DMSO (400 µL).

5.5.4. ***Attempted synthesis of BBN-TRIAZOLE-BENZ-SO$_2$[^{18}F]F***

Purified [^{18}F]-**24** (6.70 mCi) was eluted with DMSO (320 µL) directly into a microcentrifuge tube containing **N$_3$-BBN** (0.5 mg). A solution of THPTA (2.6 mg, 14.6 equiv. relative to peptide) and Cu(CH$_3$CN)$_4$PF$_6$ (1.5 mg, 9.8 equiv.) in DMSO (100 µL) was added, and the reaction was shaken thoroughly and left to react at RT for 20 min. After this time, the mixture was diluted with water (680 µL) and purified by HPLC (HPLC 4). The collected eluent (2.87 mCi) contained two closely eluting peaks (R_t = 23.4 and 23.7 min). The eluent was diluted to 24 mL with water and trapped on a tC$_{18}$ 'light' column [activated previously with EtOH (2 mL) and water (5 mL)]. After washing with H$_2$O (5 mL), the ^{18}F peptide was eluted off the column with EtOH (0.3 mL), followed by saline (2.7 mL). The final formulation (10 % EtOH in saline) contained 1.99 mCi of impure **BBN-TRIAZOLE-BENZ-SO$_2$[^{18}F]F** (51 % DC crude yield from start of bioconjugate synthesis). Total synthesis time for bioconjugation was 85 min.

5.6. Experimental Procedures

5.6.1. *Assessing hydrolytic stability of sulfonyl fluoride standards in buffered solution.*

Arylsulfonyl fluoride standards in MeOH (**21**, **22** and **24**) or diethyl ether (**23**, **25**) were prepared (9.8 µM) and aliquots (50 µL) were removed and concentrated in microcentrifuge tubes over a stream of helium. Each aliquot was incubated in PBS (75 µL, 150 mM, pH 7.2) at 37 °C for 15, 70 or 150 min. After the appointed time, the sample was diluted with acetonitrile (150 µL) and let stand 15 min, then a portion (75 µL) was injected into HPLC for analysis. HPLC parameters used were as follows: Compound **24**, HPLC 12. Compounds **21** and **23**, HPLC 13. Compounds **22** and **25**, HPLC 14. An estimation of percent stability was calculated as follows:

$$\frac{absorbance\ units\ of\ the\ peak\ of\ interest}{(total\ absorbance - \ absorbance\ units\ of\ a\ blank\ sample)} \times 100\ (Eq. 8)$$

This approach assumes that the difference in extinction coefficients between a sulfonyl fluoride and its corresponding sulfonic acid is negligible. The experiment was performed three times for each compound.

5.6.2. *Determination of Apparent Specific Activities of Compounds [^{18}F]-22 and [^{18}F]-24.*

Non-radioactive arylsulfonyl fluoride was dissolved in MeCN (2 mM). This stock solution was serially diluted by 10 into four separate containers using MeCN and an aliquot of each (50 µL) was assayed by analytical HPLC (HPLC 18). Each sample was injected three times and the average measure of UV- absorbing material associated with the ^{19}F bifunctional molecule at each concentration was used to generate a straight line representing absorbance at 260 nm with respect to compound concentration (R^2 > 0.9998). After purification of the radioactive version, an aliquot of known activity in MeCN was assayed using identical HPLC conditions and the amount of UV- absorbing material co-eluting with the radio-detection signal was estimated relative to the mass standard curve. Apparent specific activities were reported in GBq of injected activity per µmol of associated prosthetic group. [^{18}F]-**22**: R_t = 11.7 min. [^{18}F]-**24**: R_t = 9.0 min.

5.6.3. *Serum Stability Study of BBN-OX-MESIT-SO_2[^{18}F]F.*

BBN-OX-MESIT-SO_2[^{18}F]F in DMSO (34.4- 44.4 MBq) was diluted 1:9 with fresh mouse serum and heated to 37 °C. As a control, a second portion of ^{18}F peptide was treated in an identical fashion with PBS (150 mM, pH 7.2) in place of mouse serum. The samples had aliquots (150 µL- 500 µL) removed after 15, 60 and 120 min. The aliquots were quenched with equal amounts of MeCN, chilled at 4 °C for 15 min, centrifuged for 3 min (15,668 × *g*), then the supernatant was removed and counted. After spotting on three separate silica gel iTLC-SG plates, the remainder of the ^{18}F peptide solution was assayed by HPLC (HPLC 17). After drying, radio-TLC was performed using 1:1 MeOH:MES buffered saline (100 mM, pH 4.7).

5.7. Results and Discussion

5.7.1. *Non-Radioactive Small Molecule Chemistry*

4-Formylbenzenesulfonyl chloride, the precursor to radioactive and non-radioactive **21** was purchased; the other sulfonyl chloride precursors were synthesized (Figure 5.4). 4-*N*-Maleimidebenzenesulfonyl chloride (**28**) and 4-(prop-2-ynyloxy)benzenesulfonyl chloride (**29**) were *para*-chlorosulfonated using and excess of chlorosulfonic acid. As is frequently observed with this reagent,[434] the nature of the substituent on the aryl ring had a marked effect on reaction results. Previously, maleimide **28** was obtained in a crude yield of 83 % (45- 50 ºC, 1 h),[430] but in our case ambient conditions for 3.5 h was enough to elicit a rapid colour change and the complete consumption of the starting material. However, we found yields of **28** (20 % after silica gel chromatography) to be hindered by the production of significant quantities of water-soluble impurities. It should be noted that the attempted chlorosulfonation of inactivated *N*-(4-chlorophenyl)-maleimide under forcing conditions (5 h, 130 ºC) yielded the same result.[435] The conversion of phenyl propargyl ether to *p*-substituted sulfonyl chloride **29** was facile and regiospecific, which is the expected result for benzoyl ethers treated with chlorosulfonic acid.[434] The yield of **29** (50 %) might have benefited from lower temperatures, as even the dropwise addition of $ClSO_3H$ at 0 ºC resulted in some heating and charring of the reaction mixture. To our knowledge, the sulfonation or chlorosulfonation of a benzaldehyde using chlorosulfonic acid has not been reported.

The production of charred products was observed when vanillin and *o*-vanillin were mixed with $ClSO_3H$.[436] Not surprisingly then, we found that 3-formyl-2,4,6-trimethylbenzenesulfonyl chloride (**27**) could not be prepared by direct treatment with $ClSO_3H$. However, **27** was eventually obtained in two steps by sulfonylation with oleum, followed by chlorination with cyanuric chloride.[437]

Bifunctional sulfonyl fluorides **21**, **22** and **24** were synthesized from their corresponding sulfonyl chlorides (4-formylbenzenesufonyl chloride, **27** and **29** respectively) using 1 M TBAF in THF (Figure 5.4). In the case of 3-formyl-2,4,6-trimethylbenzenesulfonyl chloride (**22**), pyridine was added (20 mol %), which was accompanied by an improvement in final yield compared to a similar reaction without pyridine (32 % versus 87 %). Maleimide **23** could not be obtained from **28** in acceptable yields using TBAF/THF, but was prepared in low yields (21 %) when **28** was refluxed in 1:1 mixtures of *t*-BuOH and aqueous KF. In this case, both polar and non-polar impurities were observed in the reaction mixture; both recrystallization and silica gel chromatography was required to obtain pure product.

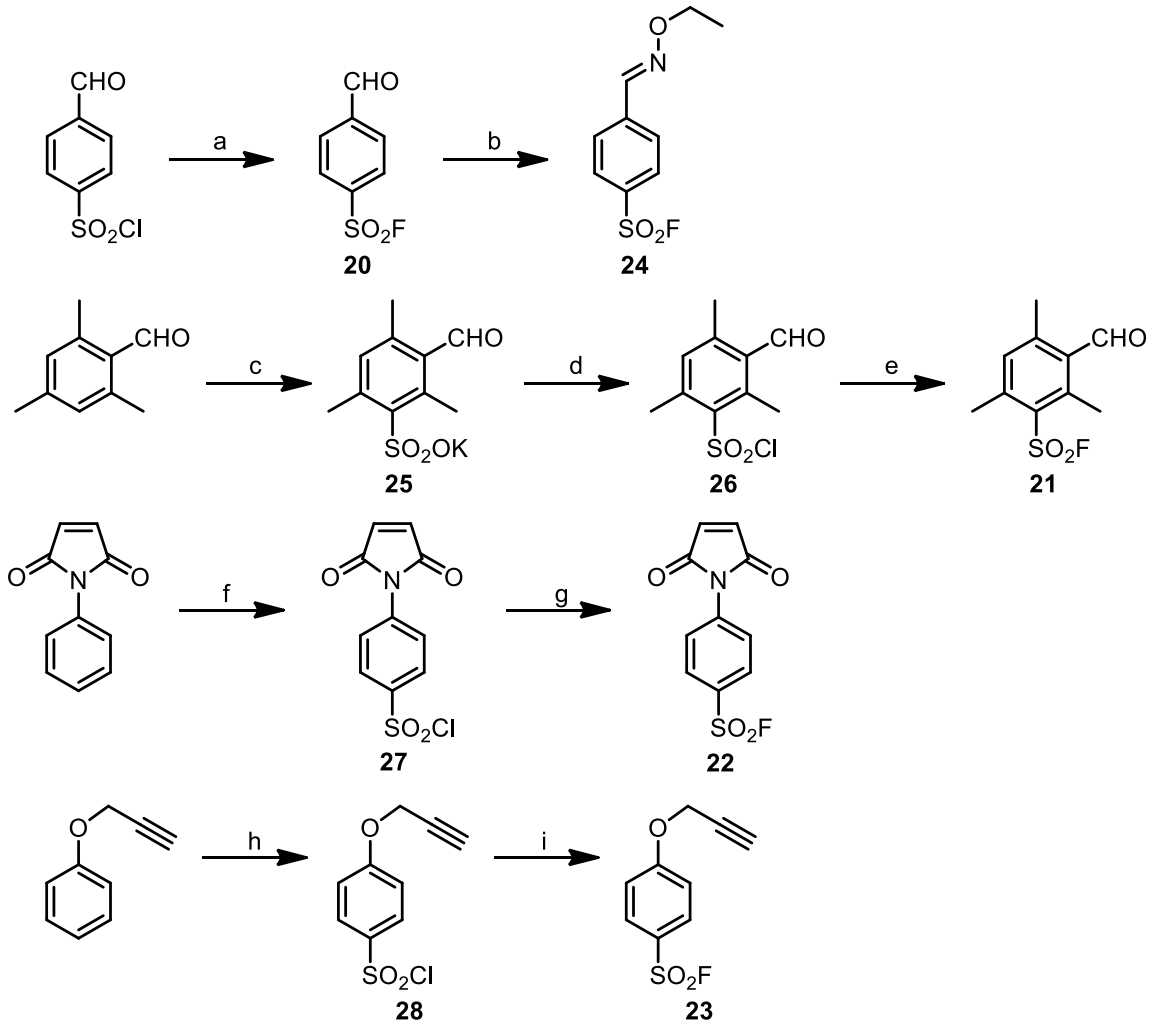

Figure 5.4. Synthesis of sulfonyl chlorides and non-radioactive sulfonyl fluorides.

a) TBAF, THF, 0°C→RT, 45 min, 69 %. b) HCl·H_2NOEt, EtOH, RT, 90 min, 61 %. c) i) oleum, 40 °C, 22 h ii) K_2CO_3, 77 %. d) 18-crown-6, cyanuric chloride, acetone, 50 °C, 48 h, 80 %. e) TBAF, pyridine (20 mol %), THF, RT (5 h) and 50 °C (24 h), 87 %. f) $ClSO_2OH$, RT, 3.5 h, 20 %. g) i) KF, 1:1 *t*-BuOH:H_2O, reflux (3.5 h) ii) pyridine, RT (30 min), 21 %. h) $ClSO_2OH$, CH_2Cl_2, 0 °C, 2 h, 50 %. i) TBAF, THF, RT (40 min) and 60°C (3.5 h), 81 %.

In order to probe the hydrolytic stability of a benzenesulfonyl fluoride bearing a 4-oxime substituent, **21** was treated with *O*-ethylhydroxyamine nucleophile to yield **25** (Figure 5.4). Buehler[438] acquired the ^{1}H NMR spectra for a series of *O*-alkylated benzaldoximes and found the *ortho*-protons of the *Z*- (anti-) isomers upfield relative to the *E*- (syn-) isomers. In a ^{1}H NMR spectrum of the crude reaction mixture of **25** we

observed a doublet (δ 7.76 ppm) upfield to one in our collected product (δ 7.85 ppm). On this basis **25** was assigned the *E* diastereomer.

To the best of our knowledge, the direct chlorosulfonation of alkylated anilines has never been reported. Despite this, an attempt was made to prepare 4-(methyl(prop-2-ynyl)amino)benzenesulfonyl chloride (**35**) in this fashion (Figure 5.5). The isolated product after quenching with water was determined to be sulfonic acid **32**. The expected mechanism to the desired *para*-sulfonated *N,N*-dialkylaniline is itself non-standard; it is known to start with the formation of a sulfamic acid complexes such as **36** (Figure 5.5). Synthesis of these reactive species using sulfur trioxide and their subsequent rearrangement have been known for many years.[439] Khelevin determined that the treatment of *N,N*-dimethyl- and diethyl- aniline with one equivalent of chlorosulfonic acid in *o*-dichlorobenzene (50- 80°C) produced the sulfonic acid by way of a first order reaction.[440] This is in contrast to the second order mechanism (*i.e.* direct sulfonation with HSO_3^+) which has been ascribed to the corresponding *N*-monoalkylanilines.[441] With a reactive complex in the rate- controlling stage established, the author also measured the effective rate constant and activation energy for the rearrangement of di(methyl-/ ethyl-)aniline-sulfotrioxide to *para*-di(methyl-/ethyl-)aminobenzene sulfonic acid and found them to be identical to the mentioned *para*-sulfonation reactions. In this fashion, the generation and disassociation of a sulfamate intermediate was confirmed. Such rearrangements are thought to start with the decomposition of the sulfamate to a radical ion pair.[442] Indeed, *N,N*-dialkylaniline radical cations have been obtained *via* one- electron transfer to Cu^{II}; reaction of these intermediates with a variety of nucleophiles installs the attacking group *para* to the dialkylamino functionality.[443] In our case one might reasonably expect the formation of sulfonic acid **37** under the conditions used, which would then be converted to sulfonyl chloride **35** in the presence of excess $ClSO_3H$, as per the established mechanism for this reagent.[434] In this case however, *p*-sulfonation is arrested and the propargyl moiety is transformed to an α-sulfoxy ketone (Figure 5.5). Addition of chlorosulfonic acid across the triple bond, followed by hydrolysis of the resulting chloro-alkene is a possible route to **32**.

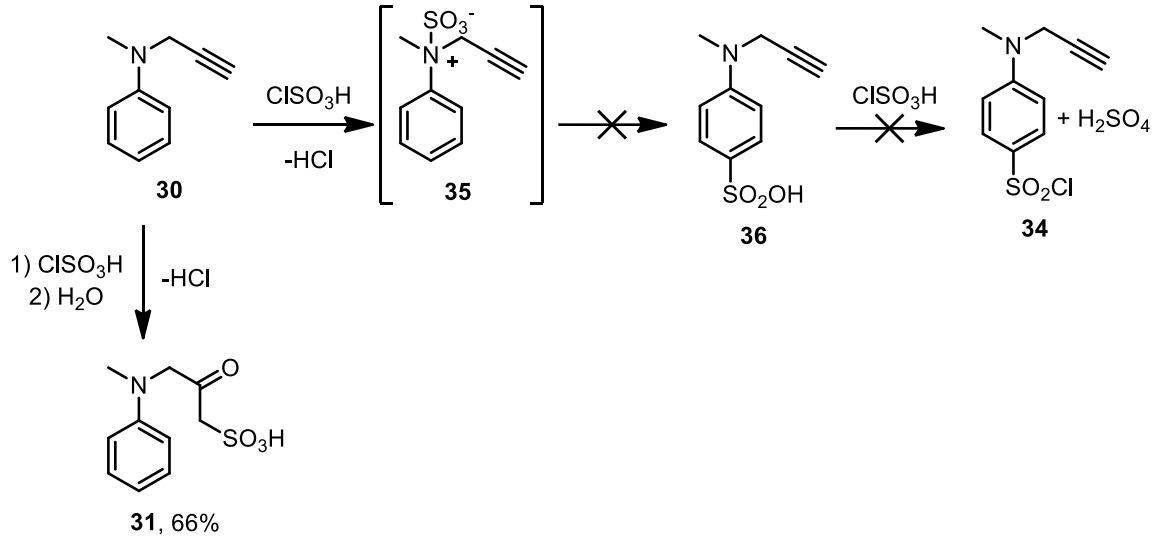

Figure 5.5. Expected and observed sulfonic acid formation.

5.7.2. *Stability of sulfonyl fluorides in buffered solution*

Some arylsulfonyl and arylalkylsulfonyl fluorides have limited stability in buffered solutions. [343, 344, 444] For instance, James[444] estimated the inactivation of PMSF based on its ability to inhibit molar equivalents of chymotrypsin in different isotonic buffers. PMSF half- lives in sodium phosphate (pH 7.0), HEPES (pH 7.5), and Tris-HCl (pH 8.0) were found to be 110, 55, and 35 min respectively (10 mM buffer, 150 mM NaCl, RT). Thus we chose to evaluate the stability of our bifunctional molecules in strong buffer [10 % DMSO in PBS (150 mM, pH 7.4)]. Mesitaldehyde analog **22** was found to be stable in 10 % DMSO in PBS (100±1 % remaining after 2.5 h) but under the same conditions only 1±1 % of **21** remained, as estimated by HPLC (Figure 5.6). We attribute this difference in stability to an increase in positive charge distribution at the benzene carbon *alpha* to the sulfur electrophile (*para* to the aldehyde group) in **21**. In addition, inductive donation of the methyl carbons in **22** might serve to depolarize the *alpha*-carbon and stabilize this sulfonyl fluoride towards nucleophilic attack by water. Alkyne- bearing prosthetic **24** exhibited good hydrolytic stability (99±1 %), but maleimide **23** showed some degradation (90±5 %). Also tested was compound **25** (Figure 5.4) as a model of the *para*-oxime linkage; it was deemed it to be essentially stable over 2.5 h (97±3 %).

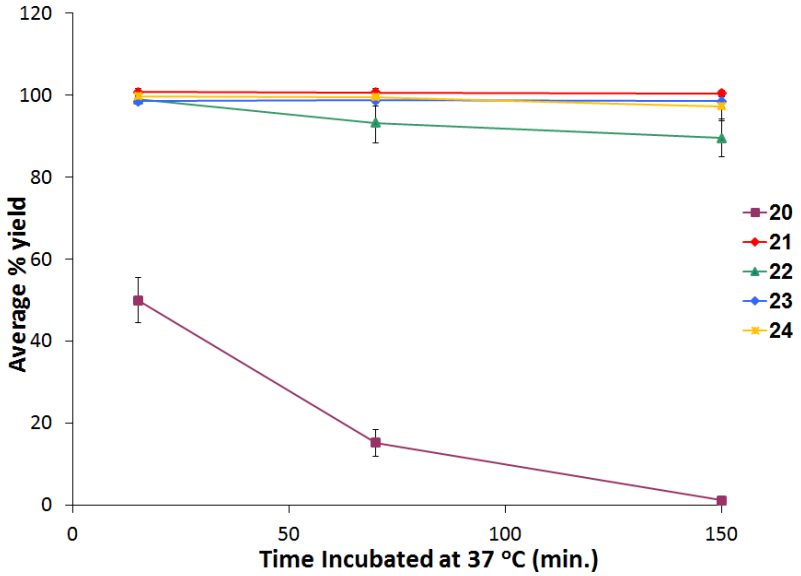

Figure 5.6. Stability of sulfonyl fluorides in buffered solution.

Percent of small molecule prosthetic **21**-**24** and **25** remaining in 10 % DMSO in PBS (pH 7.4, 150 mM) by UV-HPLC (260 nm) vs. Time. Each data point represents the average of three separate experiments. Error bars = ±SD.

It was of interest to re-synthesize bifunctional benzenesulfonyl fluorides **21**- **24** under conditions similar to those used in their radiochemical preparation (*vide infra*). Thus, 4-formylbenzene sulfonyl chloride and compounds **27**- **29** (30 mM) were each reacted with CsF in mixtures of $Cs_2CO_{3(aq)}$ (10 mg/mL) and organic co-solvent. Reactions were followed by TLC. The resulting preparative yields were very similar to those using the original protocols. For compounds **21**, **22** and **24,** *t*-BuOH was used as co-solvent; however, compound **23** was reacted in 1:1 MeCN:$Cs_2CO_{3(aq)}$. This choice was based on two related observations: a) MeCN proved the best solvent for the radiochemical synthesis of [^{18}F]-**23** (see Table 5.1, Entries 9-11) and b) the low yields of **23** can at least in part be attributed to a competing reaction where the maleimide functionality is converted to a maleamic acid moiety under basic conditions.[445] Thus the use of MeCN represents an effort to maximize chemical yields while minimizing the time **23** remains in contact with base. No improvement in the preparative yield of **23** was observed under the new conditions (22 % vs. 20 %), although purification proved much simpler, owing to a cleaner reaction mixture.

5.7.3. *Radioactive Small Molecule Chemistry*

5.7.3.1. Optimization of sulfonyl [^{18}F]fluoride synthesis and purification

Radioactive benzenesulfonyl fluorides [^{18}F]-**21**- [^{18}F]-**24** were initially prepared in 1:1 mixtures of organic solvent and an aqueous solution of cesium carbonate (10 mg/mL) at room temperature. Aliquots of the bulk Cs[^{18}F]F/$Cs_2CO_{3(aq)}$ solution could be portioned out and used for multiple [^{18}F]fluorination reactions. No azeotropic drying steps were required. After 15 min the reaction mixture was sampled for radio-TLC, then pyridine was added and the reaction was let stand another 15 min. A summary of [^{18}F]fluorination conditions explored are found in Table 5.1.

Table 5.1. Radiochemical yields by radio-TLC of bifunctional sulfonyl [^{18}F]fluorides before and after pyridine treatment.

Entry	Product	$Cs_2CO_{3(aq)}$:Co-solvent	% Yield (+15 min)	% Yield after pyridine treatment (+30 min)
1	[^{18}F]-**21**	*t*-BuOH	93±1*	89±2*
2	[^{18}F]-**21**	THF	96±1*	96±1*
3	[^{18}F]-**21**	MeCN	97±1**	90±2***
4	[^{18}F]-**21**	DMSO	No reaction**	No reaction**
5	[^{18}F]-**21**	$Cs_2CO_{3(aq)}$	19±2** (80±1**,†)	----
6	[^{18}F]-**22**	*t*-BuOH	97±1*	98±1*
7	[^{18}F]-**22**	THF	97±1**	97±1**
8	[^{18}F]-**22**	MeCN	98±1**	97±1**
9	[^{18}F]-**22**	*t*-BuOH	28±1**	18±2**
10	[^{18}F]-**22**	THF	72±2*	0.6±0.1*
11	[^{18}F]-**22**	MeCN	91±1**	18±2**
12	[^{18}F]-**23**	*t*-BuOH	29±2*	100±1*
13	[^{18}F]-**23**	THF	29±1*	99±1*
14	[^{18}F]-**23**	MeCN	84±1**	100±1**

Note: *Average of 3 traces. **Average of 4 traces. †Sampled after addition of DMSO (200 µL), between 15-16 min. Error = ±SD.

The study began with [^{18}F]-**21**, which was produced efficiently by way of halogen exchange from precursor compound 4-formylbenzenesulfonyl chloride when *t*-BuOH

was used as co-solvent (Table 5.1, Entry 1). A representative radio-TLC trace of the reaction mixture is shown in Figure 5.7. Similar results were observed upon synthesis of mesitaldehyde derivative [^{18}F]-**22** from **27** using identical conditions (Table 5.1, Entry 6 and Figure 5.7). Hindered protic solvents have recently been identified as an excellent media for S_N2 [^{18}F]fluorination reactions, presumably because of their capacity to reduce the charge association between Cs^+ and [^{18}F]F^- by hydrogen bonding to the salt and moderately solvating the free fluoride ion.[103] It was also suggested that the enhanced rate of nucleophilic aliphatic [^{18}F]fluorinations using mesylate precursor relative to other leaving groups may be the result of additional hydrogen bonding of *t*-BuOH solvent to the sulfonyl moiety. It is possible that protic *t*-BuOH lowers the energy of an S_N1-type sulfonoxy anion transition state in this scenario as well; however, the bulk of the literature favours an S_N2 mechanism for sulfonyl halide exchanges.[446] In this case, excellent radiochemical yields of [^{18}F]-**21** and [^{18}F]-**22** were observed even in 1:1 mixtures of THF/$Cs_2CO_{3(aq)}$ and MeCN/$Cs_2CO_{3(aq)}$, where no alcoholic proton donation is possible (Table 5.1, Entries 2, 3, 7 & 8).

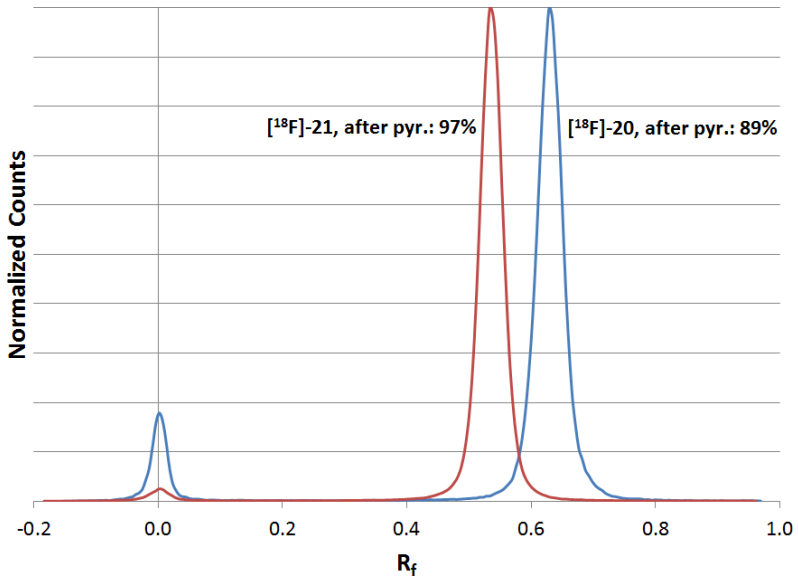

Figure 5.7. Representative radio-TLCs for the synthesis of [^{18}F]-21 and [^{18}F]-22.

[^{18}F]-**21** (Table 5.1, Entry 1; blue line) and [^{18}F]-**22** (Table 5.1, Entry 6; red line), in both cases after pyridine treatment. Vertical scale is linear. For each trace, radioactive counts are reported relative to maximum signal strength.

Polar aprotic solvents such as DMSO are essential when utilizing $K_{2.2.2}$/K[^{18}F]F complex, but the presence of DMSO completely inhibits the formation of [^{18}F]-**21** under

the reported conditions (Table 5.1, Entry 4). The same is true when DMSO is employed and dried $K_{2.2.2.}$/K[^{18}F]F fluoride source is used (data not shown).

It was of significant interest to determine if bifunctional benzenesulfonyl fluorides could be radiochemically prepared in the absence of organic solvent. However, direct analysis of this reaction by radio-TLC was not expected to provide reliable data, as the product compound is unlikely to be soluble in water. The observed radiochemical yield of a [^{18}F]-**21** reaction mixture employing only $Cs_2CO_{3(aq)}$ (10 mg/mL) as the solvent was found to be comparatively low (Table 5.1, Entry 5). Addition of DMSO to the reaction mixture, followed by immediate re-sampling, was associated with a marked increase in the measured radiochemical yield (Table 5.1, Entry 5). As it was shown that sulfonyl fluoride formation does not proceed in the presence of DMSO under similar conditions, this increase in the measured yield is attributed to the improved solvation of [^{18}F]-**21**.

Maleimide- bearing arenes such as **23** and **28** are susceptible to base- mediated ring opening. This makes them incompatible with typical ^{18}F labelling conditions that utilize alkali salts, $K_{2.2.2.}$ cryptand, and elevated temperatures.[225] When *t*-BuOH was used as a co-solvent under the standard conditions, labelling yields of [^{18}F]-**23** by radio-TLC were low, and decreased slightly after incubation with pyridine (Table 5.1, Entry 9). Moderate yields of [^{18}F]-**23** were observed when THF was used as a co-solvent, but the compound degraded almost completely after addition of pyridine (Table 5.1, Entry 10 and Figure 5.8). MeCN as co-solvent provided the best yields of [^{18}F]-**23**, but again significant degradation occurred upon pyridine treatment. (Table 5.1, Entry 11).

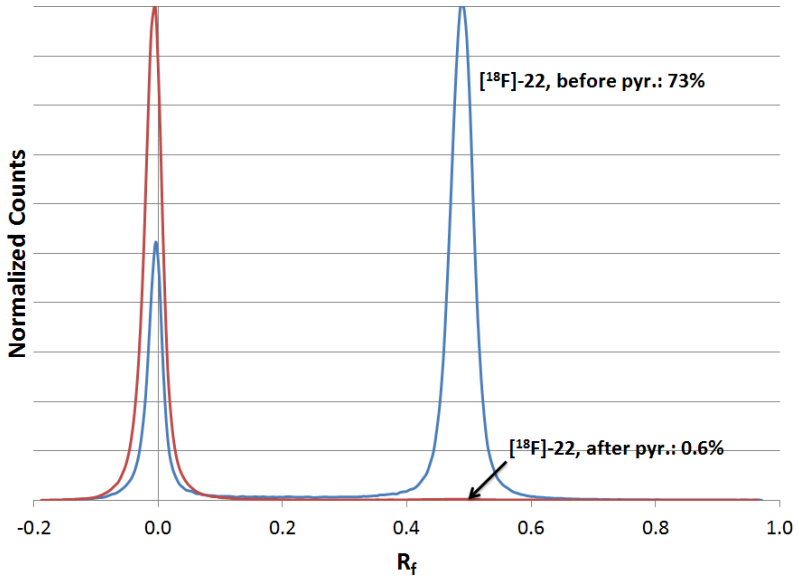

Figure 5.8. Representative radio-TLCs for the synthesis of [^{18}F]-23.

Figure shows yield of [^{18}F]F-**23** in 1:1 THF:$Cs_2CO_{3(aq)}$, before (blue line) and after (red line) pyridine treatment (Table 5.1, Entry 10). For each trace, radioactive counts are reported relative to maximum signal strength.

Pyridine is known to catalyze a number of acylation reactions, including the hydrolysis[447] and methanolysis[448] of benzenesulfonyl chlorides. In these cases, the mechanism of catalysis has been shown to be nucleophilic. Therefore, it is not surprising that yields of 4-(prop-2-ynyloxy)benzenesulfonyl fluoride ([^{18}F]-**24**) improved markedly upon addition of pyridine (Table 5.1, Entry 12 and Figure 5.9), as the formation of a reactive *N*-sulfonylpyridinium chloride ion pair allows for the facile acylation of fluoride with pyridine as the leaving group. Building on this result we improved upon our earlier two- step approach in which the [^{18}F]fluoride and pyridine are added sequentially in favour of a shorter protocol in which all three solvents (*t*-BuOH, $Cs_2CO_{3(aq)}$ and pyridine) are added at the same time. As a result, excellent radiochemical yields of [^{18}F]-**24** (99±1 % by radio-TLC) could be achieved in 15 (versus 30) min, with no apparent effect on either chemical or radiochemical purity. This optimized protocol was also deemed acceptable for the preparation of formylated compound [^{18}F]-**22** (96±1 % by radio-TLC). These yields represent the average of four traces in four separate experiments.

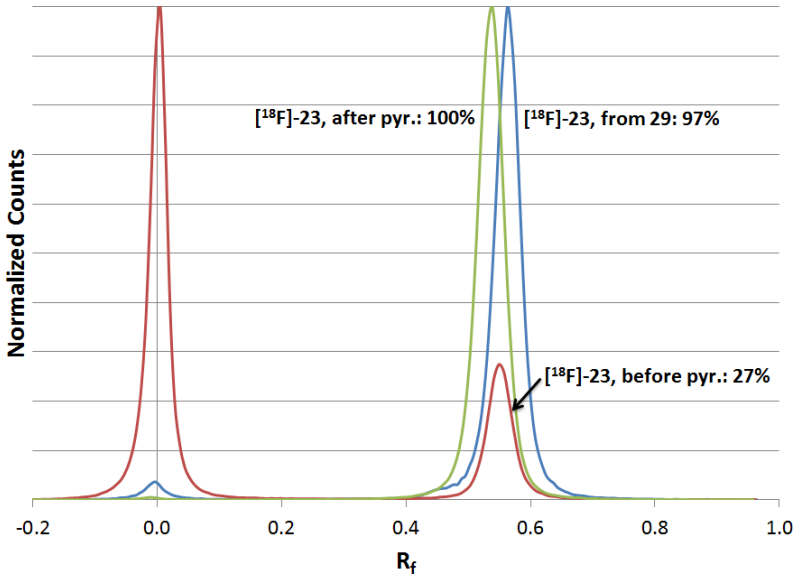

Figure 5.9. Representative radio-TLCs for the synthesis of [^{18}F]-24.

Figure shows yield of [^{18}F]F-**24** in 1:1 *t*-BuOH:$Cs_2CO_{3(aq)}$ before (red line) and after (green line) pyridine treatment (Table 5.1, Entry 12). The blue line depicts [^{18}F]-**24** as obtained from DMAP salt **30** (Table 5.3, Entry 4). For each trace, radioactive counts are reported relative to maximum signal strength.

5.7.3.2. Preparative synthesis of [^{18}F]-22 and [^{18}F]-24

In light of these initial yield and stability results, compounds [^{18}F]-**22** and [^{18}F]-**24** were chosen as candidates for preparative radiosynthesis and bioconjugation experiments. Established reaction conditions involved the incubation of sulfonyl chloride precursor (30 mM) in mixtures of Cs[^{18}F]F/$Cs_2CO_{3(aq)}$, *t*-BuOH, and pyridine (1:1:0.8, 280 µL) for 15 min a RT (Figure 5.11). It would be desirable to obtain purified ^{18}F prosthetic without resorting to HPLC purification. Thus, the initial protocol for the purification of [^{18}F]-**24** involved dilution of the reaction mixture with diethyl ether (700 µL) and fractional elution through a silica gel SPE column with ether (6 mL). The collected fractions (1 mL) were checked for activity, pooled (usually fractions 3 and 4), and concentrated at RT under a stream of helium. Table 5.2 provides a summary of the preparative parameters employed. Overall, this purification approach was unwieldy and subjected the synthesist to significant hand exposure. Furthermore, the effective removal of pyridine from the purified product was not achieved by this method (See Figure 5.10). CuAAC chemistry notwithstanding, one can envision many ligation chemistries (and targeting molecules) that would not tolerate the presence of nitrogen base. The replacement of a silica gel

purification step with one that utilized reverse phase tC_{18} sorbent was accompanied with a marked improvement in the NDC, collected yield of [^{18}F]-**24** (Table 5.2).

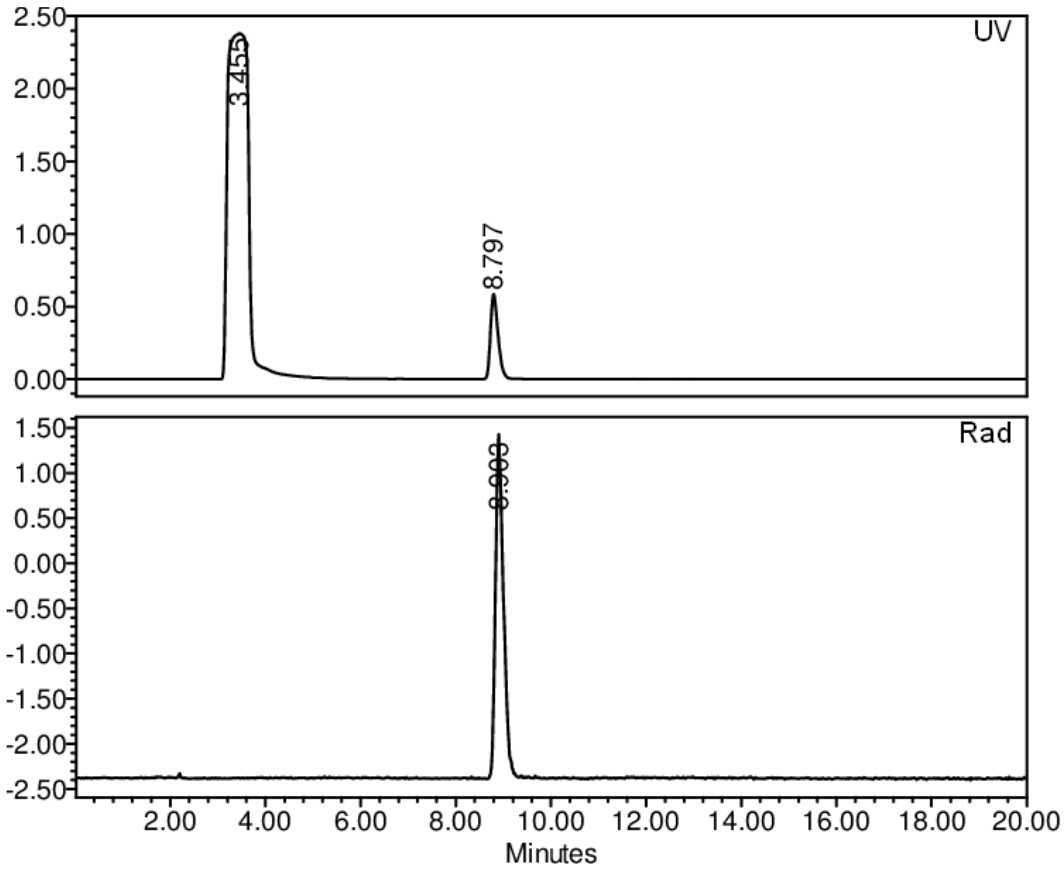

Figure 5.10. Co-injection HPLC trace of [^{18}F]-24 after silica gel SPE purification.

HPLC 18 Top: UV detection (260 nm, absorbance units) Bottom: Rad detection, mV. Non-radioactive **24** standard was added prior to injection. R_t pyridine = 3.5 min.

Table 5.2. Summary of Preparative Parameters of [^{18}F]-22 and [^{18}F]-24.

Peptide	**[^{18}F]-24**	**[^{18}F]-24**	**[^{18}F]-22**
Type of SPE Purification	Silica	tC_{18}	tC_{18}
Prep Yield, DC	78±6 %*	94±5 %**	88±8 %*
Prep Yield, NDC	52±5 %*	79±5 %**	73±7 %*
Protocol Time	50- 80 min	25- 30 min	27- 31 min

Note: *n =4. **n = 3.

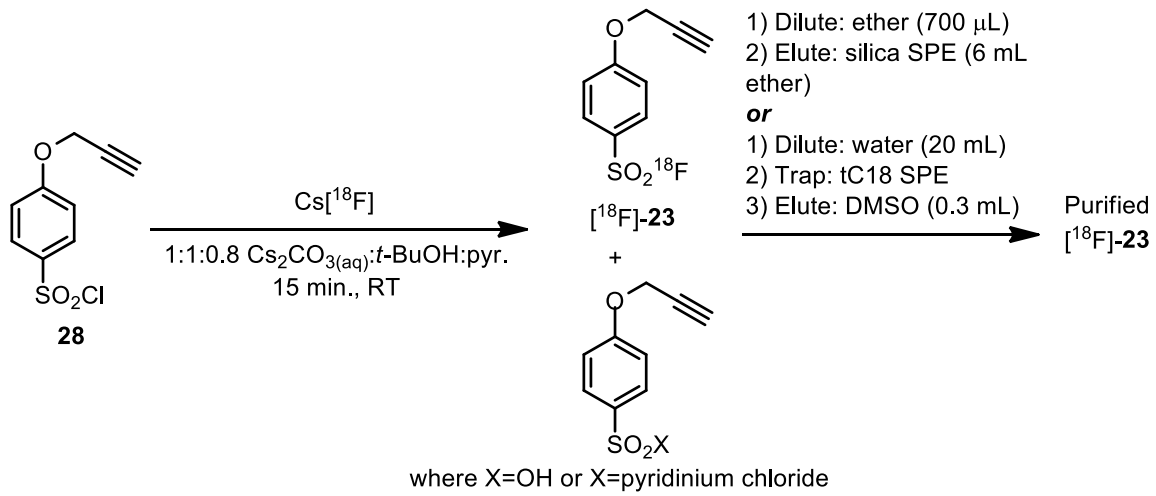

Figure 5.11. Preparative synthesis and purification of prosthetic group [^{18}F]-24.

Preparative syntheses of [^{18}F]-**22** were carried out in a manner identical to the optimized conditions for [^{18}F]-**24**. After purification on tC_{18} sorbent, excellent yields from SOS were obtained (73±7 % NDC, 88±8 % DC, *n*=6). Total synthesis time was 27- 31 min from SOS, or 47- 71 min from EOB. Figure 5.12 shows a HPLC trace (HPLC 18) of [^{18}F]-**22** after tC_{18} SPE purification. The UV chromatogram reveals little in the way of other chemical impurities, suggesting that the SPE step was efficient in separating [^{18}F]-**22** from any non- radioactive mesitaldehyde species that might compete with the prosthetic group during subsequent bioconjugations. Under the reported HPLC conditions, the R_t of sulfonyl chloride precursor **6** is 13.7 min and the R_t of sulfonate **16** is 6.4 min. The bulk of the pyridine was also removed (R_t = 3.3 min).

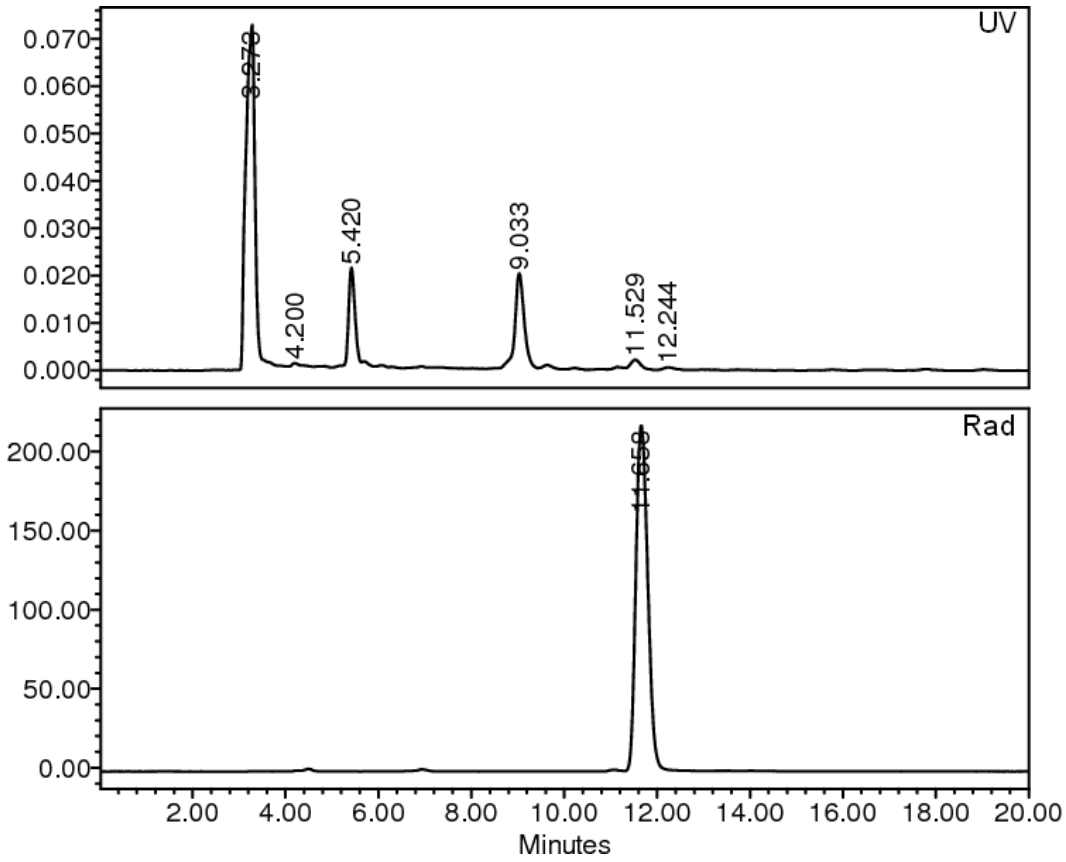

Figure 5.12. Radio-HPLC of [^{18}F]-22 after tC$_{18}$ SPE purification.

HPLC 18 Upper trace: UV detection (260 nm, absorbance units). Lower trace: radioactive detection (mV). Precursor sulfonyl chloride **27** elutes at 13.7 min.

The apparent specific activity of [^{18}F]-**22** and [^{18}F]-**24** after tC$_{18}$ purification was estimated to be 105±2 GBq/μmol (n = 4) and 63±8 GBq/μmol (n = 4) respectively, based on the UV-HPLC signal co-eluting with radiotracer relative to a mass standard curve.

5.7.3.3. DMAP salts as sulfonyl [^{18}F]fluoride precursors

In general, *N*-sulfonylpyridinium chlorides are difficult to isolate under atmospheric conditions, but *N*-sulfonyldialkylaminopyridinium salts are resonance-stabilized and in a few cases have been prepared.[449] Notably, DMAP derivative **33** (Figure 5.13) was used to tosylate tyrosine residues on chains A and B of oxidized bovine insulin and human calcitonin at pH 10-11.5.[432] Although 4-dialkylamino-substituted pyridines have been used as acylation catalysts for some time,[450] to our knowledge there have been no reports of *N*-sulfonyldialkylaminopyridinium salts being

used for the synthesis of arylsulfonyl fluorides. However, in light of our observations we synthesized **33** according to published protocol[432] (DMAP, 0 °C, EtOAc) and attempted to fluorinate it with KF in mixtures of 1:1 THF:$Cs_2CO_{3(aq)}$ (Figure 5.13). Qualitative TLC suggested good yields of tosyl fluoride (**34**) in the reaction mixture; we attribute the low recovered yield (37 %) to the reactivity of **34** towards DMAP (and unreacted DMAP salt) during product extraction. Indeed, a bifunctional analogue of **33**, alkynylated DMAP salt **30**, was also synthesized in excellent yields (98 %) and later used to prepare **24** (84 %, Figure 5.13). The same reaction conditions as those used to prepare **34** were employed, but the work-up was modified. Specifically, the reaction mixture was not diluted with water prior to extraction, and the extract was filtered immediately through silica gel. Unfortunately, an attempt to produce formylated compound **38** by the above method resulted in a hygroscopic solid that was very difficult to isolate. Overall, this previously unreported sulfonyl transfer reaction is an attractive alternative to the synthesis of certain sulfonyl fluorides by way of Cl-to-F exchange, which is sometimes sluggish without forcing conditions and often requires careful separation of the two sulfonyl halides.

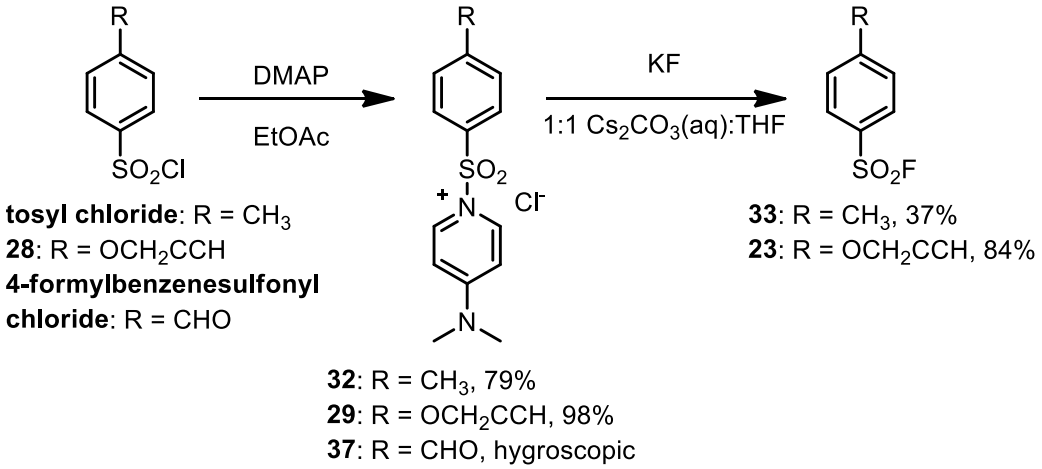

Figure 5.13. Synthesis of benzenesulfonyl fluorides 24 and 34 from N-sulfonyldimethylaminopyridinium salts 30 and 33 respectively.

[^{18}F]-Labelled tosyl fluoride ([^{18}F]-**34**) was synthesized from its *N*-sulfonyldimethylaminopyridinium precursor (**33**). Gratifyingly, excellent yields by radio-TLC were observed in mixtures of THF and $Cs_2CO_{3(aq)}$ after 15 min at RT (Table 5.3, Entry 1). Solvent mixtures composed of 1:1 *t*-BuOH:$Cs_2CO_{3(aq)}$ also work well (Table

5.3, Entry 2). Because salt **33** is water- soluble and exhibits a viable half-life in aqueous solutions ($t_{1/2}$= 14.5 h, pH 6.0 at 36°C),[432] we also attempted to radiolabel under aqueous conditions only (Cs[^{18}F]F/$Cs_2CO_{3(aq)}$), with excellent radiochemical yields of [^{18}F]-**34** observed after quenching with DMSO (Table 5.3, Entry 3). In this case the small radioactive peak at the trace origin, usually ascribed to free [^{18}F]F^-, appears to be a composite of two unresolved peaks, suggesting that a polar radiochemical impurity has formed. We further validated this new ^{18}F- labelling approach by converting bifunctional DMAP derivative **30** to [^{18}F]-**24** in 1:1 THF:$Cs_2CO_{3(aq)}$ and 100 % $Cs_2CO_{3(aq)}$ (Table 5.3, Entries 4 & 5 and Figure 5.9). In addition, we verified that [^{18}F]-**24** could be extracted from the bulk 1:1 THF:$Cs_2CO_{3(aq)}$ mixture in using the reverse phase SPE method described above. In this fashion, excellent preparative yields of [^{18}F]-**24** were achieved (78 % NDC yield from SOS, 92 % DC).

Table 5.3. Radiochemical yields by radio-TLC of [^{18}F]-24 and [^{18}F]-34 from N-sulfonyldimethylaminopyridinium salts 30 and 33 respectively.

Entry	Product	Precursor	$Cs_2CO_{3(aq)}$:Co-solvent	% Yield (+15 min)
1	[^{18}F]-**34**	**33**	*t*-BuOH	100±1**
2	[^{18}F]-**34**	**33**	THF	99±1**
3	[^{18}F]-**34**	**33**	$Cs_2CO_{3(aq)}$	8±1 (98±1)**,†
4	[^{18}F]-**24**	**30**	THF	99±1**
5	[^{18}F]-**24**	**30**	$Cs_2CO_{3(aq)}$	7±1 (97±1)*,†

Note: *Average of 3 traces. *Average of 4 traces. †Sampled after addition of DMSO (200 µL), between 15-16 min. Error = ±SD.

5.7.4. *Non-Radioactive Bioconjugate Chemistry*

For the coupling to formylated sulfonyl fluoride prosthetics such as **22**, 9-amino acid bombesin analogue (aminooxy acetic) [D-Tyr^6,βAla^{11},Thi^{13},Nle^{14}]BBN(6-14) (**BBN-ONH_2**) was prepared by collaborators at Université de Sherbrooke using standard Fmoc protocols. Non-radioactive **BBN-OX-MESIT-SO_2F** standard was obtained by mixing of **BBN-ONH_2** and **22** in DMSO followed by semi-preparative HPLC purification (Figure 5.14). The large difference in retention times between labelled and unlabelled material (ΔR_t = 4.5 min) is notable because it suggests that a significant degree of lipophilic character is conferred to the peptide targeting vector upon bioconjugation.

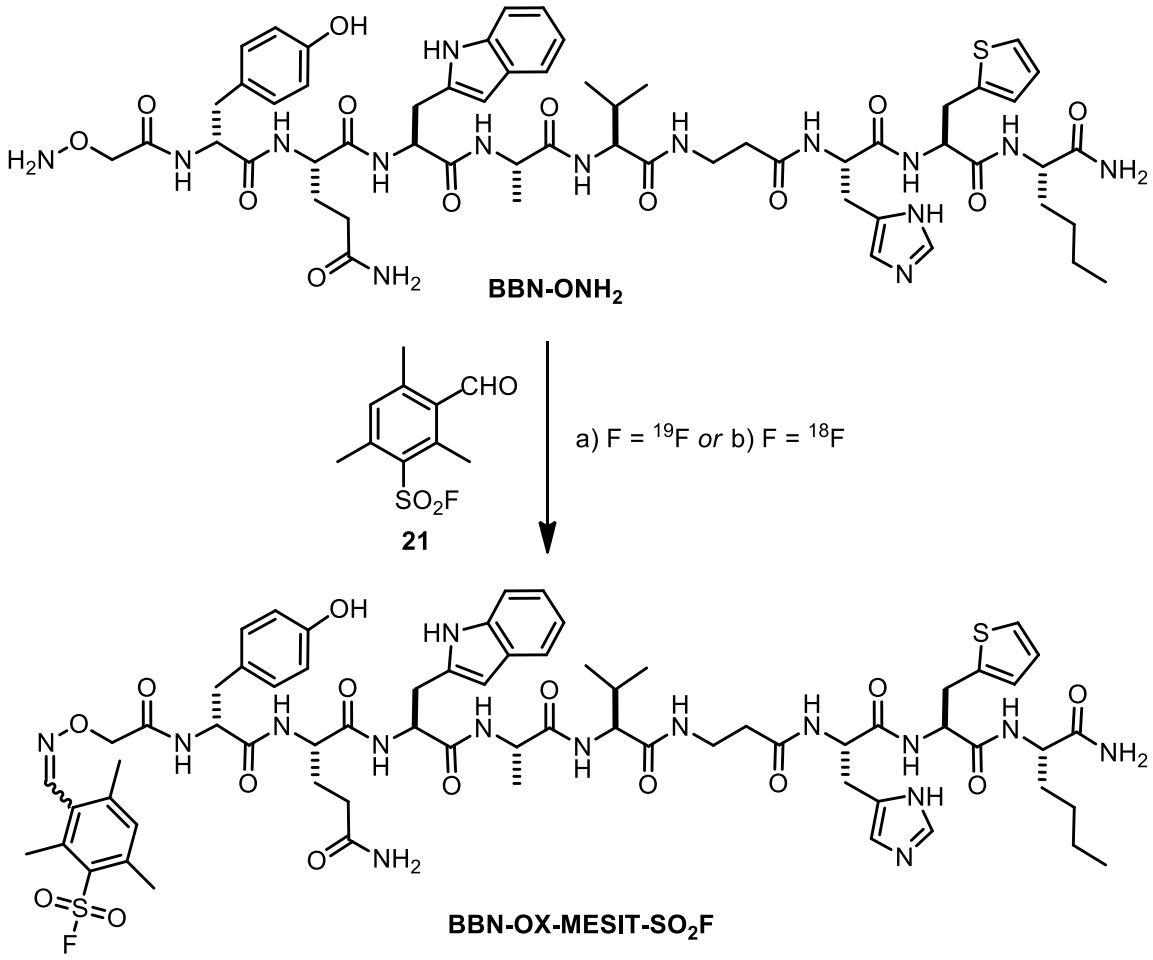

Figure 5.14. Preparation of BBN-OX-MESIT-SO_2F peptide.

a) ^{19}F prosthetic **22**, DMSO, 5 h. b) ^{18}F prosthetic [^{18}F]-**21**, see Table 12.

Results arising from the coupling of **N_3-BBN** with **24** in the presence of $Cu(CH_3CN)_4BF_4$ and TBTA were unexpected. HPLC assay of the reaction mixture at 1 hour revealed complete consumption of **BBN-N_3** (13.1 min; HPLC 17) corresponded with the presence of two closely eluting peaks (14.7 & 14.9 min; see Figure 5.16). These peaks, when collected together, exhibited the expected mass of **BBN-TRIAZOLE-BENZ-SO_2F** when assayed by MALDI-TOF (A1. 6, Appendix). However, as was observed during CuAAC preparations of **F-PEG-BBN** and **F-PEG-BVD**, a significant signal corresponding to $[M+^{63}Cu]^+$ (~50 % of base peak) is also present. Replacing TBTA catalyst with THPTA did not change the observed reaction outcome. It could be reasonably hypothesized that at least one of the product peaks corresponds to copper-

associated **BBN-OAlk-SO_2F**. However, the incubation of another CuAAC reaction mixture with copper- scavenging Chelex® 100 resin (200 mg in PBS, 30 min) resulted in a diminishment of *both peaks* and an increase of a single peak at 17.5 min (Figure 5.17). This peak was inconsistently observed in other reaction mixtures, and a radioactive version was seen during attempted preparations of **BBN-TRIAZOLE-SO_2[^{18}F]F** (Figure 5.18). Considering that the species at 17.5 min can be made radioactive (*i.e.* ^{18}F labelled) and furthermore, elutes at the expected time from N_3 precursor (ΔR_t = +4.4 min), it was postulated to be non-cuprated **BBN-TRIAZOLE-SO_2[^{18}F]F**. However, when this peak was collected after a non-radioactive reaction and assayed by MALDI-TOF, it exhibited a base *m/z* 300 Da smaller than the desired peptide. Further discussion related to the formation of Cu-peptide adducts can be found in Section 5.7.7.

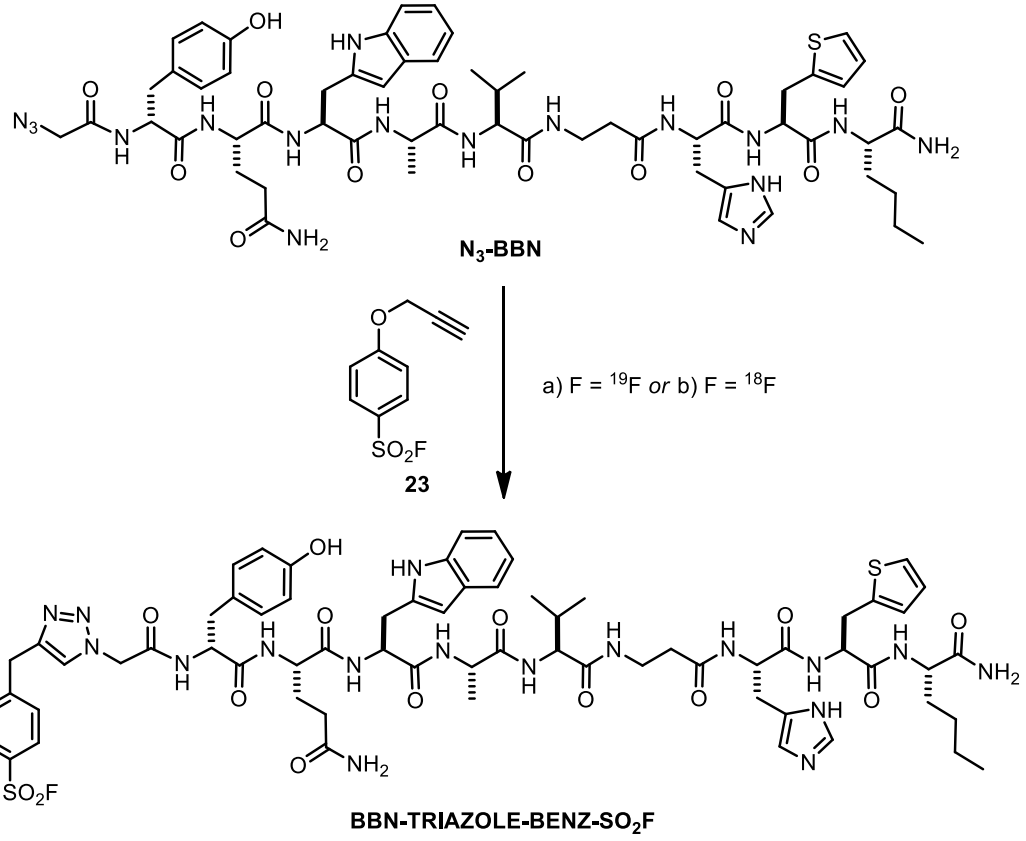

Figure 5.15. Attempted synthesis of BBN-TRIAZOLE-BENZ-SO_2F peptide.

a) ^{19}F prosthetic **24**, $Cu(CH_3CN)_4BF_4$, TBTA, DMSO, RT, 1 h. b) ^{18}F prosthetic [^{18}F]-**24** $Cu(CH_3CN)_4PF_6$, THPTA (or TBTA), DMSO, RT, 20 min. Peptide could not obtained as a single chemical species as determined by HPLC.

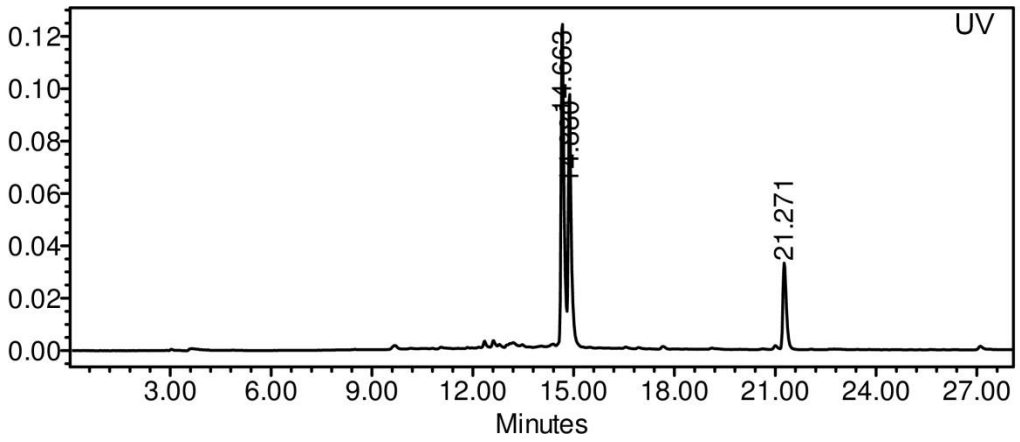

Figure 5.16. Preparative HPLC trace of non-radioactive BBN-TRIAZOLE-BENZ-SO_2F synthesis.

HPLC 17. Y-axis: UV absorbance at 280 nm (absorbance units). At 1 h. Precursor peptide **N_3-BBN** elutes at 13.1 min (now consumed). Prosthetic **24** elutes at 21.3 min.

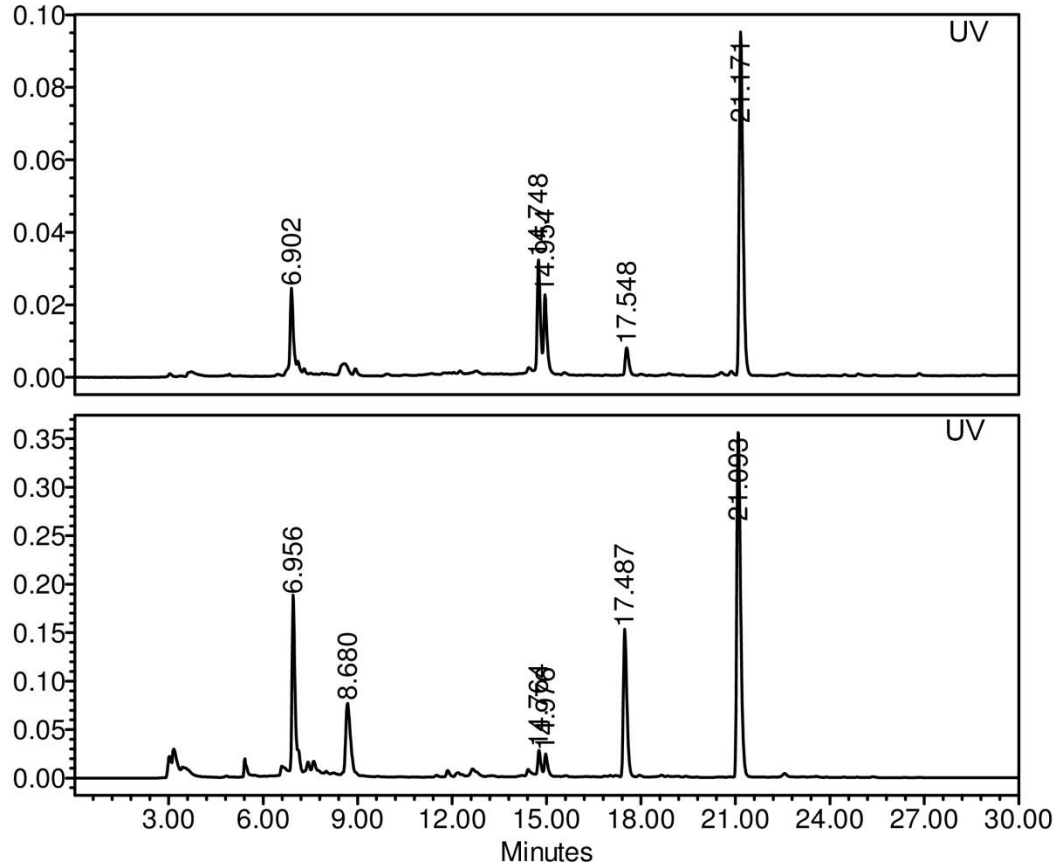

Figure 5.17. UV-HPLC before (top) and after (bottom) incubation in Chelex® 100.

HPLC 17. X-axis: min. Y-axis: UV absorbance at 280 nm (absorbance units). At 30 min incubation. R_t of THPTA = 6.9 min.

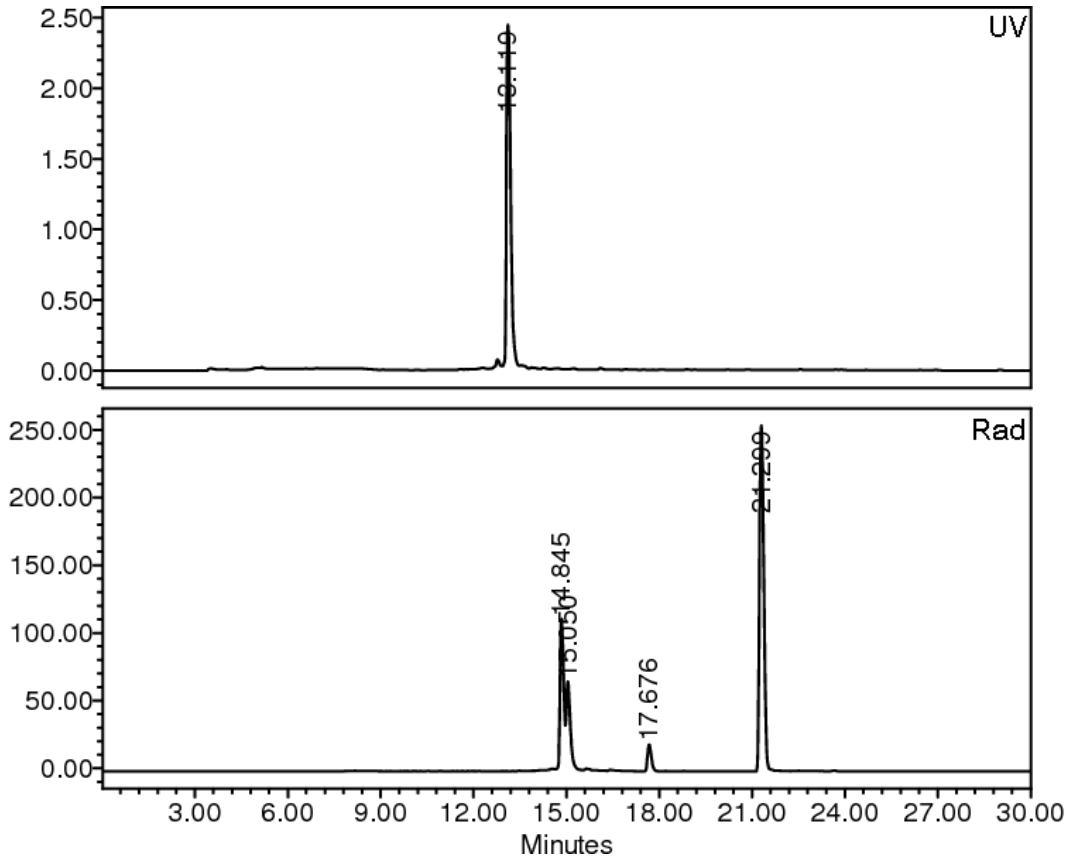

Figure 5.18. Radio-HPLC of BBN-TRIAZOLE-BENZ-SO2[^{18}F]F reaction mixture.

HPLC 17. Top: Y-axis = UV absorbance at 280 nm (absorbance units). Bottom: Y-axis = Radiation detection (mV). Cu^{I}/TBTA, DMSO, 10 min, RT. Precursor peptide **N_3-BBN** elutes at 13.1 min. Prosthetic **24** elutes at 21.3 min.

5.7.5. *Radioactive Bioconjugate Chemistry*

Acceptable conjugation yields of radioactive 3-formyl-2,4,6-trimethylbenzenesulfonyl [^{18}F]fluoride ([^{18}F]-**22**) to **BBN-ONH$_2$** by way of oxime formation required some optimization (Figure 5.14 and Table 5.4). As oxime bond formation occurs most rapidly in aqueous solutions at pH 3-5,[451] additional test reactions were carried out in the presence of 5 % AcOH and 2-(*N*-morpholino)ethanesulfonic acid (MES) buffered saline (100 mM, pH 4.7). Full preparative radiosyntheses of sulfonyl [^{18}F]fluoride- modified **BBN-OX-MESIT-SO$_2$[^{18}F]F** was eventually carried out according to the parameters outlined in Table 5.4, Entry 5.

Table 5.4. Parameters tested for the synthesis of BBN-OX-MESIT-SO$_2$[^{18}F]F.

Entry	DMSO:Co-solvent	Time (min)	Temperature	% Yield by HPLC
1	DMSO	20	RT	29
2	MES buffered saline*	20	RT	34
3	5 % AcOH	20	RT	51
4	5 % AcOH	30	RT	52
5	5 % AcOH	30	37 °C	64

Note: All reactions utilized 0.5 mg precursor peptide (**BBN-ONH$_2$**) and 400 µL total solvent. *100 mM, pH 4.7.

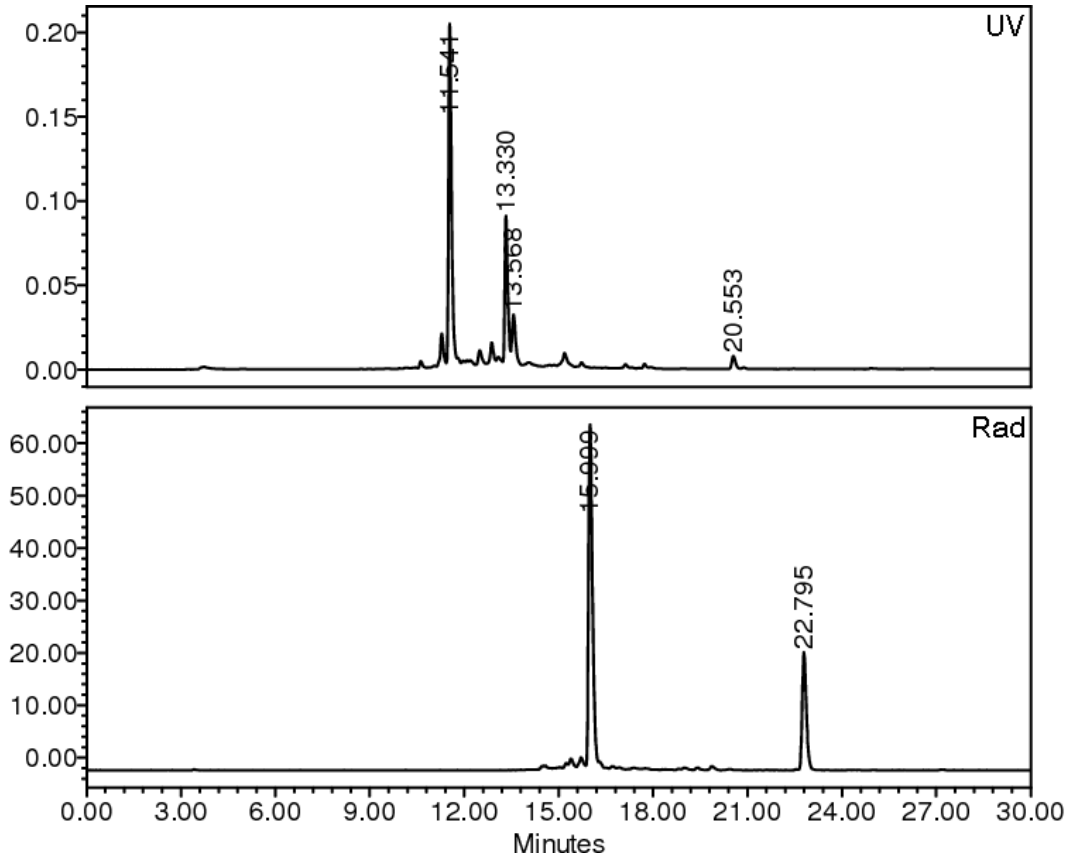

Figure 5.19. HPLC trace of BBN-OX-MESIT-SO$_2$[^{18}F]F reaction mixture.

HPLC 17. Top: Y-axis = UV absorbance at 280 nm (absorbance units). Bottom: Y-axis = Radiation detection (meV). Reaction conditions: 3:1 DMSO:5 % AcOH, 37 °C, 30 min. R_t of **BBN-ONH$_2$** = 11.5 min. R_t of **BBN-OX-MESIT-SO$_2$[^{18}F]F** = 16.0 min. R_t of [^{18}F]-**22** = 22.8 min.

An important requirement for cellular receptor imaging is that the final tracer formulation be reasonably free of functionally similar impurities that might compete with

the radiopharmaceutical for receptor targets *in vivo*. In this case, **BBN-OX-MESIT-SO_2[^{18}F]F** was well separated from peptide precursor using the HPLC purification reported. The radio-peptide was removed from HPLC eluent by way of a second tC_{18} extraction and formulated in 10 % EtOH in saline. A radio-HPLC trace of the final formulation is shown in Figure 5.20. Note that the accompanying spectroscopic chromatogram (λ_{max} = 280 nm, top trace) fails to detect any measurable amount of UV-absorbing material associated with the ^{18}F peptide. **BBN-OX-MESIT-SO_2[^{18}F]F** was obtained in DC preparative yields of 35± 6 % (*n* = 4) from SOS. Total synthesis time was 105- 109 min from SOS. The distribution coefficient of radioactive peptide **BBN-OX-MESIT-SO_2[^{18}F]F** was obtained following modifications to the standard procedure as described by Wilson *et al.*[452] In short, the radio-peptide was extracted into 1-octanol prior to measuring its distribution into octanol/PBS (20 mM, pH 7.4), thus ensuring that no co-contaminant polar radioactive impurity (such as [^{18}F]F^-) was present. The log $D_{[7.4]}$ value for was found be 1.91±0.01 (*n*=4 measurements), which suggests that **BBN-OX-MESIT-SO_2[^{18}F]F** is a rather lipophilic BBN(6-14) analogue.

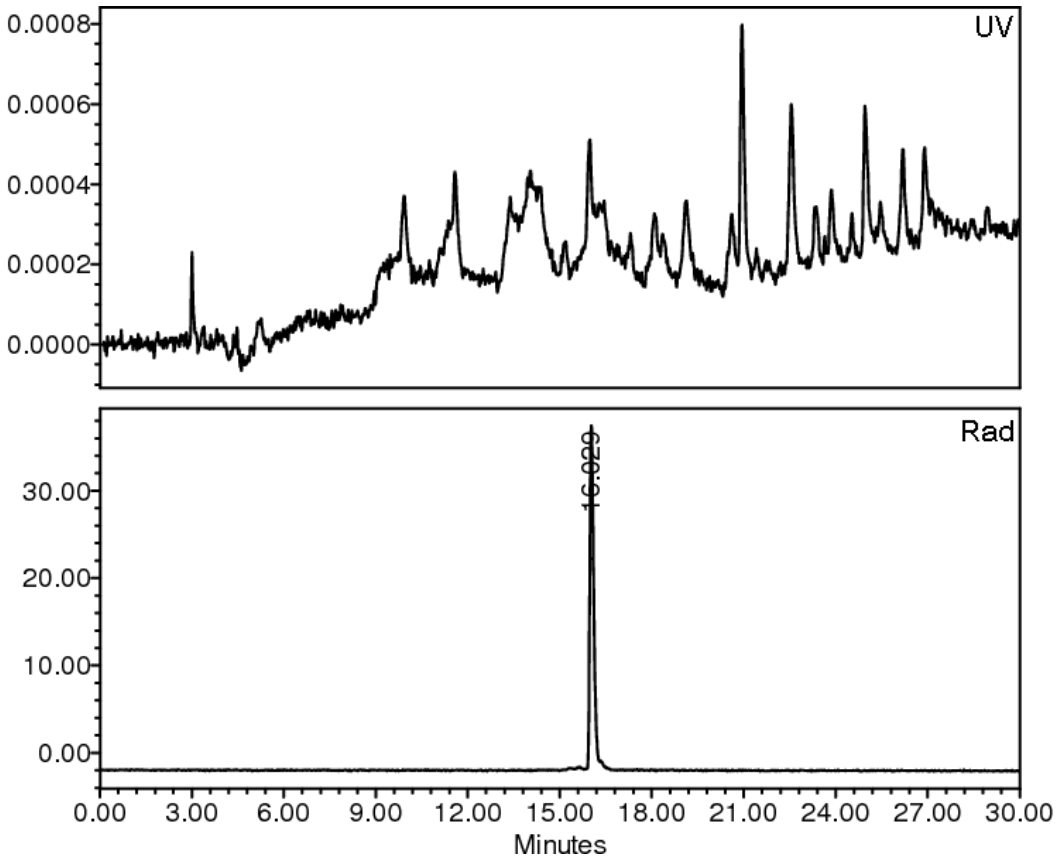

Figure 5.20. Radio-HPLC of BBN-OX-MESIT-SO$_2$[^{18}F]F after final formulation.

HPLC 17**.** Top: Y-axis = UV absorbance at 280 nm (arbitrary units). Bottom: Y-axis = Radiation detection (meV). Note that the UV-HPLC signal is essentially at baseline.

5.7.6. *Stability of Sulfonyl [^{18}F]Fluoride- Modified Peptide in Mouse Serum*

The stability of **BBN-OX-MESIT-SO$_2$[^{18}F]F** in 10 % DMSO in murine serum was originally tested by HPLC. After 15, 60 and 120 min at 37 °C, a portion of the incubation mixtures were quenched with equal amounts of MeCN, chilled (4 °C), centrifuged, and the supernatant was assayed by HPLC (HPLC 17). At the 15 min time point, 45- 57 % of the total radioactivity remained in the precipitate, which suggests that a significant amount of the peptide non-specifically binds to serum protein. Association with blood proteins is the established *in vivo* fate of many lipophilic pharmaceuticals, including certain radiolabelled peptide analogues.[453] After two hours, control mixtures (10 % DMSO in PBS, 37 °C, quenched with acetonitrile) appear identical to QC traces of the final formulation. However, **BBN-OX-MESIT-SO$_2$[^{18}F]F** in serum is extensively

converted to other radiolabelled metabolites in less than 15 min. As shown in Figure 5.21, the major decomposition product (R_t = 14.9 min) constitutes 45±4 % of the total detected radioactivity. (*n*=3 separate experiments). Very little or no radioactive signal was observed early in these chromatograms where one would expect to observe free fluoride. In contrast, HPLC traces at 60 and 120 min contain both free fluoride and the product signal, but both peaks are very small relative to the injected activity. Furthermore, the chromatograph baselines are not uniform, indicating that $[^{18}F]F^-$ is 'bleeding' off the HPLC column during the acquisition of these traces. This further suggests that at these time points, significant defluorination of the radio-peptide has occurred.

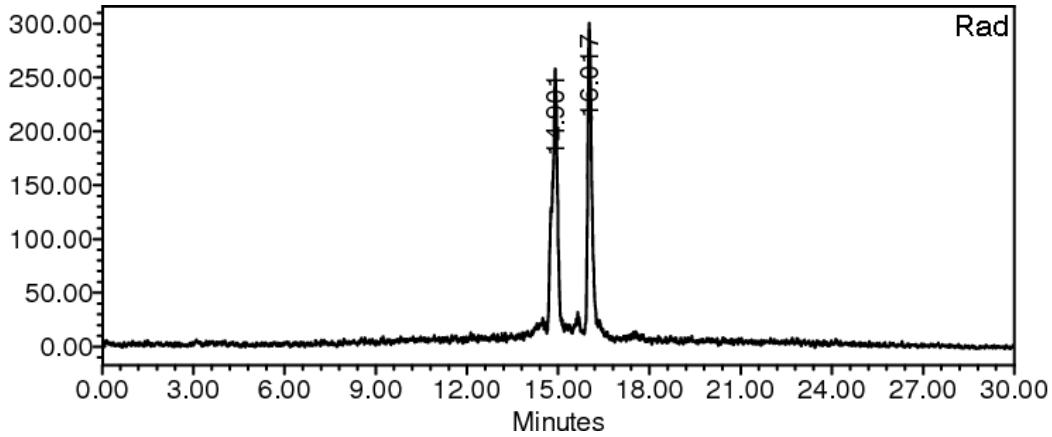

Figure 5.21. Radio-HPLC of BBN-OX-MESIT-SO$_2$[^{18}F]F after incubation in mouse serum.

HPLC 17. Y-axis = radiation detection (meV). Incubation conditions were 15 min at 37 °C. **BBN-OX-MESIT-SO$_2$[^{18}F]F** elutes at 16.0 min, while the major decomposition product elutes at 14.9 min.

These observations highlight the difficultly in assessing the true extent of ^{18}F radiotracer defluorination by way of reverse phase HPLC. This is primarily because $[^{18}F]F^-$ can potentially adsorb onto C_{18} sorbents and thus be removed from the recorded chromatogram. Therefore a radio-TLC method employing normal phase silica iTLC-SG plates was developed to assess the relative amount of dissolved ^{18}F peptide after incubation in serum. Using 1:1 MeOH:MES buffered saline as eluent, $[^{18}F]F^-$ in 1:1 MeCN:10 % DMSO in mouse serum exhibits an R_f of ~0.1. (Figure 5.22). In contrast, when the same solution of $[^{18}F]F^-$ is run in 1:1 MeOH: ammonium acetate (0.1 M), or 1:1 MeOH:PBS buffer (0.15 M, pH 7.2), radioactivity can be found throughout the length of

the plate. The nature by which MES affixes free [^{18}F]fluoride near the origin of the iTLC plate is not yet understood, but this observation should undoubtedly be of interest to others seeking a simple means to measure the extent of radio-defluorinaion of polar ^{18}F tracers. Under similar conditions, **BBN-OX-MESIT-SO$_2$[^{18}F]F** and related species are separated from free [^{18}F]fluoride (R_f = ~0.9; Figure 5.23). However, it should be noted that individual [^{18}F]fluorinated peptide degradation products cannot be distinguished using this technique. Thus, the observed radioactivity present at 0.7- 1.0 R_f after 15 min in serum [43±4 % (*n*=3 traces) and 35±1 % (*n*=3 traces) in two separate experiments] represents only an estimation of the percent remaining of sulfonyl [^{18}F]fluoride- bearing species relative to the total radioactivity in the serum solution.

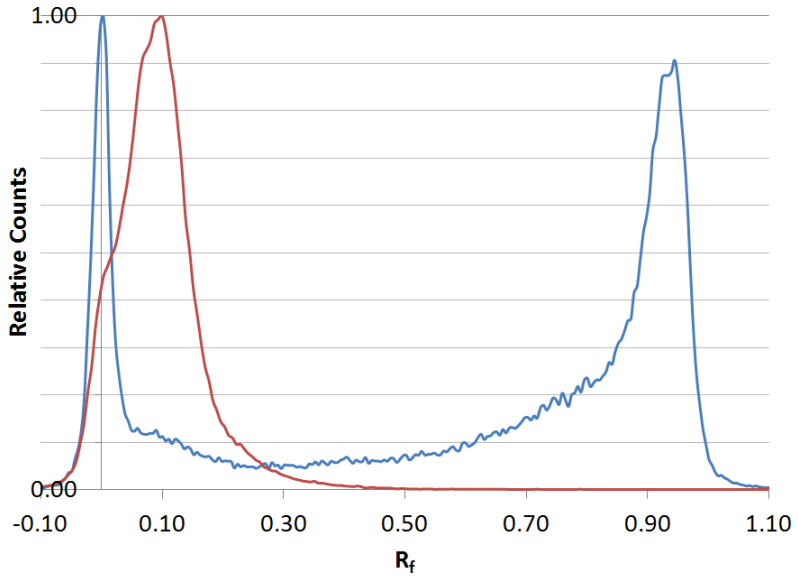

Figure 5.22. Radio-TLCs of [^{18}F]F$^-$ in serum assay mixture.

Figure shows free [^{18}F]fluoride in 1:1 MeCN:10 % DMSO in mouse serum when 1:1 MeOH:PBS (150 mM, pH 7.2) is used as eluent (blue line), versus 1:1 MeOH:MES (100 mM, pH 4.7, red line). For each trace, radioactive counts are reported relative to maximum signal strength.

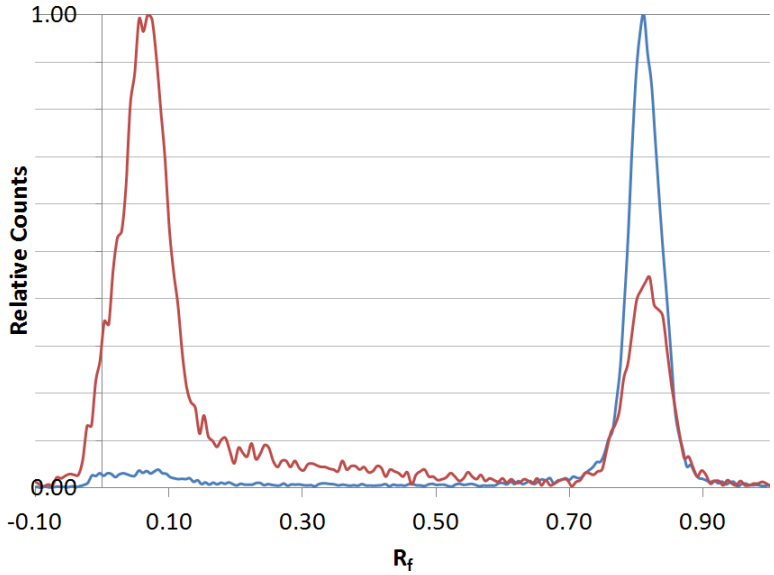

Figure 5.23. Radio-TLCs of BBN-OX-MESIT-SO$_2$[^{18}F]F before and after incubation in serum.

Figure shows **BBN-OX-MESIT-SO$_2$[^{18}F]F** after incubation in 1:1 MeCN:10 % DMSO in PBS at 37 ºC for 15 min (blue line), versus incubation in 1:1 MeCN:10 % DMSO in mouse serum under the same conditions (red line). For each trace, radioactive counts are reported relative to maximum signal strength. In both traces, 1:1 MeOH:PBS (150 mM, pH 7.2) was used as eluent.

5.7.7. *Further comments on the formation of Cu-peptide adducts*

Some CuAAC bioconjugations carried out in both Chapters 4 and 5 resulted in the formation Cu-peptide adducts. To summarize, the MALDI-TOF spectra of HPLC-purified **F-PEG-BVD**, **F-PEG-BBN** and **BBN-OAlk-BENZ-SO$_2$F** (Figure 4.2, Figure 4.2, and Figure 5.15 respectively) contained [M+Cu]$^+$ ions. In contrast, peptides **F-ALK-BVD**, **F-ALK-BBN**, **F-ALK-BBN-PEG** and **F-PEG-BBN-PEG** did not exhibit evidence of Cu association. A worthwhile examination of these observations would benefit from a survey of the potential binding elements at play. The association of Cu with [1,2,3]-triazole moieties has already been discussed in context of CuAAC catalysts TBTA and THPTA (Section 1.4.2). However, PEG moieties, sulfur- containing amino acid residues, and basic amine amino acids can also serve as copper- chelating functionalities, as described below.

Polymers of ethylene oxide and chloride ion can inhibit the electrochemical deposition of copper in acidic (sulfate) solutions, and it is in this context that the study of PEG/Cu interactions has taken place. Yokoi *et al*. first posited the notion that the

polyethylene glycol chains in such solutions wrap around Cu^{I} and Cu^{II} ions to form pseudo-crown moieties (Figure 5.24a), which then associate with chloride ions adsorbed to the copper surface.[454] However, later authors have noted that in order to accommodate a bridging chloride ion at the surface of the electrode, the complex as proposed by Yokai *et al.* would need to expand to a rare seven-coordinate system. In aqueous solutions lacking Cl^-, a Cu^{II}(-oxyethylene-)$\cdot 5H_2O$ complex (Figure 5.24b) was proposed by Suryanarayana *et al.*,[455] and others argued for a similar structure in acid chloride baths.[456] More recently, Raman spectroscopic investigations have suggested that Cu^{I} is complexed in deposition solutions in a three- coordinate fashion by way of a Cu^{I}-Cl bond and two oxyethylene groups [Cu^{I}(-oxyethylene-)$_2$(Cl); Figure 5.24c].[457] Regardless of the reducing species, it has been established that PEG chains exhibit significant conformational differences depending on the nature of the surrounding solvent. Thus Stoychev and Tsvetanov[456] suggest that in lipophilic media, the oxygen molecules form an electronegative cavity which is suitable for the complexation of cations. In water, however, the oxygen atoms may hydrogen bond with solvent molecules and thus metal chelation is not possible. The authors note an inherent instability associated with these complexes. They attribute this instability to the strong potential of the bulk water to act as a competing ligand, as well as the lack of a strictly defined geometry in the chelating PEG architecture. Of course, distinct differences exist between the copper electroplating process and the conditions by which copper is absconded into the above peptides; specifically, electrolytic baths employ large PEG polymers in low pH/ high Cl^- envirnoments. However, weak cathodic inhibition has been observed even in the absence of chloride, and this phenomena has attributed to the formation of Cu^{I}(-oxyethylene-)$_3\cdot H_2O$ and Cu^{II}(-oxyethylene-)$_4\cdot 2H_2O$ complexes (Figure 5.24d).[456] With regard to PEG size, it was reported that chains as short as tetraethylene glycol (TEG) can initiate absorptive inhibition in plating solutions;[458] the jump in required overpotential between diethylene glycol (two ether oxygen atoms) and TEG (three) is striking. A number of experimental observations, including the large excess of Cu^{I} (but not Cu^{II}) relative to TEG on the surface of the electrode points to a Cu^{I} complex being responsible for the observed effects.

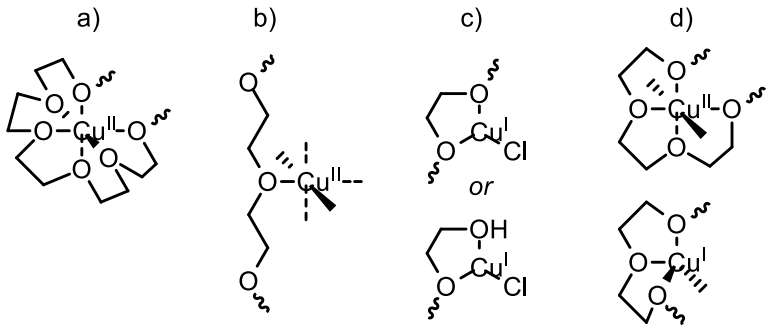

Figure 5.24. The nature of Cu-PEG association in copper deposition solutions as postulated by different researchers.

Coordinating water molecules are shown only as sticks for clarity.

Copper is essential to a variety of biological processes, including electron transfer and dioxygen chemistry (*e.g.* reduction, superoxide degradation, incorporation and transport).[459] As a result, copper- bioligand interactions have been widely studied.[460] Among bioactive peptides that bind copper, MALDI-TOF has proven a valuable investigative tool because the resulting adducts are intrinsically charged and in general analyte ions form abundantly upon laser desorption. Unlike $[M+H]^+$ ions, in which the proton can be considered 'mobile', Cu is thought to anchor to particular side chains over the course of the analytical process.[461, 462] Wu *et al*. calculated theoretical binding energies of a series of Cu^I-peptide ligand systems and found the order of monodendate binding strength to be Arg>His>Lys>Cys>Ser; bidentate models exhibited similar behaviour: Arg>Lys>His>Gn>Asn>Glu>Asp.[463] The same group obtained metastable ionization fragmentation patterns for a series of bioactive peptides and results suggest that Arg, Lys and His residues are overwhelmingly responsible for $[M+Cu]^+$ peptide formation. Competition between these residues is common and position within the primary sequence is a critical factor for binding.* It should be noted however, that while an understanding of a Cu-peptide's gas-phase ionization chemistry can offer important insights, different criteria must be met if a stable (*i.e.* HPLC-

* For instance, *N*-terminal arginines show a significantly higher affinity for Cu^I compared to internal arginines, suggesting a bidendate mode of chelation that includes both guanidine group and N-terminal amine.[462]

purifiable) adduct is to form in solution. First, one might anticipate the importance of multidentate chelation sites so that stable coordination spheres can be achieved. Second, Cu binding to peptides tends to increase with increasing pH, as more basic residues are become deprotonated and thus available to bind the metal.[464]

Concerning our observations specifically, we first note that while the presence of $[M+Cu]^+$ ions in the MALDI-TOF spectra coincide with appearance of two closely eluting HPLC peaks, it has not been shown conclusively that these peaks represent labelled and unlabelled material. It is also possible that the peaks represent *coordination isomers*, that arise from an asymmetric binding motif. Similar HPLC events have been reported previously under NCA conditions, when attempts were made stabilize ^{99m}Tc-HYNIC chelates with secondary ligands.[465] Another possibility is that collected mixture(s) are composed of Cu-peptide product and a degraded peptide species (Cu-associated or otherwise), although this scenario should be easier to recognize using MALDI-TOF.

With regard to the possibility that the core peptide sequence(s) are responsible for Cu binding, we note that BVD analogues **F-ALK-BVD** and **F-PEG-BVD** contain two arginines, which are separated by a single leucine residue. The fact that **F-PEG-BVD** binds copper while **F-ALK-BVD** does not suggests that arginine does not participate in Cu binding. Furthermore, both peptides were prepared in the presence of buffer [2:1 DMSO:PBS (pH 7.2)], an environment in which the guanidino head groups (pKa ~12.5) are principally charged. In contrast, the imidazole group of histidine is largely neutral at physiological pH, and histidines can be found in the binding domains of virtually all proteins which use copper in a co-factor role.[460],* The BBN analogues described here ([d-Tyr^6, βAla^{11}, Thi^{13}, Nle^{14}]BBN(6-14)) contain a single histidine (His^{12}). However, this monodendate ligand is unlikely to bind copper on its own and is well removed from the

* Apart from histidine, the other key Cu binders *in vivo* are cysteine and methionine. These sulfur- bearing amino acids work in concert with histidine in the blue copper (type 1) and Cu_A protein classes. Not all copper proteins require His, however; intracellular copper traffickers retain Cu^I by means of only two or three spatially optimized Cys or Met groups.[466]

terminus bearing the pendant molecule. An unnatural 3-thienylalanine (Thi) residue, which replaces Phe in the native peptide fragment, can been found adjacent to His^{12}. However, the thiazole ring is not particularly basic (pKa ~2.5) and sequence engineering experiments with the blue copper protein azurin have shown that replacing a key histidine with 3-thienylalanine severely inhibits the metalloprotein's ability to bind copper.[467] Thus it seems unlikely that the Thi^{13} residue participates in the formation of the observed Cu-BBN adducts.

Upon consideration of the potential role of the 2-fluoropyridine- based pendant group(s) in binding Cu, a straightforward paradigm does not emerge. A majority of Cu^{I} complexes are tetrahedral, but many stable two- and three- coordinate compounds are also possible.[468] [^{18}F]-**16**- labelled peptides **F-PEG-BBN** and **F-PEG-BVD** have two ethereal oxygen atoms (disregarding the pyridolic oxygen) with which to bind copper. Furthermore, it is indeed possible that the [1,2,3]-triazole moiety and/ or the pyridine nitrogen could work in conjugation with the mini-PEG chain to coordinate Cu^{I} at additional sites. The fact that these peptides exhibit evidence of copper binding by MALDI-TOF- while their non-PEGylated analogues (**F-ALK-BVD** and **F-ALK-BBN**) do not- is suggestive of the role of the prosthetic in this phenomenon. However, no Cu-peptide is observed in the spectrum of a third [^{18}F]-**16**- bearing peptide, **F-PEG-BBN-PEG**. Furthermore, both **F-PEG-BBN-PEG** and **F-ALK-BBN-PEG** contain an auxiliary, internal amino-TEG pendant group which does not appear to bind Cu to a significant extent. Any notion that the observations herein can be explained in a straightforward and general fashion is further dismissed by the fact that **BBN-TRIAZOLE-BENZ-SO_2F** also forms an adduct with Cu during bioconjugate CuAAC reactions. Among the potential ligating functionalities discussed thus far, **BBN-TRIAZOLE -BENZ-SO_2F** contains only a [1,2,3]-triazole and a distant histidine. It is tempting to evoke a sulfonate-Cu interaction (in concert with the triazole) to explain the presence of $[M+Cu]^+$ ions in the MALDI-TOF. However, this would necessitate the loss of [^{18}F]F^-, and because both peaks can be made radioactive (Figure 5.18), both almost certainly contain intact sulfonyl [^{18}F]fluoride.

If an inclusive explanation to the above observations is available, its discovery will require the implementation of additional investigative techniques (and possibly, different peptide sequences). Comprehensive examinations of peptide fragmentation

ion spectra, in conjunction with computational analysis, have been used to predict the preferred gas- phase Cu^{I} binding sites for a few specific Cu-peptide adducts.[462, 463, 469] While this information may have some predictive value, it is unlikely to assist the practical preparation of ^{18}F peptide radiopharmaceuticals which tend to associate with copper. Scavenging Cu through the addition of complexation or precipitation agents either before or after HPLC purification might be possible, but this represents an undesirable strategy in terms of radiosynthetic efficiency, peptide integrity, and drug quality control. Furthermore, such an approach might be considered unacceptable for clinical use if the complete removal of copper cannot be verified by radio-HPLC (as in cases of **[^{18}F]F-PEG-BBN** and **[^{18}F]F-PEG-BVD**).

5.8. Conclusion

The elevated temperatures and anhydrous conditions required to create C-^{18}F bonds by way of nucleophilic aromatic and nucleophilic aliphatic substitution reactions are incompatible with many potential biological targeting agents. We hypothesized that a bifunctional benzenesulfonyl fluoride moiety might be found that was sufficiently stable *in vivo* to successfully serve as an easy-to-prepare, ^{18}F- bearing prosthetic for PET biomarkers. To this end, a straightforward protocol was developed for the radiosynthetic preparation of 4-formyl, 3-formyl, 4-maleimido and 4-oxylalkynl- benzenesulfonyl fluorides (**21**- **24**). These novel ^{18}F prosthetics were radiosynthesized in high yields in equal volumes of basic cyclotron target [^{18}O]H_2O and organic co-solvent at room temperature from their corresponding sulfonyl chlorides. *Preparation of anhydrous $K_{2.2.2}$/K[^{18}F]F complex was not required.* Except in the case of maleimide **23**, excess pyridine could be used to selectively convert the sulfonyl chloride precursor to a reactive *N*-sulfonylpyridinium chloride intermediate. Radiochemical yields were not diminished by this approach, and in the case of less reactive **24** yields saw improvement. Furthermore, the destruction of sulfonyl chloride precursor allowed for simple SPE extraction of ^{18}F prosthetic from the bulk reaction mixture.

Recent successes preparing robust, electron- poor tri[^{18}F]fluoroarylborates (see Section 1.6.1) speak well for a radiobioconjugate strategy by which modifications to an aryl ring might inductively stabilize an ^{18}F bearing pendant group towards defluorination.

By analogy, we successfully prepared electron- rich arylsulfonyl fluorides that were stable in strongly buffered, aqueous solutions (150 mM PBS). Owing to their observed stability under these conditions, 3-formyl-2,4,6-trimethylbenzenesulfonyl fluoride (**22**) and 4-(prop-2-ynyloxy)benzenesulfonyl fluoride (**24**) were chosen for further study. The *in situ* degradation of benzenesulfonyl chloride precursor in the presence of pyridine permitted the efficient and reproducible preparative synthesis of their radioactive versions, without the need for time- consuming HPLC purification of the prosthetic group. To the best of our knowledge, the NDC, collected yields of [^{18}F]-**22** and [^{18}F]-**24** (73±7 % and 79±5 % from SOS respectively) achieved in this work constitute a high watermark for the preparation of an ^{18}F labelling agent without automated assistance. Finally, in light of our previously unreported observations regarding the utility of pyridine for the nucleophilic catalysis of sulfonyl halide exchange, an *N*-sulfonyl-dimethylaminopyridinium chloride salt (**30**) was synthesized and used to prepare both ^{19}F- and ^{18}F- labelled **24** in excellent chemical (84 %) and radiochemical yields (78 % NDC from SOS).

We chose to assess the utility of [^{18}F]-**22** and [^{18}F]-**24** as prosthetic ^{18}F labelling agents for biological PET tracers using the 14-amino acid neuropeptide bombesin(6-14) (BBN) as a 'proof-of-principle' targeting vector. [^{18}F]-**24** was coupled to an azide-bearing analogue of bombesin (**BBN-TRIAZOLE-BENZ-SO$_2$[^{18}F]F**) *via* [1,2,3]-triazole formation (CuAAC chemistry). Unfortunately, **BBN-TRIAZOLE-BENZ-SO$_2$[^{18}F]F** associates Cu catalyst and a means to disassociate the resulting adduct was not established. More successful was the radiosynthesis of [^{18}F]-**22**- modified **BBN-OX-MESIT-SO$_2$[^{18}F]F** peptide *via* oxime ligation to an oxyamino- bearing bombesin analogue. Although the carbonyl addition- elimination reaction was not quantitative, the outstanding efficiency and reproducibility inherent in the overall radiosynthetic protocol allowed for preparation of ^{18}F peptide in yields competitive with other, significantly more complex syntheses [35±6 % DC, 18±3 % NDC (*n* = 4) from SOS]. The full synthesis of **BBN-OX-MESIT-SO$_2$[^{18}F]F** can be completed in less than 110 min.

The sulfonyl fluorinated peptide analogue **BBN-OX-MESIT-SO$_2$[^{18}F]F** was found to be stable in 10 % DMSO in PBS over two hours at physiological temperature and pH. Under similar conditions in mouse serum, however, **BBN-OX-MESIT-SO$_2$[^{18}F]F** showed signs of defluorination. An accurate estimation of the rate of sulfonyl [^{18}F]fluoride

hydrolysis was complicated by the fact that enzymatic modification of the ^{18}F peptide and complexation with serum proteins also occurs. The interrelation between these three processes remains to be determined, but further insights might be gleaned through the labelling of alternative targeting vectors. However, it must be conceded that even if defluorination in the peri-receptor space can be avoided, sulfonyl [^{18}F]fluoride- labelled radioprobes may still be unsuitable for the imaging of cell surface receptors and other targets that would see the sulfonyl fluoride moiety brought in close proximity protein nucleophiles. Yet perhaps this potential intrinsic limitation could be ameliorated through the use of long tethering chains separating receptor ligand and prosthetic group.

To conclude, we suggest that the foremost idea garnered from this work may be the notion that functionally complex molecules might be reliably and chemoselectively labelled with *moderately reactive* arylsulfonyl fluorides. SO_2F- modified bioconjugates could serve as precursors to a wide variety of chimeric compounds, including radioprobes. With regard to PET chemistry specifically, one could conceive of a SO_2F-bearing biomolecule being labelled directly with [^{11}C]CH_3I. It is anticipated that the resulting SO_2[^{11}C]CH_3 pendant group would be sufficiently stable to allow for *in vivo* imaging with fast- clearing biological targeting agents (such as peptides). A similar strategy could be employed for the straightforward preparation of ^{11}C- labelled small molecules which contain a methyl sulfone in their pharmacophore. Regardless of whether or not the utility of arylsulfonyl[^{18}F]fluorides for PET imaging is established, it is hoped that the chemistries outlined here will assist other parties in their efforts exploring this underutilized functionality.

6. Final Remarks

The disparity of projects outlined in this thesis serve to make attempts at broad commentary challenging and somewhat irrelevant. However, it is worth reviewing the most impactful and insightful results gleaned from each of these efforts. With the application of [^{18}F]FPy5yne for the labelling of an antisense oligonucleotide (Chapter 3), the role of this compound as a *general* pre-synthetic ^{18}F labelling agent is confirmed. At the time of its publication[288], the protocol described here represented- to our knowledge- the only reported use of CuAAC technology for the preparation of nucleic acid- based radioprobes. The synthesis of high specific activity, bioactive ^{18}F peptides in a sustained and reproducible way (Chapter 4) allowed for comprehensive pre-clinical PET investigations into the use of neuropeptide receptor overexpression as means to target and diagnose certain cancers. To our knowledge, this is the first example of a 2-[^{18}F]fluoropyridine- modified peptide or protein being used to obtain a successful PET image. Undoubtedly, synthetic details outlined here will assist in the labelling of alternative (and hopefully, superior) targeting vectors. Finally, in a novel effort to transcend some of the longstanding challenges and limitations associated with 'classical' [^{18}F]F$^-$ incorporation chemistry (*e.g.* high temperatures, complex radiosyntheses, and basic, anhydrous conditions), a highly efficient route for the preparation of bifunctional benzenesulfonyl [^{18}F]fluorides was established (Chapter 5). That NDC *preparative* yields of >70 % could be obtained says much about the optimized protocol, which requires no heating or drydown step to ^{18}F- label by way of halogen exchange. Selective degradation of sulfonyl chloride precursor offers an innovative means to obtain high specific activity material, without the need for HPLC purification. Among those strategies seeking to fundamentally advance ^{18}F PET chemistry beyond its reliance on C-F bond-forming reactions, this approach stands out as the only one that does not require a phase transfer additive (*e.g.* $K_{.2.2.2.}$, *n*-Bu_4NHCO_3) to enhance the nucleophilicity of the [^{18}F]F$^-$.

References

[1] G. Hevesy, *Biochem J* **1923**, *17*, 439-445.

[2] O. Chiewitz, G. Hevesy, *Nature* **1935**, *136*, 754-755.

[3] S. Carlsson, *Acta Oncol* **1995**, *34*, 1095-1102.

[4] E. O. Lawrence, D. Cooksey, *Phys Rev* **1936**, *50*, 1131-1140.

[5] E. Fermi, *Am J Phys* **1952**, *20*.

[6] *Science* **1946**, *103*, 697-705.

[7] B. Cassen, L. Curtis, C. W. Reed, *Nucleonics* **1950**, *6*, 78-81.

[8] B. Cassen, L. Curtis, C. Reed, R. Libby, *Nucleonics* **1951**, *9*, 46-50.

[9] D. E. Kuhl, R. H. Chamberlain, J. Hale, R. O. Gorson, *Radiology* **1956**, *66*, 730-739.

[10] W. H. Blahd, *Semin Nucl Med* **1996**, *26*, 165-170.

[11] H. O. Anger, *Nature* **1952**, *170*, 200-201.

[12] H. O. Anger, *Rev Sci Instrum* **1958**, *29*, 27-33.

[13] E. Tapscott, *J Nucl Med Technol* **2005**, *33*, 250-253.

[14] D. E. Kuhl, R. Q. Edwards, *Radiology* **1963**, *80*, 653-662.

[15] R. J. Jaszczak, *Phys Med Biol* **2006**, *51*, R99-115.

[16] R. J. Jaszczak, P. H. Murphy, D. Huard, J. A. Burdine, *J Nucl Med* **1977**, *18*, 373-380.

[17] J. W. Keyes, Jr., N. Orlandea, W. J. Heetderks, P. F. Leonard, W. L. Rogers, *J Nucl Med* **1977**, *18*, 381-387.

[18] T. B. Saleh, in *Basic Sciences of Nuclear Medicine* (Ed.: M. M. Khalil), Springer, Berlin; Heidelberg, **2011**.

[19] J. Környei, K. Ozker, *Technetium-99m: Manufacture of Kits, Vol. 466*, IAEA Publishing Section, Vienna, Austria, **2008**.

[20] R. J. Gibbons, *Heart* **2000**, *83*, 355-360.

[21] J. M. Lo, W. T. Huang, C. H. Kao, C. S. Yang, *Ann Nucl Med Sci* **2001**, *14*, 215-222; S. Zerarka, L. Pellerin, D. Slosman, P. J. Magistretti, *J Cerebr Blood F Met* **2001**, *21*, 456-468; R. D. Neirinckx, J. F. Burke, R. C. Harrison, A. M. Forster, A. R. Andersen, N. A. Lassen, *J Cerebr Blood F Met* **1988**, *8*.

[22] G. B. Saha, *Physics and radiobiology of nuclear medicine*, 3rd ed., Springer, New York, **2006**.

[23] R. T. Overman, H. M. Clark, *Radioisotope techniques*, McGraw-Hill, New York,, **1960**.

[24] W. H. Sweet, *New Engl J Med* **1951**, *245*, 875-878; F. R. Wrenn, M. L. Good, P. Handler, *Science* **1951**, *113*, 525-527.

[25] G. L. Brownell, W. H. Sweet, *Nucleonics* **1953**, *11*, 40-45.

[26] C. J. Thompson, Y. L. Yamamoto, E. Meyer, E. *Proc. SPIE, Application of Optical Instrumentation in Medicine V,* **1976**, *96*, 263–268.

[27] M. M. Khalil, in *Basic Sciences of Nuclear Medicine* (Ed.: M. M. Khalil), Springer, Berlin; Heidelberg, **2011**.

[28] M. E. Daube-Witherspoon, I. G. Zubal, J. S. Karp, *Semin Nucl Med* **2003**, *33*, 28-41.

[29] D. L. Bailey, in *Positron emission tomography: basic sciences* (Ed.: D. L. Bailey), Springer, London; New York, **2005**.

[30] D. L. Bailey, J. S. Karp, S. Surti, in *Positron emission tomography: basic sciences* (Ed.: D. L. Bailey), Springer, London ; New York, **2005**.

[31] G. B. Saha, *Basics of PET Imaging: Physics, Chemistry and Regulations*, Springer, New York, **2005**.

[32] C. Melcher, J. Schweitzer, *IEEE Trans Nucl Sci* **1992**, *39*, 502-505.

[33] J. S. Huber, W. W. Moses, W. F. Jones, C. C. Watson, *Phys Med Biol* **2002**, *47*, 3535-3541.

[34] P. Vaska, A. Bolotnikov, G. Carini, G. Camarda, J. F. Pratte, F. A. Dilmanian, S. J. Park, R. B. James, in *Nuclear Science Symposium/Medical Imaging Conference*, Fajardo, **2005**.

[35] M. I. Lopes, V. Chepel, *Radiat Phys Chem* **2004**, *71*.

[36] C. Nahmias, *Can Assoc Radiol J* **2002**, *53*, 255-257.

[37] T. F. Massoud, S. S. Gambhir, *Gene Dev* **2003**, *17*, 545-580.

[38] M. M. Khalil, J. L. Tremoleda, T. B. Bayomy, W. Gsell, *Int J of Mol I* **2011**, *2011*, 796025.

[39] F. Kiessling, J. Huppert, M. Palmowski, *Curr Med Chem* **2009**, *16*, 627-642.

[40] P. E. Kinahan, D. W. Townsend, T. Beyer, D. Sashin, *Med Phys* **1998**, *25*, 2046-2053.

[41] T. Beyer, D. W. Townsend, T. Brun, P. E. Kinahan, M. Charron, R. Roddy, J. Jerin, J. Young, L. Byars, R. Nutt, *J Nucl Med* **2000**, *41*, 1369-1379.

[42] J. Brink, *American J Roentgenol* **2005**, *184*, S135-S137.

[43] N. R. C. (U.S.), *A glossary of terms in nuclear science and technology*, American Society of Mechanical Engineers, New York, **1957**.

[44] L. S. Cai, S. Y. Lu, V. W. Pike, *Eur J Org Chem* **2008**, 2853-2873.

[45] T. L. Ross, S. M. Ametamey, in *Basic Sciences of Nuclear Medicine* (Ed.: M. M. Khalil), Springer, Berlin; Heidelberg, **2011**.

[46] D. J. Schlyer, in *Handbook of radiopharmaceuticals: radiochemistry and applications* (Eds.: M. J. R. Welch, C. S. Redvanly), Wiley, New York, **2003**.

[47] Brookhaven National Laboratory, *Vol. 2011*, Chart of the Nuclides, http://www.nndc.bnl.gov/chart/.

[48] H. Williams, S. Robinson, P. Julyan, J. Zweit, D. Hastings, *Eur J Nucl Med Mol I* **2005**, *32*, 1473-1480.

[49] M. Lubberink, H. Herzog, *Eur J Nucl Med Mol I* **2011**, *38*, 10-18.

[50] K. Kopka, S. Wagner, in *PET-CT hybrid imaging* (Eds.: O. Schober, W. Heindel), Thieme, Stuttgart; New York, **2010**.

[51] G. B. Saha, Basics of PET Imaging: Physics, Chemistry and Regulations, Springer Science, New York, **2005**.

[52] B. Maziere, C. Loc'h, *Curr Pharm Design* **2001**, *7*, 1931-1943.

[53] L. Koehler, K. Gagnon, S. McQuarrie, F. Wuest, *Molecules* **2010**, *15*, 2686-2718.

[54] M. Kassiou, C. Loc'h, M. Bottlaender, K. Mardon, M. Ottaviani, C. Coulon, A. Katsifis, B. Maziere, *Nucl Med Biol* **2002**, *29*, 295-302.

[55] T. Sihver, K. J. Fasth, A. G. Horti, A. O. Koren, M. Bergstrom, L. Lu, G. Hagberg, H. Lundqvist, R. F. Dannals, E. D. London, A. Nordberg, B. Langstrom, *J Neurochem* **1999**, *73*, 1264-1272.

[56] N. S. Mason, C. A. Mathis, in *Positron emission tomography: basic sciences*, Springer, London; New York, **2005**.

[57] P. McQuade, D. W. McCarthy, M. J. Welch, in *Positron emission tomography: basic sciences* (Ed.: D. L. Bailey), Springer, London; New York, **2005**.

[58] M. Shokeen, C. J. Anderson, *Accounts Chem Res* **2009**, *42*.

[59] N. Di Bartolo, A. Sargeson, T. Donlevy, S. Smith, *J. Chem Soc, Dalton Trans* **2001**, 2303-2309.

[60] M. Ma, J. Karas, J. White, D. Scanlon, P. Donnelly, *Chem Commun* **2009**, 3237-3239.

[61] S. Voss, S. Smith, N. DiBartolo, L. Mclntos, E. Cyr, A. Bonab, J. Dearling, E. Carter, A. Fischman, S. Treves, S. Gillies, A. Sargeson, J. Huston, A. Packard, *P Natl Acad Sci USA* **2007**, *104*, 17489-17493.

[62] M. Fani, J. Andre, H. Maecke, *Contrast Media Mol I* **2008**, *3*, 53-63.

[63] S. Walrand, G. Flux, M. Konijnenberg, R. Valkema, E. Krenning, R. Lhommel, S. Pauwels, F. Jamar, *Eur J Nucl Med Mol I* **2011**, *38*, 57-68.

[64] K. Gould, *J Nucl Med* **1991**, *32*, 579-606.

[65] G. B. Saha, W. J. Macintyre, R. T. Go, *Semin Nucl Med* **1994**, *24*.

[66] T. J. Ruth, in *Handbook of radiopharmaceuticals: radiochemistry and applications* (Eds.: M. J. Welch, C. S. Redvanly), Wiley, New York, **2003**.

[67] M. Haji-Saeid, *Cyclotron produced radionuclides: principles and practice, Vol. 465*, IAEA Publishing Section, Vienna, Austria, **2008**.

[68] E. B. Online*, Vol. 2012*, View of a Classical Cyclotron, http://www.britannica.com/EBchecked/media/59676/Plan-view-of-a-classical-cyclotron-Subatomic-particles-introduced-into.

[69] E. O. Lawrence, M. S. Livingston, *Phys Rev* **1931**, *38*, 834-834.

[70] T. L. Ross, S. M. Ametamey, in *Basic Sciences of Nuclear Medicine* (Ed.: M. M. Khalil), Springer, Berlin; Heidelberg, **2011**.

[71] M. Berridge, S. Apana, J. Hersh, *J Labelled Compd Rad* **2009**, *52*, 543-548.

[72] E. Hess, G. Blessing, H. Coenen, S. Qaim, *Appl Radiat Isotopes* **2000**, *52*, 1431-1440.

[73] S. E. Snyder, M. R. Kilbourn, in *Handbook of radiopharmaceuticals: radiochemistry and applications* (Ed.: M. J. R. Welch, C. S. Redvanly), Wiley, New York, **2003**.

[74] T. Furuya, J. E. Klein, T. Ritter, *Synthesis (Stuttg)* **2010**, *2010*, 1804-1821.

[75] B. K. Park, N. R. Kitteringham, P. M. O'Neill, *Annu Rev Pharmacol* **2001**, *41*, 443-470.

[76] M. J. Adam, J. R. Grierson, T. J. Ruth, S. Jivan, *Appl Radiat Isotopes* **1986**, *37*, 877-882.

[77] M. Constantinou, F. I. Aigbirhio, R. G. Smith, C. A. Ramsden, V. W. Pike, *J Am Chem Soc* **2001**, *123*, 1780-1781.

[78] D. S. Wilbur, *Bioconjugate Chem* **1992**, *3*, 433-470.

[79] W. Dolbier, A. Li, C. Koch, C. Shiue, A. Kachur, *Appl Radiat Isotopes* **2001**, *54*, 73-80.

[80] D.-R. Hwang, S. R. Bergmann, in *Handbook of radiopharmaceuticals: radiochemistry and applications* (Ed.: M. J. R. Welch, C. S. Redvanly), Wiley, New York, **2003**.

[81] L.-H. Shen, M.-H. Liao, Y.-C. Tseng, *J Biomed Biotechnol* **2012**.

[82] S. J. Goldsmith, *Future Oncol* **2009**, *5*, 75-84.

[83] J. G. Cannon, in *Pharmacology for chemists*, 2nd ed., Oxford University Press, New York, **2007**.

[84] S. Vallabhajosula, in *Molecular Imaging: Radiopharmaceuticals for PET and SPECT*, Springer, Berlin; Heidelberg, **2009**.

[85] M. Namavari, A. Bishop, N. Satyamurthy, G. Bida, J. Barrio, *Applied Radiation and Isotopes* **1992**, *43*, 989-996.

[86] J. Bergman, O. Solin, *Nucl Med Biol* **1997**, *24*, 677-683.

[87] J. K. Vahatalo, O. Eskola, J. Bergman, S. Forsback, P. Lehikoinen, J. Jaaskelainen, O. Solin, *J Labelled Compd Rad* **2002**, *45*, 697-704.

[88] S. Forsback, O. Eskola, M. Haaparanta, J. Bergman, O. Solin, *Radiochimica Acta* **2008**, *96*, 845-848.

[89] E. Lee, A. Kamlet, D. Powers, C. Neumann, G. Boursalian, T. Furuya, D. Choi, J. Hooker, T. Ritter, *Science* **2011**, *334*, 639-642.

[90] R. M. Hoyte, S. S. Lin, D. R. Christman, H. L. Atkins, W. Hauser, A. P. Wolf, *J Nucl Med* **1971**, *12*, 280-286; G. Firnau, C. Nahmias, S. Garnett, *J Med Chem* **1973**, *16*, 416-418; M. Argentini, C. Wiese, R. Weinreich, *J Fluorine Chem* **1994**, *68*, 141-144.

[91] M. F. Ghorab, J. M. Winfield, *J Fluorine Chem* **1990**, *49*, 367-383.

[92] J. S. Wilson, M. A. Avila-Rodriguez, R. R. Johnson, A. Zyuzin, S. A. McQuarrie, *Appl Radiat Isotopes* **2008**, *66*, 565-570.

[93] J. E. House, *Inorganic Chemistry*, Academic Press, Burlington; San Diego; London, **2008**.

[94] J. W. Brodack, M. R. Kilbourn, M. J. Welch, J. A. Katzenellenbogen, *Appl Radiat Isotopes* **1986**, *37*, 217-221.

[95] D. O. Kiesewetter, W. C. Eckelman, R. M. Cohen, R. D. Finn, S. M. Larson, *Appl Radiat Isotopes* **1986**, *37*, 1181-1188; K. Hamacher, H. H. Coenen, *Appl Radiat Isotopes* **2002**, *57*, 853-856; M. M. Alauddin, J. Balatoni, J. Gelovani, *J Labelled Compd Rad* **2005**, *48*, 941-950.

[96] T. Irie, K. Fukushi, T. Ido, T. Nozaki, Y. Kasida, *Int J Appl Radiat Isot* **1984**, *35*, 517-520; E. Briard, V. W. Pike, *J Labelled Compd Rad* **2004**, *47*, 217-232; S. Fischer, A. Hiller, M. Scheunemann, W. Deuther-Conrad, A. Hoepping, M. Diekers, F. Wegner, P. Brust, J. Steinbach, *J Labelled Compd Rad* **2008**, *51*, 123-131.

[97] P. Baudot, M. Jacque, M. Robin, *Toxicol Appl Pharmacol* **1977**, *41*, 113-118.

[98] O. A. Mascaretti, *Aldrichimica Acta* **1993**, *26*, 47-58.

[99] D. R. Hwang, C. S. Dence, T. A. Bonasera, M. J. Welch, *Appl Radiat Isotopes* **1989**, *40*, 117-126.

[100] R. Schirrmacher, P. Lucas, E. Schirrmacher, B. Waengler, C. Waengler, *Tetrahedron Lett* **2011**, *52*, 1973-1976.

[101] U. Roehn, J. Becaud, L. J. Mu, A. Srinivasan, T. Stellfeld, A. Fitzner, K. Graham, L. Dinkelborg, A. P. Schubiger, S. M. Ametamey, *J Fluorine Chem* **2009**, *130*, 902-912; S. Farrokhzad, M. Diksic, L. Y. Yamamoto, W. Feindel, *Can J Chem* **1984**, *62*, 2107-2112.

[102] D. W. Kim, D. S. Ahn, Y. H. Oh, S. Lee, H. S. Kil, S. J. Oh, S. J. Lee, J. S. Kim, J. S. Ryu, D. H. Moon, D. Y. Chi, *J Am Chem Soc* **2006**, *128*, 16394-16397.

[103] D. W. Kim, H. J. Jeong, S. T. Litn, M. H. Sohn, J. A. Katzenellenbogen, D. Y. Chi, *J Org Chem* **2008**, *73*, 957-962.

[104] S. Oh, C. Mosdzianowski, D. Chi, J. Kim, S. Kang, J. Ryu, J. Yeo, D. Moon, *Nucl Med Biol* **2004**, *31*, 803-809.

[105] M. S. Haka, M. R. Kilbourn, G. L. Watkins, S. A. Toorongian, *J Labelled Compd Rad* **1989**, *27*, 823-833.

[106] H. R. Sun, S. G. DiMagno, *J Fluorine Chem* **2007**, *128*, 806-812.

[107] H. H. Coenen, in *PET chemistry: the driving force in molecular imaging* (Eds.: A. Schubiger, L. Lehmann, M. Friebe), Springer, Berlin; New York, **2007**.

[108] M. A. Carroll, V. W. Pike, D. A. Widdowson, *Tetrahedron Lett* **2000**, *41*, 5393-5396.

[109] F. M. Beringer, A. Brierley, M. Drexler, E. M. Gindler, C. C. Lumpkin, *J Am Chem Soc* **1953**, *75*, 2708-2712.

[110] A. Shah, V. Pike, D. Widdowson, *J Chem Soc, Perkin Trans 1* **1998**, 2043-2046.

[111] K. M. Lancer, G. H. Wiegand, *J Org Chem* **1976**, *41*, 3360-3364.

[112] V. PIKE, F. AIGBIRHIO, *J Chem Soc Chem Comm* **1995**, 2215-2216.

[113] T. Ross, J. Ermert, C. Hocke, H. Coenen, *J Am Chem Soc* **2007**, *129*, 8018-8025.

[114] S. Martin-Santamaria, M. A. Carroll, C. M. Carroll, C. D. Carter, V. W. Pike, H. S. Rzepa, D. A. Widdowson, *Chem Commun* **2000**, 649-650.

[115] J.-H. Chun, S. Lu, V. W. Pike, *Eur J Org Chem* **2011**, 4439-4447.

[116] E. Kharasch, K. Thummel, *Anesthesiology* **1993**, *79*, 795-807.

[117] P. Mutch, G. Dear, I. Ismail, *J Pharm Pharmacol* **2001**, *53*, 403-408; K. H. Mitchell, C. E. Rogge, T. Gierahn, B. G. Fox, *Proc Natl Acad Sci U.S.A.* **2003**, *100*; A. Harkey, H.-J. Kim, S. Kandagatla, G. M. Raner, *Biotechnol Lett* **2012**, *34*.

[118] J. S. Fowler, T. Ido, in *Handbook of radiopharmaceuticals: radiochemistry and applications* (Eds.: M. J. Welch, C. S. Redvanly), Wiley, New York, **2003**.

[119] D. Le Bars, *J Fluorine Chem* **2006**, *127*, 1488-1493.

[120] H. Hricak, B. I. Choi, A. M. Scott, K. Sugimura, A. Muellner, G. K. von Schulthess, M. F. Reiser, M. M. Graham, N. R. Dunnick, S. M. Larson, *Radiology* **2010**, *257*, 498-506.

[121] R. J. Hicks, *Cancer Imaging* **2004**, *4*, 22-24.

[122] S. J. Kim, S. H. Hwang, I. J. Kim, M. K. Lee, C. H. Lee, S. Y. Lee, E. Y. Lee, *J Exp Clin Cancer Res* **2010**, *29*, 69.

[123] T. Ido, C. Wan, V. Casella, J. Fowler, A. Wolf, M. Reivich, D. Kuhl, *J Labelled Compd Radiopharm* **1978**, *14*, 175-183.

[124] R. Ehrenkaufer, J. Potocki, D. Jewett, *J Nucl Med* **1984**, *25*, 333-337.

[125] C. Shiue, K. To, A. Wolf, *J Labelled Compd Radiopharm* **1983**, *20*, 157-162.

[126] A. R. Braun, R. E. Carson, H. R. Adams, R. D. Finn, B. E. Francis, P. Herscovitch, *Nucl Med Biol* **1994**, *21*, 857-863.

[127] K. Hamacher, H. Coenen, G. Stocklin, *J Nucl Med* **1986**, *27*, 235-238.

[128] G. C. Finger, D. R. F. Dickerson, J. Hamer, L. D. Starr, H. S. Gutowsky, *J Org Chem* **1963**, *28*, 1666-&.

[129] G. Bartoli, P. Todesco, A. Latrofa, F. Naso, *J Chem Soc, Perkin Trans 1* **1972**, 2671.

[130] F. Dolle, in *PET chemistry: the driving force in molecular imaging* (Eds.: A. Schubiger, L. Lehmann, M. Friebe), Springer, Berlin; New York, **2007**.

[131] F. Dolle, *Curr Pharm Design* **2005**, *11*, 3221-3235.

[132] E. J. Knust, C. Mullerplatz, M. Schuller, *J Radioanal Chem* **1982**, *74*, 283-291.

[133] J. Ballinger, B. Bowen, G. Firnau, E. Garnett, F. Teare, *Int J Appl Radiat Isot* **1984**, *35*, 1125-1128.

[134] L. Dolci, F. Dolle, S. Jubeau, F. Vaufrey, C. Crouzel, *J Labelled Compd Rad* **1999**, *42*, 975-985.

[135] M. Karramkam, F. Hinnen, F. Vaufrey, F. Dolle, *J Labelled Compd Rad* **2003**, *46*, 979-992.

[136] H. Beer, M. Haeberli, S. Ametamey, P. Schubiger, *J Labelled Compd Rad* **1995**, *36*, 933-945; A. Abrahim, P. Angelberger, K. Kletter, M. Muller, C. Joukhadar, T. Erker, O. Langer, *J Labelled Compd Rad* **2006**, *49*, 345-356.

[137] M. Carroll, J. Nairne, J. Woodcraft, *J Labelled Compd Rad* **2007**, *50*, 452-454.

[138] G. Roger, B. Lagnel, J. Rouden, L. Besret, H. Valette, S. Demphel, J. Gopisetti, C. Coulon, M. Ottaviani, L. Wrenn, S. Letchworth, G. Bohme, J. Benavides, M. Lasne, M. Bottlaender, F. Dolle, *Bioorgan Med Chem* **2003**, *11*, 5333-5343.

[139] L. Dolci, F. Dolle, H. Valette, F. Vaufrey, C. Fuseau, M. Bottlaender, C. Crouzel, *Bioorgan Med Chem* **1999**, *7*, 467-479; G. Roger, W. Saba, H. Valette, F. Hinnen, C. Coulon, M. Ottaviani, M. Bottlaender, F. Dolle, *Bioorgan Med Chem* **2006**, *14*, 3848-3858; G. Roger, F. Hinnen, H. Valette, W. Saba, M. Bottlaender, F. Dollee, *J Labelled Compd Rad* **2006**, *49*, 489-504.

[140] F. Dolle, L. Dolci, H. Valette, F. Hinnen, F. Vaufrey, I. Guenther, C. Fuseau, C. Coulon, M. Bottlaender, C. Crouzel, *J Med Chem* **1999**, *42*, 2251-2259.

[141] M. Karramkam, F. Hinnen, M. Berrehouma, C. Hlavacek, F. Vaufrey, C. Halldin, J. McCarron, V. Pike, F. Dolle, *Bioorgan Med Chem* **2003**, *11*, 2769-2782.

[142] R. Schirrmacher, U. Muhlhausen, B. Wangler, E. Schirrmacher, J. Reinhard, G. Nagel, B. Kaina, M. Piel, M. Wiessler, F. Rosch, *Tetrahedron Lett* **2002**, *43*, 6301-6304.

[143] I. Greguric, S. Taylor, T. Pham, N. Wyatt, C. Jiang, T. Bourdier, C. Loc'h, P. Roselt, O. Neels, A. Katsifis, *Aust J Chem* **2011**, *64*, 873-879.

[144] A. Nunn, *Cancer Biother Radio* **2007**, *22*, 722-739.

[145] M. R. Zalutsky, J. S. Lewis, in *Handbook of radiopharmaceuticals: radiochemistry and applications* (Eds.: M. J. Welch, C. S. Redvanly), Wiley, New York, **2003**.

[146] S. Vallabhajosula, J. Harwig, W. Wolf, *Int J Nucl Med Biol* **1981**, *8*, 363-370.

[147] A. Duatti, *Curr Drug Targets* **2004**, *5*, 753-760.

[148] H. J. Wester, M. Schottelius, in *PET chemistry: the driving force in molecular imaging* (Eds.: P. A. Schubiger, L. Lehmann, M. Friebe), Springer, Berlin; New York, **2007**.

[149] L. C. Knight, in *Handbook of radiopharmaceuticals: radiochemistry and applications* (Ed.: M. J. R. Welch, C. S. Redvanly), Wiley, New York, **2003**.

[150] J. G. Krupnick, J. L. Benovic, *Annu Rev Pharmacol* **1998**, *38*, 289-319.

[151] D. Josephs, J. Spicer, M. O'Doherty, *Target Oncol* **2009**, *4*, 151-168.

[152] I. Dijkgraaf, O. C. Boerman, W. J. Oyen, F. H. Corstens, M. Gotthardt, *Anticancer Agents Med Chem* **2007**, *7*, 543-551.

[153] R. Ting, C. W. Harwig, J. Lo, Y. Li, M. J. Adam, T. J. Ruth, D. M. Perrin, *J Org Chem* **2008**, *73*, 4662-4670.

[154] T. Maina, M. de Jong, in International Symposium on Technetium and Other Radiometals in Chemistry and Medicine, Bressanone, Italy, **2010**.

[155] M. Schottelius, H. J. Wester, *Methods* **2009**, *48*, 161-177.

[156] L. Gentilucci, R. De Marco, L. Cerisoli, *Curr Pharm Design* **2010**, *16*, 3185-3203.

[157] C. Smith, G. Sieckman, N. Owen, D. Hayes, D. Mazuru, W. Volkert, T. Hoffman, *Anticancer Res* **2003**, *23*, 63-70.

[158] P. Antunes, M. Ginj, M. Walter, J. Chen, J. Reubi, H. Maecke, *Bioconjugate Chem* **2007**, *18*, 84-92.

[159] H. J. Wester, M. Schottelius, T. Poethko, K. Bruus-Jensen, M. Schwaiger, *Cancer Biother Radio* **2004**, *19*, 231-244.

[160] F. Veronese, G. Pasut, *Drug Discov Today* **2005**, *10*, 1451-1458.

[161] H. Zhang, J. Schuhmacher, B. Waser, D. Wild, M. Eisenhut, J. Reubi, H. Maecke, *Eur J Nucl Med Mol I* **2007**, *34*, 1198-1208.

[162] Z. H. Wu, Z. B. Li, W. B. Cai, L. He, F. T. Chin, F. Li, X. Y. Chen, *Eur J Nucl Med Mol I* **2007**, *34*, 1823-1831.

[163] C. K. Younes, R. Boisgard, B. Tavitian, *Curr Pharm Design* **2002**, *8*, 1451-1466.

[164] S. D. Patil, D. G. Rhodes, D. J. Burgess, *Aaps J* **2005**, *7*, E61-77.

[165] http://www.isispharm.com/Pipeline/Therapeutic-Areas/Other.htm#Vitravene.

[166] S. S. Gambhir, J. R. Barrio, H. R. Herschman, M. E. Phelps, *J Nucl Cardiol* **1999**, *6*, 219-233.

[167] S. Crooke, Biochim Biophys Acta, Gene Struct Expression **1999**, 1489, 31-44.

[168] S. M. Freier, C. F. Bennett, P. D. Cook, S. T. Crooke, L. L. Cummins, N. M. Dean, D. J. Ecker, R. H. Griffey, C. J. Guinosso, D. Kornbrust, J. Leeds, E. A. Lesnik, B. P. Monia, Y. S. Sanghvi, J. E. Zuckerman, *J Cell Biochem* **1995**, 205-205.

[169] J. Kurreck, E. Wyszko, C. Gillen, V. Erdmann, *Nucleic Acids Res* **2002**, *30*, 1911-1918.

[170] R. M. Crooke, M. J. Graham, M. J. Martin, K. M. Lemonidis, T. Wyrzykiewiecz, L. L. Cummins, *J Pharmacol Exp Ther* **2000**, *292*, 140-149.

[171] P. S. Eder, R. J. DeVine, J. M. Dagle, J. A. Walder, *Antisense Res Dev* **1991**, *1*, 141-151.

[172] R. S. Geary, R. Z. Yu, A. A. Levin, *Curr Opin Invest Dr* **2001**, *2*, 562-573.

[173] A. S. Dutta, in *The textbook of pharmaceutical medicine*, 6th ed. (Ed.: J. P. Griffin), Wiley-Blackwell, Chichester; Hoboken, **2009**.

[174] S. T. Crooke, *Method Enzymol* **2000**, *313*, 3-45.

[175] B. P. Monia, E. A. Lesnik, C. Gonzalez, W. F. Lima, D. Mcgee, C. J. Guinosso, A. M. Kawasaki, P. D. Cook, S. M. Freier, *J Biol Chem* **1993**, *268*, 14514-14522.

[176] E. R. Kandimalla, A. Manning, Q. Y. Zhao, D. R. Shaw, R. A. Byrn, V. Sasisekharan, S. Agrawal, *Nucleic Acids Res* **1997**, *25*, 370-378.

[177] R. L. Beane, R. Ram, S. Gabillet, K. Arar, B. P. Monia, D. R. Corey, *Biochemistry* **2007**, *46*, 7572-7580.

[178] R. M. Hudziak, E. Barofsky, D. F. Barofsky, D. L. Weller, S. B. Huang, D. D. Weller, *Antisense Nucleic A* **1996**, *6*, 267-272.

[179] J. Summerton, D. Weller, *Antisense Nucleic A* **1997**, *7*, 187-195.

[180] J. Summerton, D. Weller, *Nucleos Nucleot* **1997**, *16*, 889-898.

[181] S. Karkare, D. Bhatnagar, *Appl Microbiol Biotechnol* **2006**, *71*, 575-586.

[182] J. Heasman, *Dev Biol* **2002**, *243*, 209-214.

[183] P. E. Nielsen, *Method Enzymol* **2000**, *313*, 156-164.

[184] J. Kurreck, *Eur J Biochem* **2003**, *270*, 1628-1644.

[185] R. Robinson, *Plos Biol* **2004**, *2*, 18-20.

[186] V. Wacheck, U. Zangemeister-Wittke, *Crit Rev Oncol Hemat* **2006**, *59*, 65-73.

[187] B. Tavitian, *Gut* **2003**, *52*, 40-47.

[188] D. Eulberg, S. Klussmann, *Chembiochem* **2003**, *4*, 979-983.

[189] R. L. Juliano, X. Ming, O. Nakagawa, *Bioconjugate Chem* **2012**, *23*, 147-157.

[190] B. Yu, X. Zhao, L. J. Lee, R. J. Lee, *Aaps Journal* **2009**, *11*, 195-203.

[191] C. Wolfrum, S. Shi, K. Jayaprakash, M. Jayaraman, G. Wang, R. Pandey, K. Rajeev, T. Nakayama, K. Charrise, E. Ndungo, T. Zimmermann, V. Koteliansky, M. Manoharan, M. Stoffel, *Nat Biotechnol* **2007**, *25*, 1149-1157.

[192] S. Li, H. M. Deshmukh, L. Huang, *Pharm Res* **1998**, *15*, 1540-1545.

[193] W. Zhou, X. Yuan, A. Wilson, L. J. Yang, M. Mokotoff, B. Pitt, S. Li, *Bioconjugate Chem* **2002**, *13*, 1220-1225.

[194] Z. M. Qian, H. Y. Li, H. Z. Sun, K. Ho, *Pharmacol Rev* **2002**, *54*, 561-587.

[195] J. O. McNamara, E. R. Andrechek, Y. Wang, K. D Viles, R. E. Rempel, E. Gilboa, B. A. Sullenger, P. H. Giangrande, *Nat Biotechnol* **2006**, *24*, 1005-1015.

[196] J. P. Dassie, X.-y. Liu, G. S. Thomas, R. M. Whitaker, K. W. Thiel, K. R. Stockdale, D. K. Meyerholz, A. P. McCaffrey, J. O. McNamara, II, P. H. Giangrande, *Nat Biotechnol* **2009**, *27*, 839-U895.

[197] J. Gump, R. June, S. Dowdy, *J Biol Chem* **2010**, *285*, 1500-1507.

[198] H. Margus, K. Padari, M. Pooga, *Mol Ther* **2012**, *20*, 525-533.

[199] P. Lundberg, S. El-Andaloussi, T. Sutlu, H. Johansson, U. Langel, *Faseb J* **2007**, *21*, 2664-2671.

[200] S. H. Kang, M. J. Cho, R. Kole, *Biochemistry* **1998**, *37*, 6235-6239.

[201] P. Lundin, H. Johansson, P. Guterstam, T. Holm, M. Hansen, U. Langel, S. E. L. Andaloussi, *Bioconjugate Chem* **2008**, *19*, 2535-2542.

[202] M. W. Reed, D. Fraga, D. E. Schwartz, J. Scholler, R. D. Hinrichsen, *Bioconjugate Chem* **1995**, *6*, 101-108.

[203] S. Ghosh, P. Kao, A. Mccue, H. Chappelle, *Bioconjugate Chem* **1990**, *1*, 71-76.

[204] D. Forget, D. Boturyn, E. Defrancq, J. Lhomme, P. Dumy, *Chem-Eur J* **2001**, *7*, 3976-3984.

[205] D. Forget, O. Renaudet, D. Boturyn, E. Defrancq, P. Dumy, *Tetrahedron Lett* **2001**, *42*, 9171-9174; D. Forget, D. Boturyn, O. Renaudet, E. Defrancq, P. Dumy, *Nucleos Nucleot Nucl* **2003**, *22*, 1427-1429; Y. Singh, E. Defrancq, P. Dumy, *J Org Chem* **2004**, *69*, 8544-8546; N. Spinelli, O. P. Edupuganti, E. Defrancq, P. Dumy, *Org Lett* **2007**, *9*, 219-222.

[206] O. P. Edupuganti, O. Renaudet, E. Defrancq, P. Dumy, *Bioorg Med Chem Lett* **2004**, *14*, 2839-2842.

[207] R. Juliano, T. Tuschl, J. Rossi, *Ann NY Acad Sci* **2006**, *1082*, 18-26.

[208] M. R. Alam, V. Dixit, H. Kang, Z.-B. Li, X. Chen, J. Trejo, M. Fisher, R. L. Juliano, *Nucleic Acids Res* **2008**, *36*, 2764-2776.

[209] X. Ming, M. R. Alam, M. Fisher, Y. Yan, X. Chen, R. L. Juliano, *Nucleic Acids Res* **2010**, *38*, 6567-6576.

[210] F. Wuest, *Amino Acids* **2005**, *29*, 323-339.

[211] L. Lang, W. C. Eckelman, *Appl Radiat Isot* **1994**, *45*, 1155-1163.

[212] X. Z. Zhang, W. B. Cai, F. Cao, E. Schreibmann, Y. Wu, J. C. Wu, L. Xing, X. Y. Chen, *J Nucl Med* **2006**, *47*, 492-501.

[213] X. Y. Chen, R. Park, Y. P. Hou, V. Khankaldyyan, I. Gonzales-Gomez, M. Tohme, J. R. Bading, W. E. Laug, P. S. Conti, *Eur J Nucl Med Mol I* **2004**, *31*, 1081-1089; X. Y. Chen, R. Park, A. H. Shahinian, M. Tohme, V. Khankaldyyan, M. H. Bozorgzadeh, J. R. Bading, R. Moats, W. E. Laug, P. S. Conti, *Nucl Med Biol* **2004**, *31*, 179-189; X. Zhang, Z. Xiong, Y. Wu, W. Cai, J. Tseng, S. Gambhir, X. Chen, *J Nucl Med* **2006**, *47*, 113-121.

[214] Z. Cheng, L. Zhang, E. Graves, Z. M. Xiong, M. Dandekar, X. Y. Chen, S. S. Gambhir, *J Nucl Med* **2007**, *48*, 987-994.

[215] J. Toretsky, A. Levenson, I. N. Weinberg, J. F. Tait, A. Uren, R. C. Mease, *Nucl Med Biol* **2004**, *31*, 747-752.

[216] J. L. Li, J. O. Trent, P. J. Bates, C. K. Ng, *J Labelled Compd Rad* **2007**, *50*, 1255-1259; J. L. Li, J. O. Trent, P. J. Bates, C. K. Ng, *J Labelled Compd Rad* **2006**, *49*, 1213-1221.

[217] E. Hedberg, B. Langstrom, *Acta Chem Scand* **1998**, *52*, 1034-1039.

[218] L. Lang, W. C. Eckelman, *Appl Radiat Isot* **1997**, *48*, 169-173.

[219] G. Tang, W. B. Zeng, M. X. Yu, G. Kabalka, *J Labelled Compd Rad* **2008**, *51*, 68-71.

[220] C. Y. Shiue, A. P. Wolf, J. F. Hainfeld, *Journal of Labelled Compounds and Radiopharmaceuticals* **1989**, *26*, 287-289.

[221] T. Toyokuni, J. C. Walsh, A. Dominguez, M. E. Phelps, J. R. Barrio, S. S. Gambhir, N. Satyamurthy, *Bioconjugate Chem* **2003**, *14*, 1253-1259.

[222] M. Berndt, J. Pietzsch, F. Wuest, *Nucl Med Biol* **2007**, *34*, 5-15.

[223] C. Hultsch, M. Berndt, R. Bergmann, F. Wuest, *Appl Radiat Isotopes* **2007**, *65*, 818-826.

[224] F. Wuest, L. Koehler, M. Berndt, J. Pietzsch, *Amino Acids* **2009**, *36*, 283-295.

[225] B. de Bruin, B. Kuhnast, F. Hinnen, L. Yaouancq, M. Amessou, L. Johannes, A. Samson, R. Boisgard, B. Tavitian, F. Dolle, *Bioconjugate Chem* **2005**, *16*, 406-420.

[226] W. B. Cai, X. Z. Zhang, Y. Wu, X. Chen, *J Nucl Med* **2006**, *47*, 1172-1180.

[227] B. Kuhnast, F. Dolle, S. Terrazzino, B. Rousseau, C. Loc'h, F. Vaufrey, F. Hinnen, I. Doignon, F. Pillon, C. David, C. Crouzel, B. Tavitian, *Bioconjugate Chem* **2000**, *11*, 627-636.

[228] F. Dolle, F. Hinnen, F. Vaufrey, B. Tavitian, C. Crouzel, *J Labelled Compd Rad* **1997**, *39*, 319-330.

[229] I. Koslowsky, S. Shahhosseini, J. Wilson, J. Mercer, *J Labelled Compd Rad* **2008**, *51*, 352-356.

[230] R. Boisgard, B. Kuhnast, S. Vonhoff, C. Younes, F. Hinnen, J. M. Verbavatz, B. Rousseau, J. Furste, B. Wlotzka, F. Dolle, S. Klussmann, B. Tavitian, *Eur J Nucl Med Mol I* **2005**, *32*, 470-477.

[231] B. Kuhnast, S. Klussmann, F. Hinnen, R. Boisgard, B. Rousseau, J. P. Furste, B. Tavitian, F. Dolle, *J Labelled Compd Rad* **2003**, *46*, 1205-1219.

[232] B. Kuhnast, F. Dolle, B. Tavitian, *J Labelled Compd Rad* **2002**, *45*, 1-11.

[233] B. Kuhnast, F. Hinnen, R. Boisgard, B. Tavitian, F. Dolle, *J Labelled Compd Rad* **2003**, *46*, 1093-1103.

[234] H. C. Kolb, M. G. Finn, K. B. Sharpless, *Angew Chem Int Edit* **2001**, *40*, 2004-+.

[235] H. C. Kolb, K. B. Sharpless, *Drug Discov Today* **2003**, *8*, 1128-1137.

[236] N. Ishibashi, T. Kuwamura, H. Sano, F. Yamamoto, T. Haradahira, K. Suzuki, T. Suhara, S. Sasaki, M. Maeda, *J Labelled Compd Rad* **2000**, *43*, 375-383.

[237] K. Bruus-Jensen, T. Poethko, M. Schottelius, A. Hauser, M. Schwaiger, H. J. Wester, *Nucl Med Biol* **2006**, *33*, 173-183; Y. S. Lee, J. M. Jeong, H. W. Kim, Y. S. Chang, Y. J. Kim, M. K. Hong, G. B. Rai, D. Y. Chi, W. J. Kang, J. H. Kang, D. S. Lee, J. K. Chung, M. C. Lee, Y. G. Suh, *Nucl Med Biol* **2006**, *33*, 677-683; A. Dirksen, P. E. Dawson, *Bioconjug Chem* **2008**, *19*, 2543-2548.

[238] M. Pretze, F. Wuest, T. Peppel, M. Kockerling, C. Mamat, *Tetrahedron Lett* **2010**, *51*, 6410-6414; A. Gaeta, J. Woodcraft, S. Plant, J. Goggi, P. Jones, M. Battle, W. Trigg, S. K. Luthra, M. Glaser, *Bioorg Med Chem Lett* **2010**, *20*, 4649-4652.

[239] D. J. Vugts, A. Vervoort, M. Stigter-van Walsum, G. W. M. Visser, M. S. Robillard, R. M. Versteegen, R. C. M. Vulders, J. D. M. Herscheid, G. A. M. S. van Dongen, *Bioconjugate Chem* **2011**, *22*, 2072-2081.

[240] W. P. Jencks, in *Progress in physical organic chemistry* (Eds.: S. G. Cohen, A. Streitwieser, R. W. Taft), Wiley, New York, **1963**.

[241] J. Shao, J. P. Tam, *J Am Chem Soc* **1995**, *117*, 3893-3899.

[242] T. S. Zatsepin, D. A. Stetsenko, M. J. Gait, T. S. Oretskaya, *Bioconjugate Chem* **2005**, *16*, 471-489.

[243] T. Poethko, M. Schottelius, G. Thumshirn, M. Herz, R. Haubner, G. Henriksen, H. Kessler, M. Schwaiger, H. J. Wester, *Radiochimica Acta* **2004**, *92*, 317-327.

[244] M. Schottelius, T. Poethko, M. Herz, J. C. Reubi, H. Kessler, M. Schwaiger, H. J. Wester, *Clin Cancer Res* **2004**, *10*, 3593-3606.

[245] M. Glaser, M. Morrison, M. Solbakken, J. Arukwe, H. Karlsen, U. Wiggen, S. Champion, G. M. Kindberg, A. Cuthbertson, *Bioconjugate Chem* **2008**, *19*, 951-957.

[246] M. Namavari, Z. Cheng, R. Zhang, A. De, J. Levi, J. K. Hoerner, S. S. Yaghoubi, F. A. Syud, S. S. Gambhir, *Bioconjugate Chem* **2009**, *20*, 432-436.

[247] R. Huisgen, in *1,3-Dipolarcycloaddition Chemistry, Vol. 1* (Ed.: A. Padwa), Wiley, **1984**.

[248] V. V. Rostovtsev, L. G. Green, V. V. Fokin, K. B. Sharpless, *Angew Chem Int Edit* **2002**, *41*, 2596.

[249] C. W. Tornoe, C. Christensen, M. Meldal, *J Org Chem* **2002**, *67*, 3057-3064.

[250] A. D. Moorhouse, J. E. Moses, *Chemmedchem* **2008**, *3*, 715-723.

[251] P. Appukkuttan, W. Dehaen, V. V. Fokin, E. Van der Eycken, *Org Lett* **2004**, *6*, 4223-4225.

[252] X. Li, *Chem Asian J* **2011**, *6*, 2606-2616.

[253] A. J. Dirks, J. J. L. M. Cornelissen, F. L. van Delft, J. C. M. van Hest, R. J. M. Nolte, A. E. Rowan, F. P. J. T. Rutjes, *QSAR Comb Sci* **2007**, *26*, 1200-1210.

[254] F. Amblard, J. H. Cho, R. F. Schinazi, *Chem Rev* **2009**, *109*, 4207-4220; P. M. E. Gramlich, C. T. Wirges, A. Manetto, T. Carell, *Angew Chem Int Edit* **2008**, *47*, 8350-8358.

[255] S. Sen Gupta, J. Kuzelka, P. Singh, W. G. Lewis, M. Manchester, M. G. Finn, *Bioconjugate Chem* **2005**, *16*, 1572-1579; Q. Wang, T. R. Chan, R. Hilgraf, V. V. Fokin, K. B. Sharpless, M. G. Finn, *J Am Chem Soc* **2003**, *125*, 3192-3193.

[256] A. J. Link, D. A. Tirrell, *J Am Chem Soc* **2003**, *125*, 11164-11165; K. E. Beatty, F. Xie, Q. Wang, D. A. Tirrell, *J Am Chem Soc* **2005**, *127*, 14150-14151.

[257] A. J. Link, M. K. S. Vink, D. A. Tirrell, *J Am Chem Soc* **2004**, *126*, 10598-10602.

[258] J. M. Baskin, J. A. Prescher, S. T. Laughlin, N. J. Agard, P. V. Chang, I. A. Miller, A. Lo, J. A. Codelli, C. R. Bertozzi, *P Natl Acad Sci USA* **2007**, *104*, 16793-16797.

[259] J. P. Alexander, B. F. Cravatt, *Chem Biol* **2005**, *12*, 1179-1187.

[260] A. V. Ustinov, V. A. Korshun, *Russ Chem Bull* **2006**, *55*, 1268-1274.

[261] C. J. Burrows, J. G. Muller, *Chem Rev* **1998**, *98*, 1109-1151.

[262] W. L. Baker, J. Goode, L. Cooper, *Mikrochim Acta* **1992**, *106*, 143-152.

[263] R. H. Nagaraj, V. M. Monnier, *Biochim Biophys Acta, Protein Struct* **1995**, *1253*, 75-84.

[264] N. Shangari, T. S. Chan, K. Chan, S. H. Wu, P. J. O'Brien, *Mol Nutr Food Res* **2007**, *51*, 445-455.

[265] N. J. Agard, J. A. Prescher, C. R. Bertozzi, *J Am Chem Soc* **2004**, *126*, 15046-15047; P. V. Chang, J. A. Prescher, E. M. Sletten, J. M. Baskin, I. A. Miller, N. J. Agard, A. Lo, C. R. Bertozzi, *P Natl Acad Sci USA* **2010**, *107*, 1821-1826.

[266] T. R. Chan, R. Hilgraf, K. B. Sharpless, V. V. Fokin, *Org Lett* **2004**, *6*, 2853-2855.

[267] V. O. Rodionov, V. V. Fokin, M. G. Finn, *Angew Chem Int Edit* **2005**, *44*, 2210-2215.

[268] A. E. Speers, G. C. Adam, B. F. Cravatt, *J Am Chem Soc* **2003**, *125*, 4686-4687.

[269] N. K. Devaraj, G. P. Miller, W. Ebina, B. Kakaradov, J. P. Collman, E. T. Kool, C. E. D. Chidsey, *J Am Chem Soc* **2005**, *127*, 8600-8601.

[270] V. Hong, A. K. Udit, R. A. Evans, M. G. Finn, *Chembiochem* **2008**, *9*, 1481-1486.

[271] V. Hong, S. I. Presolski, C. Ma, M. G. Finn, *Angew Chem Int Edit* **2009**, *48*, 9879-9883.

[272] J. Marik, J. L. Sutcliffe, *Tetrahedron Lett* **2006**, *47*, 6681-6684.

[273] M. Glaser, E. Arstad, *Bioconjugate Chem* **2007**, *18*, 989-993.

[274] L. Iddon, J. Leyton, B. Indrevoll, M. Glaser, E. G. Robins, A. J. George, A. Cuthbertson, S. K. Luthra, E. O. Aboagye, *Bioorg Med Chem Lett* **2011**, *21*, 3122-3127.

[275] J. Leyton, L. Iddon, M. Perumal, B. Indrevoll, M. Glaser, E. Robins, A. J. George, A. Cuthbertson, S. K. Luthra, E. O. Aboagye, *J Nucl Med* **2011**, *52*, 1441-1448.

[276] Z. B. Li, Z. Wu, K. Chen, F. T. Chin, X. Chen, *Bioconjugate Chem* **2007**, *18*, 1987-1994.

[277] H. S. Gill, J. Marik, *Nat Protoc* **2011**, *6*, 1718-1725.

[278] T. Ramenda, R. Bergmann, F. Wuest, *Lett Drug Des Discovery* **2007**, *4*, 279-285.

[279] D. Thonon, C. Kech, J. Paris, C. Lemaire, A. Luxen, *Bioconjugate Chem* **2009**, *20*, 817-823.

[280] L. S. Campbell-Verduyn, L. Mirfeizi, A. K. Schoonen, R. A. Dierckx, P. H. Elsinga, B. L. Feringa, *Angew Chem Int Edit* **2011**, *50*, 11117-11120.

[281] R. L. Weller, S. R. Rajski, *Org Lett* **2005**, *7*, 2141-2144.

[282] A. H. El-Sagheer, *Nucleos Nucleot Nucl* **2009**, *28*, 315-323.

[283] J. Gierlich, G. A. Burley, P. M. E. Gramlich, D. M. Hammond, T. Carell, *Org Lett* **2006**, *8*, 3639-3642.

[284] T. S. Seo, Z. M. Li, H. Ruparel, J. Y. Ju, *J Org Chem* **2003**, *68*, 609-612.

[285] C. Bouillon, A. Meyer, S. Vidal, A. Jochum, Y. Chevolot, J. P. Cloarec, J. P. Praly, J. J. Vasseur, F. Morvan, *J Org Chem* **2006**, *71*, 4700-4702.

[286] D. H. Kim, Y. S. Choe, K. H. Jung, K. H. Lee, J. Y. Choi, Y. Choi, B. T. Kim, *Arch Pharm Res* **2008**, *31*, 587-593.

[287] U. Sirion, H. J. Kim, J. H. Lee, J. W. Seo, B. S. Lee, S. J. Lee, S. J. Oh, D. Y. Chi, *Tetrahedron Lett* **2007**, *48*, 3953-3957.

[288] J. A. H. Inkster, M. J. Adam, T. Storr, T. J. Ruth, *Nucleos Nucleot Nucl* **2009**, *28*, 1131-1143.

[289] T. Shiraishi, Y. Kitamura, Y. Ueno, Y. Kitade, *Chem Commun* **2011**, *47*, 2691-2693.

[290] F. Mercier, J. Paris, G. Kaisin, D. Thonon, J. Flagothier, N. Teller, C. Lemaire, A. Luxen, *Bioconjugate Chem* **2011**, *22*, 108-114.

[291] T. Kuboyama, M. Nakahara, M. Yoshino, Y. Cui, T. Sako, Y. Wada, T. Imanishi, S. Obika, Y. Watanabe, M. Suzuki, H. Doi, *Bioorgan Med Chem* **2011**, *19*, 249-255.

[292] J. K. Amartey, I. Al-Jammaz, B. Al-Otaibi, C. Esguerra, *Nucl Med Biol* **2002**, *29*, 817-823; I. Al Jammaz, B. Al-Otaibi, S. Okarvi, J. Amartey, *J Labelled Compd Rad* **2006**, *49*, 125-137.

[293] B. Kuhnast, A. de Bruin, F. Hinnen, B. Tavitian, F. Dolle, *Bioconjugate Chem* **2004**, *15*, 617-627.

[294] T. Viel, B. Kuhnast, F. Hinnen, R. Boisgard, B. Tavitian, F. Dolle, *J Labelled Compd Rad* **2007**, *50*, 1159-1168.

[295] T. Viel, R. Boisgard, B. Kuhnast, B. Jego, K. Siquier-Pernet, F. Hinnen, F. Dolle, B. Tavitian, *Oligonucleotides* **2008**, *18*, 201-212.

[296] B. Kuhnast, F. Hinnen, R. Hamzavi, R. Boisgard, B. Tavitian, P. E. Nielsen, F. Dolle, *J Labelled Compd Rad* **2005**, *48*, 51-61.

[297] E. von Guggenberg, J. A. Sader, J. S. Wilson, S. Shahhosseini, I. Koslowsky, F. Wuest, J. R. Mercer, *Appl Radiat Isotopes* **2009**, *67*, 1670-1675.

[298] C. L. Denholt, B. Kuhnast, F. Dolle, F. Hinnen, P. R. Hansen, N. Gillings, A. Kjaer, *J Labelled Compd Rad* **2010**, *53*, 774-778.

[299] B. Kuhnast, F. Hinnen, B. Tavitian, F. Dolle, *J Labelled Compd Rad* **2008**, *51*, 336-342.

[300] A. C. Valdivia, M. Estrada, T. Hadizad, D. J. Stewart, R. S. Beanlands, J. N. DaSilva, *J Labelled Compd Rad* **2012**, *55*, 57-60.

[301] T. J. Ruth, A. P. Wolf, *Radiochim. Acta* **1979,** *26*, 21.

[302] G. E. Smith, H. L. Sladen, S. C. G. Biagini, P. J. Blower, *Dalton Trans* **2011**, *40*, 6196-6205.

[303] R. Ting, M. J. Adam, T. J. Ruth, D. M. Perrin, *J Am Chem Soc* **2005**, *127*, 13094-13095.

[304] R. Ting, J. Lo, M. J. Adam, T. J. Ruth, D. M. Perrin, *J Fluorine Chem* **2008**, *129*, 349-358.

[305] R. Ting, C. Harwig, U. auf dem Keller, S. McCormick, P. Austin, C. M. Overall, M. J. Aclam, T. J. Ruth, D. M. Perrin, *J Am Chem Soc* **2008**, *130*, 12045-12055.

[306] R. Ting, T. A. Aguilera, J. L. Crisp, D. J. Hall, W. C. Eckelman, D. R. Vera, R. Y. Tsien, *Bioconjugate Chem* **2010**, *21*, 1811-1819.

[307] U. A. D. Keller, C. L. Bellac, Y. Li, Y. M. Lou, P. F. Lange, R. Ting, C. Harwig, R. Kappelhoff, S. Dedhar, M. J. Adam, T. J. Ruth, F. Benard, D. M. Perrin, C. M. Overall, *Cancer Res* **2010**, *70*, 7562-7569; Y. Li, R. Ting, C. Harwig, U. Keller, C. Bellac, P. Lange, J. Inkster, P. Schaffer, M. Adam, T. Ruth, C. Overall, D. Perrin, *Medchemcomm* **2011**, *2*, 942-949.

[308] Y.-R. Luo, Comprehensive Handbook of Chemical Bond Energies, CRC Press, Boca Raton, **2007**.

[309] W. J. McBride, R. M. Sharkey, H. Karacay, C. A. D'Souza, E. A. Rossi, P. Laverman, C. H. Chang, O. C. Boerman, D. M. Goldenberg, *J Nucl Med* **2009**, *50*, 991-998.

[310] P. Laverman, W. J. McBride, R. M. Sharkey, A. Eek, L. Joosten, W. J. G. Oyen, D. M. Goldenberg, O. C. Boerman, *J Nucl Med* **2010**, *51*, 454-461.

[311] W. J. McBride, C. A. D'Souza, R. M. Sharkey, H. Karacay, E. A. Rossi, C. H. Chang, D. M. Goldenberg, *Bioconjugate Chem* **2010**, *21*, 1331-1340.

[312] M. S. Rosenthal, A. L. Bosch, R. J. Nickles, S. J. Gatley, *Int J Appl Radiat Isot* **1985**, *36*, 318-319.

[313] R. Schirrmacher, G. Bradtmoller, E. Schirrmacher, O. Thews, J. Tillmanns, T. Siessmeier, H. G. Buchholz, P. Bartenstein, B. Waengler, C. M. Niemeyer, K. Jurkschat, *Angew Chem Int Edit* **2006**, *45*, 6047-6050.

[314] E. Schirrmacher, B. Wangler, M. Cypryk, G. Bradtmoller, M. Schafer, M. Eisenhut, K. Jurkschat, R. Schirrmacher, *Bioconjugate Chem* **2007**, *18*, 2085-2089.

[315] L. Iovkova, B. Waengler, E. Schirrmacher, R. Schirrmacher, G. Quandt, G. Boening, M. Schuermann, K. Jurkschat, *Chem-Eur J* **2009**, *15*, 2140-2147.

[316] B. Waengler, G. Quandt, L. Iovkova, E. Schirrmacher, C. Waengler, G. Boening, M. Hacker, M. Schmoeckel, K. Jurkschat, P. Bartenstein, R. Schirrmacher, *Bioconjugate Chem* **2009**, *20*, 317-321.

[317] L. J. Mu, A. Hohne, R. A. Schubiger, S. M. Ametamey, K. Graham, J. E. Cyr, L. Dinkelborg, T. Stellfeld, A. Srinivasan, U. Voigtmann, U. Klar, *Angew Chem Int Edit* **2008**, *47*, 4922-4925.

[318] A. Hohne, L. Yu, L. J. Mu, M. Reiher, U. Voigtmann, U. Klar, K. Graham, P. A. Schubiger, S. M. Ametamey, *Chem-Eur J* **2009**, *15*, 3736-3743.

[319] A. Hoehne, L. Mu, M. Honer, P. A. Schubiger, S. M. Ametamey, K. Graham, T. Stellfeld, S. Borkowski, D. Berndorff, U. Klar, U. Voigtmann, J. E. Cyr, M. Friebe, L. Dinkelborg, A. Srinivasan, *Bioconjugate Chem* **2008**, *19*, 1871-1879.

[320] D. James, J. M. Escudier, E. Amigues, J. Schulz, C. Vitry, T. Bordenave, M. Szlosek-Pinaud, E. Fouquet, *Tetrahedron Lett* **2010**, *51*, 1230-1232.

[321] J. Schulz, D. Vimont, T. Bordenave, D. James, J. M. Escudier, M. Allard, M. Szlosek-Pinaud, E. Fouquet, *Chem-Eur J* **2011**, *17*, 3096-3100.

[322] J. L. Kice, E. A. Lunney, *J Org Chem* **1975**, *40*, 2125-2127.

[323] I. Lee, C. S. Shim, S. Y. Chung, H. Y. Kim, H. W. Lee, *J Chem Soc, Perkin Trans 2* **1988**, 1919-1923.

[324] O. M. Kamoshenkova, V. N. Boiko, *J Fluorine Chem* **2010**, *131*, 248-253.

[325] C. G. Swain, C. B. Scott, *J Am Chem Soc* **1953**, *75*, 246-248.

[326] M. E. Aberlin, C. A. Bunton, *J Org Chem* **1970**, *35*, 1825-+.

[327] B. C. Lee, D. S. Sohn, J. H. Yoon, S. M. Yang, I. Lee, *B Kor Chem Soc* **1993**, *14*, 621-625.

[328] B. R. Baker, *Accounts Chem Res* **1969**, *2*, 129-&.

[329] W. Davies, J. H. Dick, *J Am Chem Soc* **1931**, 2104-2109.

[330] T. A. Bianchi, L. A. Cate, *J Org Chem* **1977**, *42*, 2031-2032.

[331] C. L. Borders, J. L. Chambers, D. I. Macdonel, *J Org Chem* **1972**, *37*, 3549-&.

[332] D. O. Jang, J. G. Kim, *Synlett* **2010**, 3049-3052.

[333] D. W. Kim, H. J. Jeong, S. T. Lim, M. H. Sohn, *Angew Chem Int Edit* **2008**, *47*, 8404-8406.

[334] M. Tanaka, J. Iyoda, Y. Souma, *J Org Chem* **1992**, *57*, 2677-2680.

[335] Y. L. Yagupolskii, T. I. Savina, *Zh Org Khim+* **1983**, *19*, 79-82.

[336] A. J. Brouwer, T. Ceylan, T. van der Linden, R. M. J. Liskamp, *Tetrahedron Lett* **2009**, *50*, 3391-3393.

[337] M. Kirihara, S. Naito, Y. Ishizuka, H. Hanai, T. Noguchi, *Tetrahedron Lett* **2011**, *52*, 3086-3089.

[338] E. Di Cera, *Iubmb Life* **2009**, *61*, 510-515.

[339] M. Rao, A. Tanksale, M. Ghatge, V. Deshpande, *Microbiol Mol Biol R* **1998**, *62*, 597.

[340] D. E. Fahrney, A. M. Gold, *J Am Chem Soc* **1963**, *85*, 997-&.

[341] A. M. Gold, D. Fahrney, *Biochemistry* **1964**, *3*, 783-791.

[342] A. M. Gold, *Biochemistry* **1965**, *4*, 897-&.

[343] M. O. Lively, J. C. Powers, *Biochim Biophys Acta* **1978**, *525*, 171-179.

[344] T. Yoshimura, L. N. Barker, J. C. Powers, *J Biol Chem* **1982**, *257*, 5077-5084.

[345] R. Laura, D. J. Robison, D. H. Bing, *Biochemistry* **1980**, *19*, 4859-4864.

[346] T. J. Ruth, A. P. Wolf, *Radiochimica Acta* **1979**, *26*, 21-24.

[347] G. Lendvai, S. Estrada, M. Bergstrom, *Curr Med Chem* **2009**, *16*, 4445-4461.

[348] Y. M. Zhang, Y. Wang, N. Liu, Z. H. Zhu, M. Rusckowski, D. J. Hnatowich, *J Nucl Med* **2001**, *42*, 1660-1669.

[349] X. R. Liu, K. Nakamura, Y. Wang, Y. Wang, G. Z. Liu, J. He, H. L. Ding, P. Y. Lu, M. Rusckowski, A. Kubo, D. J. Hnatowich, *J Nucl Med* **2006**, *47*, 360-368.

[350] Y. Zhang, M. Rusckowski, N. Liu, C. Liu, D. Hnatowich, *Cancer Biother Radio* **2001**, *16*, 411-419.

[351] C. Ramachandran, L. L. Wellham, *Anticancer Res* **2003**, *23*, 2681-2690.

[352] K. Nakamura, C. Fan, G. Liu, S. Gupta, J. He, S. Dou, A. Kubo, M. Rusckowski, D. J. Hnatowich, *Bioconjugate Chem* **2004**, *15*, 1475-1480.

[353] K. Nakamura, Y. Wang, X. R. Liu, A. Kubo, D. J. Hnatowich, *Mol Imaging Biol* **2006**, *8*, 188-192; X. Liu, Y. Wang, K. Nakamura, A. Kubo, D. J. Hnatowich, *Cancer Gene Ther* **2008**, *15*, 126-132; X. R. Liu, K. Nakamura, Y. Wang, S. R. Zhang, J. He, G. Z. Liu, S. P. Dou, A. Kubo, M. Rusckowski, D. Hnatowich, *Mol Imaging Biol* **2006**, *8*, 278-283.

[354] K. Nakamura, Y. Wang, X. R. Liu, A. Kubol, D. J. Hnatowich, *J Nucl Med* **2007**, *48*, 1845-1852.

[355] J. G. Zheng, T. Z. Tan, *World J Gastroenterol* **2004**, *10*, 2563-2566.

[356] M. K. Dewanjee, A. K. Ghafouripour, M. Kapadvanjwala, S. Dewanjee, A. N. Serafini, D. M. Lopez, G. N. Sfakianakis, *J Nucl Med* **1994**, *35*, 1054-1063.

[357] M. K. Dewanjee, A. K. Ghafouripour, M. Kapadvanjwala, W. Ganz, W. Mallin, S. Ezuddin, A. N. Serafini, G. N. Sfakianakis, D. M. Lopez, *J Nucl Med* **1994**, *35*, P65-P65; M. K. Dewanjee, A. K. Ghafouripour, M. Subramanian, M. Hanna, M. Kapadvanjwala, A. N. Serafini, S. Ezuddin, W. Ganz, W. Mallin, G. N. Sfakianakis, *J Nucl Med* **1994**, *35*, P263-P263.

[358] A. Roivainen, T. Tolvanen, S. Salomaki, G. Lendvai, I. Velikyan, P. Numminen, M. Valila, H. Sipila, M. Bergstrom, P. Harkonen, H. Lonnberg, B. Langstrom, *J Nucl Med* **2004**, *45*, 347-355.

[359] N. Shi, R. J. Boado, W. M. Pardridge, *Proc Natl Acad Sci U S A* **2000**, *97*, 14709-14714.

[360] H. J. Lee, R. J. Boado, D. A. Braasch, D. R. Corey, W. M. Pardridge, *J Nucl Med* **2002**, *43*, 948-956.

[361] T. Suzuki, D. Wu, F. Schlachetzki, J. Y. Li, R. J. Boado, W. M. Pardridge, *J Nucl Med* **2004**, *45*, 1766-1775.

[362] H. F. Fang, X. Yue, X. X. Li, J. S. Taylor, *Nucleic Acids Res* **2005**, *33*, 6700-6711.

[363] X. K. Sun, H. F. Fang, X. X. Li, R. Rossin, M. J. Welch, J. S. Taylor, *Bioconjugate Chem* **2005**, *16*, 294-305.

[364] X. B. Tian, M. R. Aruva, W. Y. Qin, W. Z. Zhu, K. T. Duffy, E. R. Sauter, M. L. Thakur, E. Wickstrom, *J Nucl Med* **2004**, *45*, 2070-2082.

[365] X. B. Tian, M. R. Aruva, W. Y. Qin, W. Z. Zhu, E. R. Sauter, M. L. Thakur, E. Wickstrom, *Bioconjugate Chem* **2005**, *16*, 70-79.

[366] X. Tian, E. Wickstrom, *Org Lett* **2002**, *4*, 4013-4016.

[367] X. B. Tian, M. R. Aruva, K. J. Zhang, N. Shanthly, C. A. Cardi, M. L. Thakur, E. Wickstrom, *J Nucl Med* **2007**, *48*, 1699-1707.

[368] D. D. Dischino, E. J. Delaney, J. E. Emswiler, G. T. Gaughan, J. S. Prasad, S. K. Srivastava, M. F. Tweedle, *Inorg Chem* **1991**, *30*, 1265-1269.

[369] A. Chakrabarti, K. Zhang, M. R. Aruva, C. A. Cardi, A. W. Opitz, N. J. Wagner, M. L. Thakur, E. Wiskstrom, *Cancer Biol Ther* **2007**, *6*, 948-956.

[370] B. J. Hicke, A. W. Stephens, T. Gould, Y. F. Chang, C. K. Lynott, J. Heil, S. Borkowski, C. S. Hilger, G. Cook, S. Warren, P. G. Schmidt, *J Nucl Med* **2006**, *47*, 668-678.

[371] N. Liu, H. Ding, J.-L. Vanderheyden, Z. Zhu, Y. Zhang, *Nucl Med Biol* **2007**, *34*, 399-404.

[372] O. M. Merkel, D. Librizzi, A. Pfestroff, T. Schurrat, M. Behe, T. Kissel, *Bioconjugate Chem* **2009**, *20*, 174-182.

[373] D. W. Bartlett, H. Su, I. J. Hildebrandt, W. A. Weber, M. E. Davis, *P Natl Acad Sci USA* **2007**, *104*, 15549-15554.

[374] X. Tian, A. Chakrabarti, N. Amirkhanov, M. R. Aruva, K. Zhang, C. A. Cardi, S. Lai, M. L. Thakur, E. Wickstrom, *Biochem Soc Trans* **2007**, *35*, 72-76.

[375] X. H. Ou, T. Z. Tan, L. He, Y. C. Li, J. L. Li, A. R. Kuang, *Cancer Gene Ther* **2005**, *12*, 313-320; R. F. Wang, J. Shen, F. Qiu, C. L. Zhang, *J Radioanal Nucl Chem* **2007**, *273*, 19-23.

[376] E. Hedberg, H. Takechi, B. Langstrom, *J Labelled Compd Radiopharm* **1995**, *37*, 335-337.

[377] D. J. Hnatowich, K. Nakamura, *Ann Nucl Med* **2004**, *18*, 363-368.

[378] N. Khoukhi, M. Vaultier, R. Carrie, *Tetrahedron* **1987**, *43*, 1811-1822; R. P. McGeary, *Tetrahedron Lett* **1998**, *39*, 3319-3322.

[379] J. A. H. Inkster, B. Guérin, T. J. Ruth, M. J. Adam, *J Labelled Compd Rad* **2008**, *51*, 444-452.

[380] N. V. Amirkhanov, K. Zhang, M. R. Aruva, M. L. Thakur, E. Wickstrom, *Bioconjugate Chem* **2010**, *21*, 731-740.

[381] D. R. Gehlert, *Proc Soc Exp Biol Med* **1998**, *218*, 7-22.

[382] J. C. Reubi, M. Gugger, B. Waser, *Eur J Nucl Med Mol I* **2002**, *29*, 855-862.

[383] J. C. Reubi, M. Gugger, B. Waser, J. C. Schaer, *Cancer Res* **2001**, *61*, 4636-4641.

[384] M. Ruscica, E. Dozio, S. Boghossian, G. Bovo, V. M. Riano, M. Motta, P. Magni, *Endocrinology* **2006**, *147*, 1466-1473.

[385] J. Pernow, J. M. Lundberg, L. Kaijser, *Life Sci* **1987**, *40*, 47-54.

[386] A. Balasubramaniam, V. C. Dhawan, D. E. Mullins, W. T. Chance, S. Sheriff, M. Guzzi, M. Prabhakaran, E. M. Parker, *J Med Chem* **2001**, *44*, 1479-1482.

[387] M. Langer, R. La Bella, E. Garcia-Garayoa, A. Beck-Sickinger, *Bioconjugate Chem* **2001**, *12*, 1028-1034.

[388] A. J. Daniels, J. E. Matthews, R. J. Slepetis, M. Jansen, O. H. Viveros, A. Tadepalli, W. Harrington, D. Heyer, A. Landavazo, J. J. Leban, A. Spaltenstein, *P Natl Acad Sci USA* **1995**, *92*, 9067-9071.

[389] S. D. S. Jois, A. Balasubramaniam, *Peptides* **2003**, *24*, 1035-1043.

[390] B. Guerin, V. Dumulon-Perreault, M.-C. Tremblay, S. Ait-Mohand, P. Fournier, C. Dubuc, S. Authier, F. Benard, *Bioorg Med Chem Lett* **2010**, *20*, 950-953.

[391] V. Dumulon-Perreault, B. Guérin, C. Dubuc, S. Authier, M. Khan, R. Langlois, F. Benard, *J Nucl Med* **2008**, *49 (Suppl. 1)*, 97P.

[392] O. Patel, A. Shulkes, G. S. Baldwin, *Biochim Biophys Acta* **2006**, *1766*, 23-41.

[393] H. Ohki-Hamazaki, M. Iwabuchi, F. Maekawa, *Int J Dev Biol* **2005**, *49*, 293-300.

[394] J. Ischia, O. Patel, A. Shulkes, G. S. Baldwin, *Biofactors* **2009**, *35*, 69-75.

[395] R. Markwalder, J. C. Reubi, *Cancer Res* **1999**, *59*, 1152-1159.

[396] A. Anastasi, V. Erspamer, M. Bucci, *Experientia* **1971**, *27*, 166-167.

[397] S. Mantey, H. Frucht, D. H. Coy, R. T. Jensen, *Mol Pharmacol* **1993**, *43*, 762-774.

[398] R. La Bella, E. Garcia-Garayoa, M. Bahler, P. Blauenstein, R. Schibli, P. Conrath, D. Tourwe, P. A. Schubiger, *Bioconjugate Chem* **2002**, *13*, 599-604; S. R. Lane, B. Veerendra, T. L. Rold, G. L. Sieckman, T. J. Hoffman, S. S. Jurisson, C. J. Smith, *Nucl Med Biol* **2008**, *35*, 263-272; B. Nock, A. Nikolopoulou, E. Chiotellis, G. Loudos, D. Maintas, J. C. Reubi, T. Maina, *Eur J Nucl Med Mol I* **2003**, *30*, 247-258; K. S. Lin, A. Luu, K. E. Baidoo, H. Hashemzadeh-Gargari, M. K. Chen, K. Brenneman, R. Pili, M. Pomper, H. N. Wagner, *Bioconjugate Chem* **2005**, *16*, 43-50; G. Ferro-Flores, C. A. de Murphy, J. Rodriguez-Cortes, M. Pedraza-Lopez, M. Ramirez-Iglesias, *Nucl Med Commun* **2006**, *27*, 371-376; E. Gourni, M. Paravatou, P. Bouziotis, C. Zikos, M. Fani, S. Xanthopoulos, S. C. Archimandritis, E. Livaniou, A. D. Varvarigou, *Anticancer Res* **2006**, *26*, 435-438.

[399] J. Schuhmacher, H. Zhang, J. Doll, H. R. Mäcke, R. Matys, H. Hauser, M. Henze, U. Haberkorn, M. Eisenhut, *J Nucl Med* **2005**, *46*, 691-699.

[400] A. Dimitrakopoulou-Strauss, P. Hohenberger, U. Haberkorn, H. R. Macke, M. Eisenhut, L. G. Strauss, *J Nucl Med* **2007**, *48*, 1245-1250.

[401] X. Y. Chen, R. Park, Y. P. Hou, M. Tohme, A. H. Shahinian, J. R. Bading, P. S. Conti, *J Nucl Med* **2004**, *45*, 1390-1397; Y. S. Yang, X. Zhang, Z. Xiong, X. Chen, *Nucl Med Biol* **2006**, *33*, 371-380; J. J. Parry, T. S. Kelly, R. Andrews, B. E. Rogers, *Bioconjug Chem* **2007**, *18*, 1110-1117; G. B. Biddlecombe, B. E. Rogers, M. de Visser, J. J. Parry, M. de Jong, J. L. Erion, J. S. Lewis, *Bioconjug Chem* **2007**, *18*, 724-730.

[402] A. F. Prasanphanich, P. K. Nanda, T. L. Rold, L. X. Ma, M. R. Lewis, J. C. Garrison, T. J. Hoffman, G. L. Sieckman, S. D. Figueroa, C. J. Smith, *P Natl Acad Sci USA* **2007**, *104*, 12462-12467.

[403] J. C. Garrison, T. L. Rold, G. L. Sieckman, S. D. Figueroa, W. A. Volkert, S. S. Jurisson, T. J. Hoffman, *J Nucl Med* **2007**, *48*, 1327-1337.

[404] S. Ait-Mohand, P. Fournier, V. Dumulon-Perreault, G. E. Kiefer, P. Jurek, C. L. Ferreira, F. Bénard, B. Guérin, *Bioconjug Chem* **2011**, *22*, 1729-1735.

[405] J. Becaud, L. J. Mu, M. Karramkam, P. A. Schubiger, S. M. Ametamey, K. Graham, T. Stellfeld, L. Lehmann, S. Borkowski, D. Berndorff, L. Dinkelborg, A. Srinivasan, R. Smits, B. Koksch, *Bioconjugate Chem* **2009**, *20*, 2254-2261.

[406] L. Mu, M. Honer, J. Becaud, M. Martic, P. Schubiger, S. Ametamey, T. Stellfeld, K. Graham, S. Borkowski, L. Lehmann, L. Dinkelborg, A. Srinivasan, *Bioconjugate Chem* **2010**, *21*, 1864-1871.

[407] M. Honer, L. Mu, T. Stellfeld, K. Graham, M. Martic, C. R. Fischer, L. Lehmann, P. A. Schubiger, S. M. Ametamey, L. Dinkelborg, A. Srinivasan, S. Borkowski, *J Nucl Med* **2011**, *52*, 270-278.

[408] O. Jacobson, L. Zhu, Y. Ma, I. D. Weiss, X. L. Sun, G. Niu, D. O. Kiesewetter, X. Y. Chen, *Bioconjugate Chem* **2011**, *22*, 422-428.

[409] Z. B. Li, Z. H. Wu, K. Chen, E. K. Ryu, X. Y. Chen, *J Nucl Med* **2008**, *49*, 453-461.

[410] Z. Liu, Y. Yan, S. Liu, F. Wang, X. Chen, *Bioconjug Chem* **2009**, *20*, 1016-1025.

[411] D. H. Coy, J. E. Taylor, N. Y. Jiang, S. H. Kim, L. H. Wang, S. C. Huang, J. P. Moreau, J. D. Gardner, R. T. Jensen, *J Biol Chem* **1989**, *264*, 14691-14697.

[412] F. Dolle, H. Valette, M. Bottlaender, F. Hinnen, F. Vaufrey, I. Guenther, C. Crouzel, *J Labelled Compd Rad* **1998**, *41*, 451-463.

[413] I. Jlalia, F. Meganem, J. Herscovici, C. Girard, *Molecules* **2009**, *14*, 528-539.

[414] X. M. Liu, A. Thakur, D. Wang, *Biomacromolecules* **2007**, *8*, 2653-2658.

[415] S. Dandapani, D. Curran, *Chem-Eur J* **2004**, *10*, 3130-3138.

[416] Y. S. Ding, C. Y. Shiue, J. S. Fowler, A. P. Wolf, A. Plenevaux, *J Fluorine Chem* **1990**, *48*, 189-205.

[417] M. Brewster, M. Hora, J. Simpkins, N. Bodor, *Pharm Res* **1991**, *8*, 792-795.

[418] S. Davis, C. Washington, P. West, L. Illum, G. Liversidge, L. Sternson, R. Kirsh, *Ann NY Acad Sci* **1987**, *507*, 75-88.

[419] P. J. Thornalley, *Chem Biol Interact* **1998**, *111-112*, 137-151.

[420] A. Bierhaus, M. A. Hofmann, R. Ziegler, P. P. Nawroth, *Cardiovasc Res* **1998**, *37*, 586-600; N. Ahmed, O. K. Argirov, H. S. Minhas, C. A. A. Cordeiro, P. J. Thornalley, *Biochem J* **2002**, *364*, 1-14.

[421] M. A. Glomb, G. Lang, *J Agric Food Chem* **2001**, *49*, 1493-1501.

[422] U. Schwarzenbolz, T. Henle, R. Haebner, A. Klostermeyer, *Z Lebensm Unters F A* **1997**, *205*, 121-124.

[423] B. Kuhnast, A. Damont, F. Hinnen, C. Huss, F. Dolle, *J Labelled Compd Rad* **2009**, *52*, S184-S184.

[424] J. A. H. Inkster, K. Liu, S. Ait-Mohand, P. Schaffer, B. Guerin, T. J. Ruth, T. Storr, *Chemistry, A European Journal* **2012**, *18*, 11079-11087.

[425] J. P. D. Kleijn, H. J. Meeuwissen, B. Vanzanten, *Radiochem Radioa Let* **1975**, *23*, 139-143.

[426] T. R. Neal, S. Apana, M. S. Berridge, *J Labelled Compd Rad* **2005**, *48*, 557-568.

[427] M. Jelinski, Forschungszentrums Jülich (Köln), **2002**.

[428] B. Krazer, H. Zollinger, *Helvetica Chimica Acta* **1960**, *43*, 1513-1522.

[429] B. R. Baker, G. J. Lourens, *J Med Chem* **1967**, *10*, 1113.

[430] R. Cremlyn, R. Nunes, *Phosphorus Sulfur* **1987**, *31*, 245-254.

[431] E. Tayama, S. Sugai, *Tetrahedron Lett* **2007**, *48*, 6163-6166.

[432] E. Guibejampel, M. Wakselman, D. Raulais, *J Chem Soc Chem Comm* **1980**, 993-994.

[433] A. I. S. D. S. o. O. Compounds, National Institute of Advanced Industrial Science and Technology (Japan).

[434] J. P. Bassin, R. J. Cremlyn, F. J. Swinbourne, *Phosphorus Sulfur* **1991**, *56*, 245-275.

[435] A. C. Tome, J. A. S. Cavaleiro, F. M. J. Domingues, R. J. Cremlyn, *Phosphorus Sulfur* **1993**, *79*, 187-194.

[436] R. J. Cremlyn, F. J. Swinbourne, P. Fitzgerald, N. Godfrey, P. Hedges, J. Lapthorne, C. Mizon, *Indian J Chem B* **1984**, *23*.

[437] G. Blotny, *Tetrahedron Lett* **2003**, *44*, 1499-1501.

[438] E. Buehler, *J Org Chem* **1967**, *32*, 261.

[439] O. W. Willcox, *Am Chem J* **1904**, *32*, 446-476.

[440] R. N. Khelevin, *Zh Org Khim+* **1987**, *23*, 1925-1929.

[441] R. N. Khelevin, *Zhurnal Obshchei Khimii* **1985**, *55*, 184-189.

[442] J. T. Edward, J. Whiting, *Can J Chem* **1971**, *49*, 3502.

[443] M. Kirchgessner, K. Sreenath, K. Gopidas, *J Org Chem* **2006**, *71*, 9849-9852.

[444] G. T. James, *Anal Biochem* **1978**, *86*, 574-579.

[445] G. T. Hermanson, *Bioconjugate techniques*, Academic Press, San Diego, **1996**.

[446] M. Smith, J. March, *March's advanced organic chemistry: reactions, mechanisms, and structure*, 6th ed., John Wiley & Sons, Hoboken, **2007**.

[447] O. Rogne, *J Chem Soc B* **1970**, 727.

[448] O. Rogne, *J Chem Soc B* **1971**, 1334.

[449] E. F. V. Scriven, *Chem Soc Rev* **1983**, *12*, 129-161.

[450] G. Hofle, W. Steglich, H. Vorbruggen, *Angew Chem Int Ed* **1978**, *17*, 569.

[451] W. P. Jencks, *J Am Chem Soc* **1959**, *81*, 475-481.

[452] A. A. Wilson, L. Jin, A. Garcia, J. N. DaSilva, S. Houle, *Appl Radiat Isotopes* **2001**, *54*, 203-208.

[453] M. Petrik, A. Laznickova, M. Laznicek, M. R. Zalutsky, *Anticancer Res* **2007**, *27*.

[454] M. Yokoi, S. Konishi, T. Hayashi, *Denki Kagaku* **1984**, *52*, 218-223.

[455] D. Suryanarayana, P. A. Narayana, L. Kevan, *Inorg Chem* **1983**, *22*, 474-478.

[456] D. Stoychev, C. Tsvetanov, *J Appl Electrochem* **1996**, *26*, 741-749.

[457] Z. V. Feng, X. Li, A. A. Gewirth, *J Phys Chem B* **2003**, *107*, 9415-9423.

[458] D. Brazinskiene, A. Survila, *Russ J Electrochem* **2005**, *41*, 979-984.

[459] R. M. Roat-Malone, *Bioinorganic chemistry: a short course*, Wiley, Hoboken, **2002**.

[460] B. G. Malmstrom, J. Leckner, *Curr Opin Chem Biol* **1998**, *2*; J. T. Rubino, K. J. Franz, *J Inorg Biochem* **2012**, *107*.

[461] S. J. Shields, B. K. Bluhm, D. H. Russell, *Int J Mass Spectrom* **1999**, *182*, 185-195.

[462] S. J. Shields, B. K. Bluhm, D. H. Russell, *J Am Soc Mass Spectrom* **2000**, *11*.

[463] B. K. Bluhm, S. J. Shields, C. A. Bayse, M. B. Hall, D. H. Russell, *Int J Mass Spectrom* **2001**, *204*.

[464] Q. F. Ma, Y. M. Li, J. T. Du, H. D. Liu, K. Kanazawa, T. Nemoto, H. Nakanishi, Y. F. Zhao, *Peptides* **2006**, *27*, 841-849.

[465] S. Liu, D. S. Edwards, R. J. Looby, A. R. Harris, M. J. Poirier, J. A. Barrett, S. J. Heminway, T. R. Carroll, *Bioconjug Chem* **1996**, *7*, 63-71.

[466] R. A. Pufahl, C. P. Singer, K. L. Peariso, S. J. Lin, P. J. Schmidt, C. J. Fahrni, V. C. Culotta, J. E. PennerHahn, T. V. Ohalloran, *Science* **1997**, *278*.

[467] D. Garner, University of Illinois (Urbana, Illinois), **2008**.

[468] F. H. Jardine, in *Advances in inorganic chemistry and radio-chemistry, Vol. 17* (Eds.: H. J. Emelius, A. G. Sharpe), Academic Press., New York, **1975**.

[469] Z. Wu, F. A. Fernandez-Lima, D. H. Russell, *J Am Soc Mass Spectrom* **2010**, *21,* 522-533.

[470] H. Dougan, J. B. Hobbs, J. I. Weitz, D. M. Lyster, *Nucleic Acids Res* **1997**, *25*, 2897.

Appendix.

Selected MALDI-TOF Spectra

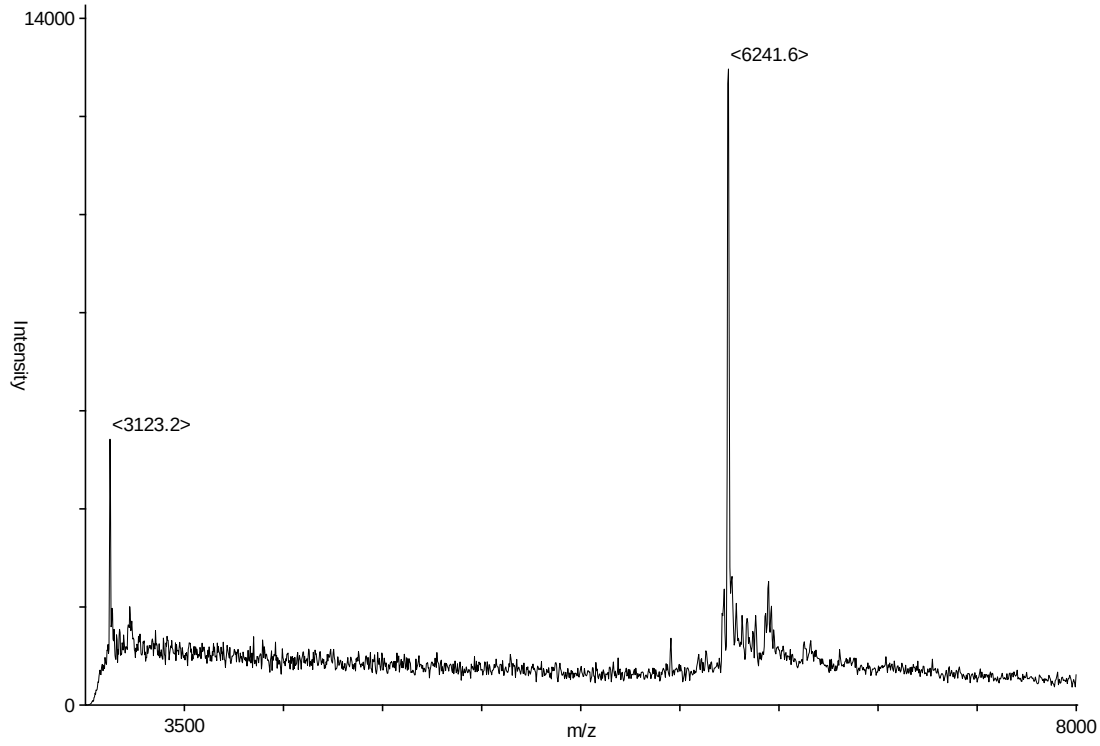

A1. 1. Spectrum of N_3-ODN.

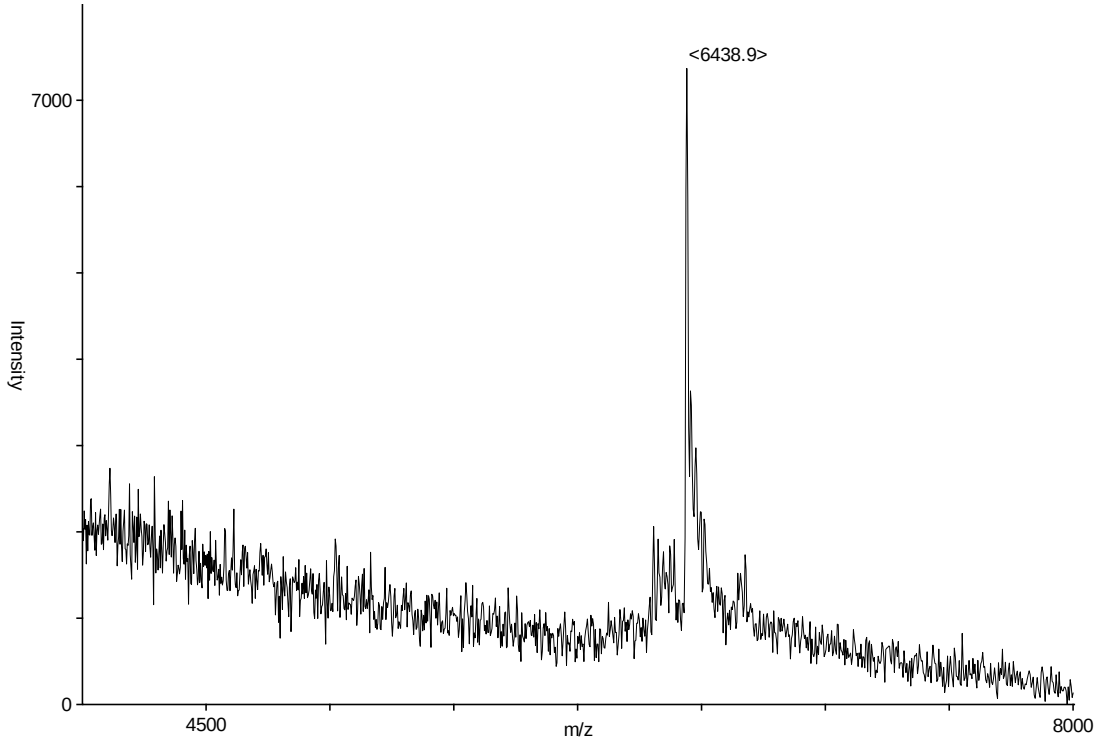

A1. 2. Spectrum of ^{19}F-ODN.

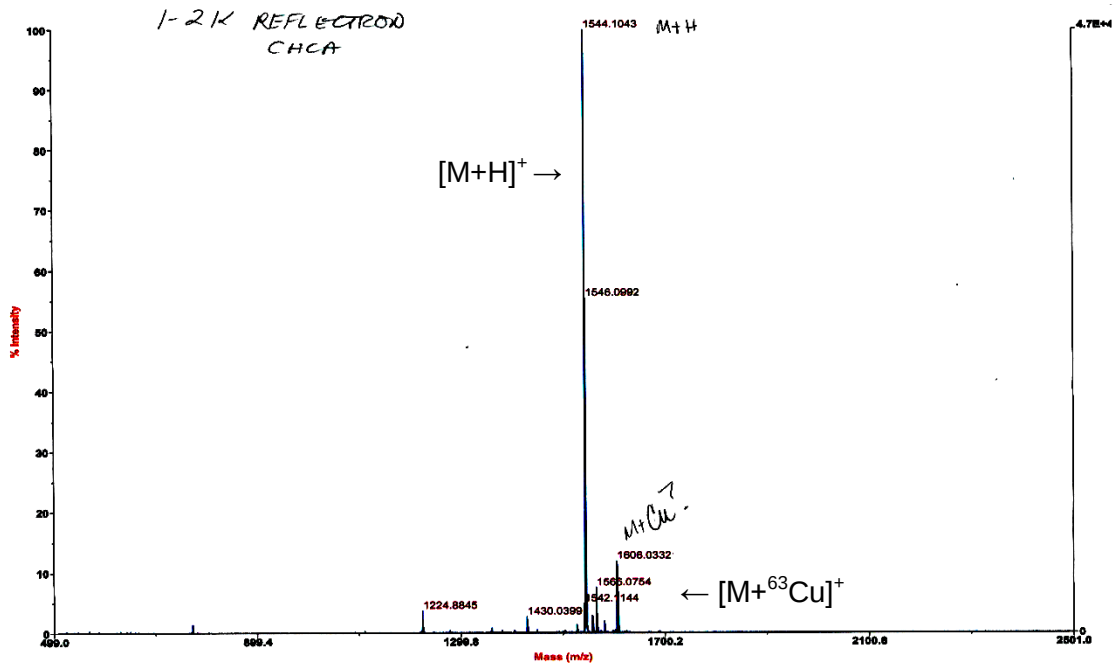

A1. 3. Spectrum of F-PEG-BVD peptide.

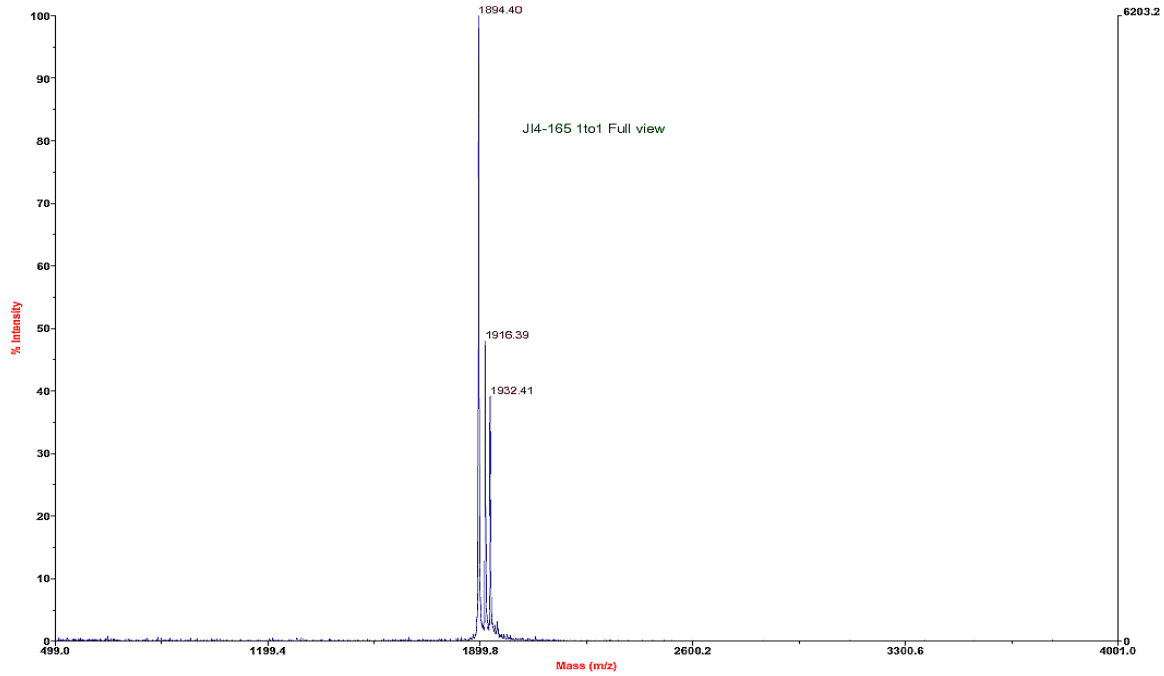

A1. 4. Spectrum of F-PEG-BBN-PEG.

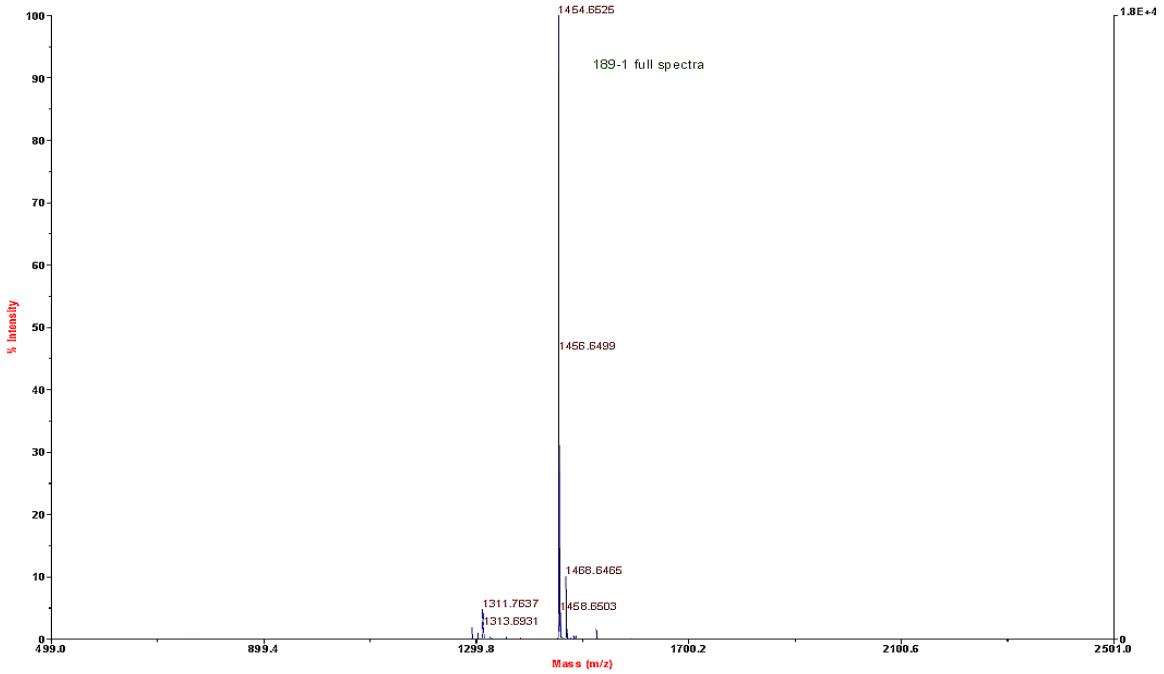

A1. 5. Spectrum of NMe_3-BBN peptide.

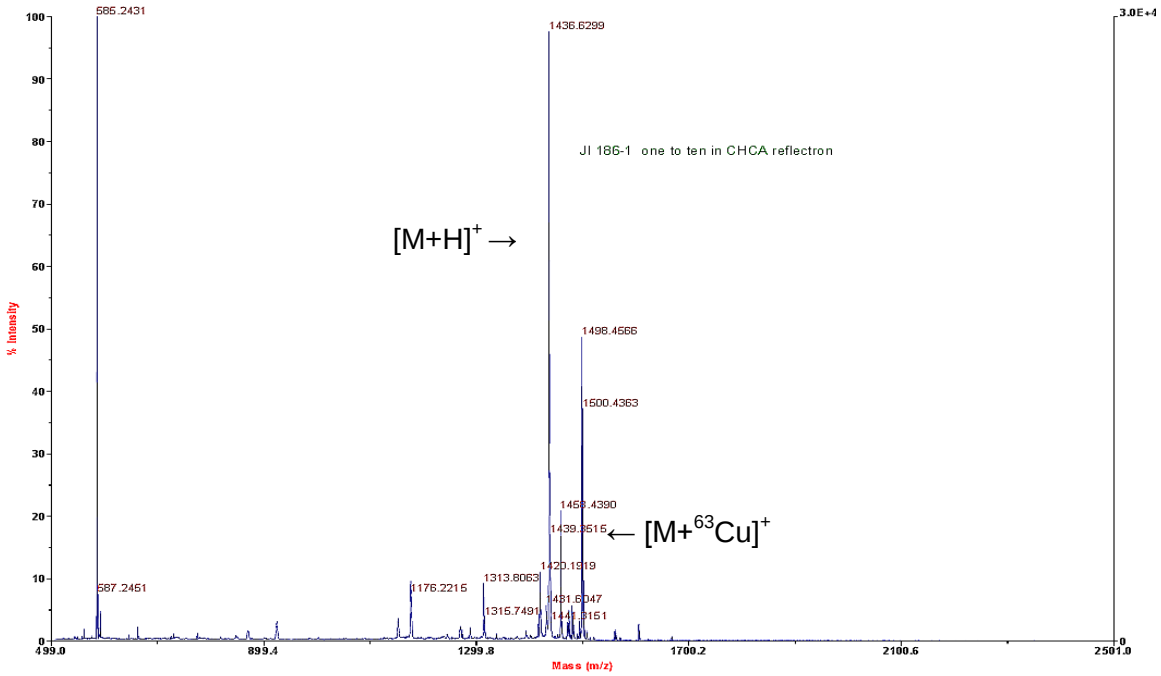

A1. 6. Spectrum of BBN-OAlk-SO_2F peptide.